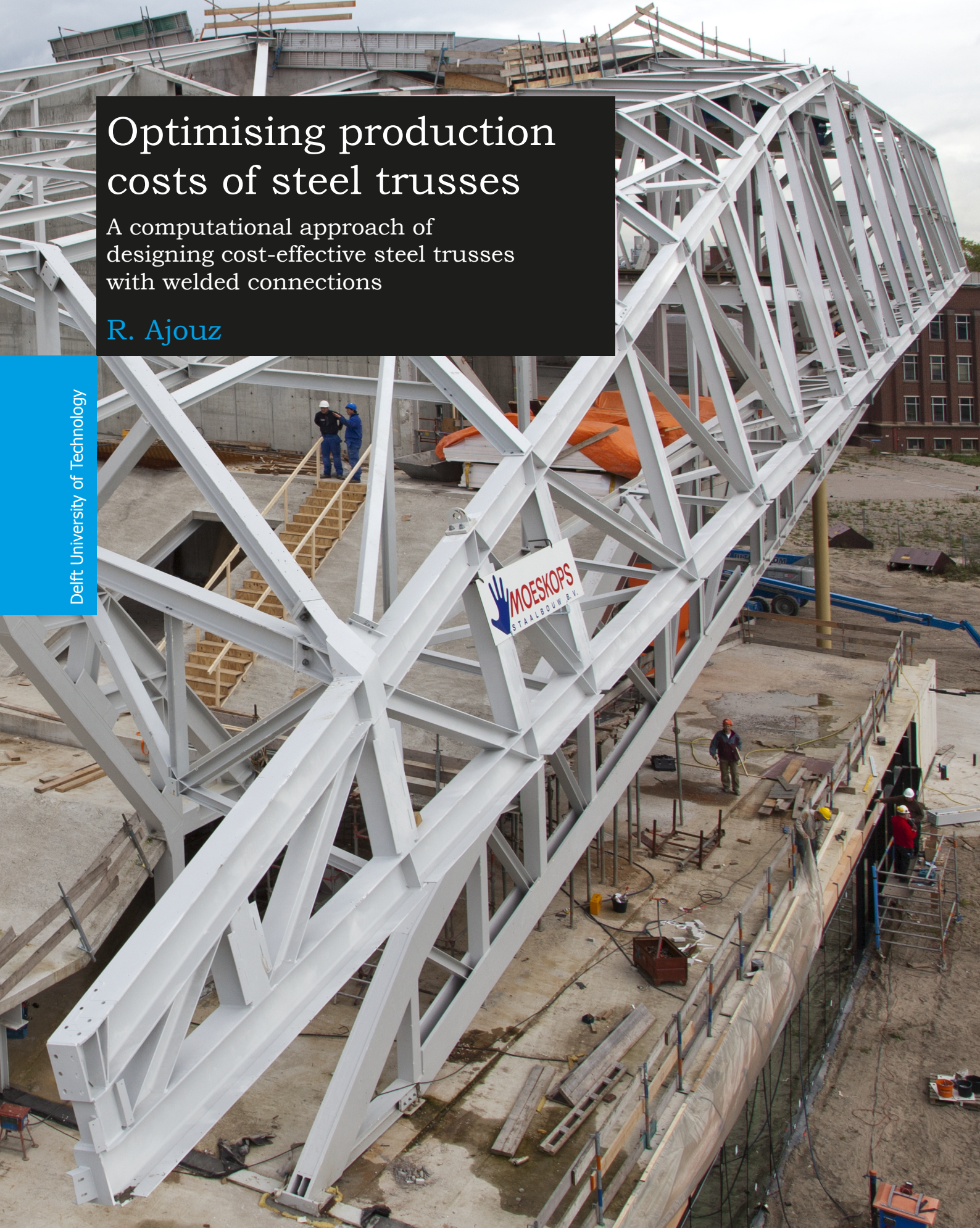


# Optimising production costs of steel trusses

A computational approach of designing cost-effective steel trusses with welded connections

R. Ajouz

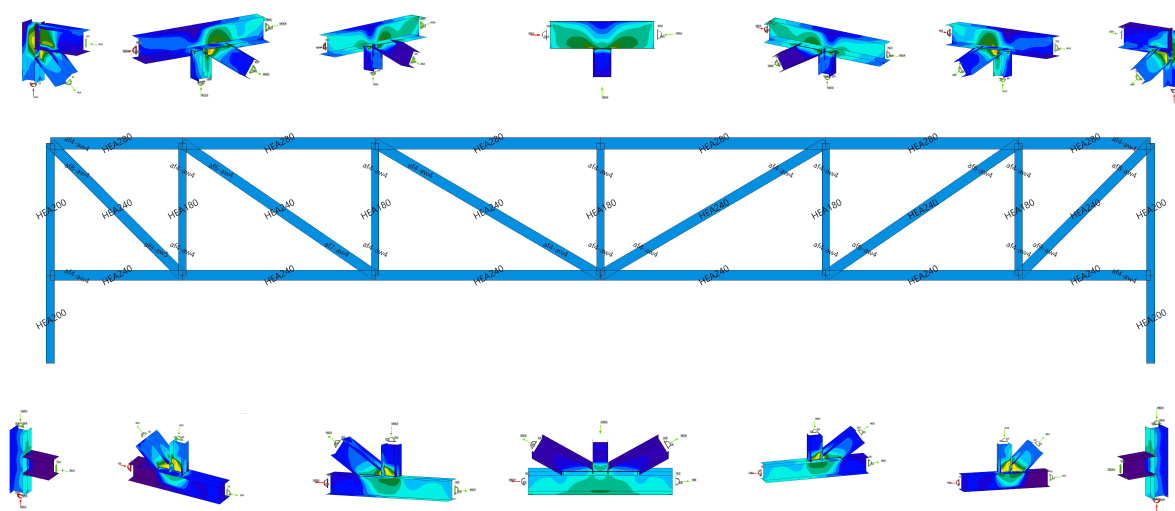
Delft University of Technology





# A computational approach of designing cost-effective steel trusses with welded connections

**R. Ajouz**



**Master of Science**  
in Building Engineering

Supervisor: Prof. dr. ir. R. Nijse  
Thesis committee: Ir. P. A. de Vries, TU Delft  
Ir. L. P. L. van der Linden, TU Delft  
Ir. J. C. van der Ploeg, ABT bv  
Advisor: Ir. F. Maatje, Bouwen met Staal



TU Delft Delft University of Technology







# Preface

This report is the result of my graduation research project for the optimization of trusses towards production costs. The graduation research is the last step towards fulfilling the requirements needed to obtain the title Master of Science in Building Engineering at the Faculty of Civil Engineering of the Delft University of Engineering.

This research project was performed at "ABT bv" in Delft, where I was tutored by the company supervisor Chris van der Ploeg. I would like to thank Chris for the time and effort to supervise my work. I was enriched by his experience both in the field of engineering and computational solutions. Under your supervision, I could develop my programming skills into a competence of which I can benefit for the rest of my career.

I would like to thank my other supervisors, Rob Nijse, Peter de Vries and Lennert van der Linden, who guided me from the start of my graduation project. Your comments and remarks were very useful to steer me in the right direction throughout the whole graduation process.

I would like to thank Frank Maatje of "Bouwen met Staal" who connected me with vital people in the Dutch steel structure industry and allowed me to participate in events of "Bouwen met Staal". I would like to thank the representatives of the steel contractors who invited me to visit their companies and helped with answering practical questions I had regarding the production process of steel structures through. Namely, I would like to thank Arjan van Dijk from Voortman steel group, Frank Reijrink from Reijrink Constructie bv and Kees Oudshoorn from Oostingh ASK Romein.

I would like to thank Costis Hatzopoulos from IDEA Statica UK for the provided support and feedback regarding the usage of the API of IDEA Statica Connection.

Finally, I would like to thank all employees of ABT for taking the time to answer my questions and giving me insight into the practice of engineering in an engineering company. I had a very pleasant and inspiring time at ABT bv during the work on my thesis. It helped me stay highly motivated and focused throughout the whole process of the graduation research.

*R. Ajouz  
Delft, December 2018*









# Contents

|          |   |           |
|----------|---|-----------|
| <b>1</b> | <b>Introduction</b>   | <b>1</b>  |
| 1.1      | Problem statement   | 3         |
| 1.2      | Scope   | 3         |
| 1.3      | Research question   | 4         |
| 1.4      | Objective   | 5         |
| 1.5      | Methodology   | 5         |
| 1.6      | Report structure  | 6         |
| <b>2</b> | <b>State of the Art</b>   | <b>9</b>  |
| 2.1      | Introduction  | 9         |
| 2.2      | State of the Art in Engineering of steel trusses including joint design | 9         |
| 2.3      | State of the Art in production of steel structures                      | 9         |
| 2.4      | Conclusion  | 12        |
| <b>3</b> | <b>Costs of Steel Structures</b>  | <b>13</b> |
| 3.1      | Introduction  | 13        |
| 3.2      | Cost models of skeletal steel structures                                | 17        |
| 3.2.1    | Method 1: Weight concept  | 17        |
| 3.2.2    | Method 2: Percentage of beam weight based on rotational capacity joint  | 17        |
| 3.2.3    | Method 3: Weld volume method  | 18        |
| 3.2.4    | Method 4: Activity Based Costing  | 20        |
| 3.3      | Cost models for welding   | 23        |
| 3.4      | Reverse engineering   | 24        |
| 3.5      | Discussion & Conclusion   | 25        |
| <b>4</b> | <b>Optimisation criteria of Trusses</b>                                 | <b>27</b> |
| 4.1      | Introduction  | 27        |
| 4.2      | Constructability  | 27        |
| 4.2.1    | Production risks caused by design                                       | 27        |
| 4.2.2    | Human error and Standardization   | 31        |
| 4.3      | Production cost   | 32        |
| 4.3.1    | Goal of cost-model  | 32        |
| 4.3.2    | Fabrication process   | 32        |
| 4.4      | Conclusion  | 41        |
| <b>5</b> | <b>Structural Analysis of Trusses</b>                                   | <b>43</b> |
| 5.1      | Introduction  | 43        |
| 5.2      | Assumed loads in research   | 43        |
| 5.3      | Assumptions for structural analysis                                     | 47        |
| 5.4      | Structural analyses with Karamba3D                                      | 49        |
| 5.4.1    | Shear-force in Eccentricity elements                                    | 52        |
| 5.5      | Conclusion  | 54        |
| <b>6</b> | <b>Welded connections in Trusses</b>                                    | <b>55</b> |
| 6.1      | Introduction  | 55        |
| 6.2      | Volume of welds   | 55        |
| 6.3      | Strength of welds   | 59        |
| 6.3.1    | Calculation Method 1: Full-strength method                              | 59        |
| 6.3.2    | Calculation Method 2: Directional method                                | 62        |
| 6.4      | Conclusion  | 68        |

|           |   |            |
|-----------|---|------------|
| <b>7</b>  | <b>Model definition</b>                                       | <b>69</b>  |
| 7.1       | Introduction  | 69         |
| 7.2       | Grasshopper + Karamba3D                                       | 69         |
| 7.3       | Framework   | 73         |
| 7.4       | IDEA Statica Connection                                       | 76         |
| 7.5       | Conclusion  | 80         |
| <b>8</b>  | <b>Cost Optimisation of Trusses</b>                           | <b>83</b>  |
| 8.1       | Parameters and boundary conditions                            | 83         |
| 8.2       | Reference Case  | 85         |
| 8.3       | Singularity in IDEA Statica Connection                        | 86         |
| 8.4       | Full-strength method analyses                                 | 87         |
| 8.4.1     | Influence of the Cross-section Family and Steel-grade         | 87         |
| 8.4.2     | Influence of the truss-height and number of truss-segments    | 92         |
| 8.4.3     | Influence of the buckling length                              | 94         |
| 8.4.4     | Influence of truss Typology                                   | 95         |
| 8.4.5     | Trusses with eccentricity joints                              | 96         |
| 8.4.6     | Trusses with variation in truss-segment length                | 98         |
| 8.5       | Directional method analyses                                   | 100        |
| 8.5.1     | Influence of mechanical scheme on weld-volume                 | 100        |
| 8.5.2     | Weld volume optimisation                                      | 101        |
| 8.6       | Conclusion  | 105        |
| <b>9</b>  | <b>Further possibilities with methodology</b>                 | <b>107</b> |
| 9.1       | Introduction  | 107        |
| 9.2       | Nationaal Militair Museum, Soesterberg                        | 107        |
| 9.3       | Sportcampus Zuiderpark  | 110        |
| 9.4       | Conclusion  | 112        |
| <b>10</b> | <b>Discussion &amp; Conclusion</b>                            | <b>113</b> |
| 10.1      | Conclusion  | 113        |
| 10.2      | Discussion  | 114        |
| 10.3      | Recommendations   | 116        |
| <b>A</b>  | <b>Appendix: Analytic analysis on cutting planes in nodes</b> | <b>119</b> |
| A.1       | Derivation of situation with static post                      | 120        |
| A.2       | Derivation of situation with dynamic post                     | 125        |
| A.3       | Derivation of situation with dynamic post and eccentricity    | 129        |
| <b>B</b>  | <b>Appendix: Welding technologies and costs</b>               | <b>133</b> |
| <b>C</b>  | <b>Appendix: Results price comparison Dutch steel traders</b> | <b>137</b> |
| C.1       | Material prices   | 138        |
| C.2       | Sawing prices   | 142        |
| C.3       | Shot-blasting and Priming                                     | 143        |
| <b>D</b>  | <b>Appendix: Test-case cost-model "Simply supported beam"</b> | <b>145</b> |
| <b>E</b>  | <b>Appendix: Surface area study on welds</b>                  | <b>153</b> |
| E.1       | skewed fillet weld  | 154        |
| E.2       | skewed but welds  | 155        |
| E.3       | triangle welds  | 156        |
| E.4       | Directional method for skew fillet welds                      | 157        |
|           | <b>Bibliography</b>   | <b>159</b> |

# 1

## Introduction

The current building industry is fragmented. Each company has own scope of expertise, which contributes to building projects. This fragmentation is also visible in the steel structure design of the utility building industry. In this industry, the structural engineers design the structure and steel contractors design the joints.

A tender is put out by a client. Multiple parties consisting of an architecture firm, an engineering firm, and a contractor team up together to create the preliminary design for the building. They work closely together in a building information model to create an integrated design of all represented disciplines, see figure 1.1. During this process, the engineering firm is responsible for designing the steel structure. They will design a steel structure that fits together with all other facets of the building. For example, the climate system, the architectural detailing etc... In this design, engineers often optimise weight in order to save material, under the assumption to lower the building costs. In this design, the joints have a coarse level of detail, and will be assumed either rigid or hinged.

When the tender is won, the contractor will look for a steel contractor who will produce and build the steel structure at the right price. The selected steel contractor will design in detail all the joints of the steel structure, which is designed by the engineering firm. The steel contractor will design these joints in the most beneficial way for his production process. Cross-sections selected by the engineer during weight optimisation can create slender structures. This can have an impact on the joints to be designed, and can create the need for more complex joints with many plates and stiffeners in order to provide sufficient structural resistance in the joint [1]. Consequently, this might result in a higher costs. On the contrary, the costs can be lower when the impact of the joints have been considered at an early phase of the project.

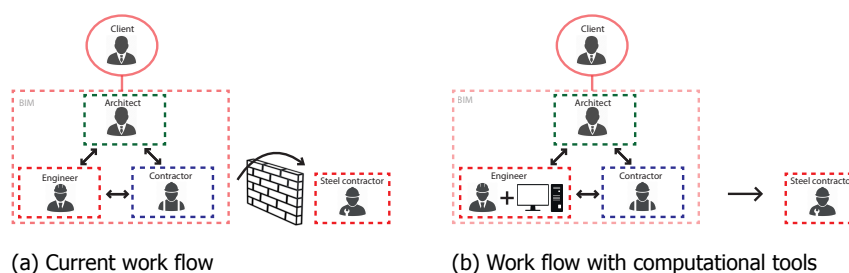


Figure 1.1: Current and suggested future workflow on the design of steel structures

Currently, designing the details takes place at a relatively late stage of the project. Mostly at a stage when the general design decision is fixed and costs of changes are high, see figure 1.2. Considering, the design of the joints at an early stage of the design process, and running an optimisation on the overall cost-effectiveness of the structure, can possibly lead to a more optimal solution for each actor in the



design process. Critical connections can be identified at this early stage where changes are still easily made at a relatively low cost. Many alternative designs are still possible, see figure 1.2. Furthermore, at this early stage, all possibilities as shape, typology and size optimisation are still applicable to the project.

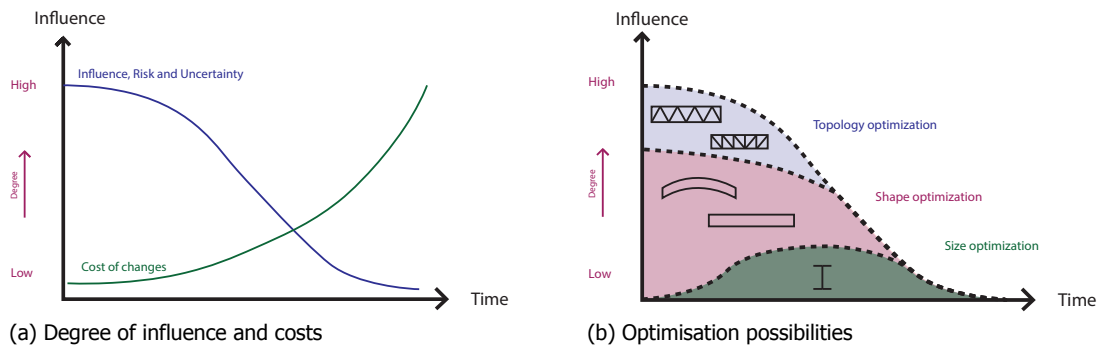


Figure 1.2: Influence, Costs and Optimisation possibilities over project lifespan

In current engineering practice, the steel contractor designs often one governing joint, which is copied to multiple similar locations of the steel structure. Standardising joints, is beneficial for reducing time needed in designing the joint, and it reduces risks of human error during production and inspection. Increased computational power that computers currently offer, allow engineers to create more complex models. Engineers can create computational tools where joint design is integrated within the automated optimisation process. This will create possibilities, to mass customise each joint based on the acting forces. The introduction of welding robots in the production process of steel structures, will make it possible to fully benefit of mass customisation, due to the lower probability of the risk of human error [2]. Most important, the use of computational tools by the engineer will allow critical joints to be identified early in the design process. This will decrease failure costs and increase project efficiency, see figure 1.1.

### Risks of not taking joints into account

Taking into account joint design in more detail at an early stadium of the project can prevent making unnecessary extra costs. For example, if a tensile element is optimised and a beam with a specific cross-sectional area is selected. At a later stage, a connection needs to be created [3, p.2]. In case of a bolted connection, holes will be drilled to facilitate the bolted connection. The drilled hole will reduce the net cross-sectional area, and can possibly lead to a too low capacity for the acting tensile force, see figure 1.3.

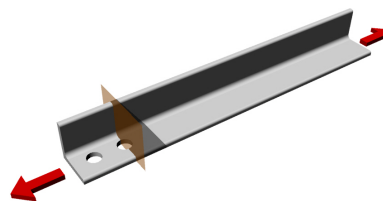


Figure 1.3: Tensile member with holes for bolted connection

To resolve this problem at a later stage, a bigger section has to be selected. However, there is a risk that this bigger section can be in conflict with other elements in the design. Another possibility will be to weld an additional plate at the position of the drilled hole to increase the local cross-sectional area. However, this can lead to extra cost for post-processing in engineering and production [4].

### Potential of taking joints into account

When joints are considered in more detail at an early phase of the design process, the aforementioned risks can be avoided. Furthermore, there are other advantages that can be achieved. According to Eurocode 3 [5], when a connection is considered to be semi-rigid, the rotational stiffness of the joint can be taken into account. The rotational stiffness will influence the moment distribution and deflections in the structure. This will give extra optimisation possibilities to save costs. With an iterative process, an optimum between the optimal beam and the potentially optimal joint can be found, see figure 1.4.

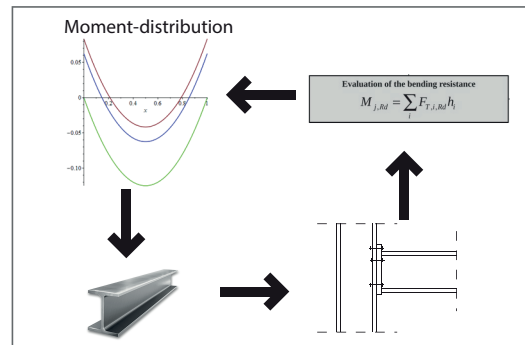


Figure 1.4: Iterative process of taking into account rotational stiffness of connections

### Production costs of steel structures

The costs of a structure is largely determined by production [6]. This includes the amount of man-hours needed to produce a certain element. Rigid connections which contain many stiffeners, are labour intensive, hence more expensive.. During the design stage, the engineer still has full control on the design. He can steer for minimum production costs, and achieve the best balance between the cost of the joints and the cost of the beams. A more complete design of the steel structure with a lower risk of failure, may allow the steel contractor to produce the structure at a lower price. Consequently, this will provide to offer the tender at a lower price, and can increase the probability of winning it.

## 1.1. Problem statement

At the early phase of steel structure design, engineers optimise often on weight and not on costs. This can create the need for expensive complex joints, and result in higher total costs, compared to when joint design has been considered at the early phase.

## 1.2. Scope

Steel structures can have two generic categories: the frame and the truss. Due to transport requirements, steel structures are manufactured in multiple prefabricated elements with bolted connections. The frames are usually big structures, this results in the fact that frames have often many bolted connections. However, trusses can be manufactured as one prefabricated element if the dimensions are within the transport limitations. This means that welded connections can be used. Welded connections are less complex than bolted connections, because bolted connections have much more parameters. Besides the welds, assumptions need to be made about the type of bolts, number of bolts, the bolt configuration and the thickness of the end-plate. Therefore, the first step to consider is to investigate the inclusion of welded connections at an early stage of the design process. Due to limited time of this research, not all types of steel structures will be analysed. For this reason, my research will focus on trusses with welded connections that fit the transport dimensions.

In addition, trusses have many parameters that influence the geometric properties and consequently the number of joints. For example the span, the height, the number of truss-segments, truss-typology etc. All these parameters can give insight in the preferable way to optimise production costs instead of solely optimising minimum weight.

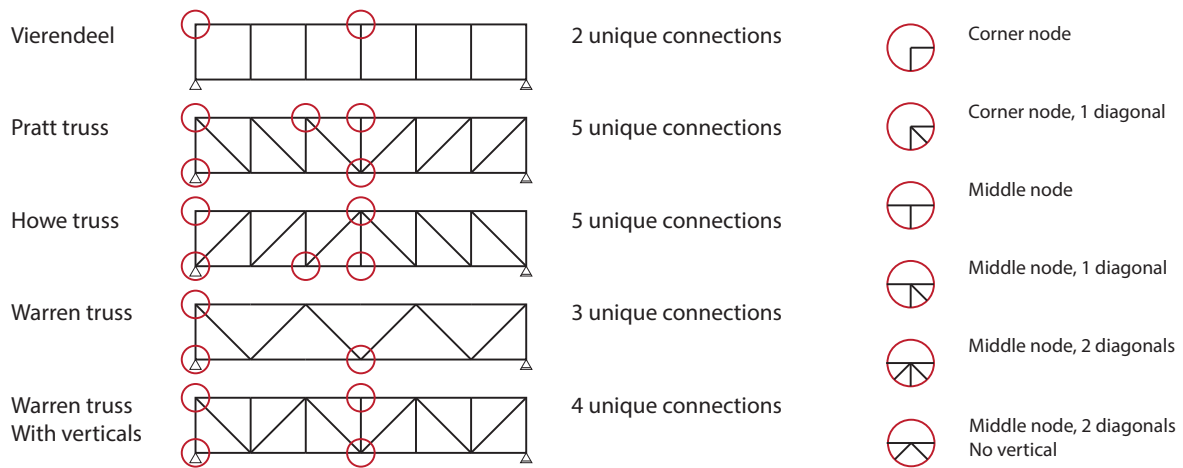


Figure 1.5: Number of unique connections for different truss typologies

| Connections<br>Joint assumptions | Truss<br>Welded<br>Hinged | Frame<br>Bolted<br>Rigid |
|----------------------------------|---------------------------|--------------------------|
|                                  |                           |                          |

Table 1.1: Comparison Truss &amp; Frame

In this research, prefabricated steel trusses with welded connections will be analysed. The types of trusses in the scope of this research are the Pratt and Warren truss. Both contain all joint configurations present in the five trusses in figure 1.5. Therefore, the methodology resulting from this research will be possible to apply to the other truss typologies.

In this research, cost-estimates are solely based on production costs. Cost for transport and site assembly will be excluded. Trusses will be designed as large as possible, within the transport limitations. The construction time is influenced by the amount of elements and not by their weight. However, the maximum size of these elements will always be limited by the transport dimensions. The goal of the cost-estimate is to give insight of how geometric variations in trusses influence production cost.

Only welded connections will be analysed in this research, with an emphasis on fillet welds. I-sections, Cold-formed Squared Hollow Sections, and Cold-formed Rectangular Hollow Sections, with steel grades of S235, S275, S355, will be analysed in this research. Higher steel grades, Circular Hollow Sections, and Hot-formed Hollow Sections are excluded because prices are not available on the online price-list, and can only be requested by an offer. This means that the offer-price will be dependent on the quantity purchased and the customer-supplier relationship. However, the methodology followed in this research will also apply to all steel grades and hollow sections when correct unit-price parameters for cost-estimation are provided.

### 1.3. Research question

In summary, taking into account joint design in the design process of trusses with welded connections can lead to complete optimised and cost-effective designs. This leads to the following question:

*"How can engineers optimise the production costs of steel trusses with welded connections?"*



## 1.4. Objective

The objective of this research is to optimise production costs of trusses with welded connections. Cost estimates created by the cost model will provide insight in cost preferences among variants.

## 1.5. Methodology

**Creating a cost model** A cost-model will be developed to optimise production costs of steel structures. The approach of this research will be as follows:

- Researching various available costing models.
- Analyzing price-lists provided by steel traders.
- Consulting steel contractors for advice and input.

Prices of material, sawing, and sandblasting in the cost-model are based on steel trader price-lists. These price-lists are available online. This makes it helpful for comparison purposes. However, these prices do not represent the prices that steel contractors pay. They usually receive discounts, based on quantities purchased and customer-supplier relationship. Hence, calculated costs in the cost-model can be overestimated compared to real-life situations.

**Creating an optimisation model** Instead of manually designing and comparing a set of trusses, a parametric model will be developed. This parametric model will increase data production and make it easy to analyse thousands of trusses. The influence of every parameter on the total production cost can be investigated. This can lead to more insight of the aspects influencing production costs.

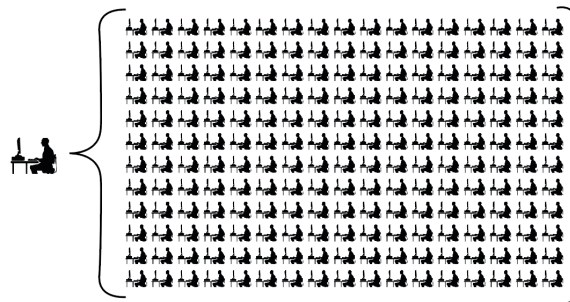


Figure 1.6: Increasing data production by using a parametric model

To achieve optimal cost-effective solutions, different parameters will be altered to reach the optimal solution. This parametric model will both analyse the main bearing structure and the detail analysis of each joint. An automated workflow will be set up to perform the following basic tasks:

- 1 Generate geometry
- 2 Evaluate forces in structure
- 3 Draw detailing
- 4 Analyse connections
- 5 Calculate prices
- 6 Store results

Various software packages have been analysed to perform each individual step in the optimisation workflow. For this research, a workflow will be set up using Grasshopper, Karamba3D, IDEA Statica Connection and additional C#-programming scripts.

Grasshopper is a visual programming plug-in for Rhinoceros, a 3D computer aided design application, in which parametric geometry can be created. Karamba3D is a plug-in for Grasshopper where structural analysis can be performed on the parametric geometry created in Grasshopper. IDEA Statica

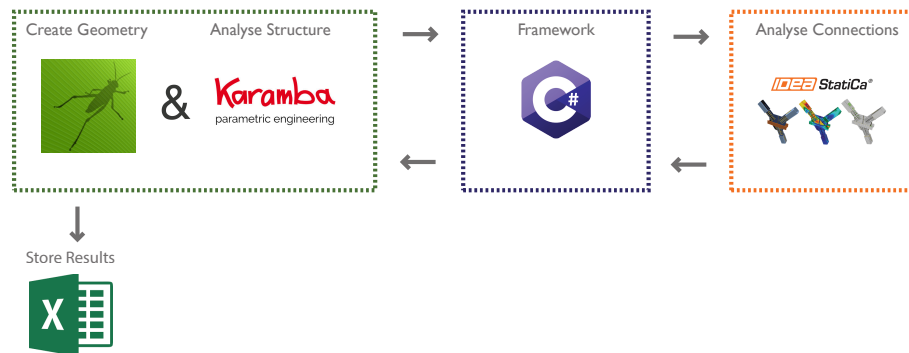


Figure 1.7: Selected Methodology for research

Connection is a finite element method based structural analysis package, designed to perform structural analysis of steel connections and joints.

This combination is selected because both Grasshopper and Karamba3D work in the same environment. This allows for a seamless data transfer and prevents the necessity of a script for communication between the programs. However, IDEA Statica Connection is a stand-alone software package written in the .NET-programming framework. The framework uses C#-programming language. Therefore, a communication link has to be set up in order to include IDEA in the automated workflow. This will be possible through an Application Programming Interface (API). An API is a set of definitions that can be used in scripts to automate workflows. The API works as an interface which makes it possible to access information and functionalities of the particular software package.

IDEA Statica Connections is selected in the optimization work-flow because it combines Euro-code's analytic calculations, with finite elements analysis. This will increase the accuracy of the results and allow the possibility to analyse unusual joints which cannot be analysed by solely using Euro-code's analytic calculation methods.

Grasshopper will be used to create a parametric wire-frame that will define the geometry of the steel structure. When the geometry is defined, supports and loads will be added. Based on the loads, cross-section profiles will be selected for the elements. This will be performed by using size optimisation available in Karamba3D. The next step will be drawing of the detailing. This will be performed in the Grasshopper environment by creating custom Grasshopper-components in C#-programming language. This custom component will also serve as a communication link to IDEA Statica Connection to send all needed information for the analysis of each joint. Afterwards, results of the analysis of the joints will be sent back to Grasshopper. The results will be used to generate a total price of the steel truss. With this optimisation model, data will be generated by "brutal force", evaluating every possible combination according the parameters ranges, and storing results in an Excel spreadsheet.

## 1.6. Report structure

The main research question will be broken down into different sub-questions. These sub-questions will be separately answered in the following chapters. Table 1.2 lists the questions which will be tackled.

In chapters 2 and 3, literature research will be performed. In chapter 4 the optimisation criteria for the model will be determined. These optimisation criteria, are costs and constructability aspects. In chapters 5 and 6, the assumptions and formulas needed for the structural analysis of the truss will be discussed. Chapter 7 defines how the optimisation criteria and the structural analysis methods will be used in the optimisation model. In chapter 8 analyses will be performed by the use of the optimisation model. Further possibilities of using the optimisation model will be discussed in chapter 9. In the last chapter the research question will be answered and conclusions will be drawn, followed by discussion and recommendations.

Table 1.2: Overview of research questions within the report structure

| Chapter | Sub-question  |
|---------|---|
| 2       | What is the current edge of technology in optimisation processes of steel trusses where joint design is included?                       |
| 2       | What is the current edge of technology in production processes of steel structures?   |
| 3       | What kind of cost-models for steel structures are used in the literature?   |
| 4       | What criteria determine the constructability of a truss?  |
| 4       | What is an appropriate cost-model to determine costs of trusses, what costs-components are included and how are these costs determined? |
| 5       | What assumptions need to be made for the structural analyses of the trusses?  |
| 6       | What determines the volume and strength of welds?   |
| 7       | How does the optimisation model work?   |
| 8       | How can cost-effective design be achieved within trusses?   |
| 8       | Will optimising on production costs lead to significant different results compared to optimising solely on weight?                      |
| 9       | What are further application possibilities of the methodology used in this research?  |





# 2

## State of the Art

### 2.1. Introduction

In this chapter will be discussed what the current state of the art is in the engineering of steel trusses where joint design is included. Furthermore, the state of the art of the production process of steel structures will be researched.

### 2.2. State of the Art in Engineering of steel trusses including joint design

**Analytic analysis of Hollow Section joints** In the literature several researches on the optimisation of hollow section steel trusses including joint design can be found. These optimisations are in most cases performed by the use of a MatLab optimisation script, where the joints of these trusses are calculated by the design codes found in NEN-EN 1993-1-8, chapter 7[7][8, p.11][9, p.20][4, p.55]. In this code the joints are checked on chord face failure, punching failure and brace failure. These calculations are based on experimental results. The reports where trusses are optimised including joint design emphasize the optimisation algorithm to perform optimisation.

**Weld volume calculation** Mela *et al.* [10] and Helminen [8, p.37] perform optimisation on cost-effectiveness of trusses. Noticeable in the optimisation process of these researches is how welding volume is determined. Here, the welding length is multiplied by the throat thickness to the power of two. In section 6.2, it will be explained why this approach is optimistic when analyzing welding volume. Furthermore these researches do not take in to consideration the adjusted welding length due to interference with other elements. How welding volume can exactly be calculated will be discussed in 4.2.1.

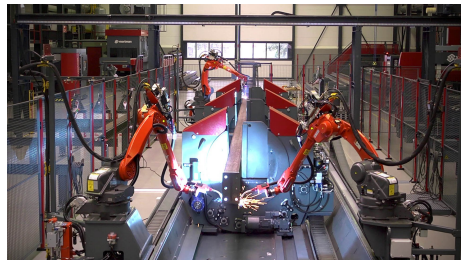
**Finite Element Method analysis** Jankowski [11] performed research on the analysis of a truss with cold-formed section and positive eccentricity nodes. In his analysis, the complete truss is modelled in a finite element analysis program, including the joints.

### 2.3. State of the Art in production of steel structures

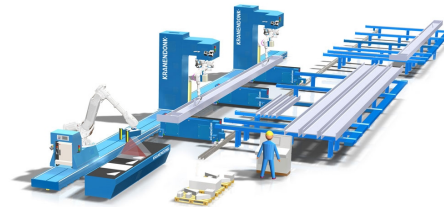
In the production industry of steel structures robots, are gradually being implemented. Currently, most steel contractors have a fully automated sawing and drilling line for both plates as beams[12][13][14], figure 2.2. But new robots make it also possible to fully assemble and weld plates and stiffeners to beams, figure 2.1. These new robots are the final piece in creating a fully automated production process and will create new possibilities.

In the current situation, assembling and welding is mostly performed manually. Here, standardization of elements and connections is preferred. Causing that workers perform the same task multiple times, which reduces the risk of human error. When robots will perform assembly and welding these

risks may be minimized. This can create possibilities of mass customizing the steel structures. Where, each beam member, each joint and each weld is optimised for their specific situation within the steel structure. In the case of automated assembling and welding this could create savings in the amount of material needed without increasing the risk of deficiencies during production.



(a) The Fabricator, Voortman Machinery



(b) Beam Stiffener Assembly line - Kranendonk

Figure 2.1: Automatic assembling and welding machines

Several companies in the Netherlands are gradually implementing these machines. Currently there are three companies that own an automated assembling and welding machine and one that owns a machine which welds automatically (BalkenLasMachine). In figure 2.4.

Beside, minor differences they all perform in equal manner. Bare sections are placed on the supply rack. Plates that need to be welded are placed on the table. A magnetic arm recognizes the plates with a camera recognition and picks it up. The plate is placed at the right location and tack welds are made. The magnetic arm will move to pick up the next plate and a welding robot arm will make the full end weld. The robot has a rotating element, this facilitates that plates can be welded at all sides of the section. When the section is finished it is placed at another rack.

Due to high investment-cost, these machines are only interesting for companies who have an annual production volume above 20.000 tons of steel [15].

Table 2.1: Advantages and Disadvantages of automated assembling and welding [15] [16, 27]

| Advantages   | Disadvantages                                       |
|--|---|
| Higher speed, arc on time 50% instead of 20%                                   | Complex joints cannot be made                       |
| Increase capacity, due to non-stop steel fabrication                           | Takes up a lot of space in factory                  |
| Reduce man-hours, due to full automation                                       | Physical limitation of welding torch, tight angles. |
| Eliminate errors, caused by human interference                                 | Max beam length                                     |
| Consistent high quality welds, due to highly accurate Panasonic welding robots | Still lot of 'Child diseases'                       |
|  | High investment costs                               |
|  | Currently not applicable for trusses                |

### Cost estimation of automated assembling and welding

Performing a production cost estimation with these robots can be challenging, because of a high level of indirect cost, which need to be considered, see figure 2.3. Indirect costs are for example: the investment cost (with interest), depreciation period, maintenance, operating and program costs. Each digital drawing needs to be checked by a programmer before it is sent to the machine.

The use of a robot to weld plates and stiffeners can have an impact on the design of steel structures. However, these robots will not be in the scope of this research project because they are not yet used for the production of trusses with welded connections, and because of the error-prone of the cost estimation assumption, due to the high percentage of indirect costs.



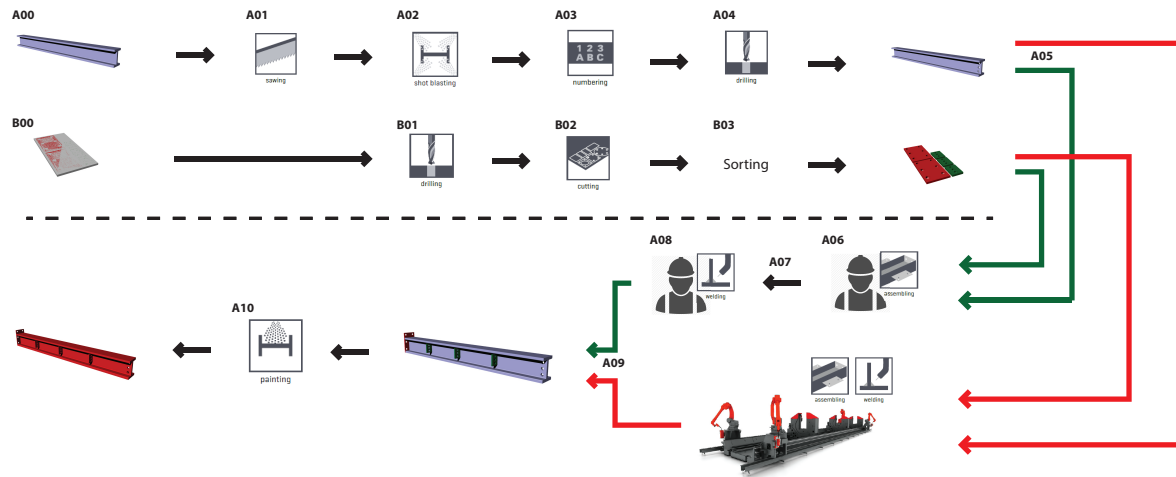


Figure 2.2: Fabrication process of beams for both manual and automated assembling and welding

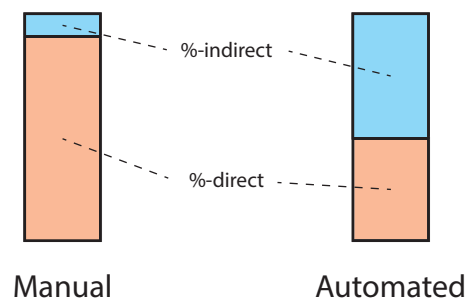


Figure 2.3: Percentage of indirect and direct costs for manual and automated fabrication



Figure 2.4: Automated assembling and welding machines in the Netherlands

## 2.4. Conclusion

Research on the optimisation of trusses where joints are included is limited. The research found is based on trusses with hollow sections, here empirical design methods of Eurocode are used to calculate the resistance of the joint. In other researches, a complete truss is modelled in a finite element program, which can create more accurate results. But it can be less suitable to use for parametric mass calculation. No research was found where software packages are combined to perform both structural analysis and detail engineering in one optimisation model.

In the production industry of steel structures, new robots are gradually being implemented. These are automated assembling and welding robots. These robots are currently limited in capabilities and cannot assemble and weld trusses. Besides, the high level of indirect costs of these robots. Costs like depreciation, programming, maintenance etc. makes it difficult to find trust-worthy values of how they influence the total production cost of a steel structure. For these reasons only manual assembling and welding will be considered in this research.

# 3

## Costs of Steel Structures

This chapter will discuss the factors which influence the costs of steel structures . These factors will be discussed briefly. In addition, a literature analysis of cost-models used for cost optimisations of steel structures will be presented.

### 3.1. Introduction

The primary goal of structural engineering is to design a structure that complies with the functional demands of the client and has sufficient structural performance. The structure should be sufficiently strong, stiff and stable. Consequently, sufficiently safe for the specific situation. When designing structures, safety factors are considered to generate extra safety in the structure . These factors lead to a higher use of material to provide this level of safety.

When the primary goal is fulfilled, the engineer can make decisions with a certain focus, depending on their preferences . Choices made within the engineering process can be based on either economic or safety considerations. Focusing on safety may lead to higher use of material which can increase the robustness of the structure. On the other hand focusing on economic considerations may lead to savings in material, which can create a lower building cost. But this may decrease the level of robustness of the structure. In figure 3.1 this balance between economic and safety considerations is displayed.

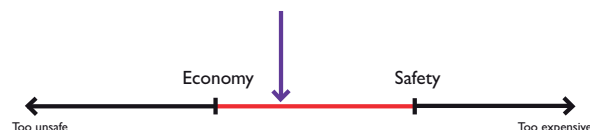


Figure 3.1: Engineers decision making

In current engineering, structures are generally not optimised on cost but on total weight[1]. Reducing weight and therefore the material to an absolute minimum will not necessarily lead to minimum cost design, due to the increased complexity of joints. In order for the engineer to come up with "the most cost-effective solution of making a safe enough structure" insight is required in the cost consequences during decision making in the design process. This insight can be acquired by the use of a cost-model during the design process. Design consideration can be based on costs.

#### Direct and indirect costs

Costs can be divided into two categories: direct costs and indirect costs. Direct costs are defined as costs which can be accurately be traced to a cost object with relatively little effort. Costs which cannot be accurately attributed to a specific cost objects are called indirect costs [17]. In table 3.1 below examples of direct and indirect cost are listed.

Table 3.1: Direct and Indirect costs

| Direct costs                       | Indirect costs                          |
|------------------------------------|---|
| Material (steel, welding material) | Power consumption                       |
| Labourer wages                     | Supervisors salary                      |
| Paint/Coating                      | Factory manager's salary                |
| Transport                          | Factory depreciation                    |
|                                    | Machine depreciation                    |
|                                    | Machine maintenance                     |
|                                    | Replacement of worn out drills and saws |

### Breakdown costs of steel structures

The cost of building a steel structure can be broken down into several components. The total cost is determined by the engineering, material needed, fabrication, fire protection, transport and construction at site [6]. However in this research the focus is to research how geometric variations affect direct costs. There are three components, which highly affect by the geometric properties of the prefabricated steel components of steel structures. These components are: fabrication, transport and site assembly, figure 3.2.

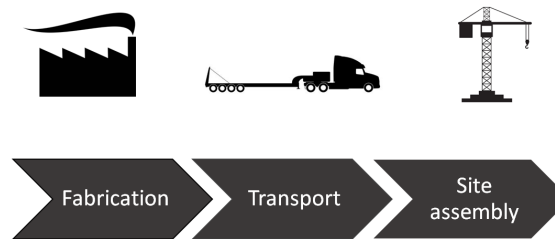


Figure 3.2: Cost dependent factors in steel structures that are design dependent

**Fabrication** Direct costs of fabrication are determined by the geometrical properties of the design. For example the number of elements and the number of connections that need to be made. In chapter 4.3, I will further elaborate on how to estimate these costs.

**Transport** Transport influences the maximum dimensions of prefabricated parts. Transport is either carried by trailers or by boat. In most cases, steel structures are transported by trailer, because most steel contractors have continuous permits to transport by trailer[12][14]. The maximum dimensions of this continuous permits are displayed in figure 3.3. Bigger dimensions are possible, but demand additional and possibly more strict permits. When steering towards cost-effective design, it could be beneficial to keep prefabricated elements within the transport dimensions of the continuous permit.

**Site assembly** Costs of site assembly are largely depended on the total building time. Longer building time leads to higher costs, because of overhead, equipment rental, possible permits etc. During site assembly, parts need to be hoisted to locations and assembled. Hoisting one small element is not much quicker than hoisting a large element[18, p.25]. Therefore, when steering towards cost-effective design, it could be beneficial to design prefabricated elements as large as possible, but constraint to transport dimensions.

### Influencers of costs

Costs of steel structures are greatly influenced by multiple factors. *"The cost associated with various connection types, material procurement and the value adding processes of detailing, fabrication, coating, transportation and erection are essentially process dependent."*[19]. Additionally costs are dominantly based on supply and demand [20]. In general low supply and high demand will lead to high prices and high supply and low demand leads to low prices. The status of supply and demand are time dependant. To create cost-effective designs of steel structures will therefore also be highly time dependant. The most cost-effective solution of today can be different within 5 years from now.



Figure 3.3: Maximum transport dimensions for road transport with a continues permit in the Netherlands

**Market** For the production of steel structures, there are three markets at present. The first market is the production of steel market, they process raw material to make steel and eventually process the steel product into steel sections. The second market is the traders who owns stocks of steel for selling it. The third market is the steel contractors who process the beams in order to make them connectable and usable in a steel structure. All of these markets influence prices based on competition, supply and demand. In table 3.2 lists the biggest companies representing these market in the Netherlands.

Table 3.2: Biggest Steel producers, Steel Section Producers and Steel contractors in the Netherlands

| Steel producer | Steel traders             | Steel contractor          |
|----------------|---------------------------|---------------------------|
| TATA Steel     | ArcelorMittal staalhandel | ASK Romein                |
| ArcelorMittal  | Deltastaal                | Hollandia structures      |
|                | Thyssenkrup               | Voortman Steel group      |
|                | Bressers Metaal           | Reijrink Staalconstructie |
|                | Geurt-Janssen             | Moeskops                  |
|                | Douma                     |                           |
|                | MCB                       |                           |

**Number of repetition** The number of repetition in a design influences the cost of the production process. It simulates serial production. Repetition will result in a learning process for the factory workers [21]. More repetition will generate more efficiency in the process, because there will be lower risk on errors. A higher efficiency in the process will lower average production time and consequently costs.

**Bulk Procurement of material** Prices of material vary dependent on the volume procured. Buying items in large volumes will allow procuring at lower price per unit. Buying small quantities will lead to the maximum price. How this price per unit varies with volume is different per company, since it is based on the customer-supplier relationship.

**Price of labour** Costs are predominantly determined by the amount of man-hours required. The amount of man-hours is then multiplied by the hourly rate. This rate is highly dependent on the prevailing economic conditions. Economic conditions vary over time and differ per country.



In figure 3.4 the hourly rate is displayed over time. A trend can be seen here that the hourly rate increases over time. This is mainly due to increasing economic prosperity since the second world war. Furthermore, countries with a higher economic prosperity have higher hourly rates.

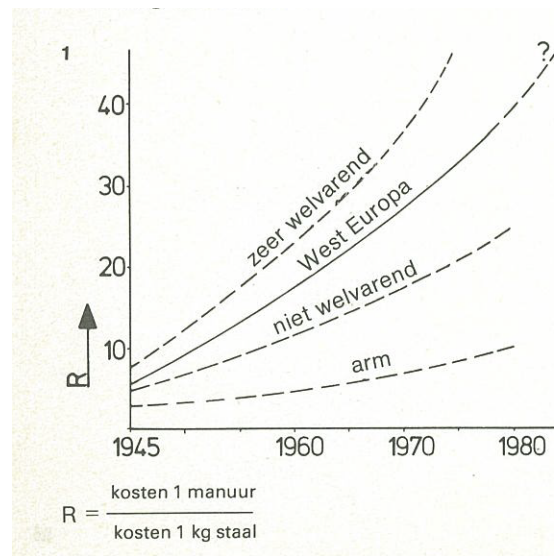


Figure 3.4: Trend relationship costs: man-hour vs material [22]

A metal welder with five years of experience will earn on average a monthly gross wage of €2200,- per month in the Netherlands[23]. Wages in Western Europe, North America & Japan are more or less the same. Eastern European countries have significantly lower wages. In the Czech republic a metal welder with five years of experience will earn on average a monthly gross wage of €880,- [23]. Developing countries have the lowest wages. For example a metal welder with five years of experience will earn on average a gross wage of €330,- per month [23].

Differences in wages are unfairly distributed among countries with different economic prosperity's. Wages in the Netherlands for metal welders are on average 700% higher than in China. A metal welder in the Netherlands earns 700% of what a Chinese metal welder earn. For material, the price of steel in the Netherlands is only 120% the price of steel in China [24]. When comparing this distribution in wages with the distribution of material, the price of material can be assumed constant. Higher wages influence the ratio between labour and material. This ratio implies that cost-effective structures will be different per country. In highly prosperous countries it can be more economical to use more material in a steel structure to prevent extra labour cost.

**Execution class** Costs of steel structures are dependent on the execution class. NEN-EN 1090-2 prescribes four different execution classes, that run from EXC1 to EXC4. Where EXC4 has the most strict requirements. The execution class can be applied to the complete structure, a part of the structure or a specific detail. The execution class has influence on the quality level of welds needs to be applied. These are noted with the symbols B, C and D according to NEN-EN-ISO 5817. Where quality level B has the highest level of requirements for the welded connection.

In this research, execution class 2 will be assumed, for the following reasons. The consequence class of the structure in the case-study of this research is assumed to be CC2. In the case-study, only static loading is present in the structure. Therefore the service-category is SC1. In this research steel-grades S235, S275 and S355 are considered. Steel grades below S355 possess production category 1 and S355 or higher contain production category 2. However they both end in EXC2. In this case, weld quality C is required.

Table 3.3: Execution class based on Consequence Class, Service Category and Production Category

| Consequence Class   |     | CC1  |      | CC2  |      | CC3  |      |
|---------------------|-----|------|------|------|------|------|------|
| Service Category    |     | SC1  | SC2  | SC1  | SC2  | SC1  | SC2  |
| Production Category | PC1 | EXC1 | EXC2 | EXC2 | EXC3 | EXC3 | EXC3 |
|                     | PC2 | EXC2 | EXC2 | EXC2 | EXC3 | EXC3 | EXC4 |

### 3.2. Cost models of skeletal steel structures

In this section, several methods for making cost-estimations are discussed. These methods have been found in the literature. Most cost models are made to calculate the cost of a steel frame structure. A cost model is used to quantify the financial consequences of the used joint typology. The overall conclusion of the literature is that using semi-rigid connections is the most economical solution compared to rigid or hinged connections. The methods discussed are arranged by the amount of complexity of the method. Starting from least complex up to most complex.

#### 3.2.1. Method 1: Weight concept

In the steel structure industry, cost estimations are mostly made based on total weight. Total weight is multiplied by the average price per kilogram of steel [25]. In the cost estimation, a percentage is added in order to include the cost of the joints. This percentage differs based on the complexity of the joints, but can be in the range of 10 % for simple joints up to 50 % for complex joints, like fully fixed moment-resisting joints.

$$\text{€} = kg * \text{€}_{kg,steel} * (100\% + \%_{additional}) \quad (3.1)$$

Where the additional percentage for the cost of joints is kept constant. This cost-model can stimulate designing a slender steel structure, because the model suggests that a lower total weight will generate a lower total price. This suggestion can be misleading. It can ultimately cause that complex joints are needed to provide sufficient structural capacity of the joint within the slender structure. Due to the plates, stiffeners and haunches these complex joints are costly. This can cause that a design with a low total weight can have a higher total cost.

#### 3.2.2. Method 2: Percentage of beam weight based on rotational capacity joint

The second method is a calculation method which goes a step further in calculating the costs. In this paragraph two models are presented one uses the rotational stiffness of bolted connections to calculate the costs. The other uses the fixity factor of bolted connections, see figure 3.3. In both models costs are not expressed as a price, but as an amount of kilograms. With the used variable (rotational stiffness or fixity factor), an estimate is made for the additional percentage that covers the costs of the connection. The result of this cost-method is a total weight. This total weight can be multiplied by a price per kilo to generate the total price.

##### Based on rotational stiffness $[S_i]$

Xu and Grierson [26] use the rotational stiffness of a joint to calculate the cost of the joint. The formula used is displayed below. This method to make a cost estimate for frames with semi-rigid connections has been used multiple times in the literature [27] [28].

$$Z(x) = \sum_{i=1}^{nm} W_i A_i \sum_{j=1}^{nbm} \sum_{l=1}^2 (\beta_{ij} R_{ij} + \beta_{ij}^0) + \sum_{i=1}^{nco} (\beta_i R_i + \beta_i^0) \quad (3.2)$$

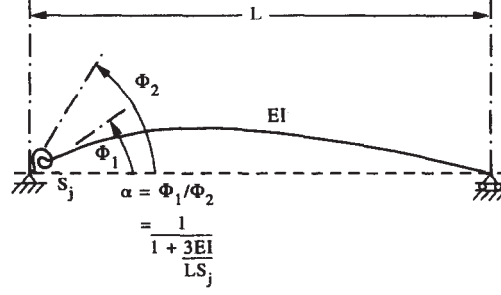


Figure 3.5: Fixity factor[29]

Table 3.4: Symbols from equation 3.2

|                             |                                 |                             |
|-----------------------------|---------------------------------|-----------------------------|
| $nm$                        | Total number of members         |                             |
| $nbm$                       | Total number of beams           |                             |
| $nco$                       | Total number of columns         |                             |
| $W_i$                       | Weight coefficient              |                             |
| $A_i$                       | Cross-sectional area            |                             |
| $R_i \& R_{ij}$             | Connection rotational stiffness |                             |
| $S_i$                       | Estimated Rotational stiffness  |                             |
| $\beta_{ij}^0 \& \beta_i^0$ | Cost of pinned ends             | $= 0.125W_iA_i$             |
| $\beta_{ij} \& \beta_i$     | Cost semi-rigid ends            | $= \frac{0.225W_iA_i}{S_i}$ |

In this model a pinned connection will cost 12.5% of the weight of the attached member. The first part of this cost formula 3.2 represents the weight of each element, the second part with the two summations describes cost of hinged connections. In table 3.4 the 12.5% for pinned joints is seen. The third part represents the additional cost for joints that possess rotational stiffness. This rotational stiffness is constrained to be in the range of 226 kNm/rad and 568.000 kNm/rad. The cost estimate of semi-rigid of this model first divided by the estimated rotational stiffness ( $S_j$ ) and then multiplied with the connection rotational stiffness ( $R_i$ ). The multiplication and division by probably an identical number makes this formula seem self-contradictory.

#### Based on Fixity factor [ $\alpha$ ]

The next model is based on the fixity factor. "The fixity factor  $\alpha$  defines the stiffness of the connection relative to the attached beam and is perhaps the most powerful and important concept for the analysis of frames with semi rigid joints. It relates quite closely to how the structure will behave in the context of the connection, far more so than the absolute value of  $S_j$ ." [29]. The fixity factor lies in a range from 0 to 1. A fixity factor of 0 resembles a fully rigid connection, a fixity factor of 1 resembles a hinged connection.

Simões [29] bases his cost model on the following statement: "Published data suggests that the cost of a steel member with IPE section is increased by 20% if it has pin-jointed end connections, and by 60% if its end-connections are bolted or welded." Therefore, the cost of a beam including connections should lie between 1.2 and 1.6. Since the relationship between costs and stiffness of a particular joint is non-linear, a quadratic formula is set up with a set of V constants [29, p.534].

$$Z_i = W_i A_1 + \sum_{k=1,2} (V_{ik}^0 + V_{ik}^1 \alpha_{ik}^1 + V_{ik}^2 \alpha_{ik}^2) \quad (3.3)$$

Using the boundary condition of the costs of pin joint connections (20%) and bolted or welded connections (60%) will result in the formula found beneath.

$$Z_i = W_i A_1 + \sum_{k=1,2} (0.2W_i A_i - 0.8W_{ik} A_{ik} \alpha_{ik}^2 - 1.6W_{ik} A_{ik} \alpha_{ik}^2) \quad (3.4)$$

#### 3.2.3. Method 3: Weld volume method

In this method the amount of welding material is used to make a cost estimate. Like method 2, this cost estimate is not expressed in a price, but in kilograms. To convert labour into the cost estimation,

the factor  $f$  is used. This factor defines the ratio between 1 kg welding material (including labour and anti-corrosion protection and 1 kg of steel (including labour). The factor  $f$  is dependent on the country, automation grade of the company and labour costs [22]. Furthermore, a constant for the welding is defined. This constant converts the height of the haunch to an estimate of the total welding length. Steenhuis *et al.* [30] assumes this factor to be 4.3.

$$kg_{total} = kg_{material} + kg_{welding} \quad (3.5)$$

$$kg_{material} = A * L_{beam} * \rho \quad (3.6)$$

$$kg_{welding} = a^2 * 4.3 * h_{haunch} * f \quad (3.7)$$

In table 3.5 a cost estimate is made for a rigid joint and a semi-rigid joint. In the table the semi-rigid joint possesses bigger beam cross-section and a smaller haunch height.

Table 3.5: Calculation example welding volume method [30, p.10]

| Cost category   | Rigid joint                                 | Semi-rigid joint                            | Savings when semi-rigid joints are used |
|---|---|---|---|
| Column material (kg steel)<br>$A * l_c * \rho$                  | $171 * 10^{-4} * 3.5 * 7850 = 470kg$        | $198 * 10^{-4} * 3.5 * 7850 = 544kg$        | $-74kg$                                 |
| Weld material haunch (kg steel)<br>$a^2 * 4.3 * h_h * \rho * f$ | $0.012^2 * 4.3 * 0.75 * 7850 * 100 = 364kg$ | $0.012^2 * 4.3 * 0.35 * 7850 * 100 = 170kg$ | $+194kg$                                |
| <b>Total</b>  |   |   | $+120kg$                                |

### Welding beads

Welds with a throat thickness bigger than 6 mm will consists of several weld beads. Scherrenberg [31] applied this concept for the cost calculation of steel portals. The number of weld beads per throat thickness can be found in table 3.6. For the cost calculation of welding, which can be found in equation 3.8, Scherrenberg [31] assumes a welding speed of 4 meter per hour for one weld bead.

$$\epsilon_{welding} = Length_{weld} * \#_{layers} * Speed_{welding} * Hourlyrate_{labour} \quad (3.8)$$

Table 3.6: Number of welding beads per throat thickness

| Throat thickness [a] | Number of weld beads | $a^2$              | $a^2$ per weld bead |
|----------------------|----------------------|--------------------|---------------------|
| 6 mm                 | 1                    | $36 \text{ mm}^2$  | $36 \text{ mm}^2$   |
| 10 mm                | 3                    | $100 \text{ mm}^2$ | $33 \text{ mm}^2$   |
| 12 mm                | 6                    | $144 \text{ mm}^2$ | $24 \text{ mm}^2$   |
| 14 mm                | 9                    | $196 \text{ mm}^2$ | $21.8 \text{ mm}^2$ |
| 16 mm                | 13                   | $256 \text{ mm}^2$ | $19.7 \text{ mm}^2$ |
| 18 mm                | 18                   | $324 \text{ mm}^2$ | $18 \text{ mm}^2$   |

In table 3.6 two columns have been added. Here the total area and the area per weld bead are displayed. Form the right table can be concluded that the area per weld bead decreases when the amount of welding layers increases.

In figure 3.6, the welding layers are illustrated. It can be clearly seen that the width of a weld bead increases and the height decreases when multiple layers are being applied.

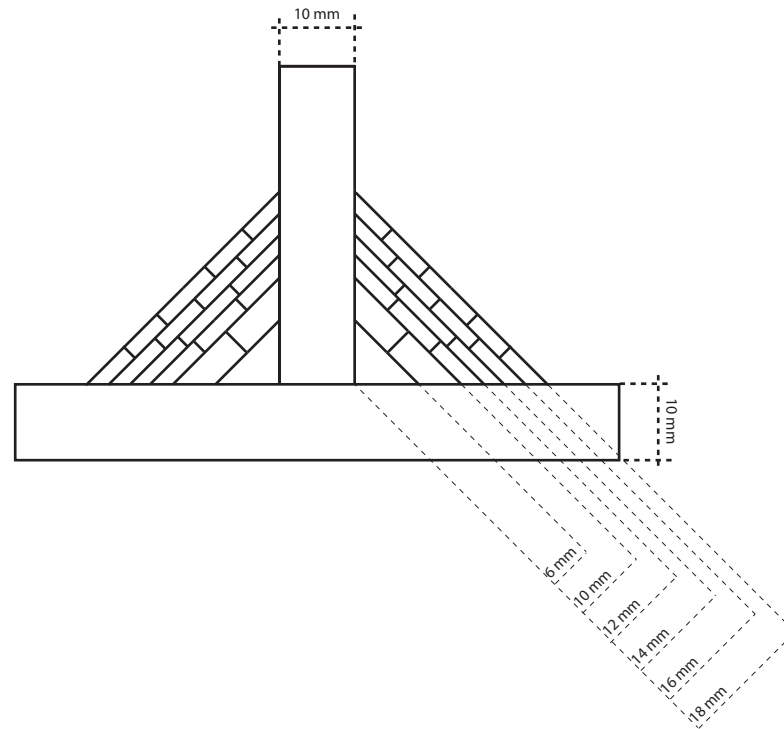


Figure 3.6: Welding beads [on scale]

#### 3.2.4. Method 4: Activity Based Costing

Activity based costing is based on the concept that not products but activities determine the costs. In activity based costing the cost per activity are determined. The sum of the costs of all activities required, generates the total cost. Since in this cost-model only activities are considered, it focuses on direct costs. Indirect costs are not taken into account. Therefore it can be concluded that this model is only applicable for processes where direct costs are a dominant contributor to total costs.

In the building industry, margins are relatively low, because competition in winning tenders is fierce, and this often results in bidding a too low price in order to win the tender [32]. The Activity Based Costing method is therefore a good method to estimate costs. In this paragraph, two models are discussed where cost estimations is based on the Activity Based Costing method.

##### Multistage production costs

In this method performed by Bel Hadj Ali *et al.* [33] [34], multiple stages in the process up to completion are considered:

- Material costs
- Fabrication costs
- Erection costs
- Foundation costs

The production costs are a summation of the superstructure costs ( $C_S$ ) and the foundation costs ( $C_F$ ).

$$C = C_S + C_F \quad (3.9)$$

Here the superstructure costs can be split into the material, fabrication and erection costs.

$$C_S = C_{Mat} + C_{Fab} + C_{Ere} \quad (3.10)$$

Material costs are based on information gathered from suppliers of steel materials and components. The fabrication costs are calculated by the time needed to fabricate the structural elements. This

time needed is converted into a price by applying a cost per hour of workshop labour. The following equation is used to calculate the amount of time required. Here two variables can be found,  $x$  is the number of holes and  $n$  is the number of identical parts. It can be noted that  $t_1$  and  $t_5$ , which stands for preparation and match marking, decreases when repetition takes place.

$$C_{Fab} = labour_{workshop} * T_{(n,x)} \quad (3.11)$$

$$T_{(n,x)} = \frac{t_1+t_5}{n} + t_3 * x + (t_2 + t_3) \quad (3.12)$$

In table 3.7 the used values in time are stated. Note that in the execution of holes no variation is made for different hole diameters. Furthermore, in the handling processes there is not a consistent time difference between manual and mechanical handling. How welding is incorporated into the model is not specified.

Table 3.7: Average time required for different elementary manufacturing operations [33]

| Timing | Category      | Description  | Manual/Automated           | Average value   |
|--------|---------------|--|----------------------------|-----------------|
| $t_1$  | Preparation   | Transfer and validation of program, changing of tools,.. | n.a.                       | 200s            |
| $t_2$  | Handling      | Part setting and clamping on the machine table           | Manual                     | 40s             |
|        |               |  | Mechanical (crane bracket) | 20s             |
| $t_3$  | Fabrication   | Execution of holes                                       | Drilling                   | 0.5-1 mm/s/hole |
|        |               |  | Punching                   | 4s/hole         |
| $t_4$  | Handling      | Cleaning and setting of part on a palette                | Manual                     | 10s             |
|        |               |  | Mechanical (crane bracket) | 55s             |
| $t_5$  | Match-Marking | Chalk marking of the last part                           | n.a.                       | 20s             |

The erection cost is calculated by multiplying the total mass of the structure with a cost constant. This cost constant includes unload, lift, place and connect of the components. The method of only using the total weight can be justified since no welds have to be done on site for all the connections and column bases considered in this study.

$$C_{Ere} = k_{Ere} M_{Str} \quad (3.13)$$

The foundation costs are calculated by multiplying the excavated volume by a cost constant. This is summed up with the multiplication of the foundation volume by a cost constant.

$$C_F = k_{Ex} V_{Ex} + k_F V_F \quad (3.14)$$

### Bouwen met Staal

In 2012 Bouwen met Staal published [35] a model to make a cost-estimate for a simple steel structure. The cost is calculated by using four main categories:

- Material
- Fabrication
- Painting/Coating
- Site Assembly

**Material** The costs of materials are determined by the price list of suppliers. In this model a net cost price for material is determined by including a surtax for scrap metal and a discount per ton. This discount is dependent on the amount of steel which is procured. This is also the case for tubes. For tubes not a fixed rate per ton is used but a percentage. When S355 is used an additional surtax is calculated. This surtax is lowered when the order is above 5000 kg.

In the formulas 3.15, 3.16 and 3.17 multiplication by a value of 1 or 0 can be found. These numbers come from a presence matrix that determines which discounts and surtaxes are applicable for a certain cross-section.



Net costs for S355 with an order of more than 5000kg:

$$\epsilon_{net} = (\epsilon_{Gross} + \frac{Surtax_{Scrap} p_{erton}}{1000} * 1 - \frac{Discount p_{erton}}{1000} * 1 + \frac{Additional price_{S355(>5000)}}{1000} * 1) * (100\% - \%_{Discount tubes} * 0) \quad (3.15)$$

Net costs for S355 with an order of less than 5000kg:

$$\epsilon_{net} = (\epsilon_{Gross} + \frac{Surtax_{Scrap} p_{erton}}{1000} * 1 - \frac{Discount p_{erton}}{1000} * 1 + \frac{Additional price_{S355(<5000)}}{1000} * 1) * (100\% - \%_{Discount tubes} * 0) \quad (3.16)$$

Net costs for S235:

$$\epsilon_{net} = (\epsilon_{Gross} + \frac{Surtax_{Scrap} p_{erton}}{1000} * 1 - \frac{Discount p_{erton}}{1000} * 1) * (100\% - \%_{Discount tubes} * 0) \quad (3.17)$$

**Fabrication** This part represents all activities starting from receiving the bear beams up to delivery at the building site, with painting and coating as the exemption. Considered processes are:

- Fabrication of connections
- Modification to the steel sections
- Detailing and drawing
- Transport

For the fabrication of connections and modification of steel sections, tables are defined that display the amount of man-hour. The amount of man-hour is dependent on the weight per meter of the to be connected beam. In figure 3.7 the amounts of man-hour of five different connections can be found. Most of these connections show a linear relationship after a certain threshold level. The base-plate is the only connection that has a non-linear relation. When the total amount of man-hours is defined, they are multiplied by an hourly rate which includes the payment of the employee and the factory overhead costs. This method is debatable since the span of the beam is not considered in the estimation of man-hour. On the other hand, the beam is selected according to the maximum bending moment. Therefore there is a relationship between specific bending moment and types of beams.

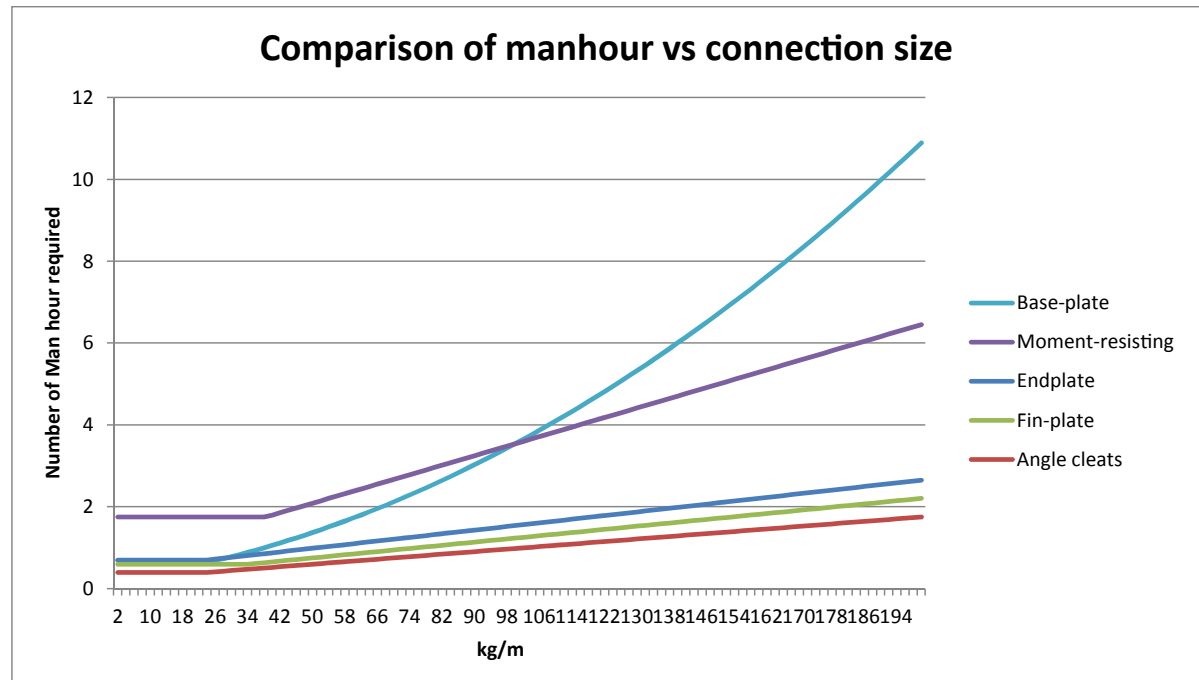


Figure 3.7: Comparison of man-hour vs connection size

For detailing a certain €/kg can be specified. For transport there is calculation key dependent on the distance to the building site and the maximum truck load in tons.

**Painting/Coating** For painting, a system of 1,2 or 3 layers can be chosen, with prices of €6, –, €10, – or €16, – per  $m^2$  respectively.

For fire-resistant coating there are 3 different types specified depending on the  $T_{critical}$  of the element. Elements with a lower  $T_{critical}$  need a thicker layer of coating, this will result in a higher price per  $m^2$ .

**Site Assembly** The cost for site assembly is taken into account in this model as well. Input for the cost calculation is the amount of building layers, workers, and equipment. Based on the number of days needed for assembly, a price is generated.

This may be a too coarse approach, since the speed of site assembly is very much dependent on weather conditions. In case of bad weather (cold, rainy, windy) the speed will be greatly influenced.

#### Feature-based Costing method for Skeletal Steel structures

Haapio [36] developed a method which gives the designer detailed information of the costs of manufacturing, transport and erecting of a steel structure. Typical to this method is the inclusion of non-productive time in the processes. Besides productive time, there is non-productive time as well. It is the preparation works which are required to flawlessly execute the process.

### 3.3. Cost models for welding

Jármai and Farkas [37] made a model to estimate the cost for the manufacturing of welded THQ beams or stiffened plates. In the model several welding technologies and several types of welding are considered. These can be found in table B.2 and B.3.

$$K = K_M + K_f = \kappa_m \rho V + \kappa_f \sum_i T_i \quad (3.18)$$

In this model the cost ratio  $\kappa_f/\kappa_m$  is introduced. With  $\kappa_m = 0.5 - 1\$/kg$  and  $\kappa_f = 0 - 1\$/min$ . A  $\kappa_f/\kappa_m = 2.0$  ratio means very high labour costs. 1.5 and 1.0 are average labour costs. And 0.5 means the labour costs of developing countries.

$$\frac{K}{\kappa_m} = \rho V + \frac{\kappa_f}{\kappa_m} (T_1 + T_2 + T_2 + T_3 + T_4 + T_5 + T_6 + T_7) \quad (3.19)$$

"Difficulty factors" are introduced in this model to cope up with uncertainties. With the difficulty factor, a differentiation for down-hand and in positional welding are made. Because down-hand welding is physically less intensive, higher average welding speeds are found. For the difficulty factor, values of 1, 2 or 3 are used.

In table 3.8 the calculation keys per activity are defined.  $T_1$  is time needed for preparation prior to welding.  $T_2 + T_3$  is the time needed for the actual welding. The number 1.3 comes from a simplification of the separate  $T_2$  &  $T_3$  [37, p.117].

Only longitudinal welds are considered in this report. When end-plates are welded to a beam, a weld along the radius of the beam's flange web connection should also be made. Further research should be done to find trustworthy values for the welding speeds of these quarter circular parts.

Table 3.8: Time calculation per activity

|                                   |   |   |
|-----------------------------------|---|---|
| Fabrication times for welding     | $T_1 = C_1 \theta_d \sqrt{\kappa \rho V}$                             | $C_1 = 1$<br>$\theta_d = \text{difficulty factor}$<br>$\kappa = \text{number of structural elements assembled}$   |
| Fabrication times for welding     | $T_2 + T_3 = 1.3 \sum C_{2i} a_{wi}^n L_{wi}$                         | $C_{2i} = \text{constant for welding technology}$<br>$a_{wi}^n = \text{throat thickness weld}$  |
| Time of flattening plates         | $T_4 = \theta_{de} (\alpha_e + b_e t^3 + \frac{1}{\alpha_e t^4}) A_p$ | $\alpha_e = 9.2 * 10^{-4} \frac{\text{min}}{\text{mm}^2}$<br>$b_e = 4.15 * 10^{-7} \frac{\text{min}}{\text{mm}^5}$<br>$\theta_{de} = \text{difficulty parameter}$<br>$t = \text{plate thickness}$<br>$A_p = \text{area of the plate}$ |
| Surface preparation time          | $T_5 = \theta_{de} \alpha_{sp} A_s$                                   | $\alpha_{sp} = 3 * 10^{-6} \frac{\text{min}}{\text{mm}^2}$<br>$\theta_{de} = \text{difficulty parameter}$<br>$A_s = \text{surface area}$  |
| Painting time                     | $T_6 = \theta_{de} (\alpha_{gc} + \alpha_{tc}) A_s$                   | $\theta_{de} = \text{difficulty parameter}$<br>$\alpha_{gc} = 3 * 10^{-6} \frac{\text{min}}{\text{mm}^2}$<br>$\alpha_{tc} = 4.15 * 10^{-6} \frac{\text{min}}{\text{mm}^2}$  |
| Cutting and edging grinding times | $T_7 = \sum_i C_7 t_i^n L_{ci}$                                       | $L_{ci} = \text{cutting length}$<br>$t_i = \text{thickness}$  |

### 3.4. Reverse engineering

An effective method to analyse the costs of steel structures is finding a set of completed project where the final price is known. By reverse engineering, costs of connections can be extracted. For this method the market should be open to share the project documents.

These documents are considered as sensitive information, because they reveal the margins companies use for profit calculation. The change of acquiring this information is expected to be low.

Another downside to reverse engineering is that you don't know the amount of margin amount of the final price. The contractor could have made a lot of profit or losses on the project.

### 3.5. Discussion & Conclusion

In this chapter a set of methods for estimating costs are discussed. The methods differ in the time needed to make an estimate which is accompanied with a certain precision and therefore reliability. In general more elaborate costing models will generate more precise cost estimates, but they take longer time.

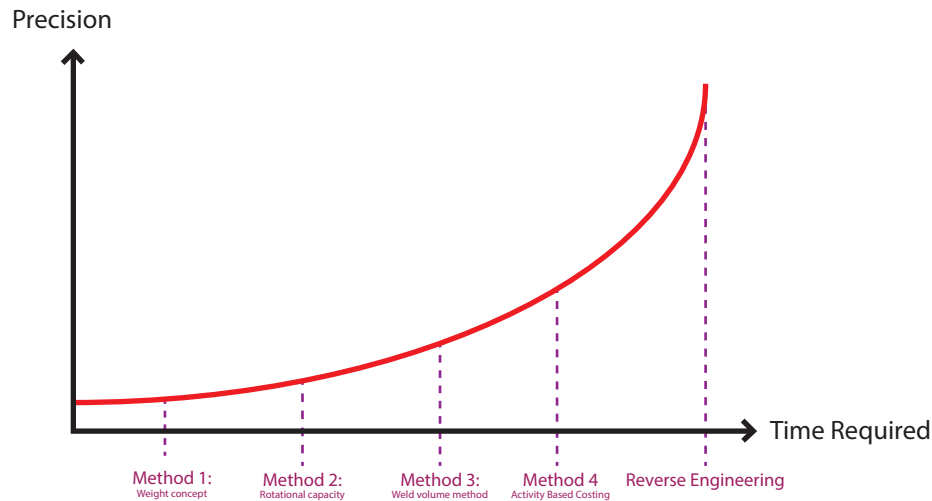


Figure 3.8: Reliability versus time per cost-estimation method

To make a good estimate of cost, it is important to have a certain level of detail in the model. The cost-model needs to be generic in order to be applicable for multiple cost calculations. The activity based cost models provide the needed level of detail. However in examples discussed a too elaborate cost estimate is made. Factors which are very project-dependent, as transport and erection are included. Also factors which are very factory-dependant, as non-productive time per production process are included. The results can be untrustworthy when a general application is used. In conclusion, there is a certain balance between making a cost model which is too elaborate and therefore too specific, and a too general model and therefore untrustworthy model.

In the cost model of this research, I will only focus on the direct costs of the production of pre-fabricated steel trusses. In this cost-model the costs for every needed process in the production are determined. Per process, one unit price is used. This will help avoiding over-complication of the cost model.

The size of these elements will be determined by the maximum transport dimensions. Transport, erection and indirect costs will be excluded in this model, because they are project and company dependent components.



# 4

## Optimisation criteria of Trusses

### 4.1. Introduction

The optimal variant in an optimisation process is dependent on the optimization criteria. In the optimisation of trusses aspects, as constructability and total production cost will be used to find optimal variants. In this chapter, I will investigate the leading constructability criteria, and how the total production cost will be assessed.

### 4.2. Constructability

In this section will discuss how trusses constructability can be analysed, and how this will affect cost-effectiveness.

#### 4.2.1. Production risks caused by design

To achieve cost-effective design in steel trusses, it is important to design the truss in such a way that production risks are avoided. When a design is created in such a way that elements need to be an exact fit, production-risks increases. In reality sizes of elements deviate because of tolerances, resulting in elements being longer or shorter than expected. When this is the case, measures should be made. In most cases, this will cause extra unwanted expenses.

Within trusses, the diagonals are the elements in the design most prone to geometric deviation[13][14][12]. This is especially the case when the joint is an overlap joint where the diagonals have double miter ends, as displayed in figure 4.1. In figure 4.2 a flow of events is displayed. These events can happen when a diagonal has deviating geometry. If these events need to take place, fabrication time of the truss will be longer. This causes increased costs. However according to ISO5817 reference 617 some deficiency is allowed. The code provides limits for the deficiency in millimeters. This limit is dependent on the quality level, the plate thickness and the throat-thickness.

#### Strategies on preventing double miter connections in diagonals

Cost-effectiveness in the design of steel trusses can be achieved by minimizing the risk of deficiencies. This can be done by designing the truss in such a manner that the joints will be gap joints, where diagonals contain only single miter ends. In figure 4.1 two strategies are displayed for achieving single miter ends in the diagonals. The first strategy is increasing the section height of the chord. This strategy causes a big increase in total weight. The second strategy is introducing eccentricities in the nodes. This will introduce bending moments. Bigger sections will be needed to carry the additional load. In this case achieving a single miter connection works in two ways, because of the eccentricity and the increased section height. In the third strategy, the overall geometry can be changed in such a way that diagonals contain small angles and therefore are more likely to produce a single miter connection. A fourth strategy is assuming a larger buckling length for the chords. This strategy is comparable with the second, but calculating with a larger buckling length could cause that less buckling supports are needed in the final design. This could result in less material needed, therefore lower costs.



|  | Typical<br><b>Pratt-truss</b><br>Joint | Typical<br><b>Warren-truss</b><br>Joint |
|--|--|---|
| <b>Design</b><br>Overlap Joint                       |  |   |
| <b>Possible reality</b><br>Overlap Joint             |  |   |
| <b>Alternative 1:</b><br>Increase chord<br>Gap Joint |  |   |
| <b>Alternative 2:</b><br>Eccentricity<br>Gap Joint   |  |   |

Figure 4.1: Risks and Measures for overlap joints of trusses

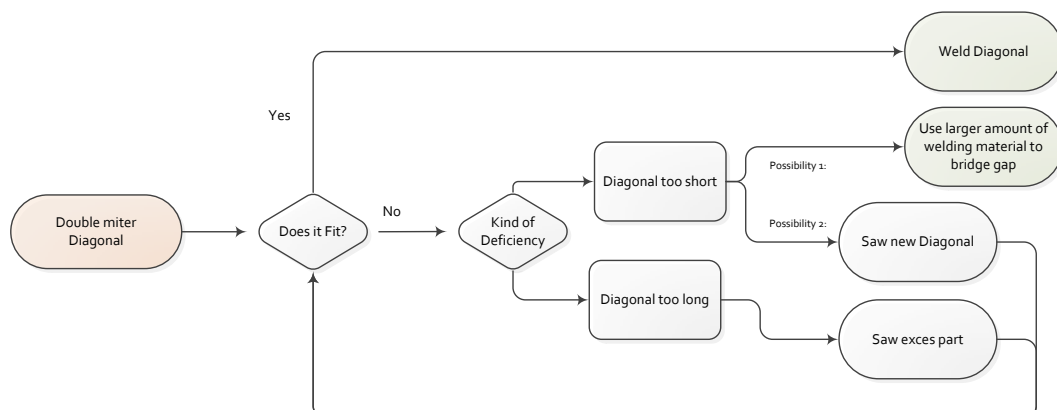


Figure 4.2: Decision making in case of deviating diagonal

### Expressing risk into cost model

Including the risk of geometric deviation of elements in the cost-model is ambitious, wrong assumptions for cost estimations can be easily made. Therefore taking into account this risk in terms of a certain additional price will not be used in the cost-model of this research. However, this cost-model will give insight in what the price-differences will be of a optimised truss overlap joints and a optimised truss with gap-joints. The truss with gap-joints will probably have a higher price, because of a higher material consumption. This price difference between the two trusses can give insight on the risk/reward of using overlap joints in a truss structure. This can lead to a conclusion whether or not it will be desired to exclude risk of geometric deviation.

### Analysis on double and single miter diagonals

The problem whether a connection has a double or single miter end can be solved mathematically. Here, the height of the diagonal is projected on the edge of the vertical (Post) and the horizontal (Chord), see figure 4.5. All parameters needed to solve the problem are listed in table 4.1. To accommodate all double miter connection situations possible in the scope of this research, there is also an angle of inclination for the vertical ( $\phi$ ) and an eccentricity ( $\varepsilon$ ) included in the list. The mathematical model produces two lines. If one of these two has a value of zero, the connection is single miter, see table 4.2. The complete derivation can be found in appendix A.

Table 4.1: Parameters

| Parameter              | Symbol        | Range                            |
|------------------------|---------------|----------------------------------|
| Half Height Vertical   | $a$           | $0 < a$                          |
| Half Height Horizontal | $b$           | $0 < b$                          |
| Half Height Diagonal   | $h$           | $0 < h$                          |
| Angle of $h$           | $\theta$      | $0^\circ < \theta < 90^\circ$    |
| Angle of $a$           | $\phi$        | $90^\circ \leq \phi < 180^\circ$ |
| Eccentricity           | $\varepsilon$ | $0 < \varepsilon$                |

Table 4.2: Decision tree for determining length of horizontal and diagonal segment

| Position Weld  | First decision             | Second decision | Length   |
|--|----------------------------|-----------------|--|
| Horizontal segment   | If $P \geq A$              |                 | $l = 2 \left  \frac{h}{\sin \theta} \right $   |
| $\vec{x} = \begin{bmatrix} Q \\ b \end{bmatrix}, \vec{y} = \begin{bmatrix} P \\ b \end{bmatrix}, \vec{z} = \begin{bmatrix} A \\ b \end{bmatrix}$ | If $P < A$                 | If $Q > A$      | $l = \sqrt{\frac{(\sin \theta \cos \phi b - \sin \theta \sin \phi \varepsilon - \cos \theta \sin \phi b + \sin \theta a + \sin \phi h)^2}{\sin \theta^2 \sin \phi^2}}$   |
|  |                            | If $Q \leq A$   | $l = 0$  |
| Diagonal segment   | If $D \leq A$ & $E \geq b$ |                 | $l = 2 * \sqrt{\frac{h^2}{(2 \cos \phi^2 - 1) \cos \theta^2 + 2 \sin \theta \cos \theta \cos \phi \sin \phi - \cos \phi^2}}$   |
| $\vec{x} = \begin{bmatrix} D \\ E \end{bmatrix}, \vec{y} = \begin{bmatrix} H \\ I \end{bmatrix}, \vec{z} = \begin{bmatrix} A \\ b \end{bmatrix}$ | If $E < b$                 | If $I > b$      | $l = \sqrt{\frac{(\sin \theta \cos \phi b - \sin \theta \sin \phi \varepsilon - \cos \theta \sin \phi b + \sin \theta a + \sin \phi h)^2}{\sin \phi^2 (2 \sin \theta \cos \theta \cos \phi \sin \phi + 2 \cos \theta^2 \cos \phi^2 - \cos \theta^2 - \cos \phi^2)}}$ |
|  |                            | If $I \leq b$   | $l = 0$  |

Figure 4.3 displays how the total length varies over a different angle. For this graph  $a, b$  and  $h$  are assumed as 1. The graph shows that an angle of 45 degrees is the most desirable when a minimum length needs to be achieved. This can be desirable in case of welding volume optimisation. However these double miter connections increase risks of failure in production.

### Analysis on single miter end connections

The equations in 4.2 can also be useful to investigate when single miter connections occurs. This can be investigated in the same two strategies as discussed in figure 4.1. Rewriting the equation in terms of height of the chord  $b$  or eccentricity  $\varepsilon$  could provide valuable information on how single miter connections can be achieved. For this analysis  $\phi = 90^\circ$  for simplification purposes.

The ideal situation for production is when the diagonal is only connected to the chord. In mathematical expression this happens when greater than the x-coordinate of  $\vec{z}$ , or  $P > A$ .

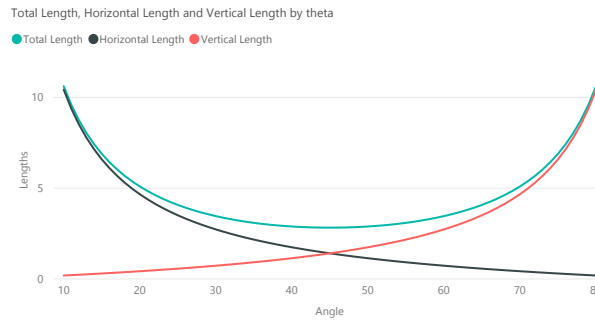
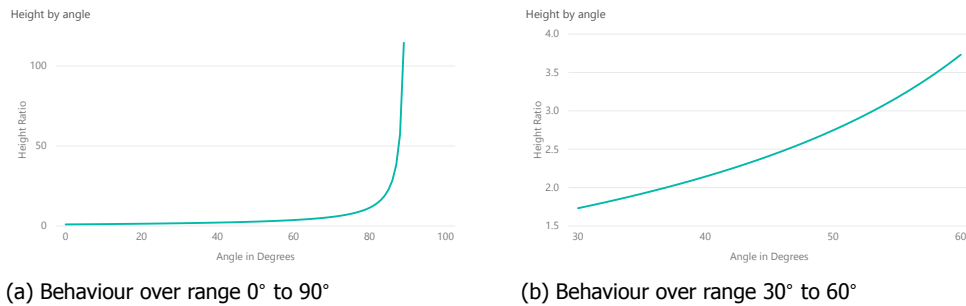
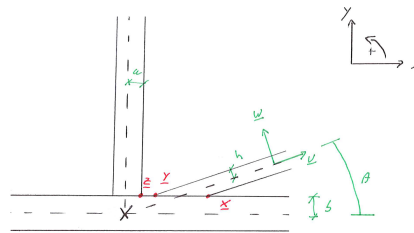


Figure 4.3: Vertical and horizontal interaction lengths over different angle when  $a, b$  and  $h$  are assumed as 1



(a) Behaviour over range 0° to 90°

(b) Behaviour over range 30° to 60°



(c) Desired situation

Figure 4.4: Height ratio chord for single miter connection

**Increasing chord-size** In equation 4.1 this situation is expressed in  $b$ , the half height of the horizontal (chord). In this equation  $\varepsilon$  is set to zero. With this expression the additional height needed in the chord to produce a single miter connection can be calculated.

The behaviour of this equation is visualized in figure 4.4. Here,  $a$  and  $h$  are assumed to be equal. The graphs show the multiplication factor needed for the chord to obtain a single miter connection. In 4.4c the range of the graph is adjusted to 30° to 60°, because the minimum angle between two members according to NEN-EN 1993-1-8, art 7.1.2(3) is 30°. The graphs shows that a low angle  $\theta$  correlates to low ratios of increasing the chord. The minimum increase ratio according to Euro-Code's range boundaries is 1.73 for an angle of 30°. From this we can conclude that it could be beneficial to create a truss in such a way that diagonals will contain low angles towards the chord. However this will influence structural performance and therefore the size optimisation of the elements.

$$\text{for } P > A \text{ then } b > \frac{a \cdot \sin \theta + h}{\cos \theta} \quad (4.1)$$

**Introducing eccentricity** Equation 4.2 shows what value  $\varepsilon$  has to be, in order to generate a single miter connection. Compared to the equation for the required size of  $b$ , this equation will be less useful. This is because the eccentricity introduces a bending moment that will cause that a bigger chord section is chosen in the optimisation of elements. A bigger chord section may need a smaller eccentricity to obtain a single miter connection. Therefore achieving just the right amount of eccentricity to obtain a

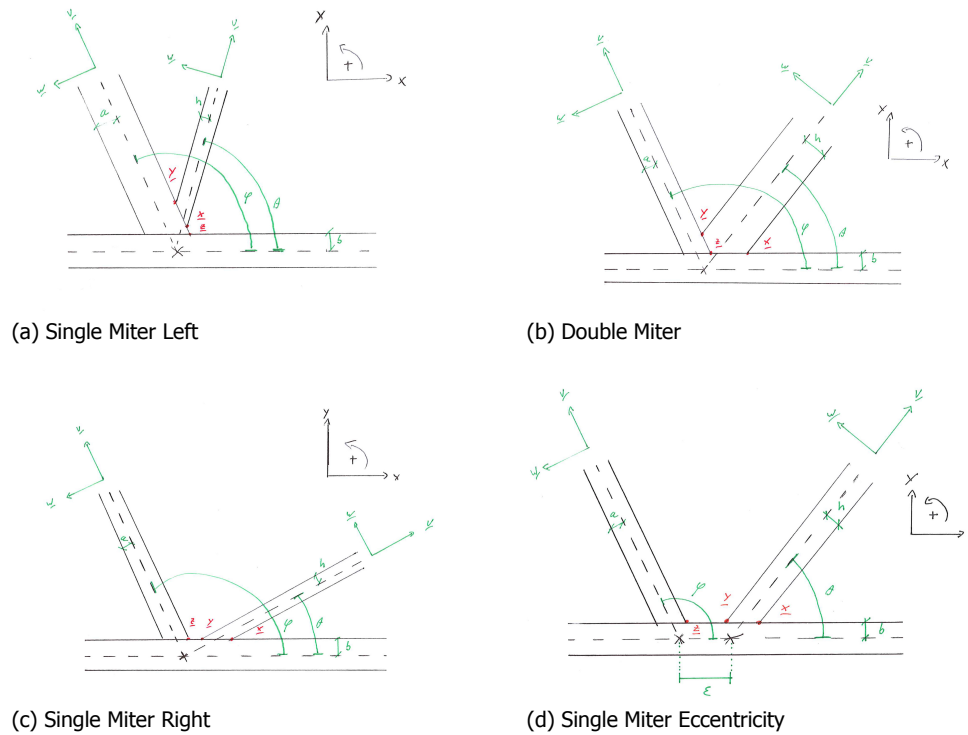


Figure 4.5: Situation drawing for single or double miter connections

single miter connection is a non-linear problem. Furthermore creating eccentricities where the segment-size in a truss is constant will also cause an inclination of the angle  $\theta$ , this adds an additional dimension to the non-linear process. However through iteration the minimum needed eccentricity can be found. In the iterative process equation 4.2 could be used to achieve together with the appropriate convergence criterion.

$$\text{for } P > A \text{ then } \varepsilon > \frac{\sin \theta * a - \cos \theta * b + h}{\sin \theta} \quad (4.2)$$

#### 4.2.2. Human error and Standardization

When designing structures, the risks of human error have to be taken into consideration. In case of welding there is preference to give as many welds as possible equal throat-thicknesses, making them standardized. This decreases the risk of human error and lowers the risk that too small throat-thicknesses are applied in welds of a connection.

Furthermore there is also a boundary on the level of precision that can be obtained during welding. A weld size of e.g. 7.5 mm be put on a drawing, since this level of precision is unrealistic for human welders. The size of a weld on a drawing is always an integer. This is a rounded up number from calculation, causing an structural over capacity in the weld instead of an under capacity.

These two factors limit the level of optimisation that is realistically possible in terms of production. When automated assembling and welding will become the standard in the steel structure production industry, it can be possible cause that these two factors do not need to be considered anymore. This will opens up the possibilities for the optimisation of the welding volume.

### 4.3. Production cost

For the cost analysis of steel trusses with welded connections, a cost model has to be set up. This section will discuss how this cost-model will work and within the optimisation model.

As concluded in previous chapter, the cost-model for this research is build up according to the Activity Based Costing Method. The activities considered are only the manufacturing activities, see figure 4.6. Transport to the building site is not considered. Erection time is excluded, and cost of foundation is excluded as well. Since production costs are very dependent on several factors. For example, the efficiency of the producer and the current economic prosperity of the country. It is important to make an adjustable cost-model. Here, users can change the parameters according to the deployment rates and process speeds of their own production process. Therefore, it is important to clearly quantify the static amounts used in the cost estimation.

These static amounts are: the surface sawing to be made, the volume of welds to be made, the surface area of surface treatment and painting. However, in this cost-model, assumptions will be made to transform these static amounts to actual prices. To simplify the cost model discounts on procurement and surtax on scrap[35] will be excluded from the cost model.

#### 4.3.1. Goal of cost-model

The goal of the cost-model is to generate a costs-estimate for the production costs of a truss with welded connections. The cost-model will be implemented in a parametric model in order to optimise trusses based on production price. The cost-model will display an estimated total production cost of the structure. With this, cost research can be performed on the ratio of prices variation between different truss-variants.

Joints in steel structures consist of several components. These components will be used as input for the cost-model. Examples of these components are the welding volume needed in the joint, the area of sawing needed and the size and thickness of plate material needed for stiffening.

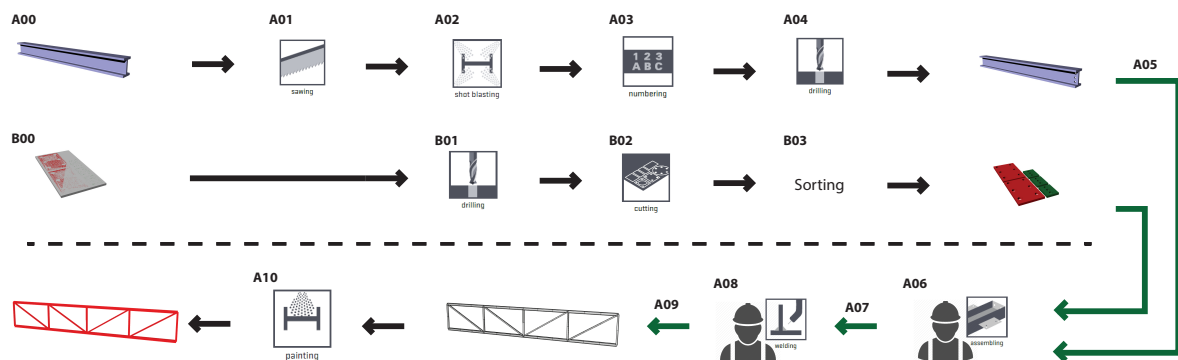


Figure 4.6: Fabrication process of trusses

#### 4.3.2. Fabrication process

During production, bare beams are being processed to make them use able and connectable for on the building site. Multiple activities take place during the fabrication process. The activities considered can be seen in figure 4.6. These activities will be discussed in the following sections. Here all activities have been numbered. All these activity are given a certain code. Processes for the beam start from A00 to A04 and for plates start from B00 to B03. During Assembling and welding these tow process come together.

##### A00. Material

A comparison has been made for five different dutch steel traders to gain knowledge about current steel prices. The names of the steel traders have been kept anonymous and are named steel trader 1[38], 2 [39], 3 [40], 4 [41] and 5 [42]. These steel traders were selected because they have a price list available in excel-format on their website. The use of excel files makes it possible to process the data relatively easy for the research purposes. Furthermore, it should be noted that these price lists

date from January 2018.

Hot formed hollow sections and sections with steel grade S460 are excluded from this research, because prices are not available in the price list on websites, and should be requested. The requested price is dependant on bulk procurement and the client costumer relation. Therefore, these requested prices between different steel traders are less useful for price comparison.

**Rolled Long Steel** In figure C.1 the gross prices per kg for long steel with a S235 steel quality are compared. The lines in the graphs show almost a horizontal relationship. The different steel traders differ from one another, but all lines follow the same slight inclination. For each graph, an extra line is added to shows the average value. All lines that display the average price lie on the horizontal axis with a price of approximately €1,40 per kilogram. Therefore a price of €1.40 for Long steel sections is assumed.

Only steel trader 1 of the five steel traders includes S355 in their product list of long steel [38]. The increase in price for these sections is 10% compared to S235. For S275 long steel no data could be found.

**Hollow sections** In figure C.2, C.3 and C.4 the gross price ranges for cold formed Square Hollow Section (SHS) and Rectangular Hollow Section beams (RHS) of three steel traders 1, 3 and 4 are displayed. These three steel traders are selected because their price list for hollow sections includes prices for S235, S275 and S355 steel quality's.

The prices of the different steel traders are not combined in one figure since these steel traders do not offer exactly the same supply of SHS and RHS beams. The horizontal axis displays the cross sectional area of the beam. This is done in order to simplify the comparison, because it filters the geometric parameters of height, width, and plate thickness. Secondly it overcomes the name difference that steel trades can have between one another.

In figure C.2, C.3 and C.4 can be seen that there is no significant difference in price per kilogram between RHS and SHS sections. However, a difference between the different steel grades can be seen. In addition, the figure shows that there is a relationship between the steel grade and the cross sectional area. All three figures show that smaller sections contain lower steel grades and bigger sections contain higher steel grades.

To gain more insight in the price range of every steel grade per steel trader, a box plot is made. In figure C.5 these box plots can be found. All three box plots show an increase in price from S235 to S275, S355. The box in the box plot represents 50% of the data. The top and bottom whiskers of the plot represent the maximum and minimum value. Because the price list contains extreme values that do not follow the expected price relationship. This extreme is the highest for steel-grade S275 at Steel trader 2. The box plot is a useful graphic tool to exclude those inconsistencies when drawing conclusions.

In table 4.3 the average price increase of the data set from S235 to S275 and from S235 to S355 are displayed for the three steel traders. This table shows that S275 is on average 5% more expensive than S235 and S355 is approximately 20% more expensive.

In figure C.5 the average price of the complete data set is given. For the price calculation of steel structures a conservative price of €3.70 per kilo is assumed for S235 hollow sections. This assumed price increases with 5% for S275 and 20% for S355.

However the price per kilo for hollow sections in this section are based on gross price list. In the case of hollow sections discounts of 50% are common when ordering bulks above 1000 kg. This is significantly different for long steel products where the price in the price-list is a realistic indication of the actual price.

**Trade lengths** Long steel has a great variation of trading lengths, starting from 8 meters up to 24 meters with a step-size of 1 meter. This means that precise lengths can be ordered, which could minimize waste when beams are cut to the precise length. However hollow sections are not available in a great variety of lengths. Common trade length for hollow sections are 6, 12, 15 and 18 meters. This can influence an optimal cost-effective design. For instance, when a design requires hollow section



Table 4.3: Difference in per cent between steel grades per steel trader

|                |      |      |      |
|----------------|------|------|------|
| Steel trader 1 | S235 | 3.31 | 100% |
|                | S275 | 3.41 | 103% |
|                | S355 | 3.92 | 118% |
| Steel trader 3 | S235 | 4.15 | 100% |
|                | S275 | 4.29 | 103% |
|                | S355 | 4.95 | 119% |
| Steel trader 4 | S235 | 2.88 | 100% |
|                | S275 | 3.11 | 108% |
|                | S355 | 3.39 | 118% |

members with a length of 6.1 meters, it means that a trade length of 12 meters needs to be ordered, where 5.9 meters will be sawn off and possibly will end up as waste.

#### A01. Sawing

From the identical set of data as in the previous paragraph, the costs of sawing per section for long steel and hollow sections have been analysed. The graphic results can be found in figures C.8, C.9 and C.3. It should be noted that these cutting prices are prices determined by the steel trader and therefore do not give exact insight into the costs that a steel contractor would make when cutting beams themselves.

**Rolled Long steel** In figure C.8 the average price range of rolled long steel is displayed for all five previously mentioned steel traders. The horizontal axis displays the cross sectional area of the beam and the vertical axis displays the price per  $m^2$ . This is a self made price that is converted from the cutting price per section in the price list. Converting this price in this manner makes comparison possible.

All different types of long steel section display approximately an equal relationship. Here, the small sections are relatively expensive put this high price quickly evens out to a constant when the cross sectional area increases. A probable cause for the higher price for small sections is the fact that a significantly bigger amount of individual cuts needs to be made to cover the same cross sectional area of  $1m^2$ . This increases handling time and therefore costs.

In figure C.8 an overall horizontal relation can be found for all types of long steel with a cross sectional area starting from  $5 \cdot 10^3 mm^2$ . Sections with a cross sectional area below this value are relatively small and therefore less prone to be chosen in a structure. Sections with a cross sectional area of less than  $5 \cdot 10^3 mm^2$  are sections up to HEA180, HEB140, IPE270, UPN260 and not a single HEM.

To simplify the cost estimate of sawing, one value will be considered. This value will be the average price in the horizontal part of the graph. The average price in this horizontal part is €5875 per  $m^2$ .

**Hollow sections** In figure C.9 and C.3 the sawing costs of hollow sections are displayed. There is a big difference in the cost to cross-sectional area relationship between the two graphs. In C.9 all value lie around the price of €10.000 per  $m^2$ , which is almost twice as expensive than the cutting price per  $m^2$  of long steel.

Figure C.3 shows a non-linear relation. It should be noted that this graph contains a small data-set. When calculating the average value of this data set the result is €9398 per  $m^2$ .

The sales-department of steel trader 1 states that the difference between the cutting price of long steel and hollow sections is because they do not saw the hollow sections themselves. The steel producer cuts them on size, and ships them on size to the steel trader.

Expertise at Oostingh ASK Romein states that there is no difference in sawing costs per  $m^2$  between long steel and hollow sections[43]. Assuming a higher sawing rate for hollow sections compared to long steel will penalize the use of hollow sections when optimising production costs, this penalty is undesirable since it does not represent the production costs that steel contractors make and will affect optimisation. In order to prevent penalizing the use of hollow sections in terms of sawing costs, the same rate for sawing of long steel will be assumed for sawing hollow sections.

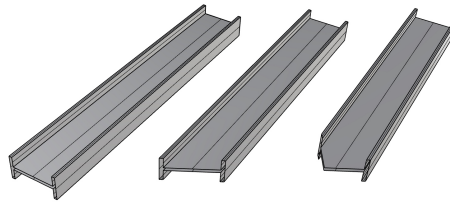


Figure 4.7: Long steel I-sections with a total of 1 (right-angled), 2 (single miter) or 3 (double miter) sawing cuts

**Number of cutting planes** There are three types of sawing cuts that can be made: right angled cuts, single miter cuts and double miter cuts. For right angled connections the beams will be sawn by one plane. In the case where a beam is connected under an angle, for example in a diagonal, cuts need to be made in multiple planes. Steel traders multiply the sawing price by the amount of sawing cuts [38][40].

The total sawing price assumed in this research will be the sawing cost multiplied with the amount of sawing cuts for an element. An element has two sides that can either have "No cut", "Right angled cut", "Single miter cut", "Double miter cut", see figure 4.7. There will be "No cut" on cases where a beam consist out of multiple elements. In case that a element has a total of more than one sawing cuts, there will be one sawing cut deducted. This will create a more realistic price estimation, because the right angled end cut of one element also serve as the right angled start cut of the next to be sawn element in the sawing process.

Table 4.4: Cost multiplication factors per type of Sawing-cut

| Type of cut      | Sawing cuts needed |
|------------------|--------------------|
| No cut           | 0                  |
| Right angled cut | 1                  |
| Single miter cut | 2                  |
| Double miter cut | 3                  |

#### A02. Surface Treatment

Steel ordered from a steel trader can also be shot-blasted and primed if desired. The price lists of the five steel traders provide prices for this as well.

In figure C.11 the average price for only shot-blasting and both shot-blasting and priming are displayed. On the horizontal axis the weight per meter is displayed and the vertical axis shows the average price per  $m^2$ .

In these graphs HEM-sections show a higher price than the rest of the long steel sections. The average price for shot-blasting of all long steel sections is €4.85 per  $m^2$ .

The lower graph of C.11 displays the average prices of shot-blasting and priming combined. This graph shows comparable results to the graph where only the price of shot-blasting is displayed. The average increase in price when including priming, lies 18% higher than only shot-blasting.

#### A03. Numbering

Beams and plates are being numbered in the factory. Bel Hadj Ali *et al.* [33] assumes 20 seconds for chalk marking the parts. Therefore 0.33 minutes is assumed in the cost model.

#### A04. Drilling

Bel Hadj Ali *et al.* [33] also specified time for drilling which is a range of 0.5 to 1 mm/s/hole. The amount of millimeters is the thickness of the plate that is being drilled. The diameter does not seem to make a difference since it is not specified. In the model of this research a speed of 0.5 mm/s/hole

is selected, since this is the most conservative value. In the cost-model no distinction will be made between drilling in plates and drilling in beam sections.

#### A05. Internal transport

Expertise at Bouwen met Staal states that most costs in the production process are made by internal transport [44]. Internal transport can be defined as the movement when a beam needs to be transported from one assembly line to another. The number of internal transports and its efficiency is factory dependent [12][13][14]. It depends highly on the logistics layout of the factory and the number of cranes available for lifting the heavy beams.

In figure 4.8 and 4.9 two possible lay outs of a steel structure production facility are displayed. In both lay outs a sawing street for beams and a cutting line for plates can be seen. The difference can be found in the logistics of assembling and welding. In most production facilities, assembling and welding is a linear process[12][14]. The facility has multiple lines with a working table for assembling and another working table for welding. A crane is needed to hoist the beam from the assembling working table to the welding working table. This linear process can often be considered when space is limited. To prevent congestion in the production process. Both assembler and welder need to complete their work in the same time.

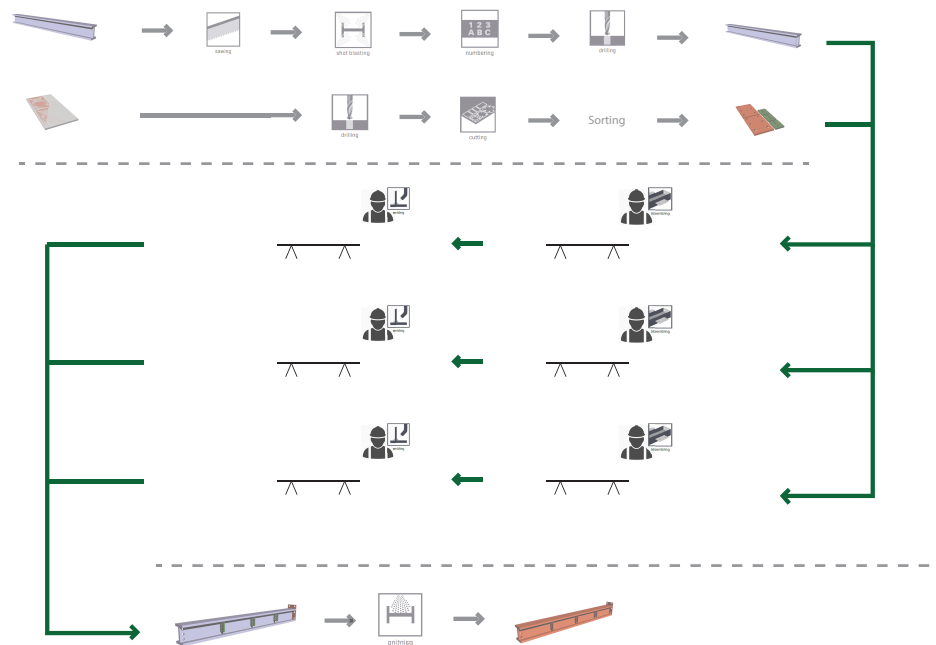


Figure 4.8: Linear process of assembling and welding

To prevent transport between assembling and welding a different lay out can be selected. This process works in an almost a circular pattern. Where workers rotate around the working tables. To prevent bottle necks in the process, multiple working tables are needed. This allows a continuous availability of work. The circular process is more efficient than the linear process because less hoisting is required. The circular process can only be applied when there is sufficient space available for a large number of working tables.

Both processes can be easily implemented in the cost-model. In case of the linear process, three hoists are assumed, one from the sawing street to the working table, one in between welding and assembling, and the last one from the welding table to the paint-shop. In case of a circular process, only 2 hoists have to be considered.

Because a linear process for assembling and welding is more common, it will also be used in the cost model of this research. Therefore three hoist in the fabrication process are assumed. The average time for a hoist will be 15 minutes per beam which is based on expertise at ASK Romein [12].

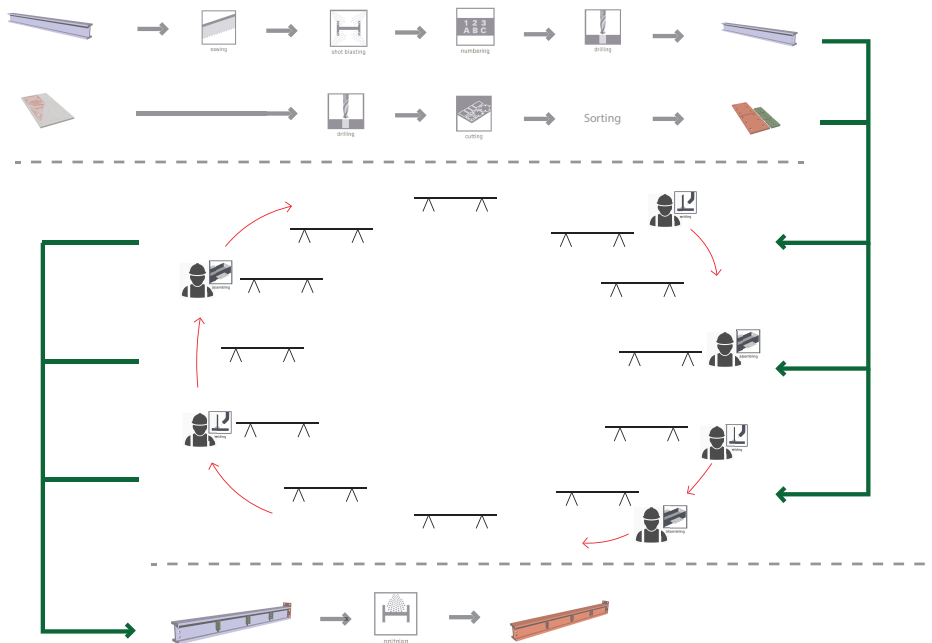


Figure 4.9: Circular process of assembling and welding

#### B00. Material Plate

The plates and stiffeners will be cut out of plates. These plates can either be hot formed (S235 and S355) or cold formed (DC01). To calculate cost, the price list of the previously mentioned five steel traders have been analysed [38][39][40][41][42].

In figure C.6 and C.7 the analysed data steel plate prices is displayed in graphs. Figure C.6 shows the average price per steel trader and the number of data entry's. This shows that steel trader 1, 2 and 3 have a more elaborate data set. Steel trader 4 and 5 possess relative high prices with their small data set.

The total average of S235 is €1.33 per kilogram. The average price of S355 is €1.30 per kilogram. Since steel trader 1 is the only steel trader that provides online prices for S355 plate steel, a conclusion that S355 is cheaper than S235 cannot be made. However, within steel trader 1 the average price between S235 and S355 are alike. Therefore, an assumption can be made that the price of S235 plate steel equals the price of S355 plate steel.

In figure C.6 the average price of cold formed steel plates (DC01) can be found as well. At every steel trader this price is higher than hot formed plate steel. On average the price of cold formed steel plates is 10 % higher than hot formed steel plates.

In figure C.7 the price relationship for varying thicknesses and total plate area are displayed per steel strength. All these graphs show a horizontal relationship. Therefore, we can conclude that neither the thickness nor the total area of a plate influences the price. However, the graph of S355 shows a non-horizontal relation. But considering the size of this data set and it only has a single resource, no conclusion can be drawn for thickness price relationship of this steel grade.

During cutting, a considerable amount of cutting waste is made, see figure 4.10. Experts at Reijrink Staal bv state that this cutting loss lies on average between 20 and 25% of the desired total weight of cut out plates, see figure 4.10.

For S235 and S355 a price of €1.30 per kilo will be assumed, with 25% of cutting waste. For cold formed plates an additional 10% will be added.

#### B01. Drilling

See A04.



Figure 4.10: Cutting waste plate cutting at steel contractor

#### B02. Plate cutting

Jármai and Farkas [37, p.123] specified multiple cutting technologies in their report. All cutting technologies have a different speed, these values can be found in table B.3 The slowest of these cutting technologies is Acetylene (normal speed), which has a time of  $T = 1.1388 * t^{0.25} * L$  for  $t = 2 - 15mm$  and  $T = 0.8529 * t^{0.364} * L$  for  $t = 10 - 40mm$ . According to the conservative approach of this research this speed for plate cutting will be chosen.

#### B03. Numbering

See A3.

#### B04. Sorting

As in Bel Hadj Ali *et al.* [33] 0.33 minutes is assumed for the sorting of plates and stiffeners.

#### A06. Assembling

A time of 5 minutes per element is assumed. This includes preparation, positioning and tack welding.

#### A07. Internal transport

See A5.

#### A08. Welding

The welding costs are dependent on multiple factors. Neessen [45] made a formula to determine the costs of welding, this formula can be found in appendix B.1. In order to use this formula a lot of information needs to be known. For example the welding technology, welding treat, protection gas, the efficiency of the welder, welding position etc. All these factors are process and company dependent. Including all these factors for welding in this cost research could increase the occurrence of errors in price calculation.

In this cost-model all welds are assumed to be welded in down-hand position by MAG welding, which is a commonly used welding technique by steel contractors [13]. To simplify the cost of welding, one rate is selected. This rate will include all the contributors of costs. This will make it more easy to adjust the rate and to research influences of different assumed welding cost rates on the optimisation process of steel structures.

Oudshoorn [43] analysed the speed of welding per throat-thickness. Results can be found in table B.5. The average of this table is a welding-speed of 150 cm<sup>3</sup>/hour. Reijrink [14] calculates with 1 to 1.2 kg of welding volume per hour. van Dijk [13] assumes a speed of 6 meter per hour for a weld with a surface area of 25 mm<sup>2</sup>. Scherrenberg [31] assumes a speed of 4 meter per hour per weld, with an surface area of 25 m<sup>2</sup>. Mela *et al.* [10] assumes 100 euro/kg. Steenhuis *et al.* [30] assumes 1 kg of welding to cost 100 times the price of a kilo of steel.

In table 4.5 the statements of the resources have been translated to cm<sup>3</sup>/hour for comparison purposes. To convert Mela *et al.* [10] and Steenhuis *et al.* [30] to a volume per hour, the assumed deployment rate of a welder in this research of 60,- per hour is used.

Table 4.5: Comparison of welding speeds per resource

| Resource                   | Resource-type    | Statement                             | Statement in cm <sup>3</sup> /hour |
|----------------------------|------------------|---------------------------------------|------------------------------------|
| Oosting ASK Romein         | Steel-contractor | Average table B.5                     | 150                                |
| Reijrink Staalconstructies | Steel-contractor | 1 to 1.2 kg/hour [14]                 | 128 to 152                         |
| Voortman Steel group       | Steel-contractor | 6 meter (a5 weld) per hour [13]       | 125                                |
| Scherrenberg               | Graduate student | 4 meter per hour per welding bead[31] | 100                                |
| Mela                       | Literature       | 100 euro/kg [10]                      | 75                                 |
| Steenhuis                  | Literature       | 140 euro/kg [30]                      | 55                                 |

In table 4.5 big differences can be seen in the assumed welding speed. In general, the literature presents relatively slow speeds and the steel-contractors present relatively high speeds. In this research a welding speed of 100 cm<sup>3</sup>/hour is assumed, this is more or less the average of table 4.5. This speed is multiplied by the hourly rate of a welder to calculate the costs. With respect to the steel contractors the assumed speed in this research is relatively slow. However, material sawing and painting prices are determined by analyzing price-lists of steel-traders instead of steel contractors. Since these costs are higher than the costs that steel contractors make themselves [43] it will justify using a slower welding speed, that will keep a realistic balance between assumed prices per process.

#### A09. Internal transport

See A5.

#### A10. Coating

In paragraph 3.2.4 several options for painting and coating are discussed. Coating against fire-protection are relatively expensive and will consume a high percentage of the fabricating costs. Since in this study the fire-safety of a structure is not part of the scope, a three-layered paint-job on four sides is assumed. Bouwen met Staal [35] assumes €16,-/m<sup>2</sup> for a three layered paint job. Mela *et al.* [10] assumes €20,-/m<sup>2</sup>, with no specification about the number of layers.

In this cost-model a price of €16,-/m<sup>2</sup> is assumed for painting. In the total to be painted, also the area of stiffeners and plates are taken into account.



### Hourly rates

The times of processes are multiplied by an hourly deployment rate in order to generate a price. The deployment rate is not a salary but a rate that external parties would pay for labour. In this cost model a distinction is made between a factory worker and a welder. The rate of a welder is higher since this rate includes equipment being used and depreciation. For the factory worker in the Netherlands we assume a deployment-rate of €40,- and for the welder in the Netherlands we assume a deployment-rate of €60,- [23].

### Summary

In table 4.6 a summary can be found of the calculation key per fabrication activity.

| Code | Name process                      | Input for generating price   | Resource                        |
|------|-----------------------------------|--|---------------------------------|
| A00  | Material Beam                     | Long steel (S235): €1.40/kg<br>Long steel (S355): €1.40 (+10%)/kg<br>Hollow section (S235): €3.70/kg<br>Hollow section (S275): €3.70 (+5%)/kg<br>Hollow section (S355): €3.70 (+20%)/kg<br>Discount Hollow sections: up to 50% | Steel trader research           |
| A01  | Sawing                            | €5875 /m <sup>2</sup><br>$Total = price * \#_{cuts}$   | Steel trader research           |
| A02  | Surface Treatment                 | Shot-blasting: €4.85/m <sup>2</sup><br>Shot-blasting & Priming: €4.85 (+18%)/m <sup>2</sup>  | Steel trader research           |
| A03  | Numbering                         | 0.33 min per unit  | Bel Hadj Ali <i>et al.</i> [33] |
| A04  | Drilling                          | 0.5 mm/min/hole  | Bel Hadj Ali <i>et al.</i> [33] |
| A05  | Internal transport                | 15 min per beam  | Company visit [12]              |
| B00  | Material Plate                    | S235: €1.30/kg<br>S355: €1.30/kg<br>DC01: €1.30 (+10%)/kg  | Steel trader research           |
| B01  | Drilling                          | 0.5 mm/min/hole  | Bel Hadj Ali <i>et al.</i> [33] |
| B02  | Cutting                           | $T = 1.1388 * t^{0.25} * L$  | Jármai and Farkas [37]          |
| B03  | Numbering                         | 0.33 min per unit  | Bel Hadj Ali <i>et al.</i> [33] |
| B04  | Sorting                           | 0.66 min per unit  | Own assumption                  |
| A06  | Assembling                        | 5 min per unit   | Own assumption                  |
| A07  | Internal transport                | 15 min per beam  | Company visit [12]              |
| A08  | Welding                           | 100 cm <sup>3</sup> /hour  | Jármai and Farkas [37]          |
|      | Minimum throat thickness: a = 4mm |  |                                 |
| A09  | Internal transport                | 15 min per beam  | Company visit [12]              |
| A10  | Coating                           | 16€/m <sup>2</sup> /type beam  | Bouwen met Staal [35]           |

Table 4.6: Summary of Input fabrication process

|                                       |       |
|---------------------------------------|-------|
| Hourly deployment-rate Factory worker | €40,- |
| Hourly deployment-rate Welder         | €60,- |

Table 4.7: Assumed hourly rates

The cost-model created in this chapter is tested by applying it on a simple case presented in appendix D. Here a singular beam with two connections is analysed. Four different typologies of connections are used. Results of this small case-study show that the biggest contributors to the total production costs are: total weight, coating and welding volume.



## 4.4. Conclusion

**Constructability** The constructability of trusses can be increased by minimizing the risks in production. In case of double miter connections, there is a high risk on deficiencies in the dimensions of the diagonals. Since the diagonals need to be a perfect fit. This risk can be minimized, by minimizing the amount of double miter connections in the truss-design.

**Cost-model** The cost-model in this research is created by analyzing price-sheets of steel-traders. These prices are gross prices where discounts are not assumed. Therefore these prices do not represent the costs that steel-contractors make. Since the costs that steel-contractor make differ per company and is sensitive information which is difficult to obtain, price-sheets of steel traders are the only resource that possess the required level of objectivity needed for comparison purposes. These price-sheets do give insight in the ratio differences between prices, which can be useful while optimising trusses on productions costs.

In appendix D a small case-study is performed on the cost model. From the results, we can conclude that weight, coating and welding volume are big contributors to the total costs. This is a conclusion drawn caused by the assumptions made in the cost model, but literature show equal distributions [36],[46].

The method of taking only production costs into consideration, allows you to work with a set of fixed, and therefore, thrust-worthy numbers. This is the welding volume, the cutting area, the sawing area, and the weight of plates and beams etc. To optimise on production costs these numbers have to be converted into a price. Finding a right value that can convert these numbers into price rates is difficult, since this is dependant on many factors. These costs differ per company, differ over time and differ per country.

In this research, it is selected to use only one unit-rate per process, because it improves controllability and adjust ability of the cost-model. When certain processes contain a wrong unit-rate, it can be easily adjusted to will provide insight into the influence of that unit-rate on the total production cost.



# 5

## Structural Analysis of Trusses

### 5.1. Introduction

In this chapter the assumptions and boundary conditions made to perform the structural analyses of trusses will be discussed.

### 5.2. Assumed loads in research

A set of assumptions are made to define the loads that will act on the truss structure. In this section, these loads will be defined.

For the cases, it is assumed that the truss structure will carry the roof of a storage facility located in Delft, the Netherlands. The storage facility will be occupied by workers, therefore consequence class II is assumed. However it should be noted that the model for optimising trusses is flexible and easy to adjust to other situations.

Table 5.1: Assumptions for load derivations

| Parameter                        | Description                |
|----------------------------------|----------------------------|
| Structure                        | Flat roof with sharp eaves |
| Consequence Class                | II                         |
| Wind Zone                        | II, rural                  |
| Category                         | H (non-accessible roof)    |
| Length truss                     | 25 m                       |
| Depth structure                  | 60 m                       |
| Center-to-center distance        | 10 m                       |
| Roof height                      | 10 m                       |
| SLS max vertical deflection roof | $L/250$                    |

#### Permanent loads

**Permanent load G** Self weight will be a variable since this load is dependent on the cross-sections selected in the optimisation process.

**Permanent load P** The permanent loads will consist of the steel-weight of the truss and the weight of roof cladding. For roof cladding and insulation, a permanent load of  $0.15 \text{ kN/m}^2$  is assumed. In this structure, it is assumed that a secondary beam lays on top of the structure with a center to center distance of 7 meters. The highest occurring load, which is the wind load of  $-0.85 \text{ kN/m}^2$ , is used together with the maximum deflection requirement of 40 mm to choose the appropriate secondary beam. For these secondary beams HEB240 are selected, resulting in an additional permanent load of  $0.12 \text{ kN/m}^2$  on the truss. In conclusion, the total permanent load is  $0.27 \text{ kN/m}^2$ .

Table 5.2:  $C_{pe,10}$  per zone

| Flat roofs                 | $C_{pe} & C_f$ per zone |                |                |                |
|----------------------------|-------------------------|----------------|----------------|----------------|
| type                       | F                       | G              | H              | I              |
| sharp eaves $C_{pe}$       | -1.8                    | -1.2           | -0.7           | +0.2/-0.2      |
| $C_f(C_{pe} + C_{pi})$     | -2.1                    | -1.7           | -1.0           | -0.5           |
| $c_s c_d * c_f * q_p(z_e)$ | $-1.79 kN/m^2$          | $-1.45 kN/m^2$ | $-0.85 kN/m^2$ | $-0.43 kN/m^2$ |

### Variable loads

**Wind-load W** For wind-region II in the Netherlands, a basic wind velocity of  $v_{b,0} = 27.0 m/s$  basic velocity pressure of  $q_b = 0.46 kN/m^2$  must be assumed [47].

To determine the characteristic wind load the following formula is used according to NEN-EN 1991-1-4, art 5.3:

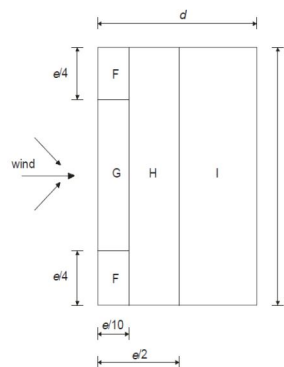
$$F_w = c_s c_d * c_f * q_p(z_e) * A_{ref} \quad (5.1)$$

Since elements assumed have a relatively small surface area and are relatively stiff, we assume that no resonance will occur. Therefore it will be assumed that  $c_s c_d = 1.0$ , NEN-EN 1991-1-4, art 6.2(1).

For a 10 meter high building located in rural area of wind zone II,  $q_p(z_e) = 0.85 kN/m^2$ , [48, gl12]. The loaded area of cladding or roof sheeting by wind load is greater than  $10 m^2$ , therefore  $C_{pe,10}$  can be used to determine the external pressure. For  $c_f$  several values should be considered, based on the location of the structure, see table 5.2.  $(c_{pe} + c_{pi}) = c_f$ .  $C_{pi}$  represents the internal pressure and is assumed to be -0.3, NEN-EN 1991-1-4, art 7.2.9(6). With these values the load of  $kN/m^2$  per zone can be calculated these loads can be found in table 5.2.

In the top of the plan, the structure is loaded with the highest wind forces, over zone F, H and I. Here  $e$  is the smallest value of  $b$  and  $2h$ . For this case this leads to  $e = 20m$ . This leads to a division of the truss into three pieces, with a length of 2, 8 and 15 meters. The load-case with three different distributed loads produces a specific bending moment, see figure 5.2. Since using three different distributed loads increases complexity of the structural analysis, a simplification is desired. To simplify, we assume a distributed load of zone H over the whole length of the truss. Which results in a higher maximum bending moment, see figure 5.2. Therefore, this simple and conservative approach can be used.

Downward wind-force will not be considered, since snow-load is the governing downward load.

Figure 5.1:  $C_{pe,10}$  for flat roofs [48, gl7]

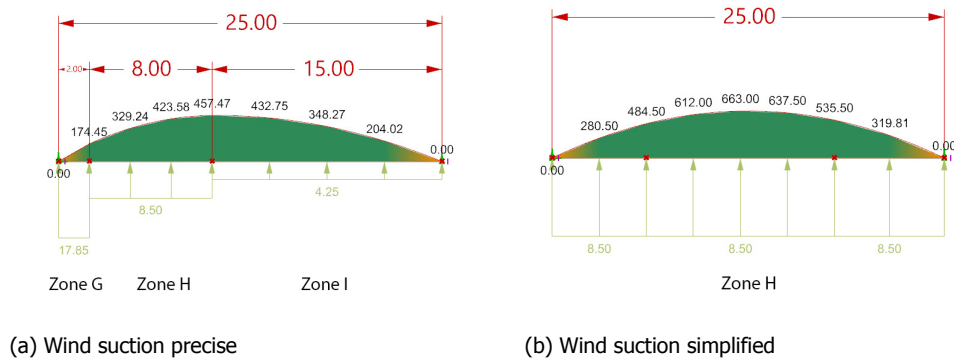


Figure 5.2: Moment distribution for wind suction

**Snow-load S** In the Netherlands a characteristic snow-load of  $s_k = 0.70 \text{ kN/m}^2$  must be assumed [47]. To calculate the design snow-load, the following formula should be used according to NEN-EN 1991-1-3, art 5.2(3a):

$$s = \mu_i C_e C_t s_k \quad (5.2)$$

Here  $\mu_i = 0.8$  because the angle of the roof is  $0^\circ$ , NEN-EN 1991-1-3, art 5.3.2.  $C_e = 1$ , since the structure has normal coverage by its surroundings.  $C_t = 1$ , since the roof has no higher thermal coefficient, as in the case of glass roofs.

In conclusion the snow-load assumed in this research is  $s = 0.56 \text{ kN/m}^2$

**Variable load for maintenance Q** According to NEN-EN 1991-1-1 art 6.3.4.2 a load of  $q_k = 1 \text{ kN/m}^2$  on  $10 \text{ m}^2$  of the roof or a point-load of  $Q_k = 1.0 \text{ kN}$  needs to be assumed. In reality this load will represent people and material standing on the roof in order to perform maintenance to the roof.

The most unfavorable  $10 \text{ m}^2$  of the  $1 \text{ kN/m}^2$  on the truss structure, is exactly in the middle. With a center-to-center distance between the trusses of 10 meters, this will result that the load is placed in a strip with a width of 1 meter. This causes a specific bending moment, see figure 5.3. However since the snow-load creates a greater Moment force, the snow-load is considered governing. Therefore, the variable load due to maintenance does not have to be taken into consideration.

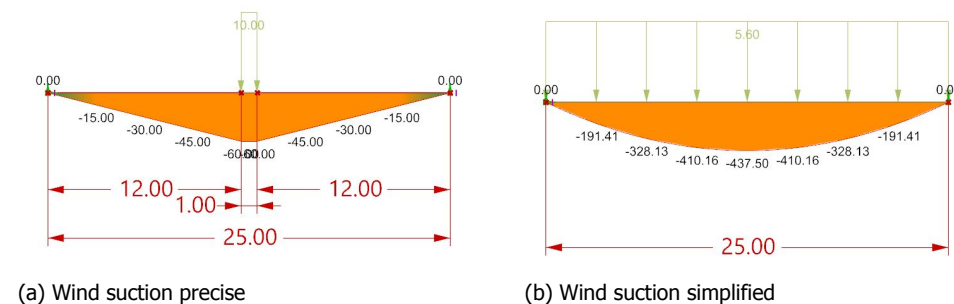


Figure 5.3: Most complex joint per design

Table 5.3: Summary: assumed loads

| Parameter | Assumed Load              |
|-----------|---------------------------|
| G         | variable                  |
| P         | $0.27 \text{ kN/m}^2$     |
| Q         | (not governing over snow) |
| W         | $-0.85 \text{ kN/m}^2$    |
| S         | $0.56 \text{ kN/m}^2$     |

### Ultimate limit State

Partial factors should be taken into consideration for the ULS load combination, in order to provide enough safety in the structure. These factors are listed in 5.4.

Table 5.4: Partial factors for load cases, NEN-EN 1990, A1.3.1

| Consequence Class | Governing | $\gamma_G$  |           | $\gamma_Q$ |
|-------------------|-----------|-------------|-----------|------------|
|                   |           | Unfavorable | Favorable |            |
| 1                 | G         | 1.2         | 0.9       | 1.35       |
|                   | Q         | 1.1         | 0.9       | 1.35       |
| 2                 | G         | 1.35        | 0.9       | 1.5        |
|                   | Q         | 1.2         | 0.9       | 1.5        |
| 3                 | G         | 1.5         | 0.9       | 1.65       |
|                   | Q         | 1.3         | 0.9       | 1.65       |

When creating load combinations, a load combination factor  $\psi$  should be used. Because the structure is a roof-structure, category H is applied. For this case  $\psi_0 = 0$  according to NEN-EN 1990, art A1.2.2. Since for all loads  $\psi_0 = 0$  the load-cases will not consist out of multiple variable loads.

Table 5.5: Load combination factors according to NEN-EN 1990, art NB.2 - A1.1

| Load              | $\psi_0$ | $\psi_1$ | $\psi_2$ |
|-------------------|----------|----------|----------|
| Category H: roofs | 0        | 0        | 0        |
| Snow-load         | 0        | 0.2      | 0        |
| Wind-load         | 0        | 0.2      | 0        |

### Permanent weight governing according to NEN-EN 1990, art 6.4.3.2 (6.10)

$$E_d = \gamma_G * G_k + \gamma_P * P + \sum \gamma_Q * \psi_0 * Q_k \quad (5.3)$$

### Variable weight governing according to NEN-EN 1990, art 6.4.3.2 (6.10)

$$E_d = \gamma_G * G_k + \gamma_P * P + \gamma_Q * Q_k + \sum \gamma_Q * \psi_0 * Q_k \quad (5.4)$$

Incidental load combination of for example earthquake and fire are not taken into account. Because it is assumed that in these situations the storage facility will be evacuated minimizing the risk of casualties.

Table 5.6: Governing ULS-loads, center-to-center distance: 10m

| Number | Load-type | Governing  | Description                                   | result                |
|--------|-----------|------------|---|-----------------------|
| 1      | ULS       | $G$        | $E_d = 1.35 * G_k + 1.35 * P$                 | $1.35 * G + 3.65kN/m$ |
| 2      | ULS       | $Q_{wind}$ | $E_d = 0.9 * G_k + 0.9 * P + 1.5 * -Q_{wind}$ | $0.9 * G - 10.32kN/m$ |
| 3      | ULS       | $Q_{snow}$ | $E_d = 1.2 * G_k + 1.2 * P + 1.5 * Q_{snow}$  | $1.2 * G + 11.64kN/m$ |

### Serviceability Limit State

When calculating SLS-load combinations. Safety factors are 1.0. The formula needed to calculate SLS-combination can be found in NEN-EN 1990, art 6.5.3 (6.15b):

$$E_d = G_k + P + \psi * Q_k \quad (5.5)$$

**Maximum deflections** With the SLS-load combinations deflections of the structure will be checked. The limit on deformation, limits the rotation at the supports of the member. Exceeding the deflection criterion could result in too great rotations at the support which could lead to damage to the cladding of the roof or of the facade. As Eurocode does not specify deformation limits, the old limits originating in the Dutch code are used (NEN6702 Belastingen en vervormingen TGB 1990). For the roof a maximum

vertical deflection of  $L/250$  is assumed. To calculate the resulting deflection the following formula is used.

$$w_{G+P} + w_Q - \text{precamber} < w_{max} = \frac{L}{250} \quad (5.6)$$

Because no precamber will be applied the following equation is used.

$$w_{G+P} + w_Q < w_{max} = \frac{L}{250} \quad (5.7)$$

Table 5.7: Governing SLS-loads, center-to-center distance: 10m

| Number | Load-type | Governing    | Description                      | result          |
|--------|-----------|--------------|----------------------------------|-----------------|
| 4      | SLS       | wind suction | $E_d = G_k + P - 1.5 * Q_{wind}$ | $G - 6.375kN/m$ |
| 5      | SLS       | snow         | $E_d = G_k + P + 1.5 * Q_{snow}$ | $G + 8.67kN/m$  |

### 5.3. Assumptions for structural analysis

#### Assumed loading scheme in research

In this research, five load combinations will be taken into account. Three ULS load-combinations and two SLS. In all five cases the load will be applied as a distributed load, acting on the top-chord of the truss. Normally, the load is applied in multiple point loads, acting at every joint in the top-chord. This is more realistic assumption, because normally secondary beams on top of the truss structure carrying the roof cause that the truss is loaded by point loads. But, assuming a distributed load is more practical for the comparing trusses that have a variation in truss-segment width, as will be discussed in section 8.4.6.

Assuming a distributed load instead of point loads acting on the top chord does not change the distribution of internal force in the truss, but it does create an additional bending-moment in the top-chord. This additional bending moment can cause the need for a bigger cross-section.

#### Assumed mechanical scheme in research

To analyse a structure, a mechanical scheme is needed. The mechanical scheme simplified representation of reality. Within mechanical scheme, connections can be assumed either hinged, rigid or semi-rigid. In reality, a connection is never completely rigid and almost never completely hinged. There will always be certain level of rotational stiffness present in the connection. However, including these rotational stiffness's in the calculation increases complexity of the analysis. Therefore, in engineering's practice often only hinged and rigid connections are used in calculations. This simplification is especially useful for manual calculations which was the standard up till the middle of the twentieth century [49, p.41].

**Hinged connections** In trusses the connections are mostly assumed to be hinged. Trusses are composed out of triangles, which are the most form-stable structural geometry. Due to this stability, bending moments stay relatively small when the connection of the truss are assumed rigid. Assuming hinged connections prevents bending moments to develop. Due to the redistribution of forces this will cause that the elimination of the shear force and the bending moment will lead to an increase of the axial force.

A structure with hinged connections will be less stiff than a structure with rigid connections. Assuming hinged connections will lead to a higher deflection, which may be a more conservative assumption when deflection is governing. Assuming hinged connections has its effect on the detail analyses of the connection. The connection will in reality always have a degree of rotational stiffness. Therefore, deformation capacity in the joint is required to allow a plastic hinge to form. Allowing a plastic hinge to form, makes the assumption of the hinged connection valid.



**Rigid connections** Assuming the connections to be rigid, will cause that no local rotation in the connection can occur. The restrained rotation will cause a shear force and a bending moment to develop. In reality a connection will never be completely rigid. Eurocode defines classification limits for the maximum rotation in which a connection can be assumed rigid, NEN-EN 1993-1-8, art 5.2.2.5. Assuming all connections of the truss structure to be rigid can cause the need for stiffeners to increase the rotational stiffness, which can be economically undesirable.

In conclusion, bending moments in trusses are relatively small. Therefore, connections can be assumed as hinged if the joint has sufficient deformation capacity. Assuming all connections to be rigid is less desirable, because there is a high probability that stiffeners are required to satisfy euro-codes conditions for assuming a connection to be rigid. For these reasons, all connections will be assumed hinged.

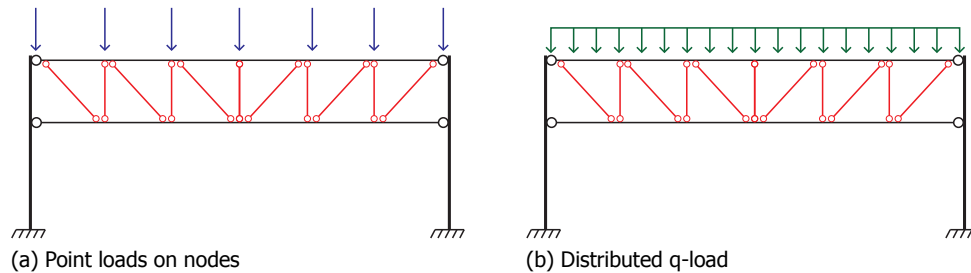


Figure 5.4: Mechanical schemes of trusses

### Assumptions for eccentric joints

As described in section 4.2, single miter connections can be created by adding an eccentricity to the joint. Therefore, the optimisation model will allow the implementation of eccentric joints. For the structural analysis of joints with eccentricities, different mechanical assumptions can be applied. Eurocode prescribes a method to include eccentricities in joints. This is done by translating the geometry of the diagonal in vertical direction, see figure 5.5. This model is based on geometric deviations that can occur as cause of tolerance in production. Which is significantly different from the purposely introducing an eccentricities in order to create single miter connections. In this research, the eccentricity is created as geometry in the wire-frame model, see figure 5.6. Since the eccentricities are created along the lines of the chords, the eccentricities are not assumed vertically but horizontally. The diagonals and post are here attached to the chords under the assumption of a hinged connection.

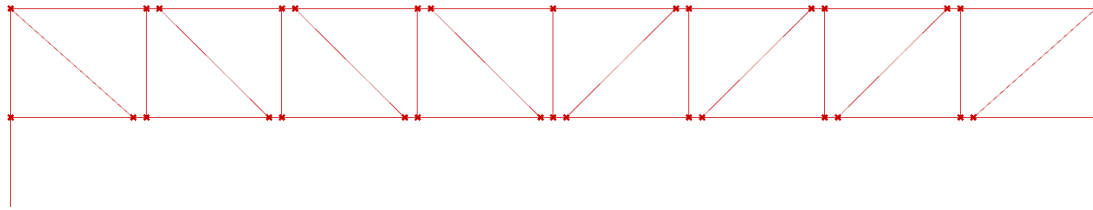


Figure 5.6: Wire-frame geometry with (exaggerated) eccentricities

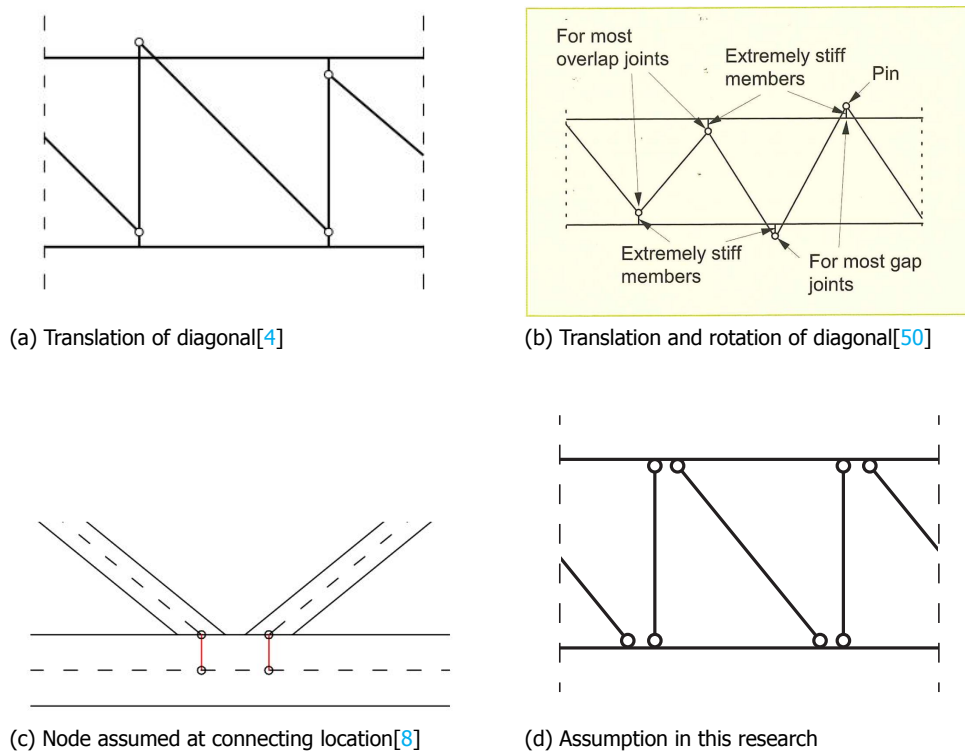


Figure 5.5: Possible assumptions for eccentricity joints[4, p.50][50, p.74][8, p.10]

## 5.4. Structural analyses with Karamba3D

Karamba3D is used for the structural analysis of the model. Karamba3D is a structural analysis plugin for Grasshopper. In Grasshopper parametric geometry is made, as presented in figure 5.6. With the components of Karamba3D supports, loads and cross-sections can be applied to this parametric geometry.

### Analysis algorithms

Karamba3D has three different analysis algorithms to analyse structures. One for First order analysis, one for Second order analysis and one for Large deformation analysis. The first order analysis assumes that the influence of axial forces on stiffness of the members is negligible. In the second order calculation this influence is taken into account. This causes that compressive force decrease a structures stiffness and tensile forces increase a structures stiffness [51, p.71]. This inclusion increases computational time of the algorithm. The large deformation analysis is to be used for non-linear geometry, like cables. Therefore this analysis is not considered in the research.

In this research the first order analysis will mainly be used to analyse truss structures, it is expected that deformations due to axial forces will not have a significant influence on the load distribution of

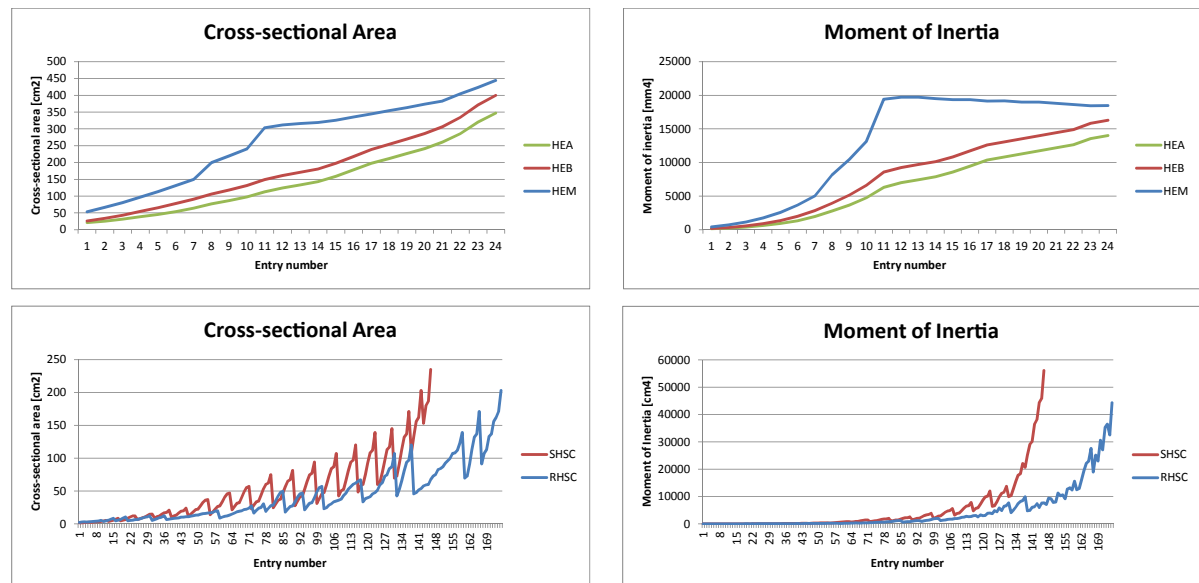


Figure 5.7: Influence of list order on optima found

trusses.

#### Size optimisation with the "Optimize Cross Sections" component

Karamba3D has the "Optimize cross section" component which performs size optimisation. In size optimisation every member in a structure is optimised to have the minimal cross-section needed to provide sufficient resistance against the acting forces. The "Optimize Cross Sections" component optimises the cross-section within a certain family per element. A family can present HEA, HEB, HEM, SHS, RHS-beams etc. In the algorithm of the component, the forces of the elements are first determined. In the second step, the first entry of the list of beams that satisfies all the utilization checks for the family is being selected. In the third step, the algorithm determines whether the distribution of forces has been changed. This can be the case in statically indeterminate structures. When the distribution of forces changes, step two will be executed again. When all utilization checks are met, the algorithm stops [51, p.87]. The optimising algorithm is bounded to the highest cross-section of a particular family. This could be for example HEA1000 in case of the HEA family. When an even heavier cross-section is needed, the algorithm will stop at this highest cross-section.

The "Optimization cross section" component is influenced by the order of the list where the beams are selected from. The component starts with the first cross-section and carries on with the next cross-section until all requirements are satisfied. Therefore, the order of the list influences the optimal result found by the cross sections. In Karamba3D these lists are ordered by the height of the cross-section. For I-sections this is an appropriate order, because in this order properties as cross-sectional area and moment of inertia that influence structural performance are in this order still monotonically discrete ordered, see figure 5.7. A order is called monotonic if and only if it is either entirely non-increasing, or entirely non-decreasing.

However, hollow sections are also firstly ordered by height. But the hollow sections with the same height are secondly ordered on width and thirdly on thickness. This can cause that the properties as for example cross-sectional area and moment of inertia to not monotonically ordered, see figure 5.7. This influences optima found within the algorithm, because it stops when all requirement are satisfied. Possibly missing the consecutive cross-sections, that would have resulted in a lower total weight of the structure. In conclusion, local optima can be missed when properties of the cross-sections are not monotonically ordered.

Results of the calculations made, can be visualized by the "Utilization" component [51, p.103]. This component has one slot that displays the details. Here the values of the calculated resistances can be found. Table 5.8 presents the calculations that are performed for the determination of the cross

Table 5.8: Utilization of elements component in Karamba3D, calculations used to determine element resistances

| Parameter           | Description  | Reference                      |
|---------------------|--|--------------------------------|
| Element             | Number of the Element in Structure                 | -                              |
| Sample point        | Start-point of element                             | -                              |
| Cross-section class | Influential factor on calculations below           | NEN-EN 1993-1-1 art 5.5        |
| $N_{Rd}$            | Axial force  | NEN-EN 1993-1-1 art 6.2.3      |
| $V_{y\_Rd}$         | Shear force y-direction                            | NEN-EN 1993-1-1 art 6.2.6      |
| $V_{z\_Rd}$         | Shear force z-direction                            | NEN-EN 1993-1-1 art 6.2.6      |
| $M_{t\_Rd}$         | Torsional moments                                  | NEN-EN 1993-1-1 art 6.2.7      |
| $M_{y\_Rd}$         | Bending moment in y-direction                      | NEN-EN 1993-1-1 art 6.2.5      |
| $M_{z\_Rd}$         | Bending moment in z-direction                      | NEN-EN 1993-1-1 art 6.2.5      |
| $M_{cr}$            | Critical bending moment Lateral torsional buckling | NEN-EN 1993-1-1 art 6.3.2.2    |
| $N_{cr\_y}$         | Critical Axial force buckling in y-direction       | NEN-EN 1993-1-1 art 6.3.1.3    |
| $N_{cr\_z}$         | Critical Axial force buckling in z-direction       | NEN-EN 1993-1-1 art 6.3.1.3    |
| $\psi_y$            | Moment distribution coefficient                    | NEN-EN 1993-1-1 art 6.3.2.3(2) |
| $C_{my}$            | Equivalent moment distribution factor              | NEN-EN 1993-1-1 Appendix B     |
| $C_{mz}$            | Equivalent moment distribution factor              | NEN-EN 1993-1-1 Appendix B     |
| $C_{mLT}$           | Equivalent moment distribution factor              | NEN-EN 1993-1-1 Appendix B     |
| $\chi_y$            | Buckling reduction factor in y-direction           | NEN-EN 1993-1-1 art 6.3.1.2    |
| $\chi_z$            | Buckling reduction factor in z-direction           | NEN-EN 1993-1-1 art 6.3.1.2    |
| $\chi_{LT\_mod}$    | Lateral torsion reduction factor                   | NEN-EN 1993-1-1 art 6.3.2.2    |
| $k_{yy}$            | Interaction factor                                 | NEN-EN 1993-1-1 Appendix B     |
| $k_{zz}$            | Interaction factor                                 | NEN-EN 1993-1-1 Appendix B     |
| $k_{yz}$            | Interaction factor                                 | NEN-EN 1993-1-1 Appendix B     |
| $k_{zy}$            | Interaction factor                                 | NEN-EN 1993-1-1 Appendix B     |

section.

The assumed buckling length of the element has a big influence on the calculated resistance. It is used to determine both the buckling resistance as the lateral torsional resistance. By default, the buckling length in Karamba3D is the length of the beam element. For trusses this can produce unsafe results for the top and bottom chord, because a too short buckling length will be assumed [51, p.76]. The "Modify Element" component in Karamba3D lets users adjust the buckling length.

For the optimisation of trusses on production costs a buckling length for the chord member of 6.25 meters is assumed. This number represents the span of 25 meters divided into four segments. Increasing the number of buckling supports of a chord will lead to a shorter buckling length. Which has a big influence and leads to a lighter cross-section needed in the chord. Since in this research only the 2D geometry of trusses is taken into account, the additional costs of having more buckling supports is not included in the total production cost calculation. It has been decided to keep the amount of buckling supports on a constant level. The assumed four segments will cause that three buckling support are needed for both the top and bottom chord for every truss variant produced. The buckling support will restrain both in plane, as out of plane buckling.

**Buckling Resistance** In Karamba3D, the reduction factor for buckling is calculated by the following equations presented in NEN-EN 1993-1-1, art 6.3.1.2.

$$\chi = \frac{1}{\phi + \sqrt{\phi^2 - \bar{\lambda}^2}}, \text{ with } \chi \leq 1.0 \quad (5.8)$$

$$\phi = 0.5[1 + \alpha(\bar{\lambda} - 0.2) + \bar{\lambda}^2], \bar{\lambda} = \sqrt{\frac{Af_y}{N_{cr}}}, N_{cr} = \frac{\pi^2 EI}{L^2} \quad (5.9)$$

**Lateral Torsional Buckling Resistance** In Karamba3D, the reduction factor for Lateral torsional buckling is calculated by the following equations presented in NEN-EN 1993-1-1, art 6.3.2.3.

$$\chi_{LT} = \frac{1}{\phi_{LT} + \sqrt{\phi_{LT}^2 - \bar{\lambda}_{LT}^2}}, \text{ with } \chi_{LT} \leq 1.0 \quad (5.10)$$

$$\phi_{LT} = 0.5[1 + \alpha_{LT}(\bar{\lambda}_{LT} - 0.2) + \bar{\lambda}_{LT}^2], \bar{\lambda}_{LT} = \sqrt{\frac{W_y f_y}{M_{cr}}} \quad (5.11)$$

$$M_{cr} = \frac{\pi}{L} \sqrt{EI_z(C + \pi^2 \frac{C_w}{L^2})}, \text{ with } C = GI_t \text{ and } C_w = EI_w \quad (5.12)$$

**Stability of Prismatic members** Both the buckling resistance factor and the lateral torsional buckling resistance factor are used to calculate the stability of elements according to following equations presented in NEN-EN 1993-1-1, art 6.3.3(4).

$$\frac{\frac{N_{Ed}}{\chi_y N_{Rk}}}{\gamma_{M1}} + k_{yy} \frac{\frac{M_{y,Ed} + \Delta M_{y,Ed}}{\chi_{LT} M_{y,Rk}}}{\gamma_{M1}} + k_{yz} \frac{\frac{M_{zy,Ed} + \Delta M_{zy,Ed}}{M_{z,Rk}}}{\gamma_{M1}} \leq 1 \quad (5.13)$$

$$\frac{\frac{N_{Ed}}{\chi_z N_{Rk}}}{\gamma_{M1}} + k_{zy} \frac{\frac{M_{y,Ed} + \Delta M_{y,Ed}}{\chi_{LT} M_{z,Rk}}}{\gamma_{M1}} + k_{zz} \frac{\frac{M_{zy,Ed} + \Delta M_{zy,Ed}}{M_{z,Rk}}}{\gamma_{M1}} \leq 1 \quad (5.14)$$

The interaction values for the cross section forces  $k_{yy}$ ,  $k_{yz}$ ,  $k_{zy}$ ,  $k_{zz}$  are calculated according to NEN-EN 1993-1-1, appendix B. In Karamba3D, the values  $C_{my}$  and  $C_{mz}$ , that are needed to calculate  $k_{yy}$ ,  $k_{yz}$ ,  $k_{zy}$ ,  $k_{zz}$ , are limited to minimum of 0.9 [51, p.80].

### 5.4.1. Shear-force in Eccentricity elements

Every element of the wire-frame geometry (see figure 5.6) is optimised to the minimal cross-section needed. Since the top and bottom chord consist of one continuous beam, all elements in the bottom chord have the same cross-section. Same holds for the top-chord. This causes that there will always be one relatively heavy loaded element that will be governing for the selection of the cross-section of the chord.

When an eccentricity is applied to the wire-frame model, it creates tiny elements that represent the eccentricity. This has an influence on the acting forces in the joint, because an additional moment force is created due to the eccentricity, see figure 5.9. The eccentricity element possess a big shear-force. This shear-force will cause that the eccentricity element will become the governing element for choosing the appropriate cross-sections. In the figure the eccentricities are exaggerated to increase readability of the figure. In reality the eccentricity will be much smaller. This causes that the lines of the diagonal and the post will still cross within the boundaries of the cross-section. This causes that the shear-force cannot develop. Therefore the eccentricity elements will be ignored when determining the cross-section of the chord in the optimisation.

Since the bending moments are also present in the neighbouring elements, these forces will not be lost when ignoring the eccentricity elements.

NEN-EN 1993-1-8 art 5.1.5(5) states that bending moments may be neglected when the positive eccentricity is less than 25% of the height of the chord. For a HEA200 profile, where the height is 200 mm, this means that the maximum positive eccentricity in vertical direction is 50 mm from the center-line of the cross-section. This rule will serve as a guideline to the maximum eccentricity possible, however a slightly greater eccentricity could still be valid since bending moments are not neglected.

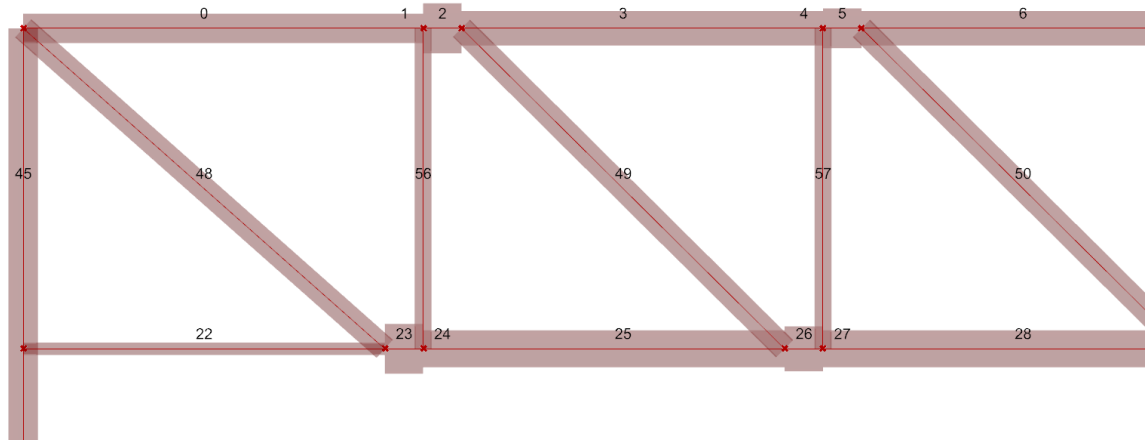


Figure 5.8: Cross-section geometry with (exaggerated) eccentricities

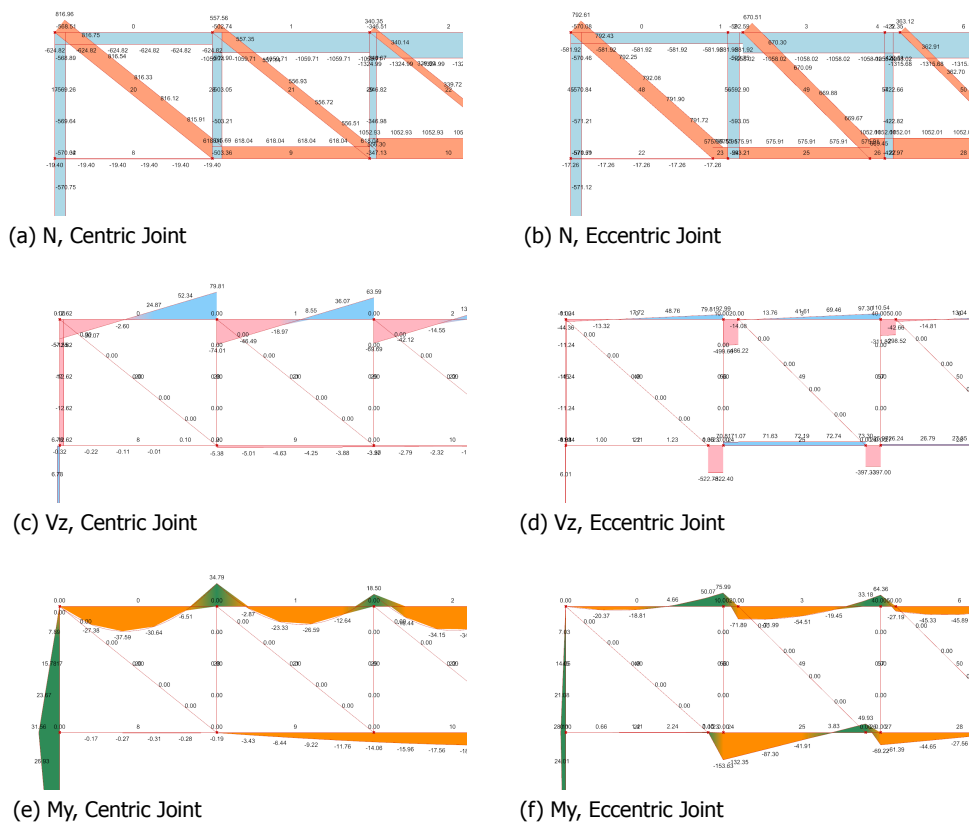


Figure 5.9: Influence of eccentricity on forces

### 5.5. Conclusion

The truss in the case-study of this research is designed to support a roof structure. This causes that five load-cases need to be considered. Three ULS load-cases and two SLS load-cases. Within these load-cases both downward as upward (wind-suction) loads are considered.

In the optimisation model, the cross-sections will be optimised for both ULS and SLS calculations with the "Optimize cross section" component in Karamba3D. This component determines the governing cross-section per group of beams. In the case of eccentric joint, the eccentricity elements have a tremendous shear force. Because this shear force cannot develop when the center of the joint falls within the perimeters of the cross-section, the suggested cross-section of these elements is ignored. The governing cross-sections of elements of the chord which are not the eccentricity elements will define the selected cross-section.



# 6

## Welded connections in Trusses

### 6.1. Introduction

In this chapter welded connection in trusses will be discussed in two main sections. The first section will discuss how weld-volume is affected. The second section will discuss how the strength of a weld can be assessed.

### 6.2. Volume of welds

In the chapter 4.3, it has been concluded that the size of the welding volume is a large contributor to the production costs. Optimising structures for the least size of welding volume could be beneficial when cost-effectiveness should be achieved. The size of welding volume of a structure is dependent on several factors:

- Type of welds
- Throat thickness
- Angle between the to be connected plates

In the following section these factors are discussed on how they influence the size of welding volume in the connections of steel structures.

#### Type of welds

In the construction field, 80% of all welds are fillet welds, 15% are butt welds. For the remaining 5 % , plug and fillet all round welds are mostly used [3, p.123]. Fillet welds do not require edge preparation, which saves costs. However, in some cases a but-weld is being selected, because it will minimize the welding volume. The savings in welding volume should weigh up against the extra costs made for edge preparation. This will be further elaborated in section 6.2.

#### Throat thickness

The strength of a weld is calculated, by its effective length, and its effective throat thickness. The throat thickness is positioned in the plane, where the cross-sectional area of the welding material is the smallest. In practice, the size of the weld-throat is displayed in millimeter with the letter a in front. For example, "a5" refers to weld with a throat thickness of 5 millimeter. The strength of welds can be calculated according to Eurocode by the directional method, or the full-strength method. The directional method is a more elaborate method and can lead to the most economic design.

The minimum throat thickness is limited. According to NEN-EN 1993-1-8, art 4.5.2(2) the minimum throat thickness of a fillet weld is 3 mm. This thickness is physically possible, but requires effort and concentration of the welder. To create a weld with such a small size the flow-rate of the welding machine needs to be adjusted. This adjusted flow-rate is not beneficial because it leads to less welding

material placed in the equal interval of time. Therefore steel contractors prefer a throat thickness of 4 or 5 mm depending on the contractor[14][13].

The minimum throat thickness required by steel contractor can be used as a starting point in the design of a truss. If the required weld size of a connection in the truss is below the minimum throat thickness, it leads to a lower utilization of the weld. This is undesirable, because it can lead to more welding volume. It is beneficial to have a high utilization in the weld because this causes that the weld is used more efficiently. By changing of the geometry or the topology of a truss, a variant can be created where the welds will have a high enough utilization, that creates weld above the minimum required size. Leading to a better cost-effectiveness in terms of welding.

On the other hand, it is also undesirable for production costs to create trusses with large weld-sizes. The size of a weld influence the cross-sectional area of the weld, which again influences the welding volume. In the case of a Tee-joint fillet weld, the cross sectional area increases quadratic as the throat thickness increases, see figure 6.1. To illustrate, "a5" and "a7" are highlighted. Due to the quadratic relationship "a7" has almost double the surface area ( $49\text{mm}^2$ ) compared to "a5" ( $25\text{mm}^2$ ). Hence, it is beneficial for the weld volume to minimize weld size.

Designing structures for solutions where the throat-thicknesses are above the minimum size as required by the steel contractors and are as small as possible can therefore lead to better cost-effective solutions. To accommodate this, sufficient welding length is needed, in order to distribute the forces and obtain a weld that suffice with small throat-thickness

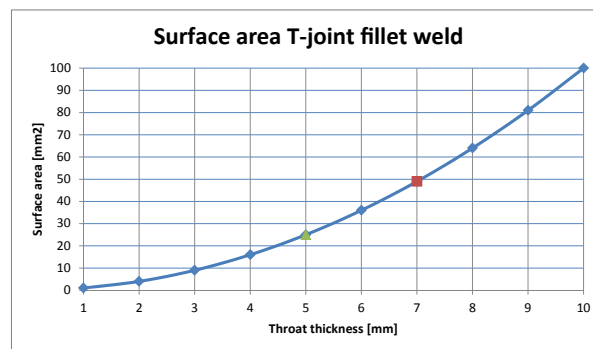


Figure 6.1: Weld Surface of T-joint fillet weld over throat thickness

### Angle of the weld

The amount of welding volume is also dependent on the angle of the weld. This angle is determined by the the plates to be connected. In this section, a closer look will be taken at how the welding surface in skewed T-joints is influenced by the angle of the weld. In the literature, the angle of a weld is often not taken into account Mela *et al.* [10].

NEN-EN 1993-1-8, art 7.1.2(3) states that the minimum angle between chord-members and braces is  $30^\circ$ . Therefore, the graphs presented in this section are limited to angles between  $30^\circ$  and  $150^\circ$ .

**Skewed fillet welds** Fillet welds are the most used welds in the utility building industry, because they perform adequately in statically loaded structures and they do not require edge preparation. In figures 6.2 and 6.3, the total surface area of the weld is per angle displayed for a double fillet weld. The surface area of the fillet weld increases quadratic from small to wide angles. In the graph of figure 6.2, it can be seen that the optimal configuration for having the least amount of welding surface is a weld with an angle of  $90^\circ$ . For further illustration on the different angles of weld multiple drawing can be found in appendix E.1.

NEN-EN 1993-1-8, art 4.3.2.1(1) states that fillet welds can be used in angles between  $60^\circ$  and  $120^\circ$ .

These boundaries are set because fillet welds with an angle outside this range will have affected structural properties. According to Eurocode, a fillet weld with an angle below  $60^\circ$  should be examined as a butt weld with a crack and a fillet weld with an angle above  $120^\circ$  should be tested by experiments defined by appendix D in EN1990.

The minimum angle of a fillet weld in production practice is  $40^\circ$ . This is because in a smaller angle, the welding torch will not be able to fit. Due to the width of the welding torch, see figure 6.4.

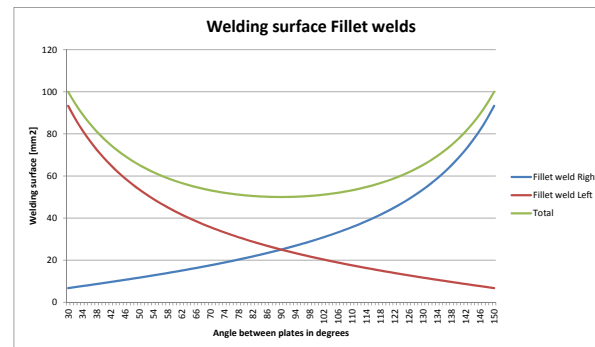


Figure 6.2: Welding surface of fillet weld per angle as graph, throat thickness = 5 mm

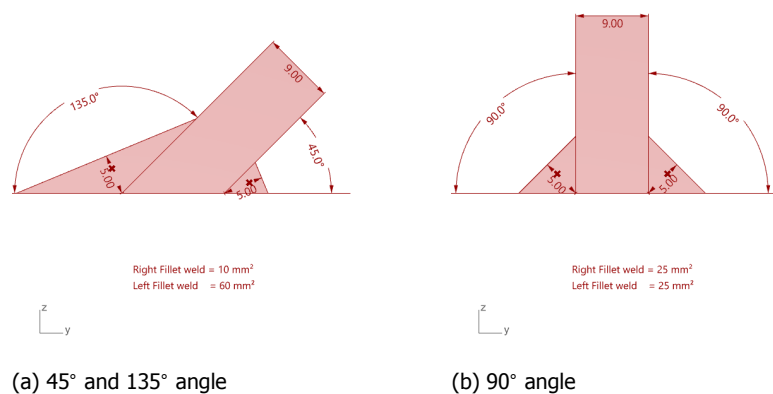


Figure 6.3: Welding surface of fillet weld per angle in detail, throat thickness = 5 mm

**Skewed butt welds** Fillet welds with a wide angle produce a significant higher welding surface. The welding surface can be reduced by choosing a butt weld instead. For the butt weld, edge preparation is needed. The benefit of less welding is measured by the cost saving generated compared to the extra costs of edge preparation, in order to produce a cost-effective design. Experts at Oostingh ASK Romein state that creating a butt welds will be beneficial for plates with a thickness greater than 20 millimeters [43]. For reference, these flange thickness occurs in section-families starting from HEA450, HEB320 or HEM100.

In figure 6.5 the welding surface for butt welds is displayed per angle. The graph starts from  $90^\circ$  because partial butt welds cannot be created in acute angles. In appendix E.2, a drawing can be found. Here, the angle of the edge preparation is displayed. The first four drawings show solutions where the angle of the prepared edge is unrealistically small.

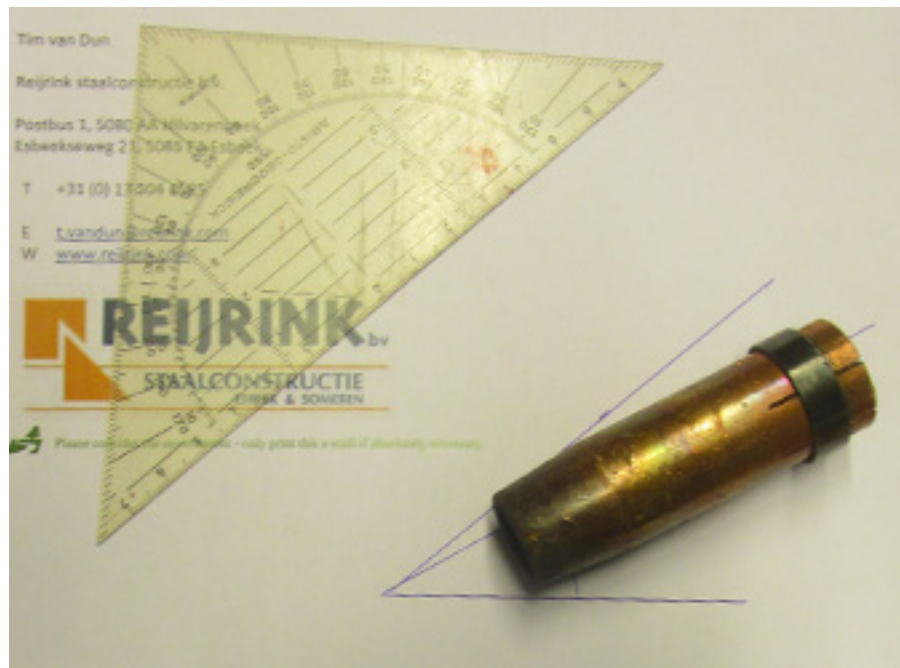


Figure 6.4: Physical limitation of accessibility of the welding torch in an angle of 30°

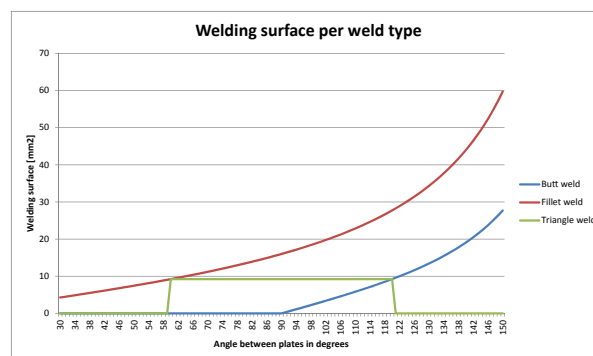


Figure 6.5: Welding surface of fillet, butt and triangle weld per angle, throat thickness = 5 mm

In figure 6.5 an additional line can be found representing a triangular weld. In engineering practice, these kinds of welds will be referred to combination welds. The weld is a combination of a fillet weld and a butt weld. A combination welds where the surface area is a triangle with corners of 60° will produce the minimum area. Experts at Oostingh ASK Romein state that the use of combination welds is only interesting for welds with a throat-thickness greater than 12 millimeters[43]. In appendix E.3 drawings can be found, the triangular weld can be seen as a combination of the fillet and butt weld. For angles between 60 and 120° this could be a welding volume beneficial solution.

In this research butt welds and combination welds will not be considered, because they are only applied if a threshold is exceeded. For butt welds this is a plate thickness of 20 millimeters, which occurs in relative big cross-sections that will not be used in the truss-structure. For combination welds a threshold of a 12 welds is set. This is a relatively big weld-size. The probability that this size occurs in trusses is low.

### 6.3. Strength of welds

In this section two calculation methods for calculating the required throat thickness of the welds of a connection will be discussed. These two methods will be used in the model for the optimisation of truss. The first method is the full-strength method, and the second method is the directional method. In the optimisation model the directional method will be implemented by using Idea Statica Connection within the workflow the model. Idea Statica combines Eurocode calculations with finite element calculations, which leads to accurate results.

The full-strength method is based on the directional method. The directional method is a simplified model provided by Eurocode where the resistance of a weld can be calculated. In the directional method, the forces transmitted by a unit length of weld are resolved into four components, see figure 6.6. These components are the vectors of the force transmitted. The main difference between the two methods is the speed of calculation and the economic use of material. The full-strength method is a fast method that generally leads to non-economic use of material. The directional method is a slower method that could lead to an economic use of material.

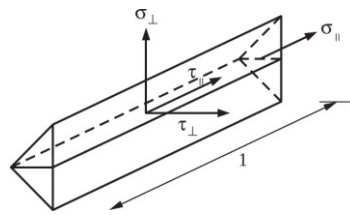


Figure 6.6: Stresses on the throat section of a fillet weld(unit length) [3, p.138]

$$\sqrt{\sigma_{\perp}^2 + 3(\tau_{\perp}^2 + \tau_{\parallel}^2)} \leq \frac{f_u}{\beta_w \gamma_{M2}} \text{ and } \sigma_{\perp} \leq 0.9 f_u / \gamma_{M2} \quad (6.1)$$

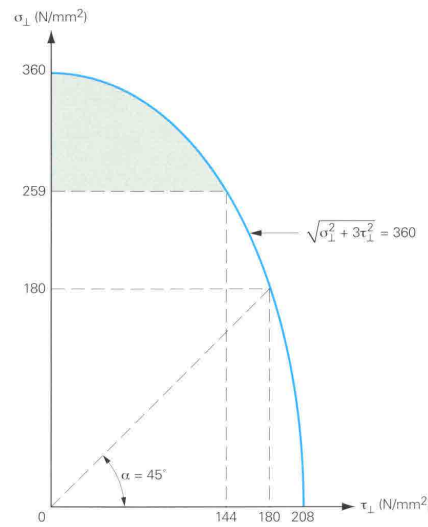


Figure 6.7: Von Mises yielding criterion for S235 [18, part 4, p.24]

#### 6.3.1. Calculation Method 1: Full-strength method

The full-strength method is a method where weld sizes are calculated under the assumption that the whole cross-section of the weakest component is yielding.

Generally, welds are designed full-strength, because it prevents that the weld is the governing element, when structural failure occurs in case of overloading. Because welds are relatively small compared to attached beams, they do not have a lot of deformation capacity while yielding. This small

amount of deformation capacity can cause a brittle failure mechanism. In general deformation capacity is desired in structures because it acts as a warning signal when a structure fails.

In the full-strength method, the required weld size is calculated by the full-strength factor. This is a number that is dependent on the lowest steel grade of the connected elements. To calculate the required weld size this factor is multiplied by the plate thickness. In equation 6.2 the derivation of the full-strength method is displayed. This derivation leads to equation 6.6, from which the full-strength factor is calculated.

The full-strength factor for different steel grades is displayed in table 6.2. Here, two columns can be found. One for double fillet welds and one for single fillet welds. Double fillet welds are used in case when I-sections need to be welded, because both sides are accessible. In the case of hollow sections the inside is inaccessible, therefore, a single fillet weld should be used. This causes that the full-strength factor is twice as big.

Table 6.1: Parameters full-strength method

| Parameter     | Description                         |
|---------------|-------------------------------------|
| $f_y$         | nominal yield strength weakest part |
| $\gamma_{M0}$ | partial safety factor               |
| $l$           | length weld                         |
| $a$           | throat thickness weld               |

$$\sqrt{\left(\frac{\sigma_{weld}}{\sqrt{2}}\right)^2 + 3\left(\left(\frac{\sigma_{weld}}{\sqrt{2}}\right)^2\right)} \leq \frac{f_u}{\beta_w \gamma_{M2}} \quad (6.2)$$

$$\sigma_{weld} \leq \frac{f_u}{\beta_w \gamma_{M2} * \sqrt{2}} \quad (6.3)$$

$$2 * a * l * \sigma_{weld} \geq t l f_y / \gamma_{M0} \quad (6.4)$$

$$N = \sigma_x * t * l \text{ with } \sigma_x = f_y / \gamma_{M0} \quad (6.5)$$

$$a \leq \frac{f_y \beta_w \gamma_{M2}}{\sqrt{2} f_u \gamma_{M1}} * t \quad (6.6)$$

Table 6.2: Minimum "full-strength" required thickness in case of double fillet and single fillet end welds(plate thickness smaller than 40 mm [3, p.144])

| Steel grade | $f_y$    | $f_u$    | $\beta_w$ | $f_{w,u,end}$ | Full-strength<br>double fillet welds | Full-strength<br>single fillet welds |
|-------------|----------|----------|-----------|---------------|--------------------------------------|--------------------------------------|
|             | $N/mm^2$ | $N/mm^2$ |           | $N/mm^2$      | I-section                            | Hollow-section                       |
| S235        | 235      | 360      | 0.80      | 255           | $a \geq 0.46 * t$                    | $a \geq 0.92 * t$                    |
| S275        | 275      | 430      | 0.85      | 286           | $a \geq 0.48 * t$                    | $a \geq 0.96 * t$                    |
| S355        | 355      | 510      | 0.90      | 321           | $a \geq 0.55 * t$                    | $a \geq 1.11 * t$                    |
| S420 M      | 420      | 520      | 1.00      | 294           | $a \geq 0.71 * t$                    | $a \geq 1.43 * t$                    |
| S420 N      | 420      | 550      | 1.00      | 311           | $a \geq 0.68 * t$                    | $a \geq 1.35 * t$                    |
| S460 M      | 460      | 550      | 1.00      | 311           | $a \geq 0.74 * t$                    | $a \geq 1.48 * t$                    |
| S460 N      | 460      | 580      | 1.00      | 328           | $a \geq 0.70 * t$                    | $a \geq 1.40 * t$                    |

The full-strength factors shown in 6.2 is calculated under the assumption that the weld has an angle of 90°. Therefore, the derivation of the full-strength method is modified in equation 6.9 to include the angle of the weld.

It is differentiated with the assumption of an angle of 90°. In this research, the full-strength method will also be used to determine the throat-thickness of connections where the angle is variable. Will the

full-strength method still be valid in such a case? In the equations below a new equation is derived for the full-strength method with a variation in the angle.

$$\omega = 0.5 * \theta \quad (6.7)$$

$$\sigma_{\perp} = \frac{f_y * t * L * \sin(\omega)}{a * L} \text{ and } \tau_{\perp} = \frac{f_y * t * L * \cos(\omega)}{a * L} \text{ and } \tau_{\parallel} = 0 \quad (6.8)$$

$$\sqrt{\left(\frac{f_y * t * L * \sin(\omega)}{a * L}\right)^2 + 3 \left(\frac{f_y * t * L * \cos(\omega)}{a * L}\right)^2} \leq \frac{f_u}{\beta_w \gamma_{M2}} \quad (6.9)$$

$$a = t * \sqrt{\frac{\beta^2 \gamma_{M2}^2 f_y^2 (2 (\cos(\omega))^2 + 1)}{f_u^2}} \quad (6.10)$$

In equation 6.10 a full-strength factor in relation to the angle  $\omega$  is derived. In graph 6.8, the equation is plotted over a range from 0° to 180° for every steel grade that is presented in table 6.2. In the figure, a vertical line at 90° is highlighted, that displays the original full-strength factors. The figure shows that small angles have a higher factor than wide angles. This is because a weld with a small angle will be predominantly stressed in shear. Since welds are weaker in shear according to the Von Mises criterion 6.7 this results in a higher full-strength factor. For obtuse angles, angles above 90°, the weld will be predominantly stressed in axial stress. This creates a lower full-strength factor. In the truss optimisation of Mela *et al.* [10] the angle is not taken into account for determining the full-strength factor. Mela *et al.* [10] uses the factors presented in table 6.2. One could argue whether this assumption is optimistic.

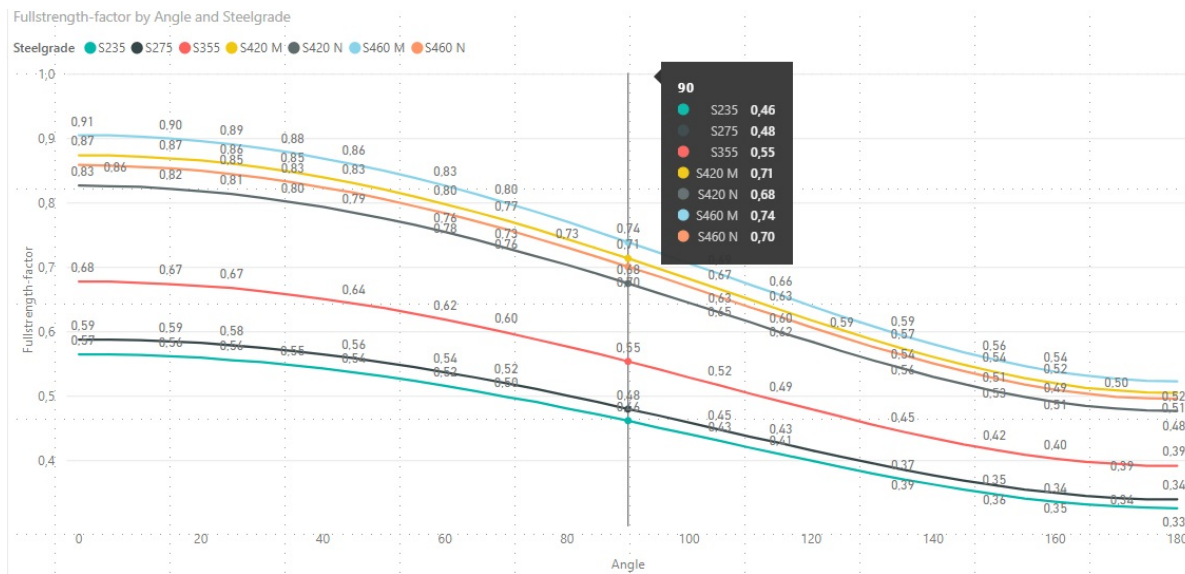


Figure 6.8: Full-strength factor over different angles

### Implementation of method in optimisation process

Figure 6.9 shows how the full-strength method will be used in the optimisation model. In this process the variables will be: the angle, the steel-grade, thickness of the plate and the minimal required throat thickness. The full-strength factor will be calculated with equation 6.10. Here the factor will be doubled in case of Hollow sections, since single fillet welds are needed. The calculated weld size is rounded up to an integer. This value is compared to the minimum required weld size. Here the maximum value is selected. This value determines the weld-size. The weld-size is calculated separately for both the web as the flange, because they can have different thicknesses.



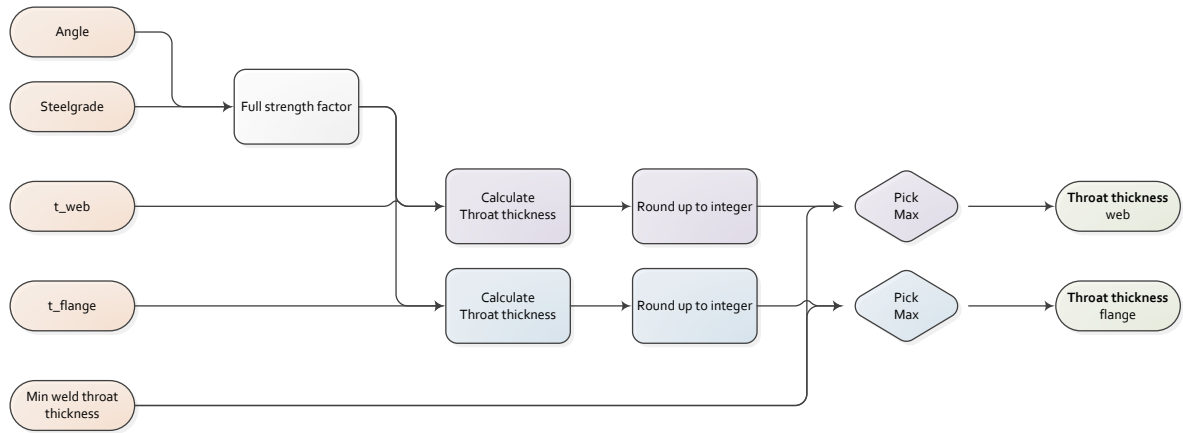


Figure 6.9: Work-flow for calculation method 1: Full-strength method

### 6.3.2. Calculation Method 2: Directional method

The concept of full-strength welds will not lead to an economic use of weld material. Designing welds with the directional method can lead to an economic use of weld material. In this section a closer look will be taken into the theoretical background of the directional method.

To investigate how the directional method affects weld sizes over different angles, equation 6.1 has been rewritten into two equations. For both equations an assumption is made that only axial forces arise in the weld. In the first derivation, the axial force will act perpendicular to the weld. In the second derivation the axial force will act in the plane of the weld.

In equation 6.12, the formula for the components of the flange plate are displayed. Here  $\theta$  is the angle between the throat and the plate and  $a$  is the throat thickness, see figure 6.10. In equation 6.14 the Von Mises criterion is rewritten in terms of the required weld size  $a$ .

$$\omega = 0.5 * \theta \quad (6.11)$$

$$\sigma_{\perp} = \frac{N * \sin(\omega)}{a * L} \text{ and } \tau_{\perp} = \frac{N * \cos(\omega)}{a * L} \text{ and } \tau_{\parallel} = 0 \quad (6.12)$$

$$\sqrt{\left(\frac{N * \sin(\omega)}{a * L}\right)^2 + 3 \left(\frac{N * \cos(\omega)}{a * L}\right)^2} \leq \frac{f_u}{\beta_w \gamma_{M2}} \text{ and } \sigma_{\perp} \leq 0.9 f_u / \gamma_{M2} \quad (6.13)$$

$$a = \sqrt{\frac{\beta^2 \gamma_{M2}^2 N^2 (2 (\cos(\omega))^2 + 1)}{L^2 f_u^2}} \quad (6.14)$$

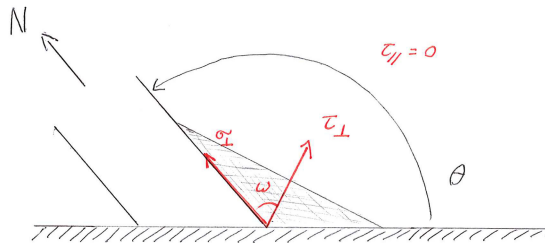


Figure 6.10: Schematic representation components flange plate of diagonal

In equation 6.15 the formula for the components of the web plate are displayed. Here  $\delta$  is the angle between the skewed plate and the base plate and  $a$  is the throat thickness, see figure 6.11. In equation 6.17 the Von Mises criterion is rewritten in terms of the required weld size  $a$ .

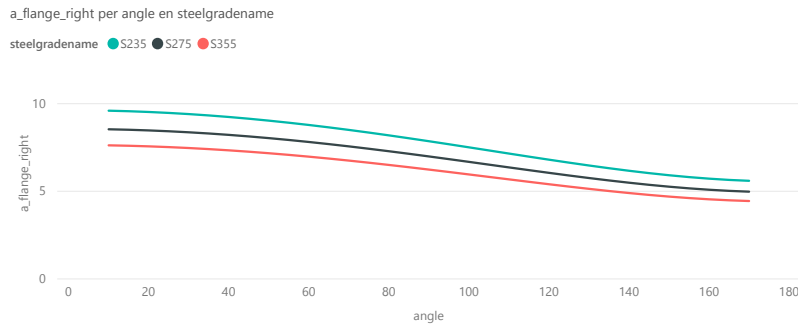


Figure 6.12: Relation  $a$  to angle in welds of flange for  $N = 400$  kN and  $L = 100$  mm

$$\sigma_{\perp} = \frac{N \cdot 0.5\sqrt{2} \cdot \sin(\delta)}{a \cdot L} \text{ and } \tau_{\perp} = \frac{N \cdot 0.5\sqrt{2} \cdot \sin(\delta)}{a \cdot L} \text{ and } \tau_{\parallel} = \frac{N \cdot \cos(\delta)}{a \cdot L} \quad (6.15)$$

$$\sqrt{\left(\frac{N \cdot 0.5\sqrt{2} \cdot \sin(\delta)}{a \cdot L}\right)^2 + 3\left(\left(\frac{N \cdot 0.5\sqrt{2} \cdot \sin(\delta)}{a \cdot L}\right)^2 + \left(\frac{N \cdot \cos(\delta)}{a \cdot L}\right)^2\right)} \leq \frac{f_u}{\beta_w \gamma_{M2}} \text{ and } \sigma_{\perp} \leq 0.9 f_u / \gamma_{M2} \quad (6.16)$$

$$a = \sqrt{\frac{\beta^2 \gamma_{M2}^2 N^2 ((\cos(\delta))^2 + 2)}{L^2 f_u^2}} \quad (6.17)$$

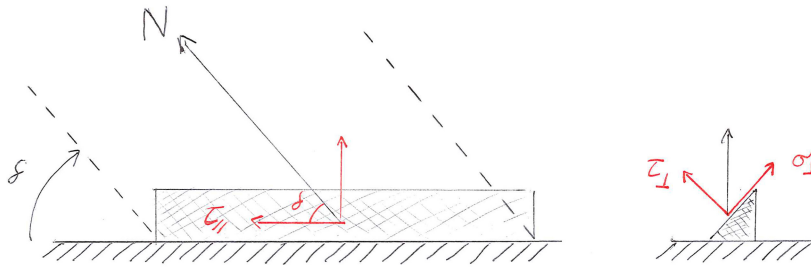


Figure 6.11: Schematic representation components web plate of diagonal

The formulas to calculate the throat thickness for fillet welds perpendicular to the vector of the axial force 6.14 and in plane with the vector of the axial force 6.17 are further examined. Here, double fillet welds are assumed which causes that total axial force is divided over the two welds.

When examining the variables in equation 6.14 and 6.17, variation in axial force, weld length and steel-grade shows a linear relationship and therefore not a notable influence on the required throat size. However the angle of the weld does show influence. In figure 6.12 an asymmetric non-linear relationship can be found, where the required throat thickness decreases when the angle increases. Fillet welds in obtuse angles have a higher structural performance than acute angles, because fillet weld in obtuse angles are predominantly loaded in axial stress. The weld has higher stress capacities in this direction due to the Von Mises criterion, see figure 6.7

In welds of the web-plate show a symmetric relationship, 6.13. Here a minimum value for the throat thickness can be found at an angle of  $90^\circ$ , which is also a direct result from the Von Mises criterion. However there is an additional requirement of maximum axial stress perpendicular to the throat found in equation 6.13 and 6.16. In the case of skew double fillet welds, the weld with the maximum throat thickness of the two is selected as governing. This will cause that weld critical in axial stress, obtuse angled welds with small throat-thicknesses, will obtain a conservative throat-thickness obtained from the acute angle weld.

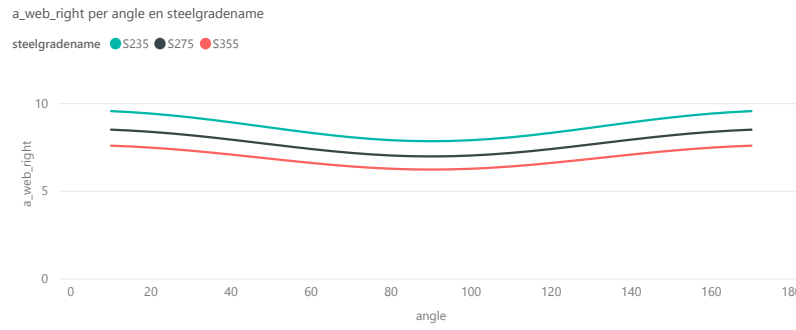


Figure 6.13: Relation  $a$  to angle in welds of web for  $N = 400$  kN and  $L = 100$  mm

### Distribution of axial force along welds

The joints in the trusses are assumed hinged. This assumption causes that only axial forces occur in the joint according to the model. In this research the axial force will be assumed to be distributed evenly along the welding-length in the directional method. Having more welding length results in a lower total welding volume of the connection, since there is more length to distribute the force. Figure 6.14 shows that in the directional method increasing the welding length reduces the total welding volume. The graphs are not smooth since the throat is rounded up before calculating the total volume, as would happen in production. In addition the thickness is not specified, because this would limit to the graph.

In the directional method it is beneficial to have more welding length, because the axial force will be more distributed, this will cause smaller weld size. Thus lower welding volumes. This is a big difference compared to the full-strength method, where more welding length is "penalized" and leads to more welding volume.

The left of figure 6.15 shows that I-section have more welding length than Hollow sections. In terms of welding volume it could be beneficial to use I-sections instead of hollow-sections, but this will produce more surface area to be painted. Which could make this possibility less attractive in terms of overall cost-effectiveness.

### Effective width

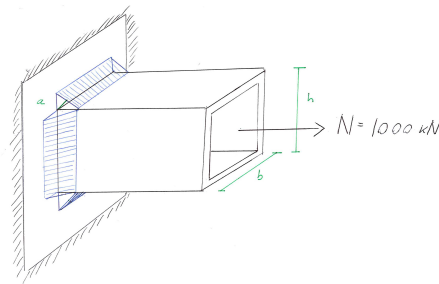
The stresses in the welds are dependent on the stiffness of the apparent material, as displayed in 6.16. This distribution can be simplified by using the effective width, equation 6.18.

The stiffness of the base plate is rarely constant. Mostly the base plate represents the flange of an I, H or box section. Here the parts near the web will be more heavily loaded than the other parts, because of its local higher stiffness. Therefore a reduced effective length should be taken into account, see figure 6.16. This effective width is used in this research for the directional method. Since the chord can deviate in section-type. In this research, all combination of effective widths should be considered, see figure 6.15. This figure shows that it is beneficial in terms of effective width to have both beam and chord-member as either Hollow-section or I-sections.

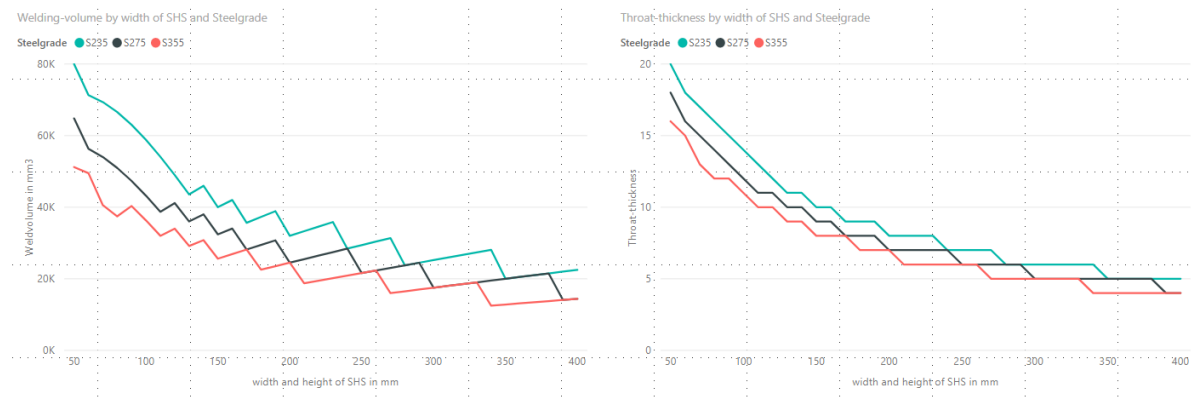
$$b_{eff} = t_w + 2s + 7kt_f, \text{ where } k = \left(\frac{t_f}{t_p}\right)\left(\frac{f_{y,f}}{f_{y,p}}\right) \text{ with } k \leq 1.0 \quad (6.18)$$

### Double miter connections

In the case of double miter connections, the weld along the web will be split into two components. This depends on the geometric configuration of the elements, as discussed in 4.2.1. In case of a split weld as in figure 6.17 one part of the weld will be predominantly loaded in axial stress and the other will be predominantly loaded in shear. The weld predominantly loaded in shear will perform worse due to the Von-Mises criterion, and will be governing for determining the throat-thickness of the web.



(a) Drawing of Situation



(b) Results

Figure 6.14: SHS section attached to an infinitely stiff plate loaded with a tensile force of 1000 kN

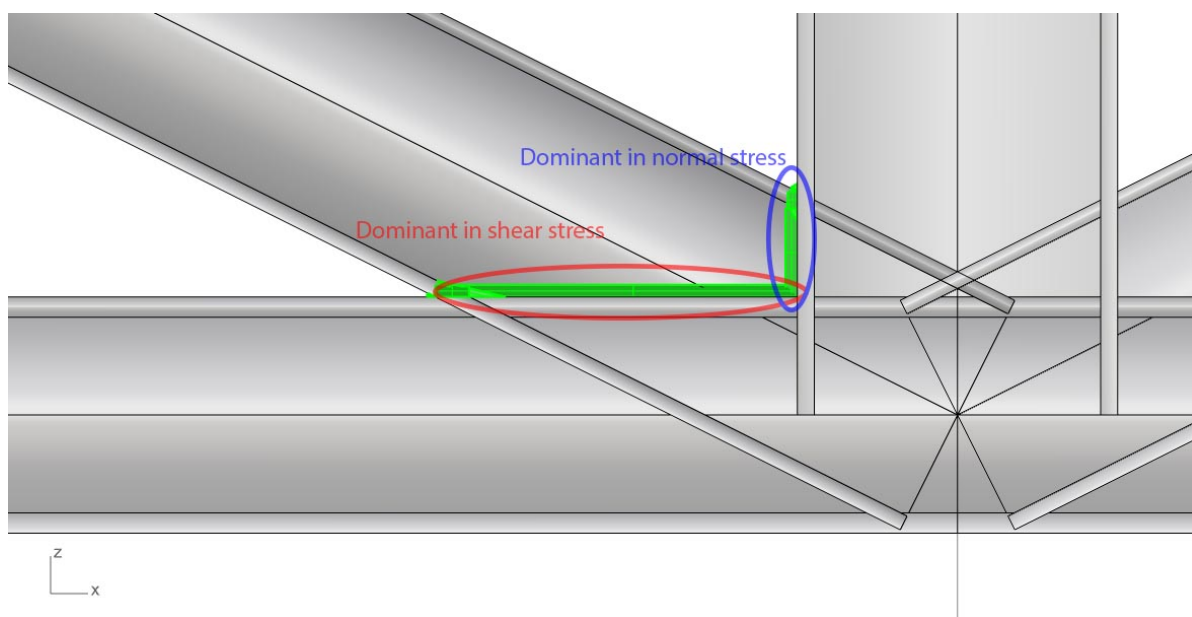


Figure 6.17: Web weld I section diagonal with two cutting planes

### Welding in cold-formed zones

Due to cold-form process of cold formed hollow sections, residual stresses occur around the corners. This causes that welding in a range of  $5t$  to the corner radius is only allowed when certain conditions are fulfilled. These conditions depend on the  $r/t$  ratio [3, p.135]. This principle can have a significant impact on variants where all members are hollow section, because it causes that only a small part can be used when calculating the resistance of the weld. Due to the effective width of the welds for

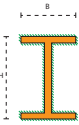
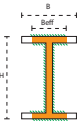
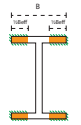
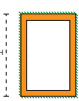
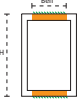
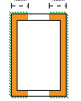
|                | $B < B_{eff}$   | $B > B_{eff}$<br>I-section chord  | $B > B_{eff}$<br>Hollow-section chord   |
|----------------|---|---|---|
| I-section      |  |  |  |
| Hollow-section |  |  |  |

Figure 6.15: Division of axial force for I-section or Hollow section

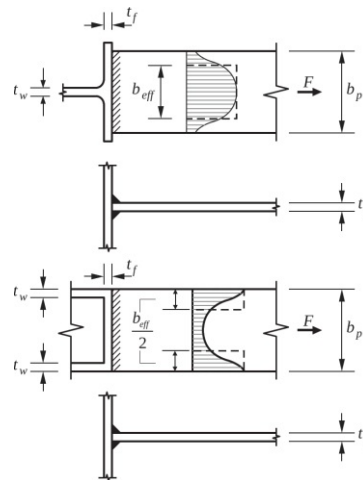


Figure 6.16: Effective width for un-stiffened tee-joints[3, p.148]

calculating the resistance will mainly be the web-welds, see figure 6.15. There is a probability that the cold-formed effective zone overlaps the effective width zone, leaving little welding length to be used for the directional method.

#### 80% criterion of welded connections

NEN-EN 1993-1-8, art 5.9(4) recommends that in general welds need to have at least 80% of the capacity of the parent material. This will allow that the welded connection has sufficient deformation capacity, which prevents brittle failure mechanisms. When optimising welds by using the directional method, the 80% criterion will serve as the minimal lower limit for the size of a weld. Following this recommendations, can limit the level of optimisation for weld volume.

#### Implementation of method in optimisation process

The distribution of forces in welds is dependent on the stiffness of the elements of a connection. This aspect makes it difficult to analyse a weld with an analytic calculation. To include behaviour due to stiffness difference IDEA Statica Connection is chosen, because IDEA Statica combines the directional method with FEM calculations, which leads to more accurate results than solely the directional method. IDEA Statica Connection will take a part in the optimisation flow through API.

IDEA Statica will be used to optimise welds. In order to perform the analysis, IDEA needs two types of files, which are the Idea Open Model (IOM) and a template. In the IOM the geometry of the joint is created, cross-sections are applied and loads are added. The IOM will be automatically created by the use of information provided by the Grasshopper+Karamba3D model. The other file is the template. The template is a predefined file that defines how the connections in the joint look like. This template is

dependent on the number of elements in the IOM. Trusses own multiple typologies of joints. Therefore in the optimisation script some cleverness will be implemented that will choose the right template with a certain IOM file.

When these two files are set, optimisation can begin. This optimisation is executed iteratively, as seen in figure 6.18. During the optimisation, the utility percentage of each weld is analysed. If the utility is above 100% in a specific weld, the throat-thickness will be increased by 1 mm. This process continues until all welds have a utility below 100%. Figure 6.19 shows how the utilization of welds decreases and the throat-thicknesses increases over the iteration in the optimisation process.

In IDEA, two cut operations are needed to create a double miter connection. This can be seen in beam DM3 and DM4 in figure 6.19. Each cut has a flange-weld and a web-weld. This makes it possible to create four different weld types with different sizes in the case of a double miter connection. However, welds are mostly standardized to one size per connection, for reasons discussed in 4.2.2.

In table 6.19, 7 differences can be seen between the number of welds of the table displaying the utilization percentage utility and the number of welds of the table displaying the throat-thickness. In "cut 1" lies the difference this is the vertical beam in the center. After calculation, results will be available for the web and both the top as the bottom flange. However, in IDEA there can only be one value set for the throat of the flange weld and the throat of the web weld. This causes that the table of throats has less columns.

Besides optimisation of welds, IDEA analyses whether the plates of the members in the joint exceed the strain criterion of 5%. When this is the case, a warning stating "failure" will be displayed in the graphic representation of the truss, see figure 8.23.

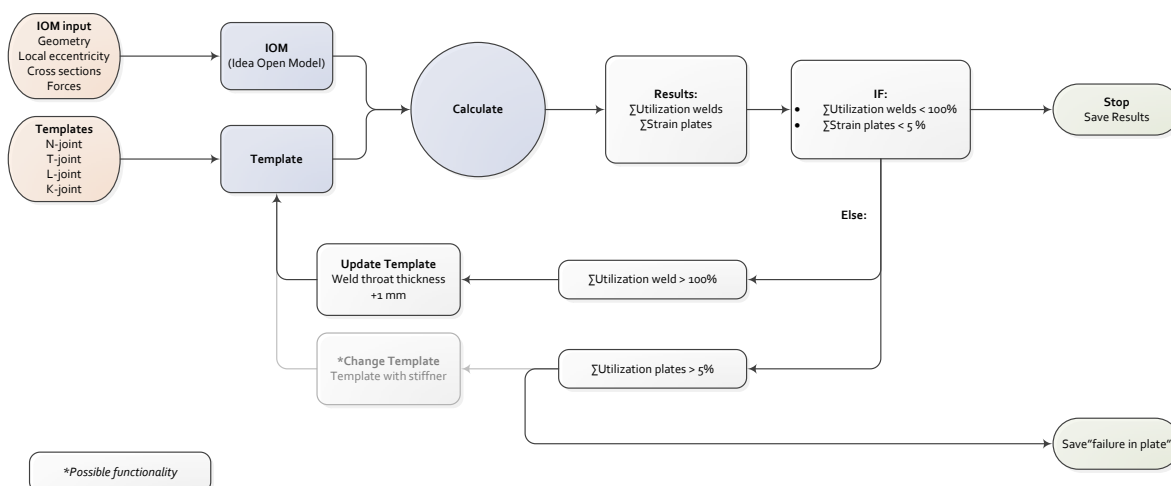
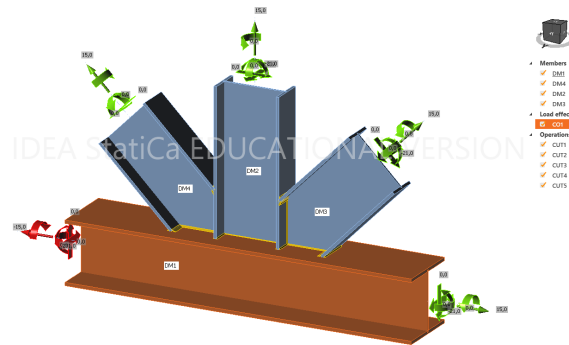
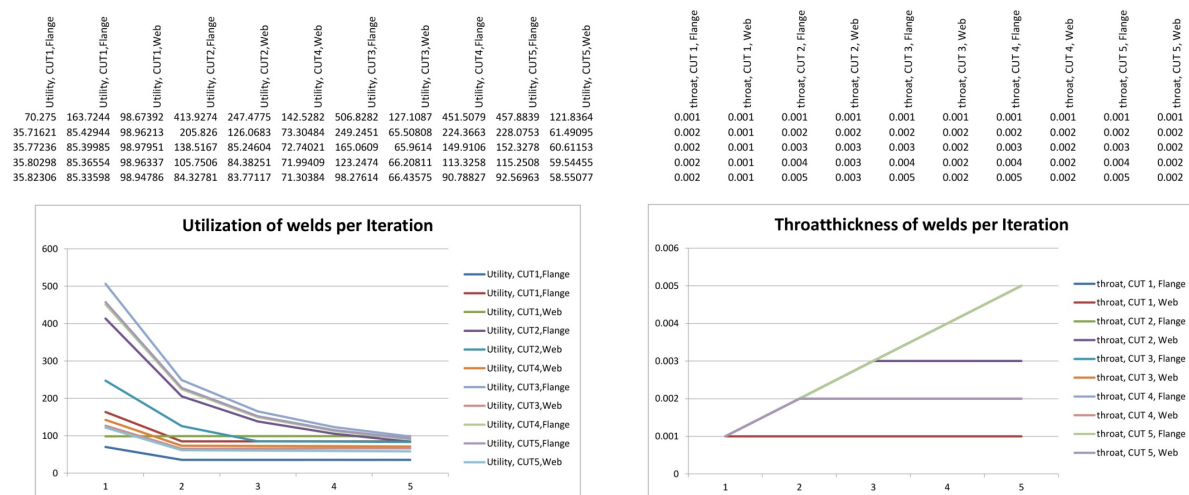


Figure 6.18: Work-flow for calculation method 3: Idea Statica Connection API



(a) Visual of connection in the IDEA Statica Connection user interface



(b) Results of optimisation process

Figure 6.19: Weld optimisation of joints in IDEA Statica Connection

## 6.4. Conclusion

The volume of a fillet weld significantly increases when the throat-thickness increases. In addition, fillet welds with wide angles create significant more welding volume than fillet welds with smaller angles.

In this research butt-welds and combinations welds will be not considered. But welds are interesting to create when plates are thicker than 20 millimeters. Combinations welds will be interesting when the throat-thickness is greater than 12 millimeters. Since these dimensions are less likely to occur for the truss-structures in the scope of this research, they will not be considered.

In this research, two methods will be used to determine the throat-thickness of a weld. First, is the full-strength method. This method from Eurocode is modified to include effect of the angle of the weld on the resistance. The second method is the directional method. This method makes it possible to optimise the sizes of welds to resist against the acting forces. This method will be used in IDEA Statica Connection by use of API. IDEA Statica combines finite element analyses with euro-code calculations. This increases accuracy since differences in stiffness are considered. However, Euro-code recommends that welded connections should have at least 80% the strength of the parent material. Following this recommendation, can cause that savings in welding volume when a applying the directional method are little.

# 7

## Model definition

### 7.1. Introduction

The work flow of the optimisation model consists out of three elements, see figure 7.1. The first element is the combination of Grasshopper with Karamba3D. They are grouped together, because they both work in the same environment. This is the main element where parameters are determined, and results are obtained. Because functionalities in Grasshopper and Karamba3D are limited, an additional script is created to fulfil these functionalities. This script is written in the C# programming language and will be referred to as the Framework. The Framework is the second element of the three elements. Besides creating extra functionalities, the Framework is used to connect the Grasshopper script with IDEA Statica Connection. The Framework will export the data of each joint in the truss structure needed for calculation in IDEA Statica Connection. IDEA Statica Connection is the third element. In IDEA Statica Connection all joints of the truss are analysed. Results of IDEA Statica will be returned through the Framework and displayed in the Grasshopper-script.

In the following sections these three elements will be discussed starting with the Grasshopper + Karamba3D, followed by the Framework. Last, I will be discuss how IDEA Statica Connection plays a role within the optimisation model.

### 7.2. Grasshopper + Karamba3D

The Grasshopper script serves as the main script where parameters are determined and results are obtained. In figure 7.2, both a print-screen of the Grasshopper script as a schematic representation can be found. As discussed in section 1.5 of this research certain steps need to be taken in the optimisation work-flow. The optimisation model has the same steps towards achieving this goal. First geometry is created. This geometry is analysed by Karamba3D with the correct loads and boundary conditions. Afterwards the joints will be designed in a custom made Grasshopper-component according

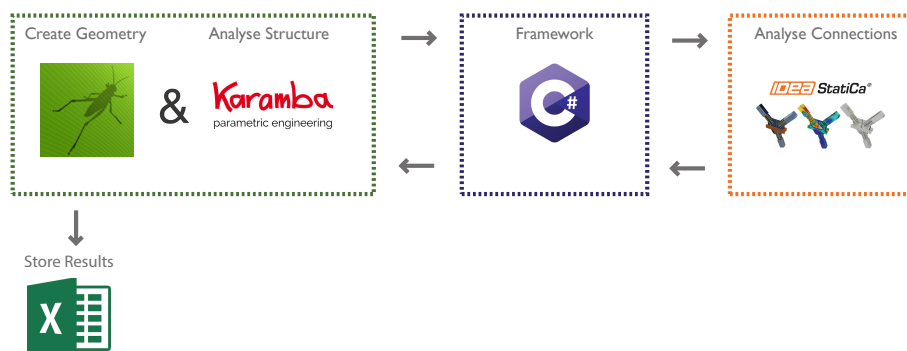
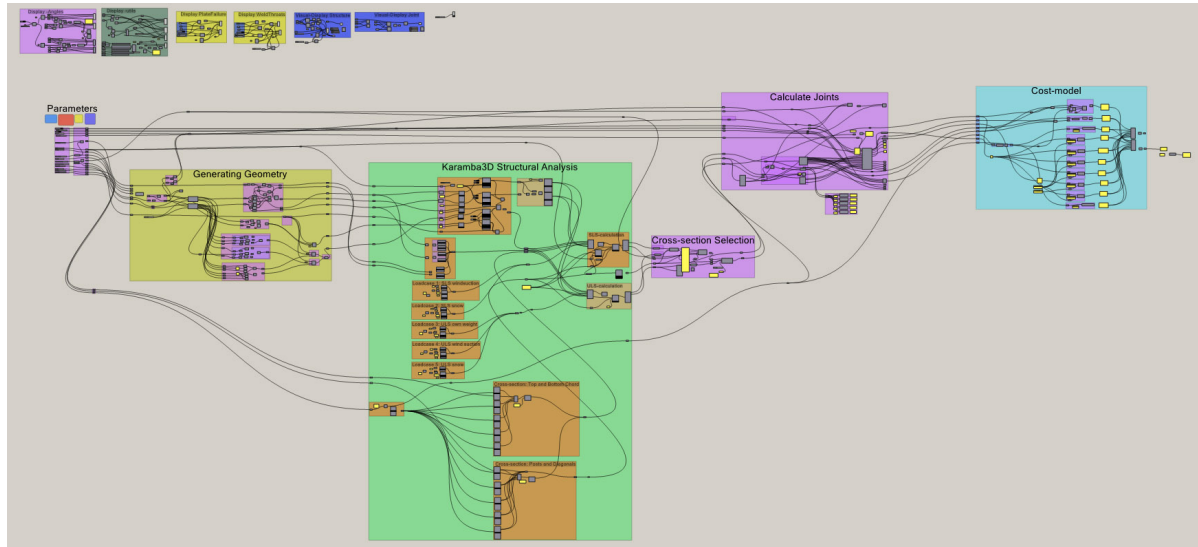


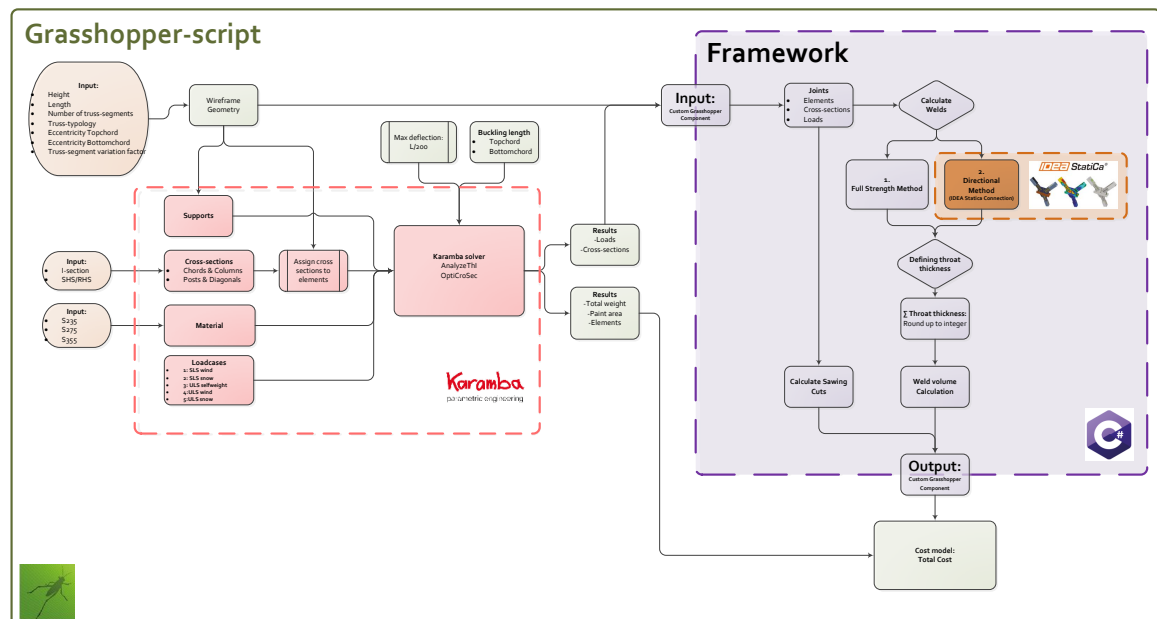
Figure 7.1: Model workflow



to the hierarchy list, which will be discussed in section 7.2. From here on, the full-strength method will be used by default to calculate the needed welding volume. In the final step, the total price of the structure will be calculated according to the cost-model.



(a) Grasshopper script



(b) Schematic overview

Figure 7.2: Work-flow for Cost-optimisation of steel structures

### Custom Grasshopper Component

Grasshopper is linked with the Framework through a custom Grasshopper component. This component imports all necessary information needed to calculate the number of sawing cuts per elements and the total welding volume of the structure. The total welding volume calculated, depends on the type of analysis method, which can either be the full-strength method or the directional method, that will be performed in IDEA through API.

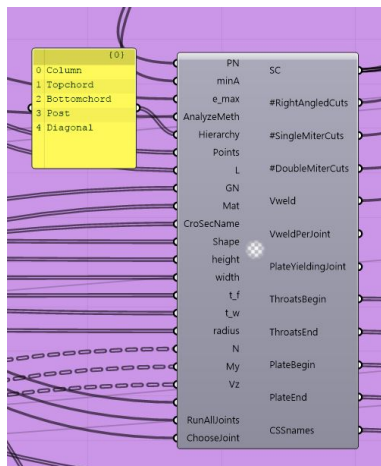


Figure 7.3: Custom Grasshopper Component

| Input     | Description  | Output | Description           |
|-----------|--|--------|-----------------------|
| PN        | Project-name   | SC     | Number of Sawing Cuts |
| minA      | Minimum throat thickness                                   | Vweld  | Total welding volume  |
| $e_{max}$ | Maximum eccentricity                                       |        |                       |
| Ana       | Analysis method, either Full Strength, Directional or IDEA |        |                       |
| H         | Hierarchy List   |        |                       |
| P         | Point that represent Joints                                |        |                       |
| L         | Lines of elements  |        |                       |
| GN        | Groupnames of elements                                     |        |                       |
| Mat       | Material of elements                                       |        |                       |
| CSS       | Cross-section of elements                                  |        |                       |
| S         | Shape of elements  |        |                       |
| h         | Cross-section height                                       |        |                       |
| w         | Cross-section width  |        |                       |
| $t_f$     | Thickness flange   |        |                       |
| $t_w$     | Thickness web  |        |                       |
| r         | Radius of cross-section                                    |        |                       |
| N         | Axial force  |        |                       |
| My        | Moment force   |        |                       |
| Vz        | Shear force  |        |                       |

Table 7.1: Description of input and output

### Hierarchy of elements in joints

In the Framework, a hierarchy list is needed to make sure that joints are created in the desired configuration. This hierarchy list is a list of the group-names of the elements in the structure. Here, the first group-name has the highest priority and the last group-name has the lowest priority. This list is needed because multiple configurations in a joint are possible, see figure 7.4. These preferences can vary per project, therefore it is desired to use a list that can be adjusted by the user.

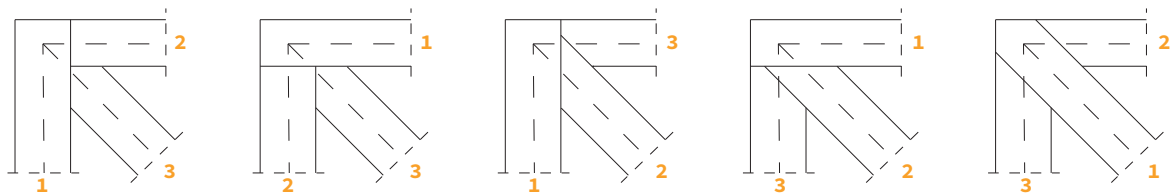


Figure 7.4: Possibilities of joint layout based on hierarchy

In the optimisation cases of this research, the following hierarchy of group-names is used: Column, Topchord, Bottomchord, Post and Diagonal. These group-names can be found in both the Pratt and Warren truss, see figure 7.5. The yellow panel with the hierarchy can be seen in figure 7.3 and serves as input for the custom Grasshopper component.

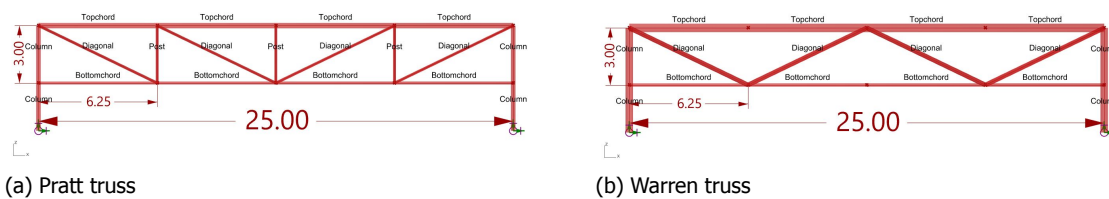


Figure 7.5: Group-name of members in both trusses

### Cost-model in Optimisation model

In 7.6 a flowchart is displayed that shows which input variables are used to generate the total cost of the truss structure. All processes discussed in chapter 4.3, can be identified with the corresponding code and name.

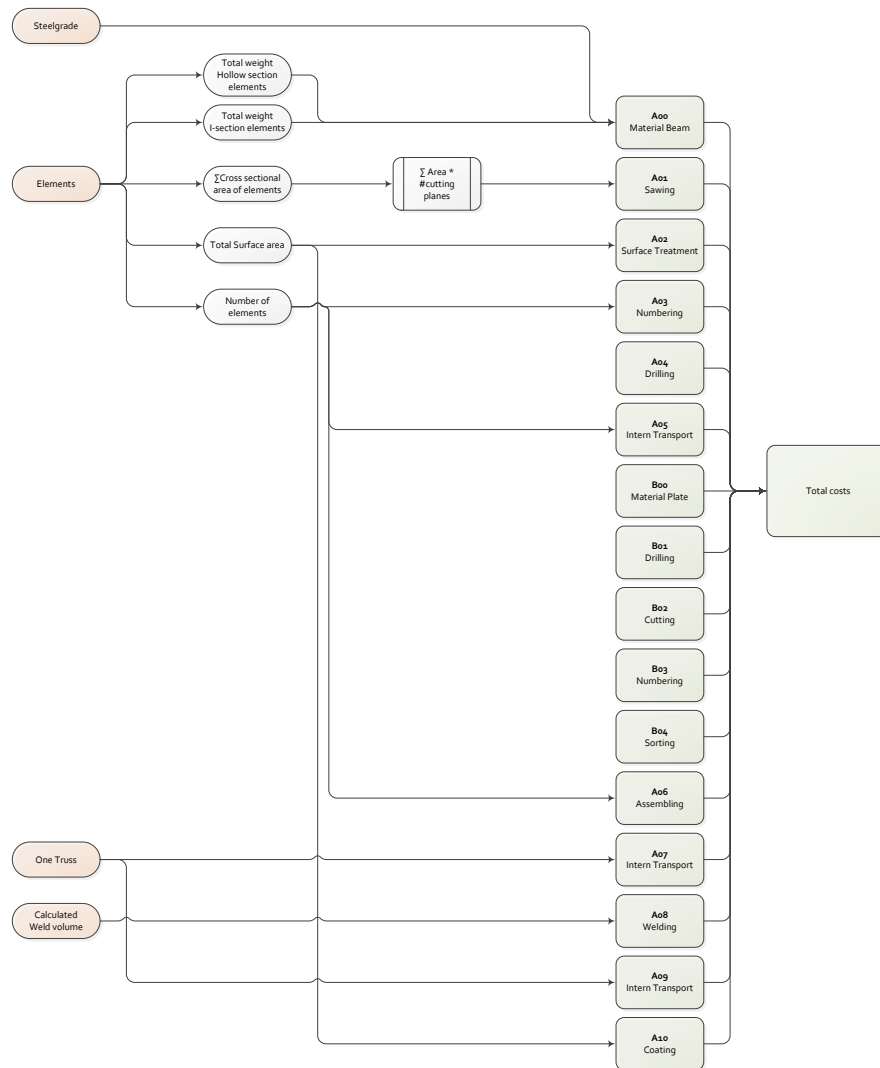


Figure 7.6: Input process for cost calculation

## 7.3. Framework

### Creating a Project

Each moment a new truss is generated in the Grasshopper script, a new project will be created in the Framework. Here all imported information from the custom Grasshopper component, will be ordered in a manner that is useful for the analysis of joints. Figure 7.7 displays how the information will be ordered. The top level in this order is the project. The project has multiple objects. For example, the load-cases, the elements, the hierarchy list and the joints.

The two most significant objects in the Framework that are part of the project are the Element-object and the Joint-object. These will be further elaborated on in the paragraphs below.

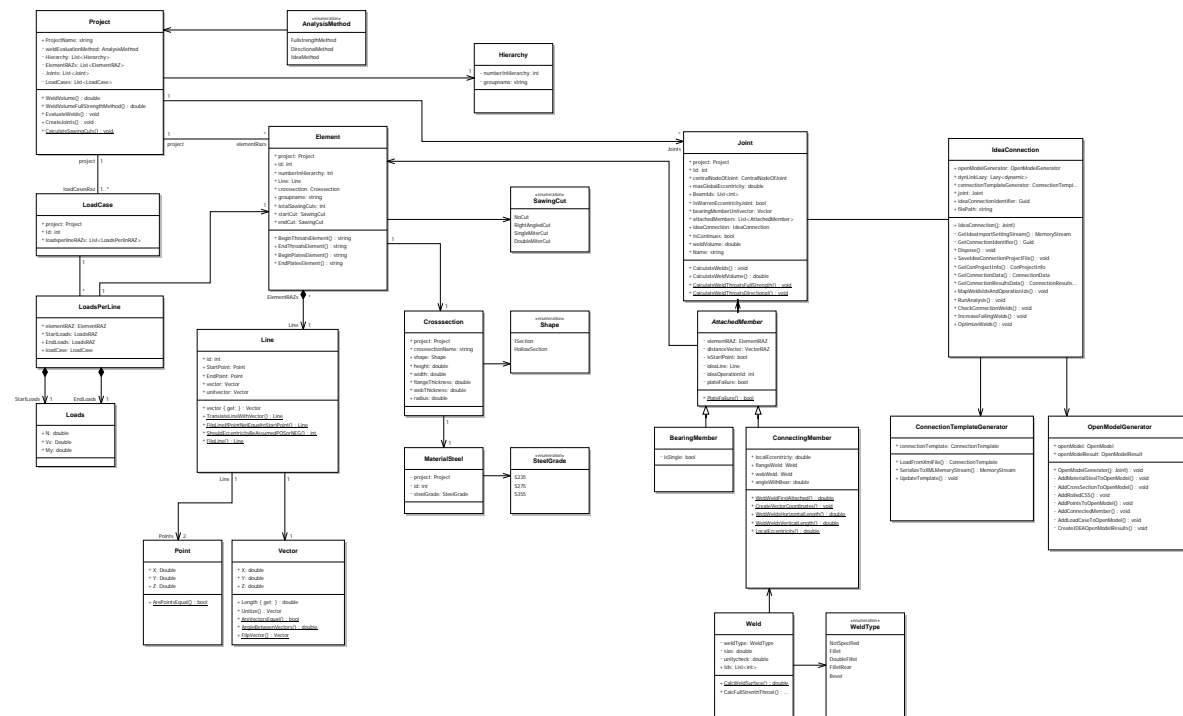


Figure 7.7: UML diagram of Framework

### Creating Element objects

From the list obtained from Karamba3D which imported imported through the custom Grasshopper component, element objects will be created. These elements have a project, an ID-number, a line, a cross-section, a group-name (figure 7.5), total number of sawing cuts needed for the elements, and a type of sawing cut for the start and the end position of the element.

### Creating Joint objects

**Tolerance-box** To create Joint objects, a tolerance box is used. This tolerance box is centered at the point where joints will be assumed, the tolerance boxes are displayed as yellow boxes in figure 7.8. The tolerance box makes it possible to obtain the appropriate elements from the model for the joint, even in the case of eccentricity joints. Since the elements with tiny line-lengths that create eccentricities in the Grasshopper model, are not needed for calculation, the following rule is used to find attached members of a joint:

*Rule: Every element that has a line with a start or endpoint that falls within the tolerance box range and a length longer than the eccentricity is an attached member of the joint.*

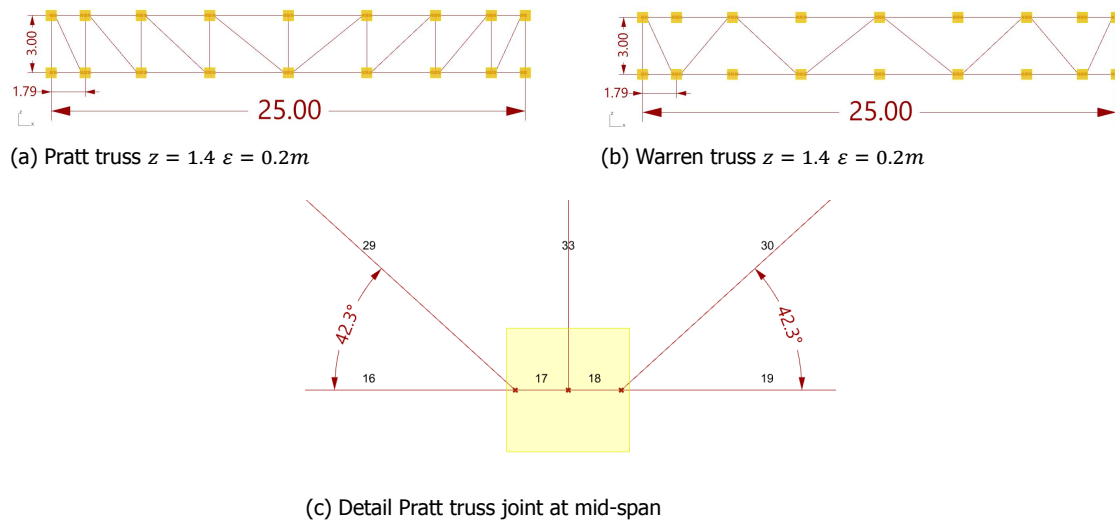


Figure 7.8: Visual representation of tolerance boxes needed to create joint objects

**Defining global eccentricity per element** To use the equations presented in table 4.2 in calculating the welding volume and the quantity of sawing cuts, a global eccentricity of the joint is needed. The global eccentricity is the vector of the eccentricity elements that starts from the central node of the joint. This vector is called the distance vector. In figure 7.8, elements 17 and 18 represent eccentricity elements. In addition, this distance vector is needed to repack the eccentric joint into a centric joint, which will make it possible to import the joint to IDEA Statica Connection. Within IDEA the eccentricity is recreated. This will be discussed in section 7.4. The distance-vector is obtained by the following rule:

*Rule: If the lines of two elements found within the tolerance box of the joint have a common point, which is not the center-point of the joint, and the lines have an identical direction vector or the inverse, then the vector from this point towards the center-point is the distance vector with a particular length that represents the global eccentricity.*

**Hierarchy, Bearing Members & Connecting Members** Attached members will be split into Bearing-Members and Connecting-Members based on the hierarchy. Bearing-Members are the one or two members with the highest hierarchy of the attached members. In the case of two Bearing-Members being present in the joint, the bearing-members create a continuous beam. In case that one Bearing-member is present in a joint, the beam is ended as displayed in figure 7.4. The Bearing-member defines the local-x axis, from where angles to connecting members will be calculated. Angles will be calculated on basis of the vector by the following equation:

$$\theta = \cos^{-1}\left(\frac{\vec{u} \cdot \vec{v}}{||\vec{u}|| \cdot ||\vec{v}||}\right) \quad (7.1)$$

It may occur that multiple connecting members have the same hierarchy, as the diagonals in Warren Trusses. In this case, the connecting member in the same hierarchy with the highest angle towards the bearing-members is higher in this sub-hierarchy. When the angles are identical, the first found element has the higher hierarchy.

**Warren Truss empty joints** In the case of Warren Trusses, it can occur that the points that are expected to be joints are not a joint, but a continuous element, see figure 7.8. This can occur because a method is applied that is both applicable for Pratt and Warren trusses. These continuous members are identified and prevented to serve a joint by the following rule:

*Rule: If the joint has only two Attached-Members that has the same direction vector or the inverse, then it is not a joint.*

**Warren Truss eccentricity joints** In the case of an eccentric joint in a Warren truss, the value of eccentricity should be doubled when calculating the length of the web weld with the equations presented in table 4.2. To identify these kind of joints the following rule applies:

*Rule: If the center-point has only two lines attached that have the same direction vector of the inverse, then the joint is a warren-joint with an eccentricity.*

### Calculation of Sawing cuts

To determine the amount of sawing cuts needed for the cost-model, the number of sawing cuts per element is needed based, on the type of sawing cut. There are several type: "No cut", "Right-angled cut", "Single miter cut", "Double miter cut", as described in section 4.3.2.

Every element in the Framework has two sawing cuts, one at the start point and one at the end point of the line of the element. The types of sawing cuts needed for both sides of the element, are calculated with the equations presented in table 4.2. By default, the start-cut and end-cut of every element is from the type "No cut". Application of the equations in the table, will generate two lengths of intersection. If one of these lengths is zero and the angle between the connection member and the bearing member is  $90^\circ$ , it is a "Right-angled cut". If one of these lengths is zero and the angle between the connection member and the bearing member is not  $90^\circ$ , it is a "Single miter cut". When two non-zero lengths are presented the sawing-cut is a "Double miter cut".

The total number of sawing cuts of the truss, and the number of double miter cuts will be sent back to the Grasshopper model.

### Calculation of Weld volume

Within the model, four situations of welded-connections are possible, see figure 7.9. First, the welding volume depends on the sections type. For an I-section more welding length is needed to create the welded connection. Second, the weld volume is influenced by the surface it is projected on. This can either be a flat surface or a kinked surface. Kinked surfaces occur when the joint has overlapping beams. In the figures, the welds of the flanges are coloured orange and the welds of the web are coloured green. The volume of the welds of the flanges is influenced by the angle of inclination of the connected member as discussed in section 6.2. The welding length of the flanges is equal to the width of the section.

The weld volume of the web is not influenced by the inclination, because it will always have an angle of  $90^\circ$ . However, the welding length is influenced by this inclination. The welding length of the web weld is calculated for both flat surface, as for kinked surface situations by using the calculations presented in table 4.2.

To calculate the welding volume the throat-thickness of the weld is needed. This throat-thickness will be calculated by default with the full-strength method. Here, the throat-thickness will be rounded to an integer and will be equal or greater than the minimal required throat thickness. The other method to determine the throat-thickness of all welds and therefore the weld-volume, is the directional method, which will be implemented by use of IDEA Statica Connection through API in the optimisation workflow.

Table 7.2: Parameters of weld volume calculation per connection

| Parameter                        | Symbol   |
|----------------------------------|----------|
| Throat-thickness of flange-welds | $a_f$    |
| Throat-thickness of web-welds    | $a_w$    |
| Width                            | $b$      |
| Vertical segment                 | $l_v$    |
| Horizontal segment               | $l_h$    |
| Angle                            | $\alpha$ |

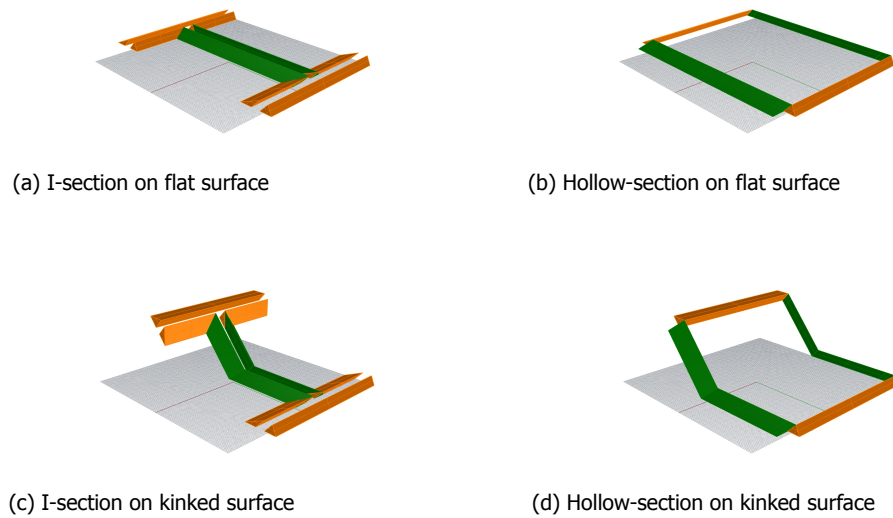


Figure 7.9: Weld-volume definitions for all possible situations

## 7.4. IDEA Statica Connection

Karamba3D and IDEA Statica connection are both software packages used for structural analysis. These two software packages have differences. The most important difference for this research, is the discrepancy between the definitions for local axes and how eccentricities in joints are created. In this section strategies will be presented that will be used to correctly import loads and geometry from the Karamba3D model to IDEA Statica connection.

The process of how welds are optimised within IDEA will not be discussed in this section, since this has been discussed in section 6.3.2.

### Import of loads from Karamba3D to IDEA Statica Connection

Karamba3D and IDEA Statica Connection has the same coordinate system[52][51, p.108]. Where the x-axis of the global coordinate system is horizontal and leads from left to right, the y-axis is horizontal and leads backwards and z-axis is vertical and leads upwards, because only 2D calculations will be performed in the XZ-plane, only "N", "Vz" and "My" will be addressed. The assumed positive direction of these forces is the following:

1. N - Positive axial force N acts in direction of the local x-axis of the member and causes tension in the cross-sections fibers.
2. Vz- Positive shear force Vz acts in the direction of the local z-axis.
3. My - Positive bending moment My causes tension in the cross sections fibers with a positive local z-axis.

To correctly import loads obtained from Karamba3D to IDEA Statica Connection, few steps need to be taken. These steps will be discussed in this paragraph and are visually displayed in figure 7.11. In this figure the local axis definition of Karamba3D and IDEA Statica Connection are drawn different on purpose, because local axes are defined differently. In Karamba3D the local axis is determined by the start and end point of the element. In IDEA the local axis is determined from the center point of the joint pointing outwards in the direction of the member.

**1: Local coordinates of Karamba3D to Framework** The local coordinates of a loaded element in Karamba3D are determined by the start and end point of the line of the element. When an element is attached to the joint with its start point, no change is needed. If the element is attached to the joint

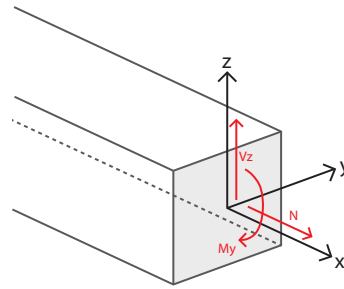


Figure 7.10: Global coordinate system of Karamba3D and IDEA Statica Connection

with its end point, both the sign of the moment force as the shear force needs to be changed.

*Rule: If element is attached with the end point to the joint, multiply shear force and moment force by -1*

**2: Framework to Local coordinates of IDEA API** The direction of a member in IDEA and therefore its local coordinates are determined by the  $\beta$  – *direction* and the  $\gamma$  – *pitch* from the central node.  $\beta$  starts from the x-axis and runs in the horizontal plane (XY-plane) with a range from  $-180^\circ$  up till  $180^\circ$ . From this direction in  $\gamma$  applies a pitch to the member. This range is constrained between  $-90^\circ$  and  $90^\circ$ .

In the scope of this research only 2D joints will be examined that are positioned in the XZ-plane. This causes that  $\beta$  is either  $-180^\circ$  for members left of the central node or is  $180^\circ$  for members right of the node, depending on the member's direction if it is left or right from the joint in the XZ-plane. This different local axis influences the positive direction of shear force and bending moments. The member's direction is left from the joint when the x-coordinate of the vector of that element is smaller than zero. To import the loads from the Framework to the IDEA API the following rule is applied:

*Rule: If the x-coordinate of the vector is smaller than 0, multiply shear force( $V_z$ ) and moment force( $M_y$ ) by -1*

**3: From API to IDEA User Interface** When the loads are defined in the API of IDEA, they have a different sign when IDEA is opened in the user interface and the loads are checked. Shear forces and bending moments are negatively imported in the user interface when are positively defined in the API. To compensate this effect, the following rule applies:

*Rule: Multiply shear force( $V_z$ ) and moment force( $M_y$ ) by -1*

### SLS and ULS analysis in Model

Both SLS and ULS calculations will be used to determine the cross-sections needed for elements in the truss structure. However, in IDEA Statica only the ULS load combinations will be used to analyse the joint, because only the utilization of elements needs to be considered and not the deflections. Only considering the ULS load combinations will reduce the calculation time needed to analyse the joint.

### Importing eccentric joints from Grasshopper to IDEA Statica Connection

Eccentric joints cannot be imported directly into IDEA Statica Connection. A centric joint needs to be imported, eccentricities in this joint will be applied afterwards. The following paragraph will explain how geometry and loads will be imported from Grasshopper+Karamba3D to IDEA Statica Connection.

IDEA defines eccentricities in a different method than the method used to define eccentricities in the Grasshopper model. In IDEA the eccentricity is defined as the shortest distance from the force towards



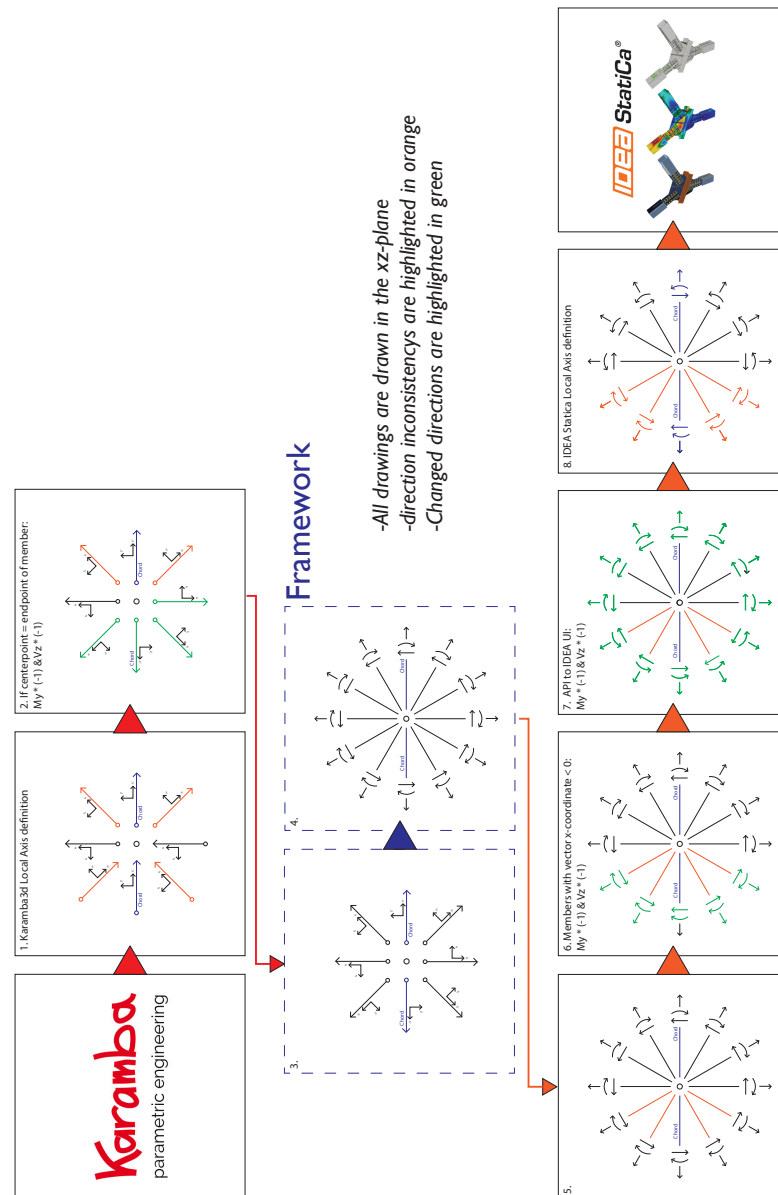


Figure 7.11: Importing load values from Karamba3D to IDEA StatiCa Connection

the node of the joint, for sake of simplicity we call this the local eccentricity,  $\varepsilon_{loc}$ . In the grasshopper model the eccentricity is the displaced distance along the line of the chord, we call this the global eccentricity. To calculate the local eccentricity needed for IDEA, equation 7.2 is used.

$$\varepsilon_{loc} = \frac{||\vec{AC} * \vec{v}||}{||\vec{v}||} \quad (7.2)$$

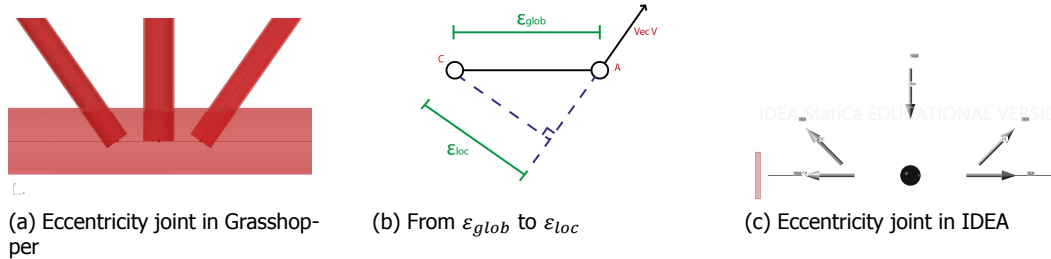


Figure 7.12: From global to local eccentricity

**Negative and positive local eccentricities in IDEA** In IDEA the eccentricity will be applied according to the local axis of the member. The local z-axis defines lateral eccentricities of the member in XZ-plane. If the member has a negative  $\gamma - pitch$ , it is located below the "horizontal plane", the local eccentricity will lead to a desired positive global eccentricity. However when a member has a positive  $\gamma - pitch$ , it is located above the "horizontal plane", the local eccentricity will lead to an undesired negative global eccentricity.

This problem can be solved by analyzing the vector of the member, where its starting point is the central-node. Here the z-coordinate of the vector should be checked. If  $\vec{v}_z < 0$  the result is desired. If  $\vec{v}_z > 0$  the result is undesired and should be multiplied by  $-1$ . This will make sure that eccentricities are implement into IDEA as needed.

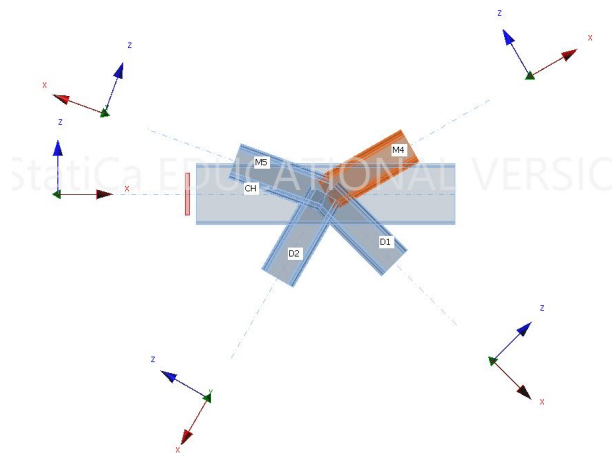


Figure 7.13: Local z-axis of members in IDEA pointing in different directions depending on above or under "horizontal plane"

**Translation of Elements-line for implementation in IDEA** In IDEA, first the geometry is created where every member is attached to the center-node. Afterwards the eccentricities are defined. However, in the Grasshopper-model the eccentricities are created within the geometry. Therefore, to allow eccentricity joint from being implemented from Grasshopper into IDEA, a strategy is needed. This is achieved by creating new line definitions for attached members of a joint in Grasshopper. These lines are translated by the global eccentricity. This creates an idealized joint with no eccentricities that

can be implemented in IDEA. Afterwards the right negative, or positive local eccentricity can be applied to the member. This will result in identical geometry compared to the Grasshopper model.

**Load definitions in case of eccentricity joints** In figure 7.14 is displayed how eccentricity joints in the model are converted to centric joints, and made eccentric again in IDEA Statica. When the eccentricity is applied to the diagonals, the forces are positioned back to their original position. The chord consists out of two members in Karamba3D. These two elements are translated as well to create the centric joint needed to import the joint into IDEA. However, IDEA defines the chord as one member. This causes that only one eccentricity can be applied to the chord member. This will cause that the additional bending moment created by the shear forces of the two chord members will be lost.

This causes that the model in IDEA will be less severely loaded. Which could potentially lead to an underestimation of the acting forces. However, these shear-forces in the chord will be relatively low, especially in the case of the bottom-chord where axial forces are dominantly present. In addition, the eccentricity will be very small, creating a small bending moment. Furthermore, the shear forces will mostly point into equal direction which will cause that they compensate each other in terms of bending moments.

When importing the loads, to eccentric joints, to IDEA, equal boundary conditions must be applied. This will be performed by importing the loads of the attached members at the side of the central-node of the joint. This will cause that force distribution over the eccentricity will be recreating within the IDEA analysis.

## 7.5. Conclusion

Beams within a steel structure are ranked according to a particular hierarchy. This hierarchy defines which beams are continuous and which are connection. The hierarchy of beams is an absolute necessity when structural design of the main structure is combined with detail engineering of the joints. The hierarchy will allow that the joints will be designed as intended within the optimisation model.

Connecting multiple software packages in a work flow, requires time and effort. Information needs to be exported and imported in methods that are required by the software package. These sets of methods are created in a Framework. The Framework will process the information according to predefined rules into desired output. Importing eccentric joints from Karamba3D to IDEA Statica connection shows a high level of complexity, since both packages define local axes and eccentricities differently. With the correct set of rules these differences can be compensated. This allows that the optimisation model works as desired and generates the desired results.

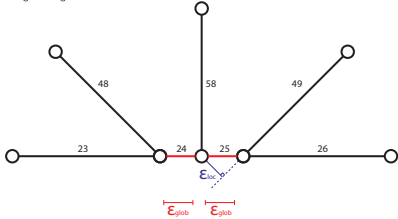
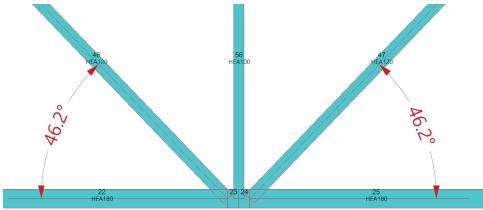
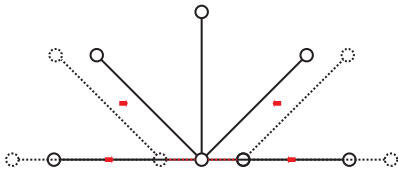
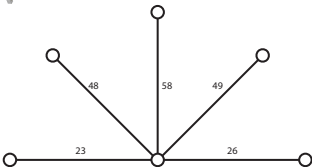
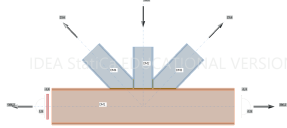
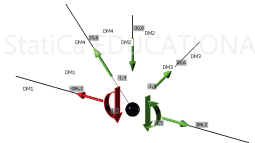
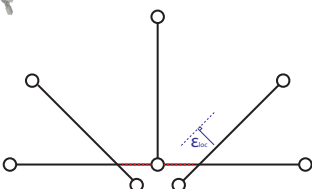
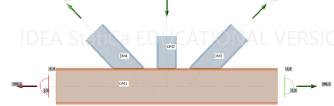
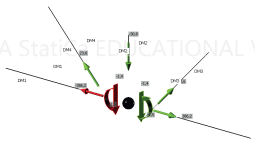
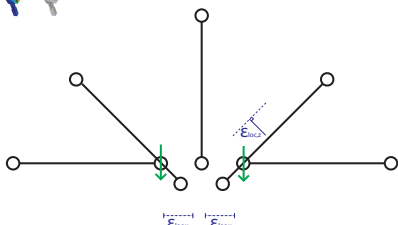
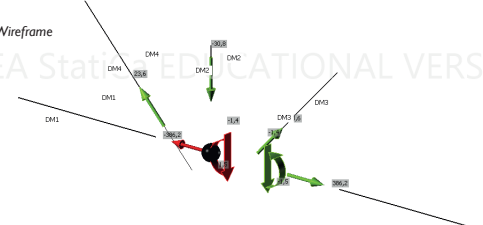
| Schematic Explanation  | Presentation in Software  |
|--|---|
| <p><b>Karamba</b><br/>parametric engineering</p>    |   |
| <p><b>Transform Eccentric joint to centric joint:</b><br/>Global eccentricity stored as local eccentricity</p>  |   |
| <p><b>Import in IDEA:</b><br/>Import as centric joint</p>    | <p>Transparent</p>  <p>Wireframe</p>   |
| <p><b>Result in IDEA:</b><br/>Loss of additional bending moment caused by chord shear forces</p>              | <p>Transparent</p>  <p>Wireframe</p>  |
| <p><b>Desired result in IDEA:</b><br/>Include additional bending moment caused by chord shear forces</p>      | <p>Loads on chord cannot be made eccentric into two directions.</p> <p>Wireframe</p>                                      |

Figure 7.14: Importing eccentric joint into IDEA StatiCa Connection



# 8

## Cost Optimisation of Trusses

The wide range of parameters available in the optimisation model creates the possibility to analyse many different types of trusses. This chapter will illustrate the possibilities that are available in the optimisation model, to optimise a truss structure. A reference truss is used to illustrate the influence of every parameter in the optimisation model. The optimisation model can perform two optimisations methods. In the first type, the weld sizes are calculated according to the full-strength method. This is a relatively fast optimisation method, which allows the production of a great set of data, but will create variants with a lower economic use of welding material. In the second type, the weld sizes are optimised by using the directional method in IDEA Statica Connection. This creates a truss with an economic use of welding material, but this optimisation method is relatively slow. Therefore, while using the optimisation model a large data set is first created with the full-strength method. Consequently, a variant is selected for this data set, for an additional weld volume analysis.

### 8.1. Parameters and boundary conditions

In table 8.1 all variables of the optimisation model are shown. The table describes per variable whether they will be used static of dynamic in this case-study.

Table 8.1: Parameters

| Number | Variable                          | Unit                 | Use in Research | Reference-truss |
|--------|-----------------------------------|----------------------|-----------------|-----------------|
| 1      | Height Structure                  | m                    | Static          | 10 m            |
| 2      | Length                            | m                    | Static          | 25 m            |
| 3      | Minimal weld size                 | mm                   | Static          | 4 mm            |
| 4      | Height Truss                      | mm                   | Dynamic         | 2500 mm         |
| 5      | Segments                          | pcs                  | Dynamic         | 8 pcs           |
| 6      | Truss-typology                    | Truss-type           | Dynamic         | Pratt           |
| 7      | Material                          | Steel-grade          | Dynamic         | S355            |
| 8      | Cross-section Chords and Columns  | Cross-section Family | Dynamic         | HEA             |
| 9      | Cross-section Diagonals and Posts | Cross-section Family | Dynamic         | HEA             |
| 10     | Buckling length chords            | m                    | Dynamic         | 6.25 m          |
| 11     | Eccentricity Topchord             | mm                   | Dynamic         | 0               |
| 12     | Eccentricity Bottomchord          | mm                   | Dynamic         | 0               |
| 13     | Variation factor                  | dimensionless        | Dynamic         | 1.0             |

#### Boundary conditions

**Height and Length** In section 3.1 the maximum transport dimensions with a continuous permit have been discussed. These maximum transport dimensions will serve as boundary conditions in the case-study. Therefore, a span of 25 meters is chosen with a maximum height of 3 meters. The maximum height of 3 meters allows that multiple truss can be stacked on one trailer.

The span of the truss structure is a static variable in the case study. Smaller spans will not be considered, since this will lead to variants with lower costs. This is because bending moments will be of a smaller magnitude. The height of the structure is a static variable as well. This height of 10 meters has been discussed in section 5.2. It has influence on the wind load that may be assumed according to Eurocode.

The height of the truss structure is chosen to be a variable with a maximum value of 3 meters. Variation in the height of the truss can lead to variants that have a higher rate of constructability. For example, a minimized number of double miter connections and a minimal angle of inclination of the diagonals.

**Buckling length** The buckling length of top and bottom chord is assumed to be 6.25 meters by default. Here, the top and bottom chord of the truss is divided into four segments, with three buckling supports. In section 8.4.3, the influence of varying the buckling length of the top and bottom chord will be investigated. For other cases, the buckling length will remain 6.25 meters, because the amount of buckling support influences the costs of the 3D structure, which falls out of the scope of this research. Keeping the buckling length equal for all variants will prevent drawing misleading conclusions when costs of creating extra buckling supports are not considered.

**Welded connections** Only welded connections are assumed in the case-study. This is also the case for the joints that connect the truss with the right and left column. Ideally these connections should be modelled as bolted connections. This would allow the truss to have dimensions that fall within the transport dimensions. Since bolted connections fall out of the scope of this research, the joints attached to the columns are assumed as welded joints. Furthermore all welds will be fillet welds with a minimal throat-thickness of 4 millimeters.

**Calculation of welds** In all variants, the amount of welding volume is calculated by using the full-strength method. Some variants will be analysed using the directional method to determine the weld volumes. Since the directional method is performed by IDEA Statica Connection through API, it is a relatively slow method. On average it takes approximately 30 minutes to optimise all the welds of a truss. Therefore, not all variants can be analysed by the use of the directional method.

**Groups of elements** The members in a truss are grouped, each group has equal cross-sections. Examples of groups in the case-study are: columns, top-chords, bottom-chords, posts and diagonals. In the case-study, columns, top-chords and bottom-chords are selected from an identical cross-section family. Post and diagonals will be from an identical cross-section family as well.

In table 8.2 the main aspects where variants will be graded on, are displayed. The total production costs will be presented as a percentage to the reference truss. To give insight into the cost build up, the four main cost contributors are displayed as well. This is the total weight of the structure, the welding volume, the surface area and the number of sawing cuts. These four main cost contributors are displayed in an amount and not in prices. This makes the values undebatable.

In addition, constructability aspects are also considered. First the amount of double miter connections is checked. It is preferable when this amount is as small as possible, because it reduces risks in production as discussed in chapter 4.2. Secondly, the angles of diagonals will be checked. The angle of inclination must be greater than the required minimum of 40. This allows enough space for the welding torch and makes it possible to easily create a connection with fillet welds.

Table 8.2: Results of variants

| Cost-aspects | Description  | Aspect           | Goal     |
|--------------|--|------------------|----------|
| 1            | Production costs percentage related to reference truss | Cost             | Minimize |
| 1a           | Weight   | Cost             |          |
| 1b           | Welding volume   | Cost             |          |
| 1c           | Surface Area   | Cost             |          |
| 1d           | Sawing Cuts  | Cost             |          |
| 2            | Number of double Miter connections                     | Constructability | Minimize |
| 3            | Inclination of Diagonal                                | Constructability | Min 40°  |

## 8.2. Reference Case

The goal of the cost-model is to provide insight in price variation between variants and not to give an exact total production cost. To display this price variation, a reference truss is used. From this reference truss, the variation of total production costs will be displayed in percentages. The reference truss is will have a production cost of 100%. Variants produced in the optimisations will have a percentage higher, lower or equal. This will make comparison evident.

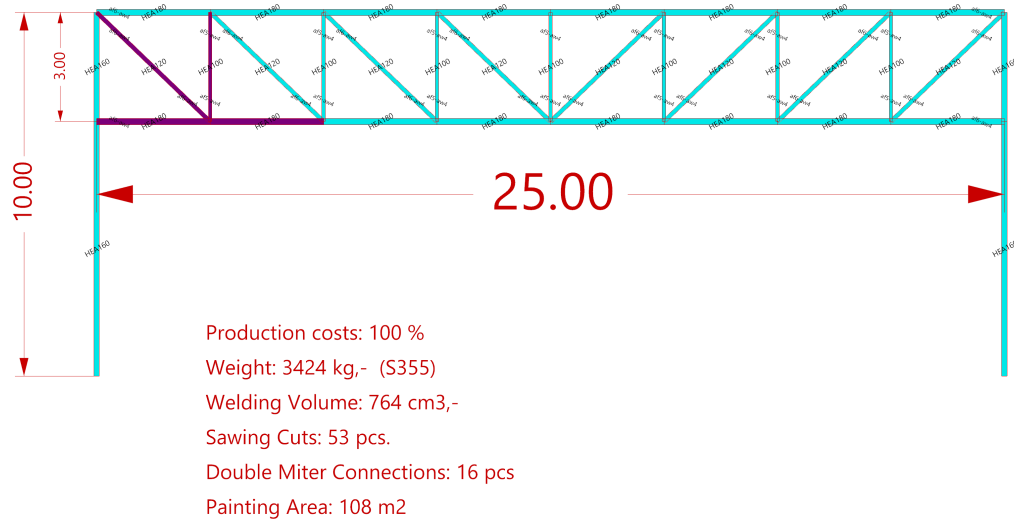
The reference truss presents a truss that would have been designed in engineering practice based on experience. In other words, without the help of an optimisation model.

For the reference truss, the Pratt-truss typology is chosen, because this typology is easier to fabricate since the posts act as spacers between the chords. The truss height is the maximum height of 3 meters. This increases the efficiency of the truss, because the arm increases the resistance capacity for bending moments.

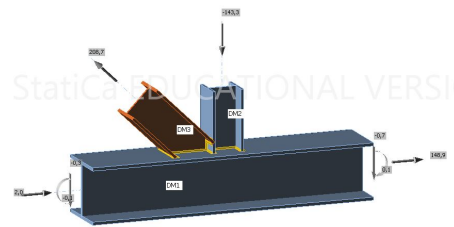
The truss has three buckling supports over its span of 25 meters, leading to four sections with a buckling length for both the bottom and top chord of 6.25 meters. A truss with 8 segments is chosen, this causes that the truss has a post at every buckling support. This causes the diagonals of the truss to have an inclination of 43.8°. S355 is chosen as steel grade, since it is the strongest steel grade in the scope of the case-study and it will most probably lead to a lighter total weight of the truss, due to the higher strength properties. In the reference case, all cross-sections are from the HEA cross-section family, because of their cheap unit price. All defined parameters for the reference truss can be found in the right columns of table 8.1.

In figure 8.1, an overview drawing is displayed. Here, the detail of most critical joint in the truss can be found. The location of this joint is highlighted in purple in the overview drawing. This joint is the most critical joint since it is the joint most closely located to the supports, here axial forces in the diagonals are the highest. Because the joint is responsible for transmitting this high axial force from the diagonal to the chord, this joint will be governing. In IDEA Statica Connection is analysed whether the plates of a member in these joints stay within the 5% strain criterion. If this strain criterion is exceeded, a bigger section is needed for the respective member. Afterwards the strain analyses will be performed again, to check whether the strain criterion is fulfilled.





(a) Truss with detail highlighted



(b) Detail with ULS Snow-load forces

Figure 8.1: Reference truss with a cost of 100%

### 8.3. Singularity in IDEA Statica Connection

In some cases IDEA Statica Connection cannot perform its finite elements analysis, because it is unable to converge due to singularity in the model. This singularity can be caused by missing parts (welds) or mesh-planes that overlap [53, 3.11]. This issue of singularity causes difficulty in finding an appropriate reference truss. Ideally, SHS sections are chosen for the posts and the diagonals of the truss, because of higher buckling resistances compared to I-sections and their absence of a weak axis compared to RHS sections. However, a variant with SHS diagonals and posts causes the mesh that represents the welds in IDEA Statica Connection to overlap, see figure 8.2. This overlap causes that the finite element analysis is not able to converge.

The overlapping welds are caused by the geometry. Changing the geometry in the IDEA model, e.g. changing the type of cross-section or the inclination of the member, can cause that welds are not overlapping anymore, and singularity does not arise. However, the geometry is created in the Grasshopper model by the parameters. It can be beneficial to create an extra check in this model to give an indication whether there is sufficient spacing between the welds. This would prevent the analysis in IDEA to fail due to singularity and increase the level of constructability of the truss.

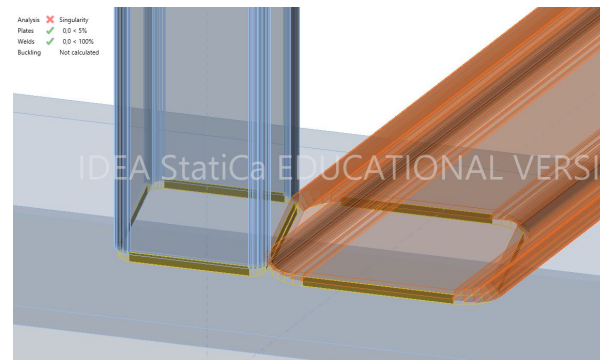


Figure 8.2: IDEA StatiCa Connection model where singularity arises due to overlapping meshes that represent welds

## 8.4. Full-strength method analyses

In this section the influence of all dynamic parameters presented, in table 8.1, will be analysed. For this analysis, the reference truss will be used as a starting point. In every section, variation will be only applied to the dynamic parameters previously discussed.

### 8.4.1. Influence of the Cross-section Family and Steel-grade

Table 8.3: Parameter range: Cross-section Family and Steel-grade

| Variable                          | Unit                 | Item-range                | Reference-truss |
|-----------------------------------|----------------------|---------------------------|-----------------|
| Cross-section Chords and Columns  | Cross-section Family | HEA, HEB, HEM, SHSC, RHSC | HEA             |
| Cross-section Diagonals and Posts | Cross-section Family | HEA, HEB, HEM, SHSC, RHSC | HEA             |
| Material                          | Steel-grade          | S235, S275, S355          | S355            |

Cross-sections are part of a cross-sectional family. The cross-section family is a list of cross-sections that are from the same type. In this research, the cross-section families considered are: HEA, HEB, HEM, SHSC and RHSC. In the model, the cross-sections of the chords and the columns are grouped and will be of a specific cross-section family. The posts and diagonals are similarly grouped to have another specific cross-section family. This section will focus on how the combination of cross-section families and steel-grades influences the production cost. In figure 8.3, three tables are displayed representing the three steel grades. Within each table, the rows present the cross-section family of the chords. The columns of the truss and the columns of the table present the cross-section family of the posts and diagonals. The total number of variants displayed in the three tables together is 75.

| S235            |  | Posts & Diagonals |        |        |        |        |
|-----------------|--|-------------------|--------|--------|--------|--------|
| Chord & Columns |  | HEA               | HEB    | HEM    | RHSC   | SHSC   |
| HEA             |  | 101.55            | 105.40 | 137.67 | 98.68  | 94.31  |
| HEB             |  | 109.29            | 113.13 | 145.40 | 106.41 | 103.45 |
| HEM             |  | 119.59            | 128.83 | 161.10 | 122.11 | 119.15 |
| RHSC            |  | 113.89            | 117.73 | 152.70 | 114.39 | 105.09 |
| SHSC            |  | 109.03            | 115.17 | 145.60 | 106.15 | 101.78 |

| S275            |  | Posts & Diagonals |        |        |        |        |
|-----------------|--|-------------------|--------|--------|--------|--------|
| Chord & Columns |  | HEA               | HEB    | HEM    | RHSC   | SHSC   |
| HEA             |  | 96.16             | 106.37 | 139.11 | 99.75  | 96.83  |
| HEB             |  | 103.94            | 114.15 | 146.89 | 107.53 | 104.60 |
| HEM             |  | 119.79            | 130.00 | 162.74 | 123.38 | 118.87 |
| RHSC            |  | 106.25            | 116.46 | 149.20 | 109.84 | 106.55 |
| SHSC            |  | 105.14            | 109.95 | 148.95 | 103.32 | 100.40 |

| S355            |  | Posts & Diagonals |        |        |        |        |
|-----------------|--|-------------------|--------|--------|--------|--------|
| Chord & Columns |  | HEA               | HEB    | HEM    | RHSC   | SHSC   |
| HEA             |  | 100.00            | 114.74 | 151.74 | 103.32 | 101.92 |
| HEB             |  | 112.29            | 123.40 | 160.39 | 111.01 | 109.62 |
| HEM             |  | 129.95            | 141.06 | 178.05 | 126.65 | 131.87 |
| RHSC            |  | 117.77            | 128.87 | 165.67 | 121.09 | 119.64 |
| SHSC            |  | 110.56            | 121.67 | 158.66 | 113.87 | 112.47 |

Figure 8.3: Cross-section family combinations in Pratt truss variants over different steel-grades

### Influence of Cross-sectional family

The tables of figure 8.3 show that any combination with HEM sections leads to a high total cost. This is caused by the thick flanges of the HEM cross-section that contribute to a higher total weight. When these cross-sections are used for the posts and diagonals, the costs are maximized. In addition the tables of figure 8.3 show that the most optimal cross section for the chords and the columns of the truss are the HEA cross-sections. This is because HEA cross-sections have thinner flanges than the HEB and HEM sections. Furthermore, HEA sections are I-sections. These have a lower unit price than

Hollow sections.

When taking a closer look at the top row of the S355 matrix, it presents HEA chords and columns. Here, the lowest costs can be found in variants where the posts and diagonals are from the cross-section family HEA, SHSC or RHSC. In the right table of figure 8.3 can be seen that the variant with SHSC posts and diagonals are lower in costs than RHSC. This is because SHSC sections have equal buckling resistances in both axes of the cross-section. RHSC-sections, on the other hand, have a strong and a weak axis, therefore more material is needed for RHSC-sections in order to have sufficient buckling resistance in the weak axis. Consequently, a bigger RHSC-section is needed. This would lead to a higher total weight, causing higher costs. HEA-sections also have a weak axis, but they show a lower total cost. In the following paragraphs, the reasons for this will be discussed.

In figure 8.4 graphs are presented to analyse the influence of the cross-section family of the post and diagonals. The graph shows that the variants with RHSC or SHS sections have a lower total weight. However, the price per kilo of steel for hollow sections is greater, hence, a higher total cost for the material needed.

The HEA variant has the least amount of welding-volume. These I-sections are welded with double fillet welds, hollow sections are welded with single fillet welds. This causes that for I-sections two smaller weld sizes can be applied instead of one big weld size, which reduces the amount of welding volume needed. Furthermore, the graph shows that the SHSC variant uses more welding volume than the RHSC variant. In figure 8.5, the type of cross-section and the weld-sizes are displayed. Because the cross-sections of the SHSC variant have a smaller perimeter and therefore less welding length, it is expected that they would have less welding volume than the RHSC variant. However, the posts of the SHSC variant have a thickness of 6mm, this causes that a 7mm weld is needed for the connection. Resulting in a higher welding volume.

The higher welding volume for the SHSC variant however, is compensated by the smaller cross-sectional area needed to be sawn, less surface area to be sand-blasted and painted, and slightly lower total weight.

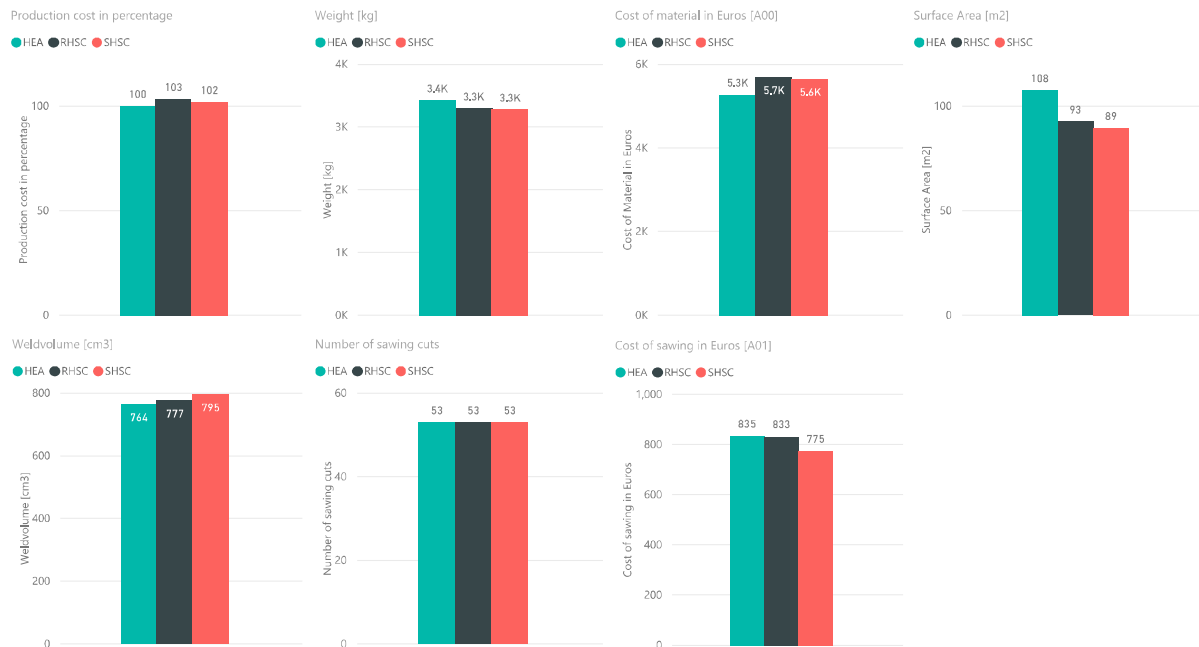


Figure 8.4: Influence of cross-section family of post and diagonal on reference truss (all S355)

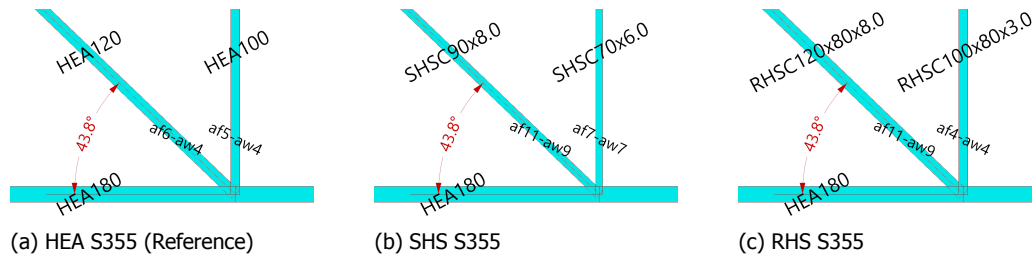


Figure 8.5: Flange-weld size (af) and Web-weld size (aw) per cross-section family of posts and diagonals

When examining the governing joint in the truss in IDEA, this is the same joint that is highlighted in figure 8.1, of the SHS and the RHS variant. They both show failure.

The SHS variant fails due to singularity in the model, which is caused by overlapping weld meshes. The overlapping weld meshes can be prevented by manually increasing the cross-section of the chord from SHSC70x6.0 to SHSC90x6.0 or adding an eccentricity. Increasing the cross-section has influence on the total production costs of the structure. In figure 8.6, it can be seen that the production costs increase due to a higher total weight, higher amount of welding volume and a greater surface area.

|  |  |
|--|--|
| Production costs: 102 %                | Production costs: 105 %                |
| Weight: 3275 kg,- (S355)               | Weight: 3354 kg,- (S355)               |
| Welding Volume: 795 cm <sup>3</sup> ,- | Welding Volume: 849 cm <sup>3</sup> ,- |
| Sawing Cuts: 53 pcs.                   | Sawing Cuts: 53 pcs.                   |
| Double Miter Connections: 16 pcs       | Double Miter Connections: 16 pcs       |
| Surface Area: 89 m <sup>2</sup>        | Surface Area: 91 m <sup>2</sup>        |
| (a) SHSC70x6.0 Post                    | (b) SHSC90x6.0 Post                    |

Figure 8.6: Results influenced by changing the cross-section of the post of the SHSC variant

The RHS variant fails because the strain limit of 5% is exceeded in the plates of the post, which is shown in figure 8.7. This failure is located near the web of the chord-section, due to the high local stiffness in this region. Increasing the cross-section of the post from RHSC100x80x3.0 to RHSC100x80x5.0 leads to a design where plate failure does not occur. However, this influences the production cost. Figure 8.8, shows the differences in results when the cross-section of the post is changed. The total cost increases from 103% to 107%. This is caused by a slight increase in the total weight and an increase in the total welding volume. In addition, the new cross-section of the post has a greater thickness. This creates a higher weld-size, determined by the full-strength method, which leads to a larger amount of welding material needed.

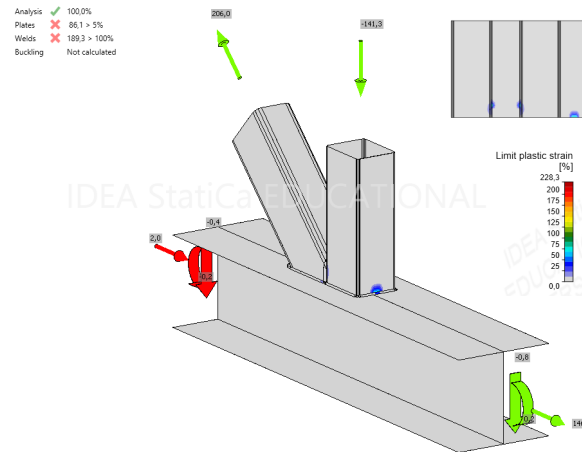


Figure 8.7: Plastic strain of the RHSC100x80x3.0 Post

|                                  |                                  |
|----------------------------------|----------------------------------|
| Production costs: 103 %          | Production costs: 107 %          |
| Weight: 3293 kg,- (S355)         | Weight: 3395 kg,- (S355)         |
| Welding Volume: 777 cm3,-        | Welding Volume: 877 cm3,-        |
| Sawing Cuts: 53 pcs.             | Sawing Cuts: 53 pcs.             |
| Double Miter Connections: 16 pcs | Double Miter Connections: 16 pcs |
| Surface Area: 93 m2              | Surface Area: 93 m2              |
| (a) RHSC100x80x3.0 Post          | (b) RHSC100x80x5.0 Post          |

Figure 8.8: Results influenced by changing the cross-section of the post of the RHSC variant

Changing the cross-section of the post and diagonals of the reference truss to Hollow sections, like SHSC and RHSC, creates higher cost variants due to a higher unit price per kilo steel for the hollow sections and the larger amount of welding volume needed. When analyzing the joints in detail, failure may occur. This can either be caused by overlapping welding meshes, which is practically not desired, or failure in the plates of the hollow section.

### Influence of Steel-grade

In figure 8.3 the middle table shows variants with steel-grade S275, which has a lower total production cost than the reference case. The following paragraph will investigate why steel-grade S275 leads to a lower production cost than the reference case which has steel-grade S355.

In graph of figure 8.9 graphs are presented to analyse the influence of the steel-grade. In these graphs, it can be seen that a higher steel-grade results in a lower total weight and less surface area. However, according to the cost-model, steel-grade S355 has a higher unit price, see table 4.6. This causes a higher material total price for S355, despite the lower total weight. The most significant difference between the steel-grades is the amount of welding volume. The welding volume is calculated according to the full-strength method. In this method, the steel-grade plays an influence on the full-strength factor, see table 6.2. In general, a higher steel-grade leads to a higher full-strength factor, due to a higher beta factor and a higher ultimate strength. This will cause that greater weld-sizes are needed, see figure 8.10. This causes a higher amount of welding volume.

However, increasing welding volume over the increasing steel-grade's yield strength cannot be seen in the graph displaying the welding volume. Moreover, the amount of welding volume is related to perimeter of a cross-section. An increased perimeter leads to an increased welding length. Increased welding length subsequently leads to more welding volume. Table 8.4 shows the cross-section per group over the different steel-grades. Here a different cross-section can be found in the groups Top-chord and Diagonal. The group Top-chord will not be of much influence since it only has two connections, one

with left column and one with the right. For steel-grade S235, the group diagonal has a HEA140 cross-section. Which is different from the other steel-grades that have HEA120 as a cross-section. This difference is caused by the higher resistance that can be achieved when higher steel-grades are used. The higher steel-grade influences the resistance of axial force, bending moment, shear force, buckling, lateral torsional buckling etc. Moreover, HEA140 has a perimeter that is approximately 17% greater than HEA120. This causes that a higher amount of welding volume is needed for the S235 variant.

In conclusion, total weight and total surface area can be decreased by using higher steel-grades. However, this does not automatically lead to a lower total cost, since the unit price of steel is higher and the amount of welding volume can increase, due to a higher beta factor that determines the weld-sizes. This conclusion is in contradiction with published articles[54][55]. These articles conclude that S235 should not be considered when designing steel, because of its higher total weight and greater surface area. The main difference is that these article include the influence of heavier structures on transport costs, which falls out of the scope of this research. When focusing solely on the production costs, a higher steel-grade does not necessarily lead to a lower total cost.

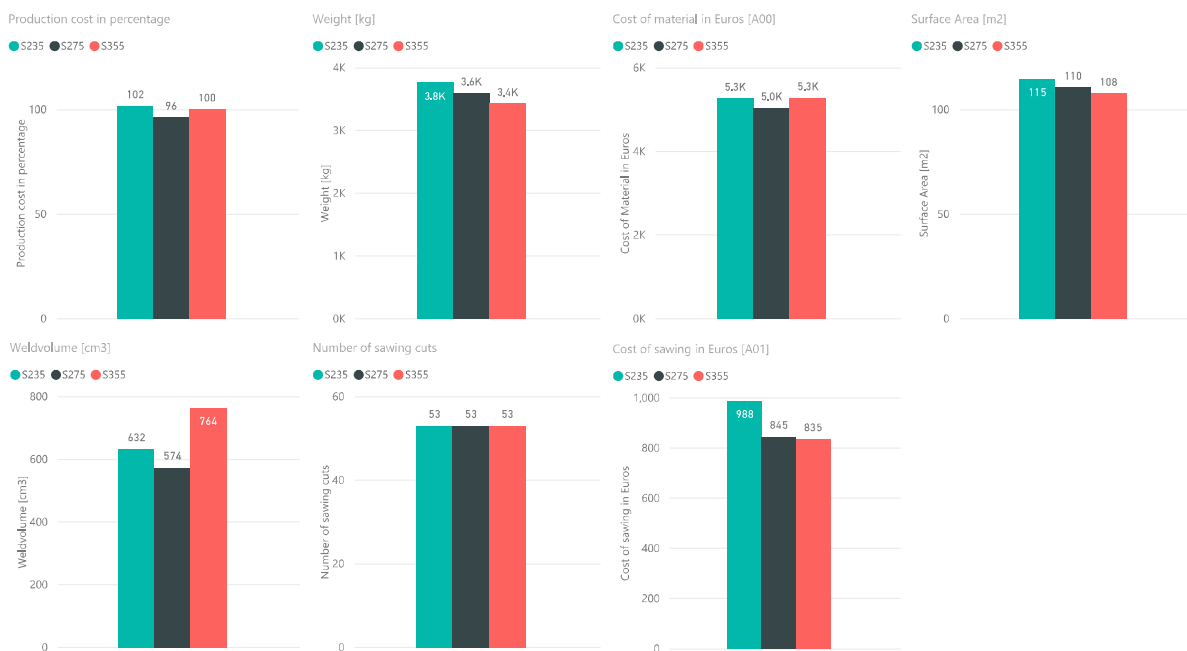


Figure 8.9: Influence of steel-grade on reference truss

Table 8.4: Cross-section per group in variation of steel-grade of reference truss

| Steel-grade | Column | Top-chord | Bottom-chord | Post   | Diagonal |
|-------------|--------|-----------|--------------|--------|----------|
| S235        | HEA160 | HEA200    | HEA180       | HEA100 | HEA140   |
| S275        | HEA160 | HEA200    | HEA180       | HEA100 | HEA120   |
| S355        | HEA160 | HEA180    | HEA180       | HEA100 | HEA120   |

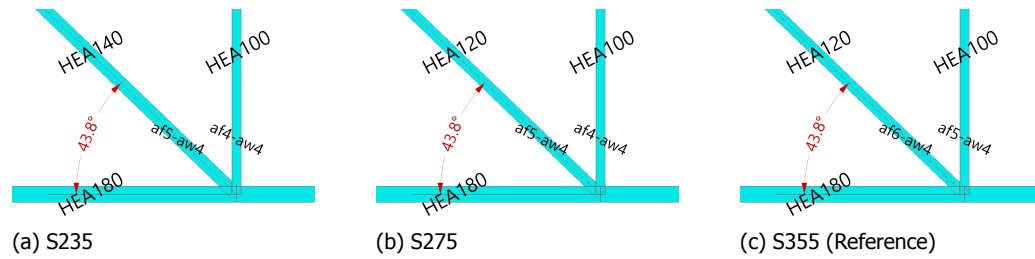


Figure 8.10: Flange-weld size (af) and Web-weld size (aw) per steel-grade

#### 8.4.2. Influence of the truss-height and number of truss-segments

Table 8.5: Parameter range: truss-height and number of truss-segments

| Variable     | Min     | Max     | Step-size | Reference-truss |
|--------------|---------|---------|-----------|-----------------|
| Height Truss | 1000 mm | 3000 mm | 100 mm    | 3000 mm         |
| Segments     | 4 pcs   | 16 pcs  | 2 pcs     | 8 pcs           |

In this case-study, the height of the truss and the number of truss-segments are the parameters influencing the wire-frame geometry of the truss. This geometry determines the distribution of forces within the structure, and therefore is of influence for which cross-sections will be selected during the optimisation.

With the parameter ranges presented in table 8.5, 147 variants are created. In figure 8.11, the table on the left shows the cost percentages for every variant. In the graph on the right side the cost percentages are displayed over the truss-heights.

The 147 variants are filtered on the angle of inclination criterion of  $40^\circ$  in figure 8.12. The graph and table generally show two relations. First, more segments will lead to more connections and therefore higher costs. Secondly, a decrease in height leads to structurally less efficient truss where bigger cross-sections are needed. This increases total weight, which leads to higher costs.

However, cross-sections are discrete variables. They have a particular resistance capacity, when this capacity is exceeded another section will be selected by the optimisation algorithm. This influences the optimal truss height and may cause that the maximum height will not lead to optimal variant. This effect is shown in the table of figure 8.11 in the column of 6 segments. Here, a decrease of total cost can be found when the height of the truss is lowered up till 2300 mm. This is due to the utilization of the members. The cross-section used in these variants are similar, decreasing the height leads to a higher utilization of the same members. This causes that decreasing the height leads to a lower amount of steel needed for the structure, resulting in a lower total cost.

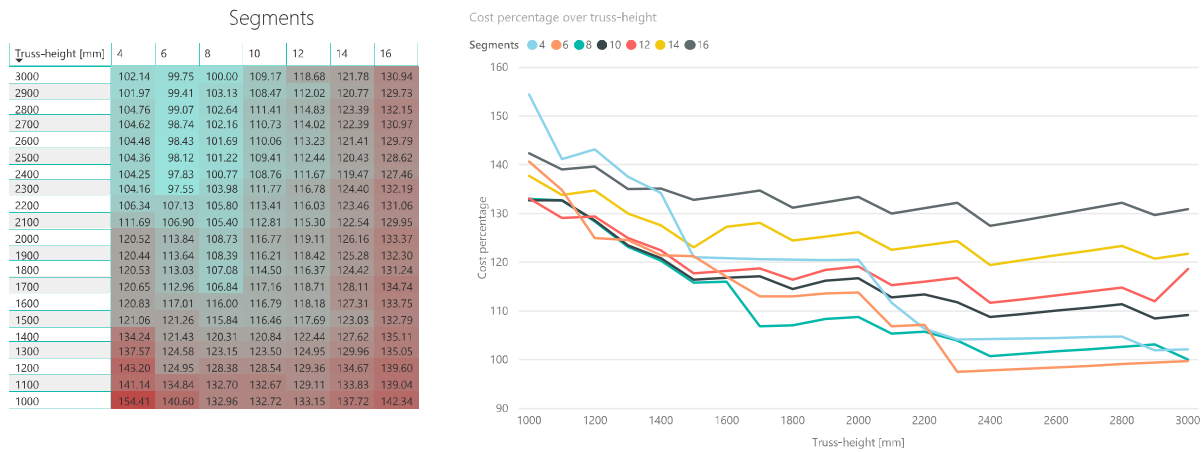
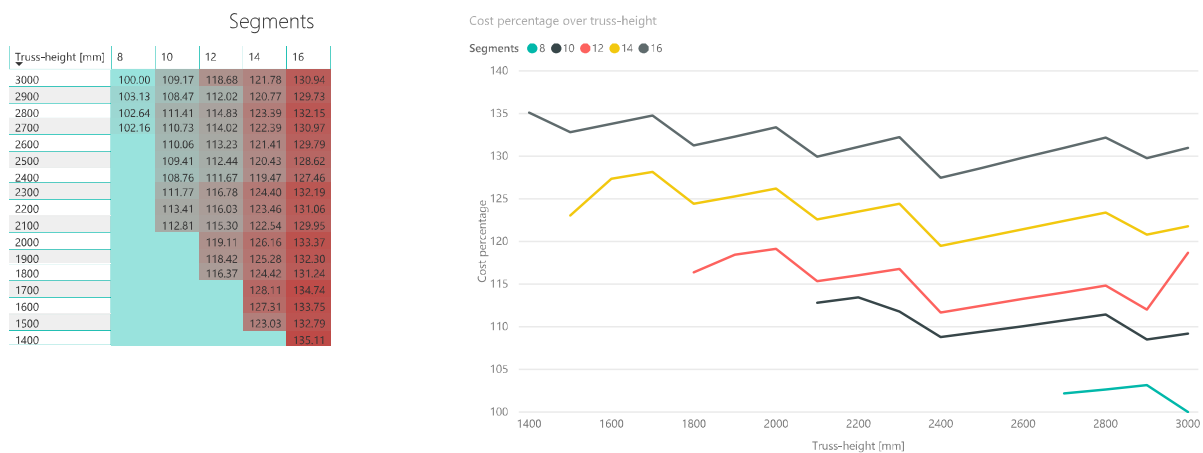
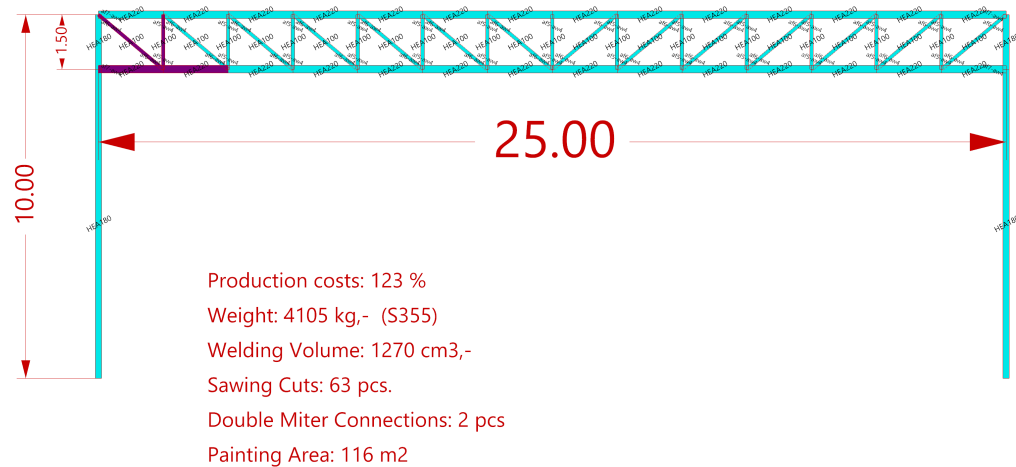


Figure 8.11: 147 variants presented in matrix

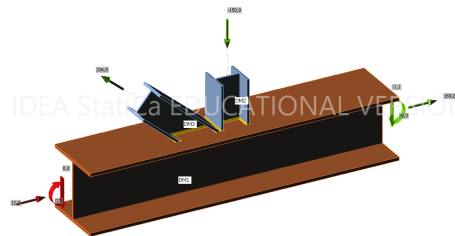
Figure 8.12: Variants with inclination of diagonal greater than  $40^\circ$ 

When the data-set presented in figure 8.12 is filtered on the minimal amount of double miter cuts, one variant is left over. This variant is presented in figure 8.13 and has 14 truss-segments. Due to its low height, the truss has a smaller arm to resist against bending moments. This causes the need for bigger sections in the chords of the truss, which is beneficial for minimizing double miter connections. However, due to its high production cost, this truss cannot be assumed as a desirable variant in the context of this case-study.





(a) Truss with detail highlighted



(b) Detail with ULS Snow-load forces

Figure 8.13: Truss with minimal amount of double miter connections

In conclusion, it is beneficial for the production cost to have the least amount of truss-segments possible. This leads to less joints being needed. However, the minimal amount of truss segments is limited to the minimal angle of inclination of the diagonal, filtering out many of the possible variants. Finding a variant that has the minimal amount of double miter connections, and where the angle of inclination of the diagonals is above the minimum, will not lead to a desirable variant, in this case of a Pratt truss with centric joints. However, it does show that creating a truss with a high level of constructability requires a different approach than optimising structures solely on total weight.

#### 8.4.3. Influence of the buckling length

In the optimisation model, an assumption is made for the buckling length of the top and bottom chord-member. This assumption is chosen to be equal for every variant, because the amount of buckling supports influences the total cost of a structure. In this research only the 2D geometry of a truss is considered and therefore production costs influences of the 3D geometry creating the buckling support is not considered. In figure 8.14, two tables are displayed. The left table shows the cost percentage and the right table shows the total weight of the variant. The rows of the table display the number of segments of the variant.

Generally, a longer buckling length leads to a bigger cross-section is needed in order to provide sufficient resistance against buckling. This bigger cross-section increases the total weight of the structure and therefore causes an increase of costs. Figure 8.14, shows that the assumed buckling length is on the conservative side of the possibilities, yet without being too conservative.

Table 8.6: Parameter range: buckling length

| Variable               | Min      | Max    | Step-size | Reference-truss |
|------------------------|----------|--------|-----------|-----------------|
| Buckling length chords | 1.5625 m | 12.5   | 1.5625 m  | 6.25 m          |
| Segments               | 4 pcs    | 16 pcs | 2 pcs     | 8 pcs           |

| Buckling length chord [m] |        |        |        |        | Buckling length chord [m] |          |          |          |          |
|---------------------------|--------|--------|--------|--------|---------------------------|----------|----------|----------|----------|
| Segments                  | 1.56   | 3.13   | 6.25   | 12.50  | Segments                  | 1.56     | 3.13     | 6.25     | 12.50    |
| 2                         | 117.88 | 117.88 | 128.71 | 144.75 | 2                         | 4,531.61 | 4,531.61 | 5,035.58 | 5,948.15 |
| 4                         | 83.23  | 88.11  | 102.14 | 131.07 | 4                         | 2,921.48 | 3,129.11 | 3,767.32 | 5,160.50 |
| 6                         | 79.30  | 84.39  | 99.75  | 126.31 | 6                         | 2,652.06 | 2,876.77 | 3,563.05 | 4,830.43 |
| 8                         | 80.53  | 85.13  | 100.00 | 130.90 | 8                         | 2,562.33 | 2,762.11 | 3,424.26 | 4,860.02 |
| 10                        | 87.81  | 94.32  | 109.17 | 140.03 | 10                        | 2,669.34 | 2,949.59 | 3,611.74 | 5,047.50 |
| 12                        | 97.35  | 103.85 | 118.68 | 143.68 | 12                        | 2,864.43 | 3,144.67 | 3,806.82 | 5,101.52 |
| 14                        | 100.49 | 106.98 | 121.78 | 152.59 | 14                        | 2,907.57 | 3,187.82 | 3,849.97 | 5,285.73 |
| 16                        | 109.68 | 116.16 | 130.94 | 161.71 | 16                        | 3,095.03 | 3,375.28 | 4,037.42 | 5,473.19 |

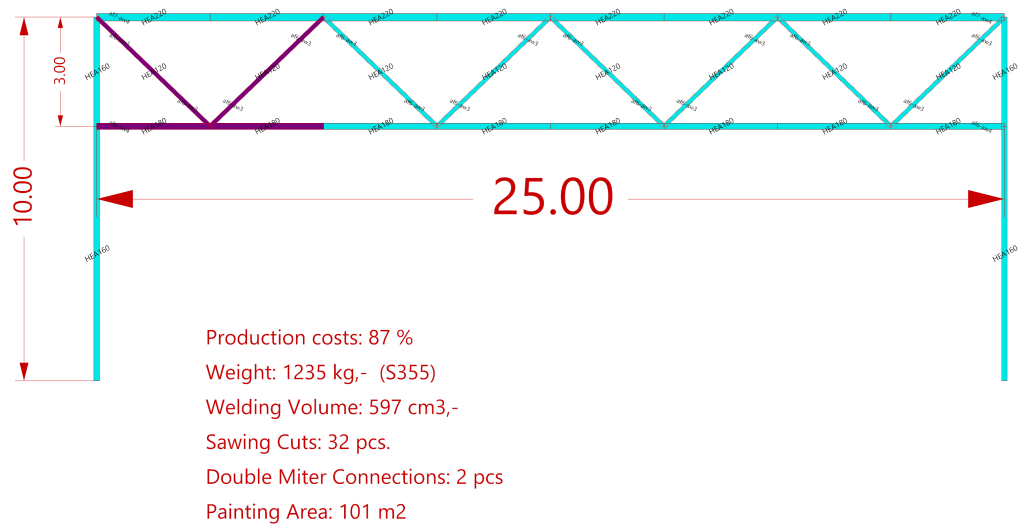
(a) Cost percentage

(b) Weight in kg

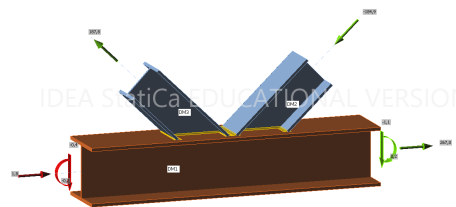
Figure 8.14: Influence of buckling length and number of divisions

#### 8.4.4. Influence of truss Typology

Changing the truss typology from a Pratt truss to a Warren truss has a significant impact on the cost percentage. This reduction is mainly caused because less beam length is used, due to the absence of posts. Figure 8.15, shows the Warren truss variant. A warren truss does not have posts. This causes that diagonals are less likely to interact with other sections increasing the change of creating single miter connections, which is beneficial for reducing production risk.



(a) Truss with detail highlighted



(b) Detail with ULS Snow-load forces

Figure 8.15: Warren Truss

#### 8.4.5. Trusses with eccentricity joints

In section 4.2.1, it has been concluded that risks in production could be reduced by creating positive eccentricities in the joints of the truss. In the optimisation script, two positive eccentricities can be applied. One for the connection of the diagonals with the top-chord and one for the connection of the diagonals with the bottom-chord.

Table 8.7: Parameter range: eccentricity top-chord &amp; bottom-chord

| Variable                 | Min  | Max    | Step-size | Reference-truss |
|--------------------------|------|--------|-----------|-----------------|
| Eccentricity Topchord    | 0 mm | 200 mm | 20 mm     | 0 mm            |
| Eccentricity Bottomchord | 0 mm | 200 mm | 20 mm     | 0 mm            |

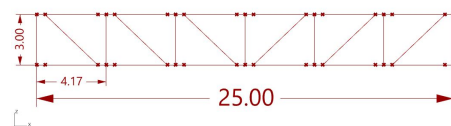
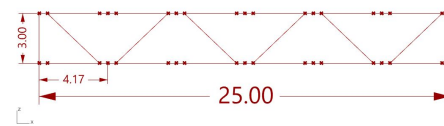
(a) Pratt truss  $\varepsilon = 0.2m$ (b) Warren truss  $\varepsilon = 0.2m$ 

Figure 8.16: Trusses with eccentric joints

Table 8.17 shows the results of the cost-percentage and the number of double miter connections per variant. Applying an eccentricity of 60 mm for both the top-chord as the bottom-chord joint produces a truss with only 2 double miter connections. Figure 8.18 shows the truss with the 60 mm eccentricities.

The inclusion of eccentricities did not influence the cross-sections of the structures compared to the reference truss. The discrete character of cross-sections may cause that there is capacity left in the beam. In this case, there is capacity left preventing the need for a different cross-section, when the eccentricity creates an additional bending moment. In figure 8.18, a cost decrease is noticed. This is caused by the reduction of sawing costs. Single miter connections only require two cuts during the sawing process, where double miter connections require three cuts. Furthermore, the eccentricity produces a steeper angle of inclination for the diagonals. This reduces the beam length needed for the diagonals and causes a decrease in total weight of 12 kg compared to the reference truss.

In section 7.4, it has been concluded that shear forces with an eccentricity produce an additional bending moment, however, this effect is lost when importing eccentric joints to IDEA Statica Connection. In this case, the two shear-forces at both ends of the chord do not point in the same direction and will not compensate each other, see figure 8.18. The shear forces found in the chord have a magnitude of 1.7 kN and 2.0 kN. Multiplied with the eccentricity, this causes an additional bending moment of 0.22 kNm. The small magnitude of the additional bending moment causes that results are not noticeably different. However, this effect can be critical when loads on the structure are much greater and can lead to an unsafe design is generated by the optimisation model. Therefore, when eccentricities are creating within the optimisation model, the influence of the additional bending moment should be checked.

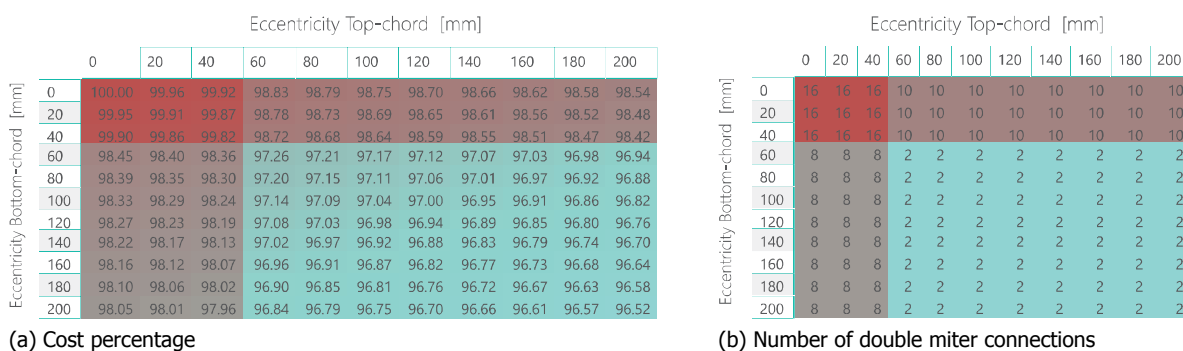
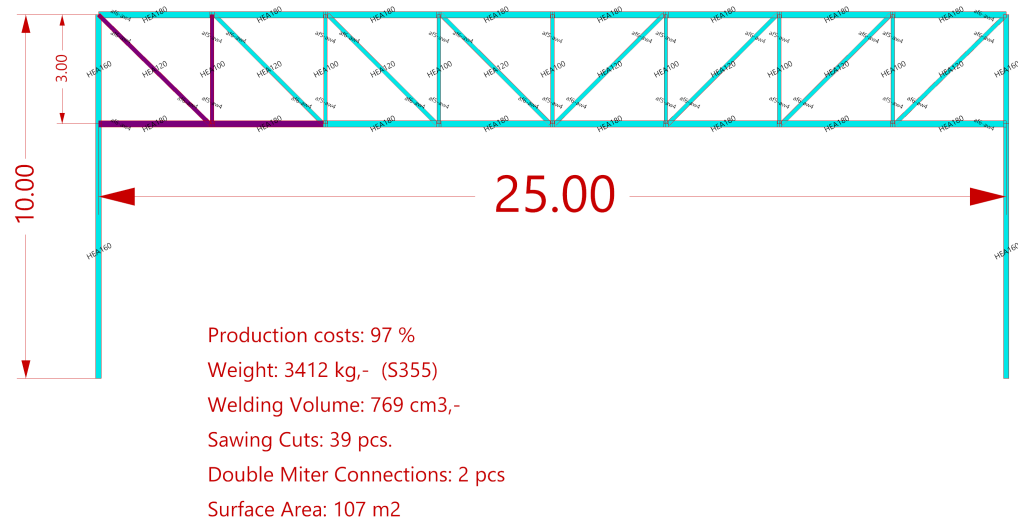


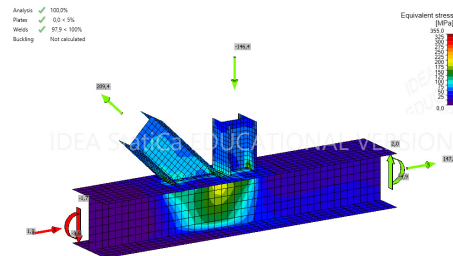
Figure 8.17: Influence of including eccentricities in the joints of the truss

In this case, applying an eccentricity to the joints does not change the cross-sections needed in the chords. This is caused by the discrete characteristics of cross-sections, that causes additional capacity to be left. In other cases, applying an eccentricity can cause the need for a different cross-section. This will increase the total weight of the structure and therefore the costs. Analyses of the optimisation model show that trusses that are higher loaded, show more sensitive responses to eccentricities.

In conclusion, depending on the situation, applying an eccentricity may or may not be beneficial. The optimisation model creates the possibility to quickly analyse the effect of applying an eccentricity to the specific situation.



(a) Truss with detail highlighted



(b) Equivalent stress in joint detail with ULS Snow-load forces

Figure 8.18: Reference truss with eccentricity of 60 mm in joints of top and bottom chord

#### 8.4.6. Trusses with variation in truss-segment length

In the case of a simply supported beam with a distributed load, the maximum moment will be in the middle of the beam while the maximum shear force will be present near the supports. This principle is applicable for trusses as well. Here it could be beneficial to have more material in the web of the truss near the supports since shear force is here at its maximum. In contrast, in the middle of the truss it is beneficial to have minimum material in the web and maximum material in the chords in order to carry the maximum moment force.

This principle can be applied to trusses by influencing the spread of points defining the individual truss-segments. Equation 8.1 defines the location of the points along a line segment. It should be noted, that this equation represents half of the chord. In application this formula is mirrored to create a symmetric distribution of points. In the equation, the desired number of segments can be filled in. This desired number of segments generates a set of points. These points are distributed according to the formula  $x^z$ . Here,  $z$  is a factor determining the spread of the points. As shown in figure 8.19 a high factor  $z$  will cause a high level of spread. In case of  $z = 1$ , the truss will have a normal spread equal to the traditional trusses. However,  $z$  should be limited to prevent the creation of diagonals with an angle outside the range of 30° and 60° as prescribed by NEN-EN 1993-1-8, art 7.1.2(3).

Table 8.8: Input parameters

| Parameter | Symbol              |
|-----------|---------------------|
| $s$       | number of segments  |
| $z$       | distribution factor |
| $l$       | length              |

$$w = \left\{ \frac{n}{s} \right\}_{n=0}^{s+1} * x^z * l \quad (8.1)$$

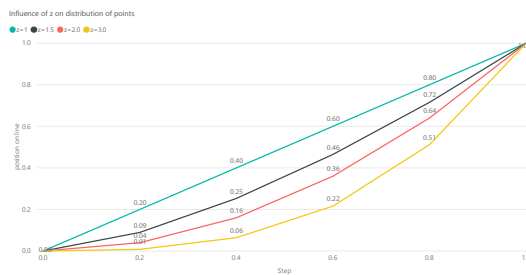
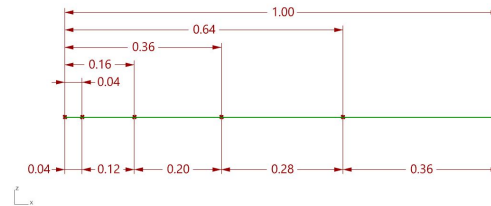
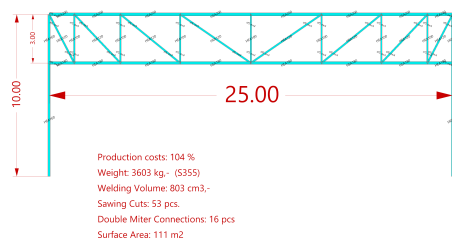
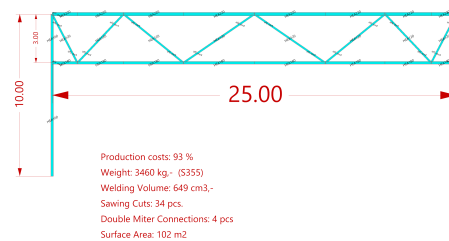
(a) 5 segments variation in  $z$ (b) 5 segments  $z = 1.5$ 

Figure 8.19: Distribution of points in case of 5 segments

In general the application of variation of truss-segment width in the truss does not lead to a lower total cost, see figure 8.21. Here, a variation of 1.0 presents a constant truss-segment width. For the Pratt truss this is the reference truss presented in figure 8.1, for the Warren truss this is the truss presented in figure 8.15. A variation lower than 1.0 leads to the opposite desired effect where more material is used in the middle of the truss, which causes a higher total cost. But using a variation factor higher than 1.0 also causes a cost increase.

In conclusion, adding a variation in the width of the truss-segments may not lead to a lower total cost. Adding a variation, increases the number of unique elements. Which can be undesirable, because it may increase risks of human error in production. Furthermore, in this case study a buckling length of 6.25 is assumed for the top and bottom chord. Normally a buckling support is created at every joint, when applying a variation of above 1.0 the chord elements in the middle will increase in length. The increased length can increase the buckling length, which can be uneconomical because the highest compressive force are found here.

(a) Pratt truss  $z = 1.5$ (b) Warren truss  $z = 1.5$ Figure 8.20: Trusses with variation in segment with  $b_i$

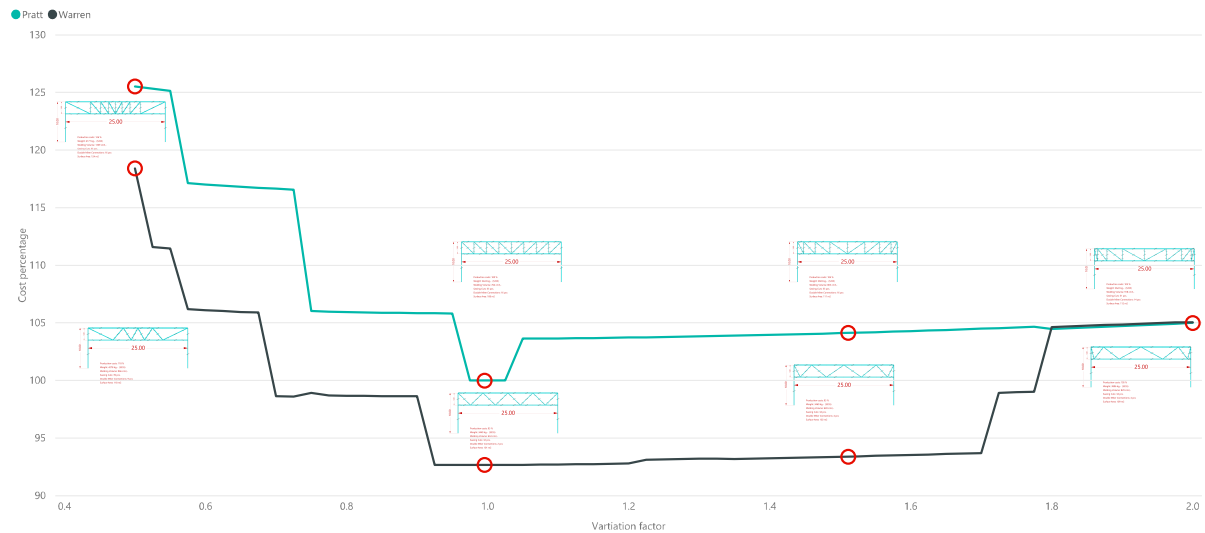


Figure 8.21: Influence of variation factor for Pratt and Warren truss

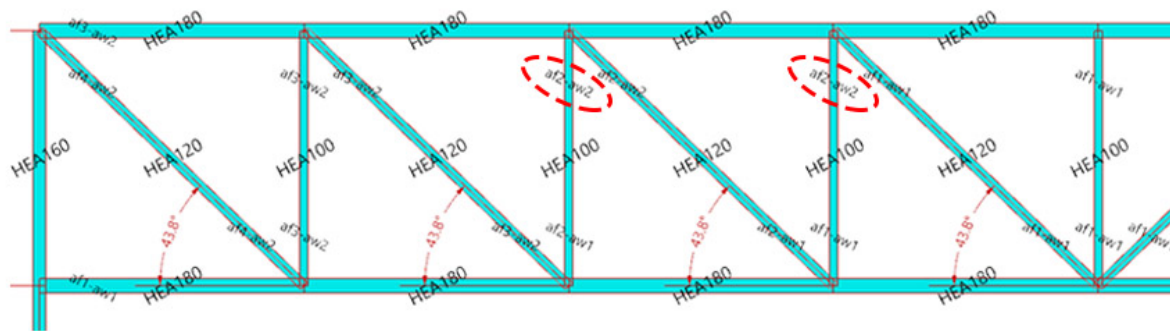
## 8.5. Directional method analyses

The API connection with IDEA Statica Connection within the optimisation model allows that each single weld of each joint can be optimised according to the directional method. In this section, we will discuss how this affects the total welding volume of a truss structure. Besides optimising the welds, the API connections with IDEA Statica Connection indicates whether the strain criterion of plates in a connection is exceeded.

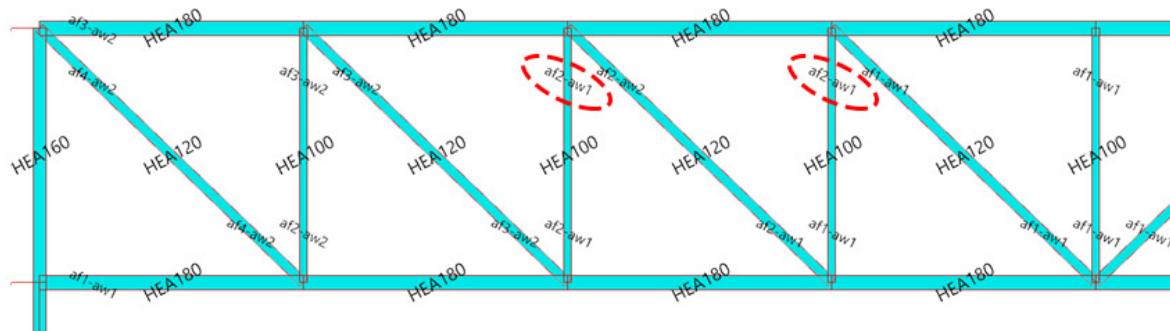
### 8.5.1. Influence of mechanical scheme on weld-volume

When all welds of the reference truss are optimised according to the directional method, none of the welds exceed the minimal threshold size of 4 mm. This causes that all welds will be the minimum of 4 mm. This is without considering the criterion that welds should at least possess 80% the strength of the parent material.

To investigate the influence of the directional method on the weld-sizes, the minimal weld-size criterion is adjusted to 1 mm. Figure 8.22 shows the weld-sizes of right half of the reference truss. The whole truss does not need to be displayed because of its symmetry. The welds are defined based on the forces. These forces are dependent on the mechanical scheme that is assumed in the beginning of the project. In chapter 5 the assumption has been made that all welded connections are assumed as hinged connections. The bottom figure of figure 8.22 shows the influence on weld-sizes when the connections are assumed rigid.



(a) Connections assumed hinged



(b) Connections assumed rigid

Figure 8.22: Weld-sizes dependent on mechanical scheme

Differences can be seen in the web-welds connecting the post with the top-chord. When the connections are assumed hinged, this leads to bigger welds than when the connections are assumed rigid. It would be expected that when connections are assumed rigid, bigger welds are needed due to the bending moment present in the connection. These bigger welds would be located in the welds of the flanges in order to resist against the bending moment. But in this case, the bending moments are relatively small causing no impact in the weld-sizes.

When connections are assumed hinged, the axial force in the connection is greater than in the case of assuming rigid connections, due to the redistribution of forces. The governing load-case, is the wind suction load-case, where the truss is loaded by a negatively distributed load. This causes that the posts are loaded in tension. Due to the higher axial force when hinges are assumed, a higher weld is needed to create sufficient resistance against the force.

When connections are assumed rigid, local rotation in the connection will not occur global analysis model. To make this assumption valid, the rotational stiffness of the connection should be checked. Because a connection will always have some degree of rotation, Eurocode defines classification limits for the maximum rotation in which a connection can be assumed rigid, NEN-EN 1993-1-8, art 5.2.2.5. It may cause that stiffening is needed to increase the rotational stiffness, which can be economically undesirable.

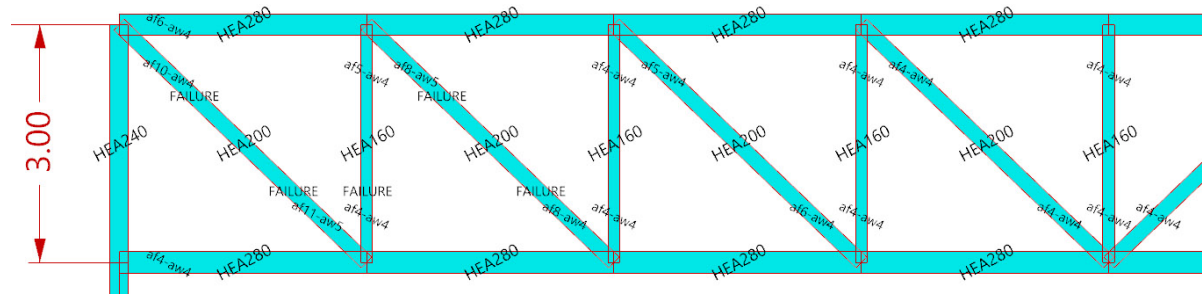
### 8.5.2. Weld volume optimisation

In the previous section, the welds of the truss were smaller than the threshold of 4 mm. In this section the same truss is analysed, but the magnitude of all five load cases is multiplied by four, see table 8.9. The cross sections are selected by the use of size optimisation with the "Optimize cross section" component of Karamba3D. When analyzing every joint in IDEA Statica Connection, the strain limit of 5% is exceeded at several locations, see figure 8.23. The word "Failure" indicates that the 5% strain criterion is exceeded of the specified beam at the nearby joint location.



Table 8.9: Load increase, center-to-center distance: 10m

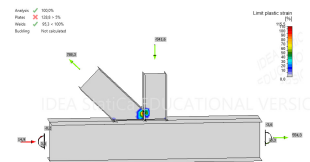
| Number | Load-type | Governing  | Original loads        | New loads             |
|--------|-----------|------------|-----------------------|-----------------------|
| 1      | ULS       | $G$        | $1.35 * G + 3.65kN/m$ | $1.35 * G + 14.4kN/m$ |
| 2      | ULS       | $Q_{wind}$ | $0.9 * G - 10.32kN/m$ | $0.9 * G - 41.28kN/m$ |
| 3      | ULS       | $Q_{snow}$ | $1.2 * G + 11.64kN/m$ | $1.2 * G + 46.56kN/m$ |
| 4      | SLS       | $Q_{wind}$ | $G - 6.375kN/m$       | $G - 25.5kN/m$        |
| 5      | SLS       | $Q_{snow}$ | $G + 8.67kN/m$        | $G + 34.68kN/m$       |



(a) Failure at multiple locations

Production costs: 192 %  
 Weight: 7127 kg,- (\$355)  
 Welding Volume: 1467 cm3,-  
 Sawing Cuts: 53 pcs.  
 Double Miter Connections: 16 pcs  
 Surface Area: 170 m2

(b) Results

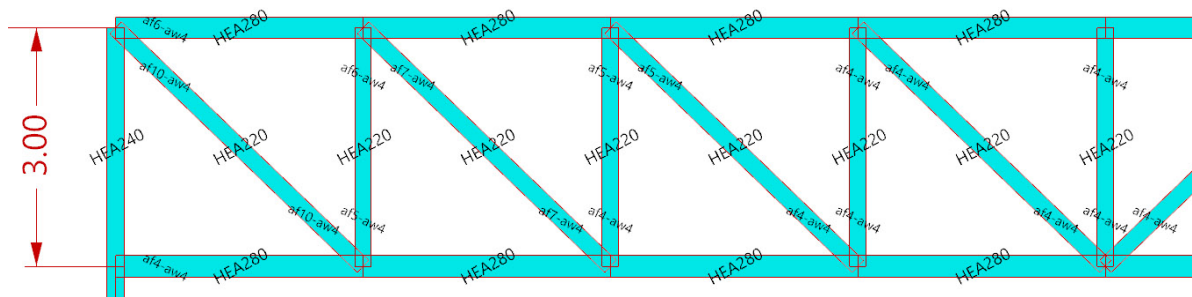


(c) Strain in joint

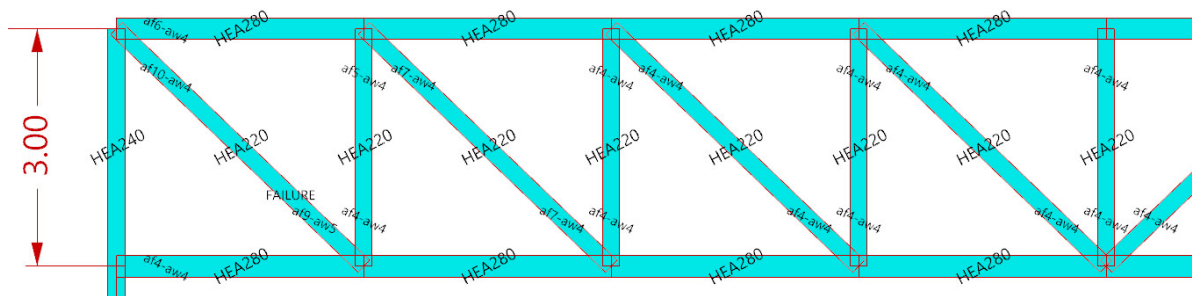
Figure 8.23: Step 1: Truss optimised with size optimisation with "Failure" warnings of connections where the strain limit has exceeded

To decrease the level of strain found in figure 8.23, there are two possibilities. First, add stiffeners. Second, modify the cross-sections. In figure 8.23, it can be seen that failure occurs in the web of the cross-sections. This thickness of the web should be increased to strengthen the web. Increasing the web thickness is achieved by increasing the web thickness.

The cross-section of the post is increased with three steps from HEA160 to HEA220 and the diagonal is increased with one step from HEA200 to HEA220. All the weld-sizes needed after this increase for both assuming the connections rigid and hinged can be seen in figure 8.24.



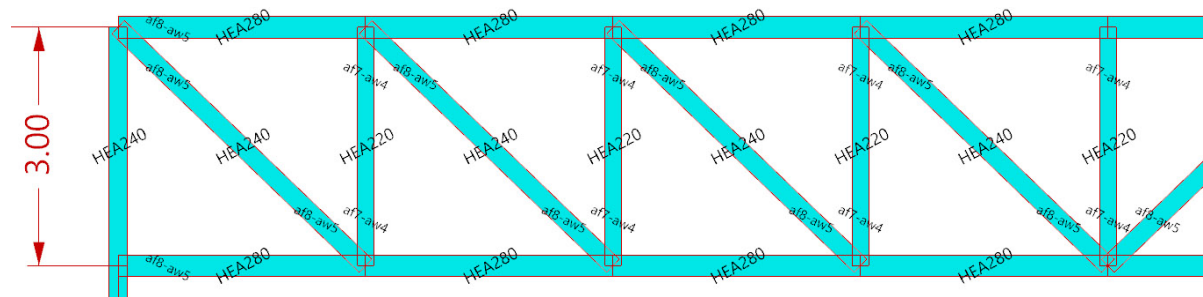
(a) Directional method: mechanical scheme with hinged connections



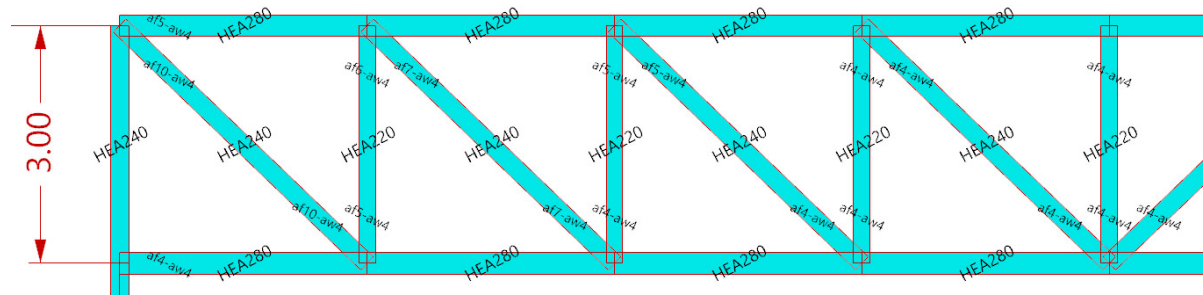
(b) Directional method: mechanical scheme with rigid connections

Figure 8.24: Step 2: Increased cross sections

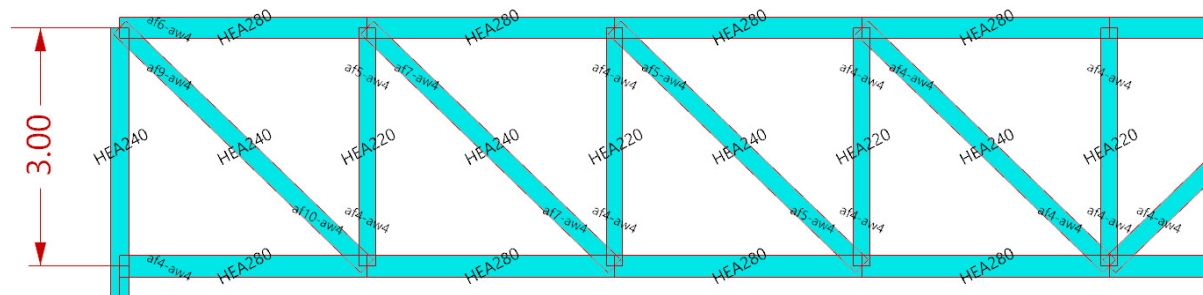
Figure 8.24 shows that plate failure occurs in the diagonal near the support when the connections are assumed rigid. This is caused by the bending moment that is introduced with the assumption of a rigid connection. Therefore an additional increase of the diagonal with one step from HEA220 to HEA240 is applied. The results of the truss after this modification can be seen in figure 8.25 & 8.26.



(a) Full-strength method



(b) Directional method: mechanical scheme with hinged connections



(c) Directional method: mechanical scheme with rigid connections

Figure 8.25: Step 3:

|                                  |                                  |                                  |
|----------------------------------|----------------------------------|----------------------------------|
| Production costs: 229 %          | Production costs: 222 %          | Production costs: 221 %          |
| Weight: 8175 kg,- (S355)         | Weight: 8175 kg,- (S355)         | Weight: 8175 kg,- (S355)         |
| Welding Volume: 2640 cm3,-       | Welding Volume: 1592 cm3,-       | Welding Volume: 1541 cm3,-       |
| Sawing Cuts: 53 pcs.             | Sawing Cuts: 53 pcs.             | Sawing Cuts: 53 pcs.             |
| Double Miter Connections: 16 pcs | Double Miter Connections: 16 pcs | Double Miter Connections: 16 pcs |
| Surface Area: 186 m2             | Surface Area: 186 m2             | Surface Area: 186 m2             |
| (a) Full-strength                | (b) Directional Hinged           | (c) Directional Rigid            |

Figure 8.26: Step 3: Results

The increased dimensions of the diagonal lead to a design where all the joints of the truss, without using stiffeners, have sufficient structural capacity. This leads to a total weight increase from 7127 kg (figure 8.23) to 8175 kg (figure 8.26). Hence, a 15% increase in weight will be needed to create a structure without stiffeners where joint do not fail. This proves that designing a structure depending only on size optimisation can lead to a fact that stiffeners will be needed to strengthen the joints. Consequently, this may result in a higher production cost of the structure. However, for certainty, it is recommended to run cost-analysis on a truss-variant with stiffeners.

In figure 8.26, results of three structures are compared. First, using the full-strength method to calculate the weld volume. Second, optimising the truss assuming that all connections are rigid. And

third, optimising the truss assuming that all connections are hinged.

In the previous section, we have seen that the variant with hinged connections has a higher amount of welding volume compared to the variant with rigid connections. When comparing the welding volume of the variant with hinged connections to the full-strength method. A volume of 1592 cm<sup>3</sup> is calculated for the hinged variant, compared to 2640 cm<sup>3</sup> for the full-strength method. This represents a 40% decrease of the welding volume.

Hence a 3% decrease in production cost will be achieved, as the production cost of the full-strength variant is 229% of the reference truss, and it decreases to 222% in case of the hinged variant. This means that when the welds are optimised using the optimisation model, 34 trusses could be built for the price of 33 trusses.

Optimisation of the welds can cause that the structure does not have sufficient deformation capacity. In the truss design class 1 cross-sections are used, these cross-sections can be analysed on their plastic design resistances. Therefore, the selection of sections during size optimisation is partly based on these plastic resistances. *"When plastic design is used, the main use of this classification is to foresee the possible need to allow a plastic hinge to form in the joint during global analysis."*[3, p.9]. Hence, deformation capacity is needed to make the assumptions of the mechanical scheme in global analyses valid. Optimising the welds of the truss, may cause that the rupture strength of the weld is lower than the yield strength of the connected parts. This can prevent a plastic hinge to form and may cause premature brittle failure of the structure.

Furthermore, welds are characterized by the presence of residual stresses as well as of geometrical imperfections [3, p.145] Residual stress and deformation caused by welding is not assumed in the design model of IDEA Statica Connection [53, 2.4].

In conclusion, sufficient deformation capacity cannot be guaranteed when optimising all the welds in the optimisation model. It is recommended to expand the model with an extra design check, to make sure that the yield strength of the plates is lower than the rupture strength of the welds, creating deformation capacity. In addition, a safety factor for designing the welds should be included to compensate the presence of residual stresses and imperfection that are not assumed in IDEA Statica Connection.

## 8.6. Conclusion

In the case-study, it has been noticed that using hollow sections for the posts and diagonals of trusses leads generally to higher production costs. Hollow sections have a higher unit price per kilogram compared to I-section. This leads to a higher total production cost, despite, the fact that by using hollow sections a lower total weight is needed, due to their beneficial structural properties of the hollow sections. In case of hollow sections, more welding volume is needed, because the welds are single fillet welds. In single fillet welds, the factor of the full-strength method is doubled. Consequently, there will be a quadratic increase in the welding volume. In addition, hollow sections have a higher probability of creating product waste, because they are only available in a limited range of trade lengths, as discussed in section 4.3.2. The procured beams will have a lower yield efficiency, and consequently a decrease in profit. However, hollow sections create a lower total surface area of the structure. When fire-resistant coating is needed, which is relatively expensive, the use of hollow sections can be desirable.

In the optimisation model, the cross-sections are optimised using size optimisation. When the final structure is analysed using IDEA Statica Connection; often, the strain criterion of the cross-sections plates near the connections is exceeded. In this case, there are two possibilities, either adding stiffeners, or modifying cross-sections. When the cross-sections are modified the joints need be analysed again. This procedure will be repeated until all joints have sufficient structural capacity.

All welds of the truss structure can be optimised in the optimisation model. However, sufficient deformation capacity in the structure cannot be guaranteed. Therefore, additional checks should be implemented.



# 9

## Further possibilities with methodology

### 9.1. Introduction

In this chapter a plan of approach will be discussed of how the cost-optimisation model can be used for building projects. Two cases will be discussed, both have a truss roof structure.

### 9.2. Nationaal Militair Museum, Soesterberg

"Nationaal Militair Museum", is a museum whose ABT bv was the structural engineer and Oostingh bv was the steel contractor. The project started in 2011 and construction finished in 2015. The museum has a rectangular shape, with dimensions of 250 by 110 meters. The roof is carried by a 4-meter-high steel truss structure that spans in two directions and has a grid size of 5 by 5 meter.

The diagonals of the original design are positioned in a specific sequence, as can be seen in figure 9.2. The reason for this sequence, is because the diagonals end in one point in the corner of the roof structure. The architect preferred this aesthetically [57][58].

However, this decision could have been critical for the final total production costs of the steel structure. In the original design, the geometry of the truss structures creates complex joints. The most complex joint connects a total of 9 elements, as shown in figure 9.3. Because of the high number of attached elements, a closed box has been designed where all elements are bolted to 9.5. Because it is not possible to tighten the nut of a bolt in a closed of box, the nut of the bolt has been welded to the plate from the inside [43].

Changing the direction of the diagonals in the truss structure, will lead to a lower maximum number of elements attached in the project's most complex joint. A maximum of 7 elements, is attached to the joint in the suggested design as can be seen in figure 9.5.



Figure 9.1: Nationaal Militair Museum, Soestberg [56]



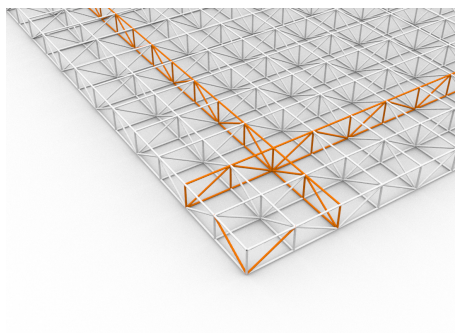
Because the number of attached elements is smaller, there will be no need for a "closed box". This can positively influence time needed for production.

In figure 9.4, a graph is displayed to show the number of joints with a particular number of connected elements occur in both the original, as the suggested design. The graph shows that in the case of the suggested design, the 7-element joint will be the most probable type of joint in the project. This can have a positive influence on mass production.

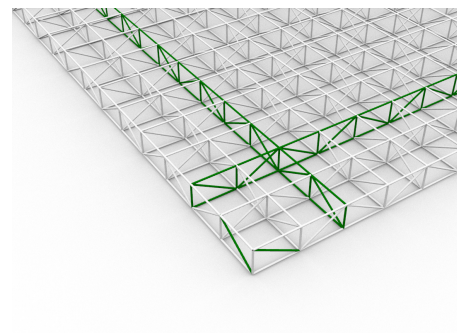
The cost-model used in this research, can be applied to quantitatively compare both designs in terms of production costs. An emphasis will be set here on the total weight and the total welding volume of the structure. To achieve this, a predefined hierarchy is needed. As discussed in section 7.2, groups of elements should be labeled with group-names. The hierarchy will be used to determine the order of dominance in a joint, to create a joint in the way the user desires. To perform this analysis, all connections are assumed to be welded connections.

With the optimization model created in this research, an analysis can be performed how changing the direction of the diagonals influences total weight and total welding volume.

Most probably will the weld volume of a bolted connection will be higher than the weld volume of the same connection welded. However, when assumptions in both cases are equal, outcomes can give insight on preferences, which can influence project decisions.

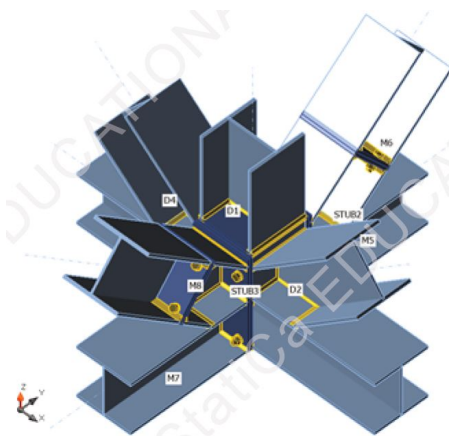


(a) Original design

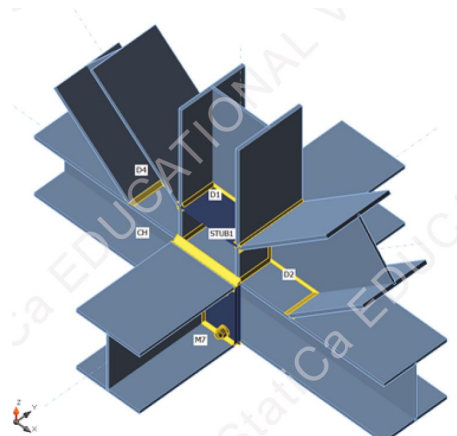


(b) Suggested design

Figure 9.2: Configuration of diagonals

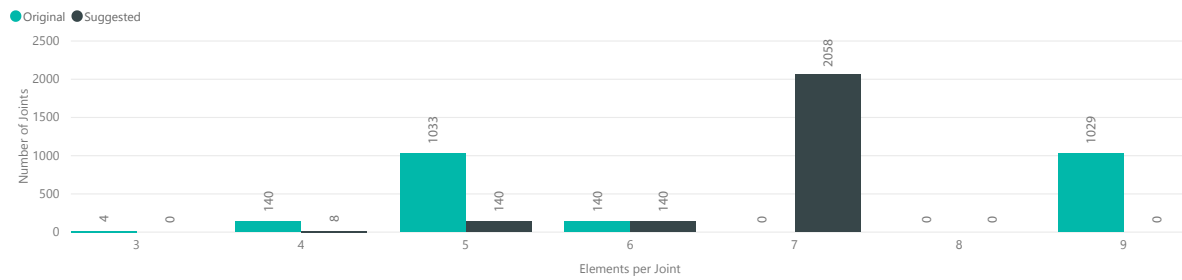



(a) Most complex joint in original design



(b) Most complex joint in suggested design

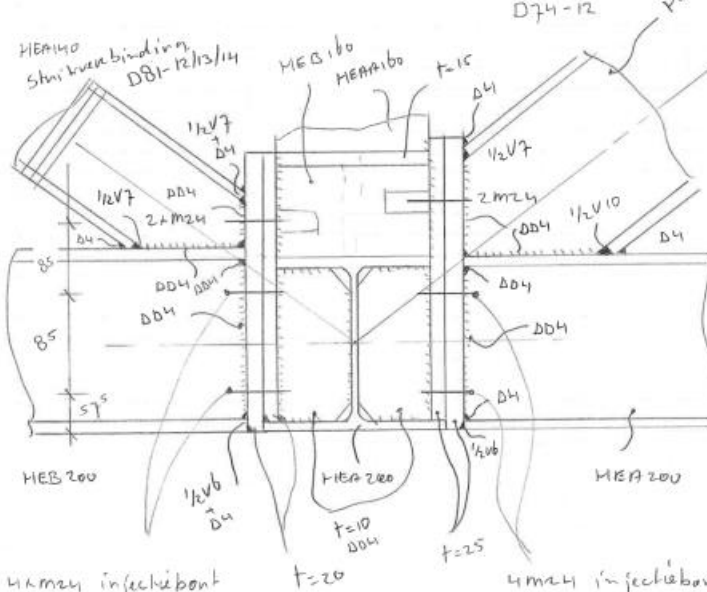
Figure 9.3: Most complex joint per design



|   |   |   |   |  |  |  |
|---|---|---|---|--|--|--|
|  | OOSTINGH STAALBOUW BV                             |   | Order : 1850-100                          |  |  |  |
|   | LAGEWEG 36, POSTBUS 3020, 2220 CA KATWIJK AAN ZEE |   | Blad : D106 - 1                           |  |  |  |
|   | TELEFOON 071-4097000 TELEFAX 071-4032557          |   | Gekonstr. : Gecontr. : Gez. : Datum : Rev |  |  |  |
|   | Betreft : Nationaal Militair Museum Soesterberg   |   | R.Hol : A                                 |  |  |  |
|   |   |   | B   |  |  |  |
|   |   | C |   |  |  |  |

Verbinding onderdruk dak as 42/2/L/P



Strijkverbinding  
D74-12

HEB200

P104

D106- 1/-

Figure 9.5: Detail drawing of welded nuts in complex joints of Nationaal Militair Museum, Soesterberg



### 9.3. Sportcampus Zuiderpark

"Sportcampus Zuiderpark", is a facility for sports whose ABT bv was the structural engineer and Oostingh bv was the steel contractor. The project started in 2011 and construction finished in 2017. The facility has an asymmetric oval shape with dimensions of 200 by 150 meters. The roof of the structure is carried by typical steel trusses that occur repeatedly in the design [59].



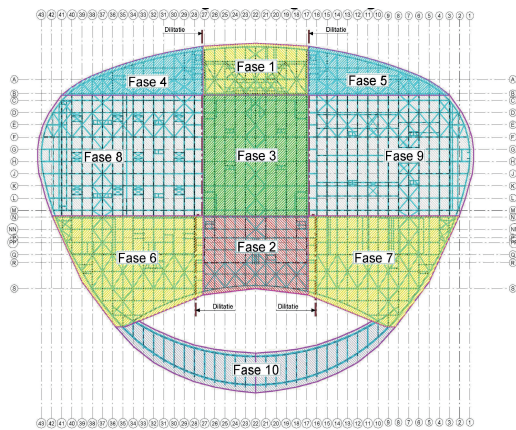
Figure 9.6: Sportcampus Zuiderpark, Den Haag [60]

In applying the cost-model to the case of Sportcampus Zuiderpark, an analysis is performed on one of the typical trusses in the roof structure. The reference truss that will be examined is the truss in phase 3 on axis 22, see figure 9.7. In the project, a production cost optimisation has already taken place by designing the truss in such a way that the diagonals possess single miter connections [59]. This is done by designing wide segments with limited height in the truss. This can be seen in figure 9.8.

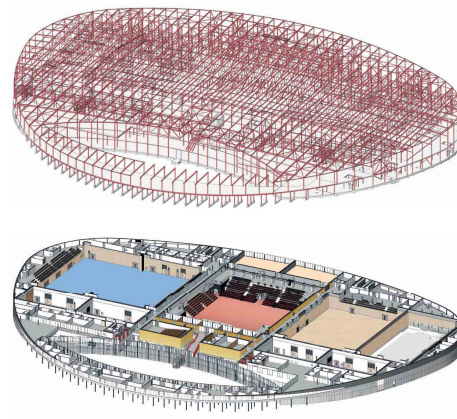
When updating the cost-model to include the possibility to having bolted connections, a new range of possibilities will be opened. In the original design, the truss is divided into 4 prefabricated truss-elements. One of the bolted connections is located in the middle of the bottom-chord. This connection can be critical due to the maximum moment, tensile stresses in the bottom-chord will be at its maximum. Designing the truss in a way where the bolted connection is resorted from the middle of the truss, can be beneficial for the structural performance of truss.

The prefabricated truss-elements can be increased in size, while still being under the maximum dimension of road transport. This would prevent that a bolted connection runs through the middle of the truss, which is the most critical part, since the highest tension force can be found here in the bottom chord. The suggested design with three prefabricated truss-elements is displayed in figure 9.8.

In the design multiple factors influence what the desired optimum will be. Conditions, such as the maximum hoist capacity of cranes, greatly influence this optimum. With these conditions, an optimisation can be run on the ideal number of prefabricated truss-elements and the ideal location of connections. By the use of sliders, one can determine at which vertical section the bolted connection has to be located. Several variants can be generated and compared. This type of optimisation process can be useful for finding optimal bolted connection configuration for the assembly-plan of a steel structure.

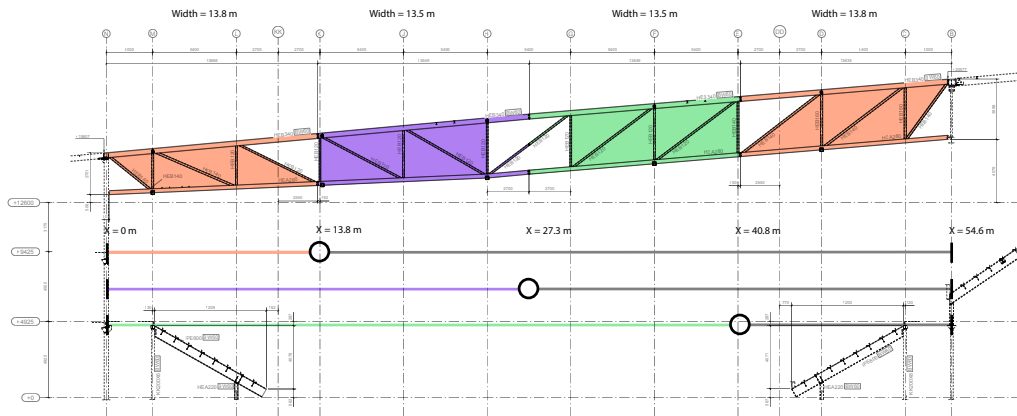


(a) Building phases

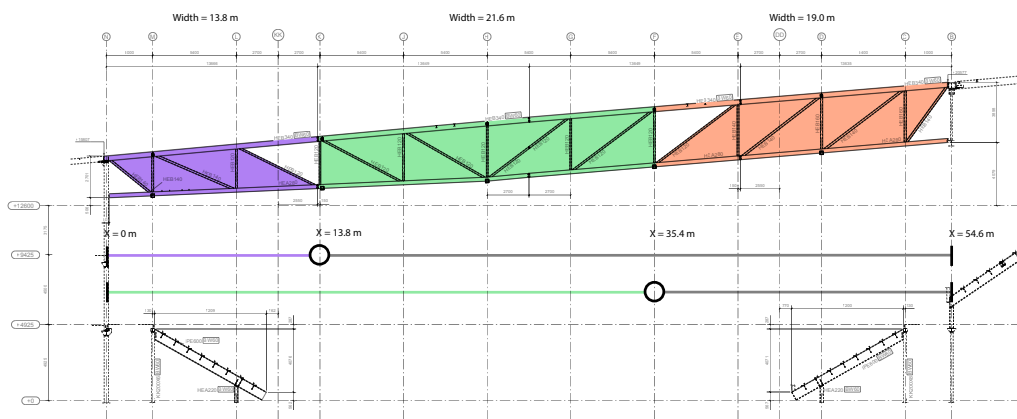


(b) 3D image

Figure 9.7: Sportcampus Zuiderpark, Den Haag [60]



(a) Original design



(b) Possible suggested design

Figure 9.8: Original and suggested design of typical truss of roof structure Sportcampus Zuiderpark, Den Haag

## 9.4. Conclusion

Taking the optimisation model to the next level, will create a wide variety of possibilities. There are two main developments applicable. First is the inclusion of bolted connections, second is making the step from 2D towards 3D geometry.

From these two improvements, including bolted connections will be a relatively easy to implement. This will create the possibility to design trusses with dimensions greater than the transport limitations. The separation of the truss into the optimal sequence of prefabricated elements, could make it possible to optimise the truss on multiple criteria. These criteria are: the production cost, the transport dimensions of the prefabricated elements and maximum weight of the prefabricated elements bounded by hoisting capacity limits. With these criteria assembly-plan optimisations could be performed.

The step from 2D geometry towards 3D geometry will be a greater step. 3D geometry will mean that more variation will be possible. This means that for the IDEA Statica Connection calculation, a lot of different templates are needed to accommodate every possibility of a 3D joint configuration within the steel structure. Here, the appropriate hierarchy-list of the groups of beams is needed in the project. Defining this list will have a higher complexity in a 3D structure. Calculation of a 3D steel structure will have a major influence on computational time. However, it can lead to a more realistic total cost of the structure. For example, in the case-study, it has been concluded that the influence different buckling lengths in the chord members due to a different amounts of buckling supports can only be studied when the 3D geometry of a truss structure is included in the optimisation model. In conclusion, 3D calculations will give a more accurate result on the total cost of a structure, but there will be an increased computational time. Therefore, 2D calculations will remain useful when shorter computational time is preferred.

# 10

## Discussion & Conclusion

### 10.1. Conclusion

In this chapter, an answer will be given to the main research question:

*"How can engineers optimise the production costs of steel trusses with welded connections?"*

The discrete characteristics of cross-sections, cause that optimisations of structures do not follow a consistent pattern. This makes the process of finding an optimal solution quite complex. Therefore, no strict rules can be found to follow when optimising costs. For example, eccentricities can be applied to the joints of a truss structure to lower failure risks during production. Furthermore, due to the discrete character of a cross-section, a capacity can be left in the chord to cope with the bending moment introduced by the eccentricity. In this case, applying an eccentricity will be beneficial. However, in other cases, the additional bending moment will cause the need for a different cross-section. In that case, the engineer should make the economic considerations between an increased weight or a higher failure risk in production.

At the early design phase, the engineer should be acquainted with the consequences that design decisions have on the joints. Increasing knowledge of the limiting effect which design decisions have on possible joint configurations, will allow for a better design decision to be made.

The optimisation model developed in this research, gives insight of the consequences that the geometry of the truss, and the selected beams in the size optimisation process, have on the joints of the structure. In the optimisation model, the strain criterion in IDEA Statica Connection proves to be useful to analyse the structural capacity of the joint. If the strain criterion is exceeded, there are a set of options available: adding plates, modifying cross-sections, or changing the geometry of the truss structure. Within this optimisation model, these changes can be easily made and analysed. This leads to an increased knowledge of how design alternation, affects the joints of the structure, and consequently a better design decision can be made .

Production cost of trusses with welded connections can only be optimised when the design of the joints is included in the optimisation process. Doing that, will mean that all values needed to determine the production cost are evaluated. These values are the total weight, the welding volume, the sawing area, surface area, the number of unique elements, etc... Contrary to production costs, these values are undebatable. Production costs are debatable values because they are factory and time dependent.

**Flexibility in application of optimisation model** This model can create optimal economic solutions of trusses for users. To create an optimal solution with the model, correct cost inputs of the production process are needed. These costs inputs are dependent on the company and the economic

prosperity of the country where the company is located. These cost inputs will determine the ratio of relevance between results as total weight, welding volume, surface area, sawing area and the number of elements of the structure. This ratio of relevance will ultimately decide what is considered to be optimal for the specific company. For example, an optimised truss for production in China can look completely different from an optimised truss for production in the Netherlands, because the ratio of relevance between labour and material can be completely different.

**Weld volume optimisation** The optimisation model optimises the welds of all the joints according to the directional method. This will create a significant decrease in welding volume compared to the full-strength method. However, deformation capacity in the joint is required to allow a plastic hinge to form. Optimising the welds of the truss, may cause that the rupture strength of the weld is lower than the yield strength of the connected parts. This can prevent a plastic hinge to form and may cause premature brittle failure of the structure.

The welding volume optimisation in the optimisation model, should be complemented with two additional checks before applying this part of the model in real-life structural design processes. First, include a check to foresee the deformation capacity. This will allow that the welding volume optimisation can be applied without risking premature brittle failure of the structure. Second, an additional safety factor for the welds should be taken into account for the possible presence of residual stresses as well as geometrical imperfections.

**Indication of plate-failure** The optimisation model shows that the cross-sections selected by the size optimisation algorithm often tend to fail at the connection. Here, the strain criterion of 5% is exceeded. This shows that size optimisation will seldom lead to structures that are constructible without stiffening. With the optimisation model failing joints can be identified.

**Hollow sections** When optimising weight, hollow sections may be preferred. However, results of the case-study show that hollow sections are undesirable when optimising costs. A hollow section has a relatively high buckling capacity and are relatively light. But due to their higher unit price and the fact that they need more welding volume for connection, makes them less attractive when optimising costs. On the other side, when surface area needs to be minimised, for example because of high priced fire-resistant coating, hollow sections can become more attractive.

In the case of hollow sections, the model cannot guarantee that an optimal solution is found. The size optimization algorithm in Karamba3D picks the first combination of cross-sections that fulfil the structural requirements as displacement and utilization. These cross-sections are selected from a list. In the case of hollow sections this list is not monotonically ordered, causing that local optima are not reached within the algorithm.

## 10.2. Discussion

**Eccentric joints** Within the optimisation model, eccentricities can be applied to joints in order to create single miter connections, which can reduce production-risks. In some cases, there is a capacity left in the chord, due to the discrete properties of cross-sections. This may cause that the additional bending moment introduced by the eccentricity, does not result in a higher total weight of the structure. It can even result in lower total costs, because sawing costs will be lower. In current engineering, joints are generally designed centric, which most probably lead that the diagonals will have double miter connections. However, these double miter connections are a benefit for the structural capacity of the joint,



because they make the joint much stiffer. This may cause that the structure is stronger than intended, creating a level robustness. When engineers would optimise towards single miter connections, this additional robustness can be lost. Because engineers are held liable for the safety of the structure, this additional robustness is beneficial for them. This can possibly retain the use of creating eccentric joints in the optimisation model.

**Steel industry: Engineering firm** The engineering firm can improve the quality of their design when joint design is included. These joint designs should not be detailed to the level a steel contractors would do. But rather a coarse level, just to gain insight of critical joints in the structures, which that can be avoided by increasing beam dimensions. Tackling these joints in an early phase can prevent lengthening project time. It can help steel contractors avoid the need for extra time in designing the joints

This can decrease the risk of project delays, and can have beneficial effects for all parties involved. However, for engineers it would mean spending more time on the design part without receiving direct compensation. In a design and build contract, the engineer creates a design together with the architect and the contractor. With this design the contractor needs to find a steel contractor who is able to manufacture and assemble the steel structure at the right price. When a higher quality design is prepared by the engineer, the contractor may be able to arrange a better price with the steel contractor because risks would be lower. This can mean that the extra time invested by the engineer is rewarded by a higher profit of the project.

**Steel industry: Steel contractor** When engineers include joint design in steel structures, it can affect steel contractors. The current situation, offers steel contractors more freedom in designing the details. The steel contractor can design the joint in the most preferable way to their production process, to save costs. This flexibility will be lost when engineers become responsible for the joint design.

**Production limitations** There are factors that limit the level of optimisation possibilities in steel structures. In current engineering practice, one governing joint will be designed in detail. This design of the joint will be copied to all other similar joint locations. This saves time needed during the engineering phase. In addition, having the same joint design at multiple locations helps reducing production risks caused by human error. Furthermore, joints are inspected randomly. When multiple joints are equal, there is a higher chance that possible deviations of the joints will be noticed during inspection. These three factors limit the level of optimisation that can be applied on a structure. Many concessions are made in order to prevent human error on multiple levels in the design and production process. This may result in less economic structures. In the future, where robots will be able to fully assemble trusses, imperfections caused by human error will play a smaller role, opening possibilities for mass customisation of joints in steel structures. This will allow possibilities in achieving greater economic solutions without significantly increasing risks. When steel structures will be produced fully automatically, this will allow that all unique weld-sizes generated by the optimisation model can effortlessly be created without increasing the risk of human-failure.

**Cost-estimation** In automated assembling and welding, savings on welding volume will play a significant role when achieving cost effectiveness of steel structures. The welding volume largely determines the time needed for production, because assembling and welding is the slowest process in the production chain and therefore acts as a bottleneck. Minimizing welding volume will minimize welding time and consequently production time, increasing factory throughput. In the cost model used for this research, welding costs are the most difficult to estimate. Because the cost of welding is highly dependent on the welder, his equipment, speed, skill level, chances of errors, and salary. These are major contributors to the cost estimation. In case of a welding robot accurate cost estimation will be easier because of constant performance. Consequently, steel contractors will be able to more accurately determine the costs of structures needed to be built, resulting in lower risks for the steel contractor and possibly lower prices for clients.

### 10.3. Recommendations

In this research, an assumption was made for the buckling length. The main reason for of this assumption, is the fact that only 2D geometry is considered in the optimisation model. The amount of buckling supports influences the 3D geometry of the truss-structure. Consequently, influencing production costs. Creating a 3D model of the truss system, will allow analysing the effect of the number of buckling supports on the production cost of the structure.

Prices of material, sawing and sand-blasting used in this research are based on steel trader price lists. However, these prices might vary in real life projects, because of price discounts offered to steel contractors. Hence, using purely the online price lists would lead to cost overestimation. To create the most realistic optimisation, it is recommended that the engineers use prices provided by the steel contractor.

Most steel contractors, use the software package "Tekla structures" to create production drawings of the steel structure. Including Tekla structures, in the workflow of the optimisation model, would create a file-to-factory model. This would mean that the drawing of an optimised truss can directly be printed.

Analyses with higher steel-grades, like S460 or S690, can be easily run with the optimisation model. Hybrid steel trusses could be analysed as well, where the posts and diagonals can consist of a lower steel-grade. This could lead to a reduction in the welding volume, because in the full strength method the weld-size is dependent on the lowest steel-grade of the connected parts.

The speed of optimising welding volume in the optimisation model, can be increased by the use of symmetry. In the current version of the optimisation model, the welds of all joints are analysed and optimised. Due to the symmetric design and the symmetric loads, couples of joints can have equal geometry and equal loads. The optimisation model can be expanded with the feature to recognize these similar joints, where only one will be analysed and results will be projected on both joints. The use of symmetry will reduce computational time needed in the optimisation model

This model can be useful to combine material procurement and structural design. Based on which beams can be purchased at low prices, a design can be made. Beams are always purchased in trading lengths. Cutting beams in lengths can result in material waste. This waste can be sold, but at lower prices, hence a lower profit. Taking into account how cutting waste can be minimised in the optimisation model could increase the possibilities of more profits for steel contractors.

The user interface of IDEA Statica Connection includes the possibility to calculate the rotational stiffness of a connection. At the moment, this functionality is not yet exposed in the API [61]. When this functionality will be exposed, it can easily be implemented in the optimisation model. Calculating the rotational stiffness in IDEA Statica Connection can take long time, especially when all connections of a structure needs to be evaluated. Therefore, it may not be interesting for parametric studies, but rather for renovation-projects, where it is needed to accurately determine the performance of the projects steel structure, whether new loading due to renovations can be applied.

#### Recommendations for Future research

The next step within this research topic is investigating bolted connections and moment resistant connections. Here the recommendation is to focus solely on total weight and welding volume, where the welds will be designed according to the full-strength method. For these types of connections, there is an economic trade off between a lighter beam and the need for plates and stiffeners or a heavier beam and no need for plates and stiffeners.

The optimisation model developed in this research can be used to find a design criterion for size optimisation. This design criterion can assess whether the joints of a truss optimised by size optimisation will still have sufficient resistance. This design criterion can be a reduced unity check. For example, a unity check of 0.8 for posts and diagonals can be a good tradeoff between weight optimisation and maintaining sufficient resistance in the joint. Such a design criterion can be easily implemented in the

current workflow of engineers.

#### Recommendations for IDEA Statica Connection

IDEA Statica Connection can add more value to the steel industry, when the software package focuses more on welding volume. Welding can create a bottleneck because it can be the slowest activity in the production process of steel structures. Optimising welding volume can result in less time is needed for welding, speeding up the process and therefore increasing factory throughput.

For IDEA, it can be interesting to include a functionality which displays the total welding volume of the joint that the user has designed. This can make it easier to compare different joint alternatives and makes it possible to quantify them. When structural performance of the two alternative joint designs is adequate, the total welding volume can give an indication of what is preferred in terms of fabrication costs.

Steel contractors may use but-welds or combination welds at strategic positions in order to minimise welding volume. Current possibilities in IDEA allow that only one weld-type for the flange and one weld-type for the web can be selected for each connection. However, in skewed plates it can be beneficial for achieving minimal welding volume to create a fillet weld on the acute angle side of the skewed plate and a butt weld on the obtuse angle side. When the total welding volume of a joint is displayed in IDEA, it will be an added value to strategically apply different weld-types to different welds.

The optimisation model of this research shows that it is technologically possible to optimize each weld of each joint of a truss structure. However, when optimising the welds, the model cannot guarantee that the joint has sufficient deformation capacity. Deformation capacity can be guaranteed when a check is implemented in IDEA to analyse whether the yield strength of the connected parts is lower than the rupture strength of the welds.

In this research, it has been found that importing eccentric joints into IDEA Statica Connection through API is not optimal. The current possible method, causes imported eccentric joints into IDEA to be less severely loaded. This is because the additional bending moment created by the shear force in the chord member cannot be recreated in IDEA. Currently, only one eccentricity can be applied to the couple of shear forces in the chord. Ideally, two eccentricities should be applicable, allowing shear forces to return to their original position of the global analysis model. This will make the detail and the global analysis more similar, which will improve quality.

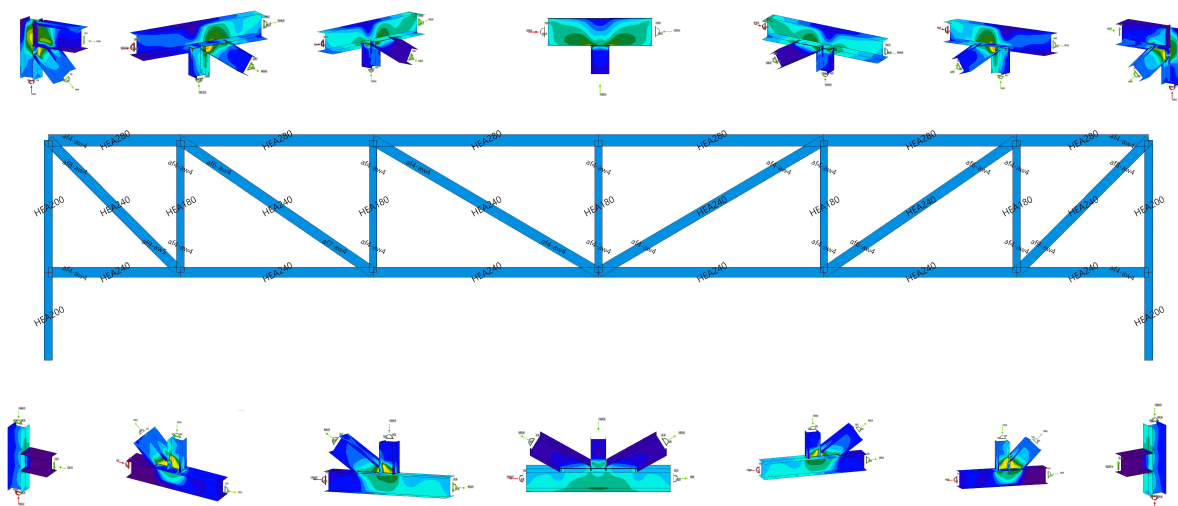


Figure 10.1: Integral analysis of the optimisation model





# A

## Appendix: Analytic analysis on cutting planes in nodes

Table A.1: Parameters

| Parameter              | Symbol        | Range                            |
|------------------------|---------------|----------------------------------|
| Half Height Vertical   | $a$           | $0 < a$                          |
| Half Height Horizontal | $b$           | $0 < b$                          |
| Half Height Diagonal   | $h$           | $0 < h$                          |
| Angle of $h$           | $\theta$      | $0^\circ < \theta < 90^\circ$    |
| Angle of $a$           | $\phi$        | $90^\circ \leq \phi < 180^\circ$ |
| Eccentricity           | $\varepsilon$ | $0 < \varepsilon$                |

$$\vec{v} = \begin{bmatrix} \cos \theta \\ \sin \theta \end{bmatrix} \quad (\text{A.1})$$

$$\vec{w} \perp \vec{v} = \vec{w} = R(90^\circ) \vec{v}, \begin{bmatrix} \cos(90^\circ) & -\sin(90^\circ) \\ \sin(90^\circ) & \cos(90^\circ) \end{bmatrix} \begin{bmatrix} \cos \theta \\ \sin \theta \end{bmatrix} = \begin{bmatrix} 0 & -1 \\ 1 & 0 \end{bmatrix} \begin{bmatrix} \cos \theta \\ \sin \theta \end{bmatrix} = \begin{bmatrix} -\sin \theta \\ \cos \theta \end{bmatrix} \quad (\text{A.2})$$

### A.1. Derivation of situation with static post

**Define  $\vec{z}$  of corner**

$$\vec{z} = \begin{bmatrix} a \\ b \end{bmatrix} \quad (\text{A.3})$$

Derivation of horizontal segment

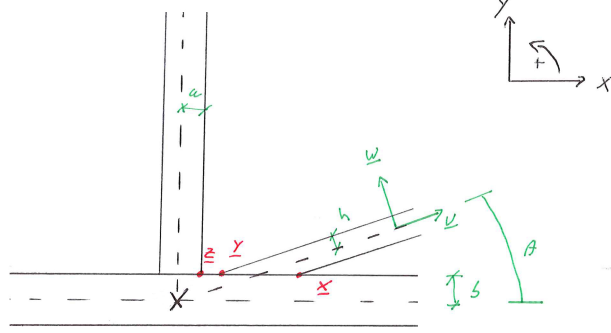


Figure A.1: Horizontal segment in situation with static post

**Define  $\vec{x}$  of horizontal segment**

$$\vec{x} = \alpha \vec{v} + \beta \vec{w} \quad (\text{A.4})$$

$$|\beta \vec{w}| = h, |\beta| = -h, \beta = -h \quad (\text{A.5})$$

$$\vec{x} = \begin{bmatrix} Q \\ b \end{bmatrix} \quad (\text{A.6})$$

$$\vec{y} = \begin{bmatrix} Q = \alpha_1 \cos \theta + h \sin \theta \\ b = \alpha_1 \sin \theta - h \cos \theta \end{bmatrix} \quad (\text{A.7})$$

$$\alpha_1 = \frac{b + \cos \theta}{\sin \theta}, Q = \frac{b + \cos \theta}{\sin \theta} \cos \theta + h \sin \theta = \frac{\cos \theta b + h}{\sin \theta} \quad (\text{A.8})$$

$$\vec{x} = \begin{bmatrix} \frac{\cos \theta b + h}{\sin \theta} \\ b \end{bmatrix} \quad (\text{A.9})$$

**Define  $\vec{y}$  of horizontal segment**

$$\vec{x} = \gamma \vec{v} + \delta \vec{w} \quad (\text{A.10})$$

$$|\delta \vec{w}| = h, |\delta| = h, \delta = h \quad (\text{A.11})$$

$$\vec{y} = \begin{bmatrix} P \\ b \end{bmatrix} \quad (\text{A.12})$$

$$\vec{y} = \begin{bmatrix} P = \gamma_1 \cos \theta - h \sin \theta \\ b = \gamma_1 \sin \theta + h \cos \theta \end{bmatrix} \quad (\text{A.13})$$

$$\gamma_1 = \frac{b + \cos \theta}{\sin \theta}, P = \frac{b + \cos \theta}{\sin \theta} \cos \theta + h \sin \theta = \frac{\cos \theta b - h}{\sin \theta} \quad (\text{A.14})$$

$$\vec{y} = \begin{bmatrix} \frac{\cos \theta b - h}{\sin \theta} \\ b \end{bmatrix} \quad (\text{A.15})$$

$$\vec{x} = \begin{bmatrix} Q \\ b \end{bmatrix}, \vec{y} = \begin{bmatrix} P \\ b \end{bmatrix}, \vec{z} = \begin{bmatrix} a \\ b \end{bmatrix} \quad (\text{A.16})$$
$$l = ||\vec{x} - \vec{y}||. \quad (\text{A.17})$$

$$l = |Q - P| \quad (\text{A.19})$$

$$l = 2 \left| \frac{h}{\sin \theta} \right| \quad (\text{A.21})$$

$$l = ||\vec{x} - \vec{z}|| \quad (\text{A.22})$$

$$l = |Q - a| \quad (\text{A.24})$$

$$l = \left| \frac{\cos \theta b - \sin \theta a + h}{\sin \theta} \right| \quad (\text{A.26})$$

$$l = 0 \tag{A.27}$$

Figure A.2: Vertical segment in situation with static post

**Define  $\vec{x}$  of vertical segment**

$$\vec{x} = \alpha \vec{v} + \beta \vec{w} \quad (\text{A.28})$$

$$|\beta \vec{w}| = h, |\beta| = -h, \beta = -h \quad (\text{A.29})$$

$$\vec{x} = \begin{bmatrix} a \\ S \end{bmatrix} \quad (\text{A.30})$$

$$\vec{y} = \begin{bmatrix} a = \alpha_2 \cos \theta + h \sin \theta \\ S = \alpha_2 \sin \theta - h \cos \theta \end{bmatrix} \quad (\text{A.31})$$

$$\alpha_2 = \frac{a-h \sin \theta}{\cos \theta}, S = \frac{a-h \sin \theta}{\cos \theta} \sin \theta - h \cos \theta = \frac{\sin \theta a - h}{\cos \theta} \quad (\text{A.32})$$

$$\vec{x} = \begin{bmatrix} a \\ \frac{\sin \theta a - h}{\cos \theta} \end{bmatrix} \quad (\text{A.33})$$

**Define  $\vec{y}$  of vertical segment**

$$\vec{y} = \gamma \vec{v} + \delta \vec{w} \quad (\text{A.34})$$

$$|\delta \vec{w}| = h, |\delta| = h, \delta = h \quad (\text{A.35})$$

$$\vec{y} = \begin{bmatrix} a \\ M \end{bmatrix} \quad (\text{A.36})$$

$$\vec{y} = \begin{bmatrix} a = \gamma_2 \cos \theta - h \sin \theta \\ M = \gamma_2 \sin \theta + h \cos \theta \end{bmatrix} \quad (\text{A.37})$$

$$\gamma_2 = \frac{a+h \sin \theta}{\cos \theta}, M = \frac{a+h \sin \theta}{\cos \theta} \sin \theta + h \cos \theta = \frac{\sin \theta a + h}{\cos \theta} \quad (\text{A.38})$$

$$\vec{y} = \begin{bmatrix} a \\ \frac{\sin \theta a + h}{\cos \theta} \end{bmatrix} \quad (\text{A.39})$$

**Decisions on Length vertical segment**

$$\vec{x} = \begin{bmatrix} a \\ S \end{bmatrix}, \vec{y} = \begin{bmatrix} a \\ M \end{bmatrix}, \vec{z} = \begin{bmatrix} a \\ b \end{bmatrix} \quad (\text{A.40})$$

If  $S \geq b$ , there will be a single cutting plane.

$$l = ||\vec{x} - \vec{y}|| \quad (\text{A.41})$$

$$l = ||\begin{bmatrix} a - a \\ S - M \end{bmatrix}|| \quad (\text{A.42})$$

$$l = |S - M| \quad (\text{A.43})$$

$$l = \left| \frac{\sin \theta a - h}{\cos \theta} - \frac{\sin \theta a + h}{\cos \theta} \right| \quad (\text{A.44})$$

$$l = 2 \left| \frac{h}{\cos \theta} \right| \quad (\text{A.45})$$

If  $S < b$  and  $M > b$ , there will be two cutting planes. Here the horizontal part will have a particular length.

$$l = ||\vec{y} - \vec{z}|| \quad (\text{A.46})$$

$$l = \left\| \begin{bmatrix} a - a \\ M - b \end{bmatrix} \right\| \quad (\text{A.47})$$

$$l = |M - b| \quad (\text{A.48})$$

$$l = \left| \frac{\sin \theta a + h}{\cos \theta} - b \right| \quad (\text{A.49})$$

$$l = \left| \frac{\cos \theta b - \sin \theta a - h}{\cos \theta} \right| \quad (\text{A.50})$$

If  $S < b$  and  $M \leq b$ , there will be no horizontal part.

$$l = 0 \quad (\text{A.51})$$

## Summary

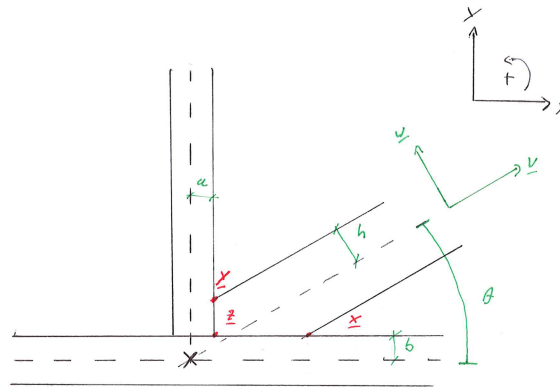


Figure A.3: Horizontal and vertical segment in situation with static post

Table A.2: Decision tree for determining length of horizontal and vertical segment

| Position Weld  | First decision | Second decision | Length   |
|--|----------------|-----------------|--|
| Horizontal segment   | If $P \geq a$  |                 | $l = 2 \left  \frac{h}{\sin \theta} \right $                               |
| $\vec{x} = \begin{bmatrix} Q \\ b \end{bmatrix}, \vec{y} = \begin{bmatrix} P \\ b \end{bmatrix}, \vec{z} = \begin{bmatrix} a \\ b \end{bmatrix}$ | If $P < a$     | If $Q > a$      | $l = \left  \frac{\cos \theta b - \sin \theta a + h}{\sin \theta} \right $ |
|  |                | If $Q \leq a$   | $l = 0$  |
| Vertical segment   | If $S \leq b$  |                 | $l = 2 \left  \frac{h}{\cos \theta} \right $                               |
| $\vec{x} = \begin{bmatrix} a \\ S \end{bmatrix}, \vec{y} = \begin{bmatrix} a \\ M \end{bmatrix}, \vec{z} = \begin{bmatrix} a \\ b \end{bmatrix}$ | If $S < a$     | If $M > a$      | $l = \left  \frac{\cos \theta b - \sin \theta a - h}{\cos \theta} \right $ |
|  |                | If $M \leq a$   | $l = 0$  |

$$\vec{x} = \begin{bmatrix} \frac{\cos \theta b + h}{\sin \theta} \\ b \end{bmatrix} \quad (\text{A.61})$$



**Define  $\vec{y}$  of horizontal segment**

$$\vec{x} = \gamma \vec{v} + \delta \vec{w} \quad (\text{A.62})$$

$$|\delta \vec{w}| = h, |\delta| = h, \delta = h \quad (\text{A.63})$$

$$\vec{y} = \begin{bmatrix} P \\ b \end{bmatrix} \quad (\text{A.64})$$

$$\vec{y} = \begin{bmatrix} P = \gamma_1 \cos \theta - h \sin \theta \\ b = \gamma_1 \sin \theta + h \cos \theta \end{bmatrix} \quad (\text{A.65})$$

$$\gamma_1 = \frac{b + \cos \theta}{\sin \theta}, P = \frac{b + \cos \theta}{\sin \theta} \cos \theta + h \sin \theta = \frac{\cos \theta b - h}{\sin \theta} \quad (\text{A.66})$$

$$\vec{y} = \begin{bmatrix} \frac{\cos \theta b - h}{\sin \theta} \\ b \end{bmatrix} \quad (\text{A.67})$$

**Decisions on Length horizontal segment**

$$\vec{x} = \begin{bmatrix} Q \\ b \end{bmatrix}, \vec{y} = \begin{bmatrix} P \\ b \end{bmatrix}, \vec{z} = \begin{bmatrix} A \\ b \end{bmatrix} \quad (\text{A.68})$$

If  $P \geq A$ , there will be a single cutting plane.

$$l = ||\vec{x} - \vec{y}||. \quad (\text{A.69})$$

$$l = 2 \left| \frac{h}{\sin \theta} \right| \quad (\text{A.70})$$

If  $P < A$  and  $Q > A$ , there will be two cutting planes. Here the horizontal part will possess a particular length.

$$l = ||\vec{x} - \vec{z}|| \quad (\text{A.71})$$

$$l = \sqrt{\frac{(\sin \theta \cos \phi b - \cos \theta \sin \phi b + \sin \theta a - \sin \phi h)^2}{\sin^2 \theta \sin^2 \phi}} \quad (\text{A.72})$$

If  $P < A$  and  $Q \leq A$ , there will be no horizontal part.

$$l = 0 \quad (\text{A.73})$$

**Derivation of Diagonal segment**

**Define  $\vec{x}$  of diagonal segment**

$$\vec{x}_a = \alpha \vec{v} + \beta \vec{w}, \vec{x}_h = \gamma \vec{v} + \delta \vec{w} \quad (\text{A.74})$$

$$\beta = -a, \delta = -h \quad (\text{A.75})$$

$$\vec{x}_a = \begin{bmatrix} D \\ E \end{bmatrix}, \vec{x}_h = \begin{bmatrix} F \\ G \end{bmatrix} \quad (\text{A.76})$$

$$\vec{x}_a = \begin{bmatrix} D = \alpha_1 \cos \phi + a \sin \phi \\ E = \alpha_1 \sin \phi - a \cos \phi \end{bmatrix}, \vec{x}_h = \begin{bmatrix} F = \gamma_1 \cos \theta + h \sin \theta \\ G = \gamma_1 \sin \theta - h \cos \theta \end{bmatrix} \quad (\text{A.77})$$

$$\vec{x}_a = \vec{x}_h, \begin{bmatrix} D \\ E \end{bmatrix} = \begin{bmatrix} F \\ G \end{bmatrix} \quad (\text{A.78})$$

$$\vec{x} = \begin{bmatrix} -\cos \theta a + \cos \phi h \\ \frac{\sin \theta \cos \phi - \cos \theta \sin \phi}{\sin \theta \cos \phi - \cos \theta \sin \phi} \end{bmatrix} \quad (\text{A.79})$$

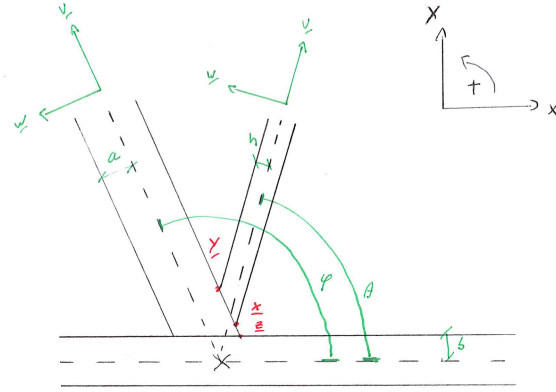


Figure A.5: Diagonal segment in situation with dynamic post

**Define  $\vec{x}$  of diagonal segment**

$$\vec{y}_a = \alpha \vec{v} + \beta \vec{w}, \vec{y}_h = \gamma \vec{v} + \delta \vec{w} \quad (\text{A.80})$$

$$\beta = -a, \delta = h \quad (\text{A.81})$$

$$\vec{x}_a = \begin{bmatrix} H \\ I \end{bmatrix}, \vec{x}_h = \begin{bmatrix} J \\ K \end{bmatrix} \quad (\text{A.82})$$

$$\vec{y}_a = \begin{bmatrix} H = \alpha_2 \cos \phi + a \sin \phi \\ I = \alpha_2 \sin \phi - a \cos \phi \end{bmatrix}, \vec{y}_h = \begin{bmatrix} J = \gamma_1 \cos \theta - h \sin \theta \\ K = \gamma_1 \sin \theta + h \cos \theta \end{bmatrix} \quad (\text{A.83})$$

$$\vec{y}_a = \vec{y}_h, \begin{bmatrix} H \\ I \end{bmatrix} = \begin{bmatrix} J \\ K \end{bmatrix} \quad (\text{A.84})$$

$$\vec{y} = \begin{bmatrix} -\cos \theta a - \cos \phi h \\ \frac{\sin \theta \cos \phi - \cos \theta \sin \phi}{\sin \theta \cos \phi - \cos \theta \sin \phi} \\ -\sin \theta a - \sin \phi h \\ \frac{\sin \theta \cos \phi - \cos \theta \sin \phi}{\sin \theta \cos \phi - \cos \theta \sin \phi} \end{bmatrix} \quad (\text{A.85})$$

**Decisions on Length diagonal segment**

$$\vec{x} = \begin{bmatrix} D \\ E \end{bmatrix}, \vec{y} = \begin{bmatrix} H \\ I \end{bmatrix}, \vec{z} = \begin{bmatrix} A \\ b \end{bmatrix} \quad (\text{A.86})$$

If  $D \leq A$  &  $E \geq b$ , there will be one cutting plane.

$$l = ||\vec{x} - \vec{y}|| \quad (\text{A.87})$$

$$l = 2 * \sqrt{-\frac{h^2}{(2 \cos \phi^2 - 1) \cos \theta^2 + 2 \sin \theta \cos \theta \cos \phi \sin \phi - \cos \phi^2}} \quad (\text{A.88})$$

IF  $D > A$  &  $E < b$  and IF  $H < A$  &  $I > b$

$$l = ||\vec{y} - \vec{z}|| \quad (\text{A.89})$$

$$l = \sqrt{-\frac{(\sin(\theta) \cos \phi b - \cos \theta \sin \phi b + \sin \theta a + \sin \phi h)^2}{\sin \phi^2 (2 \sin(\theta) \cos \theta \cos \phi \sin \phi + 2 \cos \theta^2 \cos \phi^2 - \cos \theta^2 - \cos \phi^2)}} \quad (\text{A.90})$$

IF  $D > A$  &  $E < b$  and IF  $H \geq A$  &  $I \leq b$

$$l = 0 \quad (\text{A.91})$$

## Summary

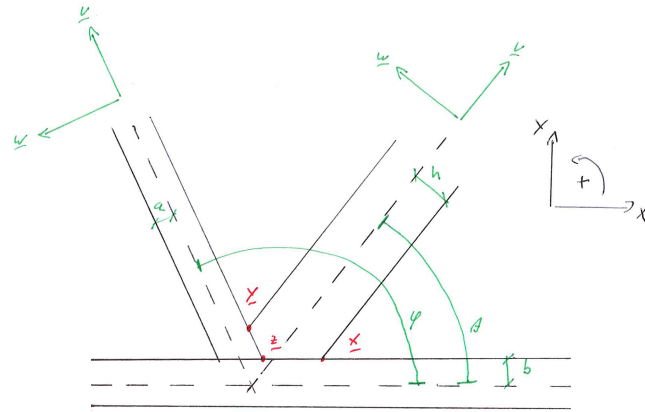


Figure A.6: Horizontal and diagonal segment in situation with dynamic post

Table A.3: Decision tree for determining length of horizontal and diagonal segment

| Position Weld  | First decision             | Second decision            | Length   |
|--|----------------------------|----------------------------|--|
| Horizontal segment   | If $P \geq A$              |                            | $l = 2 \left  \frac{h}{\sin \theta} \right $   |
| $\vec{x} = \begin{bmatrix} Q \\ b \end{bmatrix}, \vec{y} = \begin{bmatrix} P \\ b \end{bmatrix}, \vec{z} = \begin{bmatrix} A \\ b \end{bmatrix}$ | If $P < A$                 | If $Q > A$                 | $l = \sqrt{\frac{(\sin \theta \cos \phi b - \cos \theta \sin \phi b + \sin \theta a - \sin \phi h)^2}{\sin^2 \theta \sin^2 \phi}}$   |
|  |                            | If $Q \leq A$              | $l = 0$  |
| Diagonal segment   | If $D \leq A$ & $E \geq b$ |                            | $l = 2 * \sqrt{\frac{h^2}{(2 \cos \phi^2 - 1) \cos \theta^2 + 2 \sin \theta \cos \theta \cos \phi \sin \phi - \cos \phi^2}}$   |
| $\vec{x} = \begin{bmatrix} D \\ E \end{bmatrix}, \vec{y} = \begin{bmatrix} H \\ I \end{bmatrix}, \vec{z} = \begin{bmatrix} A \\ b \end{bmatrix}$ | If $D > A$ & $E < b$       | If $H < A$ & $I > b$       | $l = \sqrt{\frac{(\sin(\theta) \cos \phi b - \cos \theta \sin \phi b + \sin \theta a + \sin \phi h)^2}{\sin \phi^2 (2 \sin(\theta) \cos \theta \cos \phi \sin \phi + 2 \cos \theta^2 \cos \phi^2 - \cos \theta^2 - \cos \phi^2)}}$ |
|  |                            | If $H \geq A$ & $I \leq b$ | $l = 0$  |

### A.3. Derivation of situation with dynamic post and eccentricity

**Eccentricity vector  $\vec{\varepsilon}$**

$$\vec{\varepsilon} = \begin{bmatrix} \varepsilon \\ 0 \end{bmatrix} \quad (\text{A.92})$$

**Define  $\vec{z}$  of corner**

$$\vec{x}_a = \alpha \vec{v} + \beta \vec{w} \quad (\text{A.93})$$

$$\beta = -a \quad (\text{A.94})$$

$$\vec{z} = \begin{bmatrix} A = \alpha_1 \cos \phi + a \sin \phi \\ b = \alpha_1 \sin \phi - a \cos \phi \end{bmatrix} \quad (\text{A.95})$$

$$\vec{z} = \begin{bmatrix} \frac{a + \cos \phi b}{\sin \phi} \\ b \end{bmatrix} \quad (\text{A.96})$$

**Derivation of Horizontal segment**

**Define  $\vec{x}$  of horizontal segment**

$$\vec{x} = \alpha \vec{v} + \beta \vec{w} + \vec{\varepsilon} \quad (\text{A.97})$$

$$|\beta \vec{w}| = h, |\beta| = -h, \beta = -h \quad (\text{A.98})$$

$$\vec{x} = \begin{bmatrix} Q \\ b \end{bmatrix} \quad (\text{A.99})$$

$$\vec{y} = \begin{bmatrix} Q = \alpha_1 \cos \theta + h \sin \theta + \varepsilon \\ b = \alpha_1 \sin \theta - h \cos \theta \end{bmatrix} \quad (\text{A.100})$$

$$\alpha_1 = \frac{b + \cos \theta}{\sin \theta}, Q = \frac{b + \cos \theta}{\sin \theta} \cos \theta + h \sin \theta + \varepsilon = \frac{\cos \theta b + \sin \theta \varepsilon + h}{\sin \theta} \quad (\text{A.101})$$

$$\vec{x} = \begin{bmatrix} \frac{\cos \theta b + \sin \theta \varepsilon + h}{\sin \theta} \\ b \end{bmatrix} \quad (\text{A.102})$$

**Define  $\vec{y}$  of horizontal segment**

$$\vec{x} = \gamma \vec{v} + \delta \vec{w} + \vec{\varepsilon} \quad (\text{A.103})$$

$$|\delta \vec{w}| = h, |\delta| = h, \delta = h \quad (\text{A.104})$$

$$\vec{y} = \begin{bmatrix} P \\ b \end{bmatrix} \quad (\text{A.105})$$

$$\vec{y} = \begin{bmatrix} P = \gamma_1 \cos \theta - h \sin \theta + \varepsilon \\ b = \gamma_1 \sin \theta + h \cos \theta \end{bmatrix} \quad (\text{A.106})$$

$$\gamma_1 = \frac{b + \cos \theta}{\sin \theta}, P = \frac{b + \cos \theta}{\sin \theta} \cos \theta + h \sin \theta + \varepsilon = \frac{\cos \theta b + \sin \theta \varepsilon - h}{\sin \theta} \quad (\text{A.107})$$

$$\vec{y} = \begin{bmatrix} \frac{\cos \theta b + \sin \theta \varepsilon - h}{\sin \theta} \\ b \end{bmatrix} \quad (\text{A.108})$$

## Decisions on Length horizontal segment

$$\vec{x} = \begin{bmatrix} Q \\ b \end{bmatrix}, \vec{y} = \begin{bmatrix} P \\ b \end{bmatrix}, \vec{z} = \begin{bmatrix} A \\ b \end{bmatrix} \quad (\text{A.109})$$

If  $P \geq A$ , there will be a single cutting plane.

$$l = ||\vec{x} - \vec{y}||. \quad (\text{A.110})$$

$$l = 2 \left| \frac{h}{\sin \theta} \right| \quad (\text{A.111})$$

If  $P < A$  and  $Q > A$ , there will be two cutting planes. Here the horizontal part will possess a particular length.

$$l = ||\vec{x} - \vec{z}|| \quad (\text{A.112})$$

$$l = \sqrt{\frac{(\sin \theta \cos \phi b - \sin \theta \sin \phi \varepsilon - \cos \theta \sin \phi b + \sin \theta a + \sin \phi h)^2}{\sin^2 \theta \sin^2 \phi}} \quad (\text{A.113})$$

If  $P < A$  and  $Q \leq A$ , there will be no horizontal part.

$$l = 0 \quad (\text{A.114})$$

## Derivation of Diagonal segment

**Define  $\vec{x}$  of diagonal segment**

$$\vec{x}_a = \alpha \vec{v} + \beta \vec{w}, \vec{x}_h = \gamma \vec{v} + \delta \vec{w} + \vec{\varepsilon} \quad (\text{A.115})$$

$$\beta = -a, \delta = -h \quad (\text{A.116})$$

$$\vec{x}_a = \begin{bmatrix} D \\ E \end{bmatrix}, \vec{x}_h = \begin{bmatrix} F \\ G \end{bmatrix} \quad (\text{A.117})$$

$$\vec{x}_a = \begin{bmatrix} D = \alpha_1 \cos \phi + a \sin \phi \\ E = \alpha_1 \sin \phi - a \cos \phi \end{bmatrix}, \vec{x}_h = \begin{bmatrix} F = \gamma_1 \cos \theta + h \sin \theta + \varepsilon \\ G = \gamma_1 \sin \theta - h \cos \theta \end{bmatrix} \quad (\text{A.118})$$

$$\vec{x}_a = \vec{x}_h, \begin{bmatrix} D \\ E \end{bmatrix} = \begin{bmatrix} F \\ G \end{bmatrix} \quad (\text{A.119})$$

$$\vec{x} = \begin{bmatrix} \frac{(\sin \theta \varepsilon + h) \cos \phi - \cos \theta a}{\sin \theta \cos \phi - \cos \theta \sin \phi} \\ \frac{(\sin \phi \varepsilon - a) \sin \theta + \sin \phi h}{\sin \theta \cos \phi - \cos \theta \sin \phi} \end{bmatrix} \quad (\text{A.120})$$

**Define  $\vec{y}$  of diagonal segment**

$$\vec{y}_a = \alpha \vec{v} + \beta \vec{w}, \vec{y}_h = \gamma \vec{v} + \delta \vec{w} + \vec{\varepsilon} \quad (\text{A.121})$$

$$\beta = -a, \delta = h \quad (\text{A.122})$$

$$\vec{y}_a = \begin{bmatrix} H \\ I \end{bmatrix}, \vec{y}_h = \begin{bmatrix} J \\ K \end{bmatrix} \quad (\text{A.123})$$

$$\vec{y}_a = \begin{bmatrix} H = \alpha_2 \cos \phi + a \sin \phi \\ I = \alpha_2 \sin \phi - a \cos \phi \end{bmatrix}, \vec{y}_h = \begin{bmatrix} J = \gamma_1 \cos \theta - h \sin \theta + \varepsilon \\ K = \gamma_1 \sin \theta + h \cos \theta \end{bmatrix} \quad (\text{A.124})$$

$$\vec{y}_a = \vec{y}_h, \begin{bmatrix} H \\ I \end{bmatrix} = \begin{bmatrix} J \\ K \end{bmatrix} \quad (\text{A.125})$$

$$\vec{y} = \begin{bmatrix} \frac{(\sin \theta \varepsilon - h) \cos \phi - \cos \theta a}{\sin \theta \cos \phi - \cos \theta \sin \phi} \\ \frac{(\sin \phi \varepsilon - a) \sin \theta - \sin \phi h}{\sin \theta \cos \phi - \cos \theta \sin \phi} \end{bmatrix} \quad (\text{A.126})$$

## Decisions on Length diagonal segment

$$\vec{x} = \begin{bmatrix} D \\ E \end{bmatrix}, \vec{y} = \begin{bmatrix} H \\ I \end{bmatrix}, \vec{z} = \begin{bmatrix} A \\ b \end{bmatrix} \quad (\text{A.127})$$

If  $D \leq A$  &  $E \geq b$ , there will be one cutting plane.

$$l = ||\vec{x} - \vec{y}|| \quad (\text{A.128})$$

$$l = 2 * \sqrt{-\frac{h^2}{(2 \cos \phi^2 - 1) \cos \theta^2 + 2 \sin \theta \cos \theta \cos \phi \sin \phi - \cos \phi^2}} \quad (\text{A.129})$$

IF  $D > A$  &  $E < b$  and IF  $H < A$  &  $I > b$

$$l = ||\vec{y} - \vec{z}|| \quad (\text{A.130})$$

$$l = \sqrt{-\frac{(\sin \theta \cos \phi b - \sin \theta \sin \phi \varepsilon - \cos \theta \sin \phi b + \sin \theta * a + \sin \phi h)^2}{\sin \phi^2 (2 \sin \theta \cos \theta \cos \phi \sin \phi + 2 \cos \theta^2 \cos \phi^2 - \cos \theta^2 - \cos \phi^2)}} \quad (\text{A.131})$$

IF  $D > A$  &  $E < b$  and IF  $H \geq A$  &  $I \leq b$

$$l = 0 \quad (\text{A.132})$$

## Summary

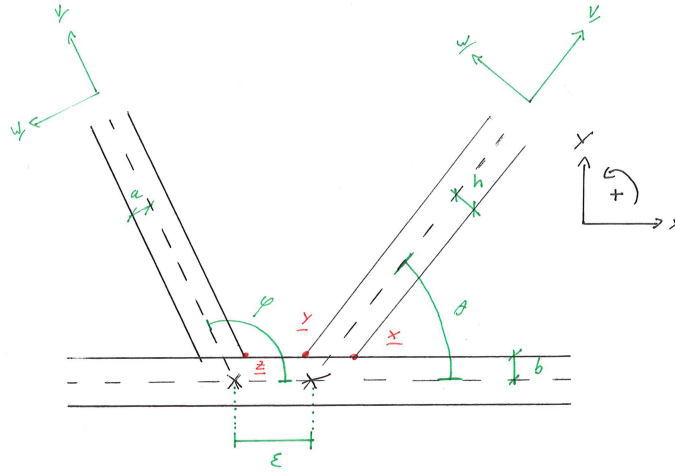


Figure A.7: Horizontal and diagonal segment in situation with dynamic post and eccentricity

Table A.4: Decision tree for determining length of horizontal and diagonal segment

| Position Weld  | First decision             | Second decision | Length   |
|--|----------------------------|-----------------|--|
| Horizontal segment   | If $P \geq A$              |                 | $l = 2 \left  \frac{h}{\sin \theta} \right $   |
| $\vec{x} = \begin{bmatrix} Q \\ b \end{bmatrix}, \vec{y} = \begin{bmatrix} P \\ b \end{bmatrix}, \vec{z} = \begin{bmatrix} A \\ b \end{bmatrix}$ | If $P < A$                 | If $Q > A$      | $l = \sqrt{\frac{(\sin \theta \cos \phi b - \sin \theta \sin \phi \epsilon - \cos \theta \sin \phi b + \sin \theta a + \sin \phi h)^2}{\sin \theta^2 \sin \phi^2}}$  |
|  |                            | If $Q \leq A$   | $l = 0$  |
| Diagonal segment   | If $D \leq A$ & $E \geq b$ |                 | $l = 2 * \sqrt{\frac{h^2}{(2 \cos \phi^2 - 1) \cos \theta^2 + 2 \sin \theta \cos \theta \cos \phi \sin \phi - \cos \phi^2}}$   |
| $\vec{x} = \begin{bmatrix} D \\ E \end{bmatrix}, \vec{y} = \begin{bmatrix} H \\ I \end{bmatrix}, \vec{z} = \begin{bmatrix} A \\ b \end{bmatrix}$ | If $E < b$                 | If $I > b$      | $l = \sqrt{-\frac{(\sin \theta \cos \phi b - \sin \theta \sin \phi \epsilon - \cos \theta \sin \phi b + \sin \theta a + \sin \phi h)^2}{\sin \phi^2 (2 \sin \theta \cos \theta \cos \phi \sin \phi + 2 \cos \theta^2 \cos \phi^2 - \cos \theta^2 - \cos \phi^2)}}$ |
|  |                            | If $I \leq b$   | $l = 0$  |

# B

## Appendix: Welding technologies and costs

**Laskosten in formule vorm**

$$W = V \times \rho \left[ \frac{100}{i} \times F \left( L + \frac{A + R + O}{1600} \times \frac{100}{B} \right) + M \times \frac{100}{\eta} + P \times \delta + \frac{1000}{60} \times \frac{V_g \times G}{F} \right]$$

SBKG.07.NF

Labels in the diagram:

- Kosten per meter laslengte
- Neersmeltsnelheid lasmetaal [kg/h]
- Afschrijving apparatuur [€/jaar]
- Rente op investering apparatuur [€/jaar]
- Onderhoud betreffende apparatuur [€/jaar]
- Kosten lastoevoegmateriaal [€/kg]
- Kosten beschermgas [€/m³]
- Verbruik beschermgas [l/min]
- Kosten laspoeder [€/kg]
- Rendement lasmateriaal [%]
- Bezettingsgraad apparatuur [%]
- Loonkosten [€/h]
- Inschakelduur lasser (duty cycle = effectieve boogtijd/totale werktijd in functie [%])
- Dichtheid lasmetaal [kg/m³]
- Volume lasnaad inclusief overdikte [mm³]
- Factor poederverbruik per kg lasdraad

Figure B.1: Formula to determine welding costs<sup>[45]</sup>



Table B.1: Discussed welding technologies in Jármai and Farkas [37, p.118]

|              |  |
|--------------|--|
| SMAW         | Shielded metal arc welding               |
| SMAW HR      | Shielded metal arc welding high recovery |
| GMAW-C       | Gas Metal arc welding with $CO_2$        |
| GMAW-M       | Gas metal arc welding with mixed gas     |
| FCAW         | Flux cored arc welding                   |
| FCAW-MC      | Metal cored arc welding                  |
| SSFCAW (ISW) | Self shielded flux cored arc welding     |
| SAW          | Submerged arc welding                    |
| GTAW         | Gas tungsten arc welding                 |

Table B.2: Welding times  $T_2$  (min/mm) in function of weld size  $\alpha_w$  (mm) for longitudinal fillet welds down-hand position [37, p.120]

| Welding technology | $\alpha_w$ [mm] | $10^3 T_2 = 10^3 C_2 \alpha_w^n$ |
|--------------------|-----------------|----------------------------------|
| SMAW               | 0-15            | $0.7889 \alpha_w^2$              |
| SMAW HR            | 0-15            | $0.5390 \alpha_w^2$              |
| GMAW-C             | 0-15            | $0.3394 \alpha_w^2$              |
| GMAW-M             | 0-15            | $0.3258 \alpha_w^2$              |
| FCAW               | 0-15            | $0.2302 \alpha_w^2$              |
| FCAW-MC HR         | 0-15            | $0.4520 \alpha_w^2$              |
| SSFCAW (ISW)       | 0-15            | $0.2090 \alpha_w^2$              |
| SAW                | 0-15            | $0.2349 \alpha_w^2$              |

Table B.3: Cutting time of plates,  $T_7$  (min/mm) in function of weld size plate thickness  $t$  (mm) [37, p.123]

| Cutting technology                | Thickness $t$ [mm] | $10^3 T_7 = 10^3 C_7 t^n$ |
|-----------------------------------|--------------------|---------------------------|
| Acetylene (normal speed)          | 2-15               | $1.1388 t^{0.25}$         |
| Acetylene (high speed)            | 2-15               | $0.9561 t^{0.25}$         |
| Stabilized gas mix (normal speed) | 2-15               | $1.1906 t^{0.25}$         |
| Stabilized gas mix (high speed)   | 2-15               | $1.0858 t^{0.25}$         |
| Propane (normal speed)            | 2-15               | $1.2941 t^{0.25}$         |
| Propane (high speed)              | 2-15               | $1.1051 t^{0.25}$         |

Table B.4: Welding times  $T_2$  [min/mm] or longitudinal fillet welds, downwards positioned, throat thickness = 6 mm [37]

|  | Welding Technology | $\alpha_w$ [mm] |     | C2     | n | [min/mm] |      | [s/mm] |          |
|--|--------------------|-----------------|-----|--------|---|----------|------|--------|----------|
|  |                    | min             | max |        |   |          |      |        |          |
| Shielded metal arc welding               | SMAW               | 0               | 15  | 0.7889 | 2 | 0.0284   | 1.70 | 76.06  | cm3/hour |
| Shielded metal arc welding high recovery | SMAW HR            | 0               | 15  | 0.539  | 2 | 0.0194   | 1.16 | 111.32 | cm3/hour |
| Gas metal arc welding with $CO_2$        | GMAW-C             | 0               | 15  | 0.3394 | 2 | 0.0122   | 0.73 | 176.78 | cm3/hour |
| Gas metal arc welding with mixed gas     | GMAW-M             | 0               | 15  | 0.3258 | 2 | 0.0117   | 0.70 | 184.16 | cm3/hour |
| Flux cored arc welding                   | FCAW               | 0               | 15  | 0.2302 | 2 | 0.0083   | 0.50 | 260.64 | cm3/hour |
| Metal cored arc welding                  | FCAW-MC            | 0               | 15  | 0.452  | 2 | 0.0163   | 0.98 | 132.74 | cm3/hour |
| Self shielded flux cored arc welding     | SSFCAW (ISW)       | 0               | 15  | 0.209  | 2 | 0.0075   | 0.45 | 287.08 | cm3/hour |
| Submerged arc welding                    | SAW                | 0               | 15  | 0.2349 | 2 | 0.0085   | 0.51 | 255.43 | cm3/hour |

Table B.5: Welding speed per throat thickness researched by Oostingh[43]

| size | throat [mm] | Plate thickness [mm] | welding beads | Surface [mm2] | Volume [mm3/meter] | min/meter | mm3/min | cm3/min | cm3/hour | gram/hour |
|------|-------------|----------------------|---------------|---------------|--------------------|-----------|---------|---------|----------|-----------|
| a4   | 4           | 10                   | 1             | 16            | 16000              | 5         | 3200    | 3.2     | 192      | 1507      |
| a5   | 5           | 10                   | 1             | 25            | 25000              | 6         | 4167    | 4.2     | 250      | 1963      |
| a6   | 6           | 15                   | 3             | 36            | 36000              | 14        | 2571    | 2.6     | 154      | 1211      |
| a7   | 7           | 15                   | 3             | 49            | 49000              | 16        | 3063    | 3.1     | 184      | 1442      |
| a8   | 8           | 15                   | 4             | 64            | 64000              | 20        | 3200    | 3.2     | 192      | 1507      |
| a9   | 9           | 15                   | 6             | 81            | 81000              | 28        | 2893    | 2.9     | 174      | 1363      |
| a10  | 10          | 20                   | 6             | 100           | 100000             | 30        | 3333    | 3.3     | 200      | 1570      |
| a11  | 11          | 20                   | 6             | 121           | 121000             | 33        | 3667    | 3.7     | 220      | 1727      |
| a12  | 12          | 25                   | 10            | 144           | 144000             | 50        | 2880    | 2.9     | 173      | 1356      |
| a13  | 13          | 25                   | 10            | 169           | 169000             | 53        | 3189    | 3.2     | 191      | 1502      |
| a14  | 14          | 30                   | 15            | 196           | 196000             | 78        | 2513    | 2.5     | 151      | 1184      |
| a15  | 15          | 30                   | 15            | 225           | 225000             | 81        | 2778    | 2.8     | 167      | 1308      |
| a16  | 16          | 30                   | 21            | 256           | 256000             | 105       | 2438    | 2.4     | 146      | 1148      |
| a17  | 17          | 40                   | 21            | 289           | 289000             | 110       | 2627    | 2.6     | 158      | 1237      |
| a18  | 18          | 40                   | 27            | 324           | 324000             | 135       | 2400    | 2.4     | 144      | 1130      |
| a19  | 19          | 40                   | 27            | 361           | 361000             | 140       | 2579    | 2.6     | 155      | 1215      |
| a20  | 20          | 40                   | 34            | 400           | 400000             | 175       | 2286    | 2.3     | 137      | 1077      |

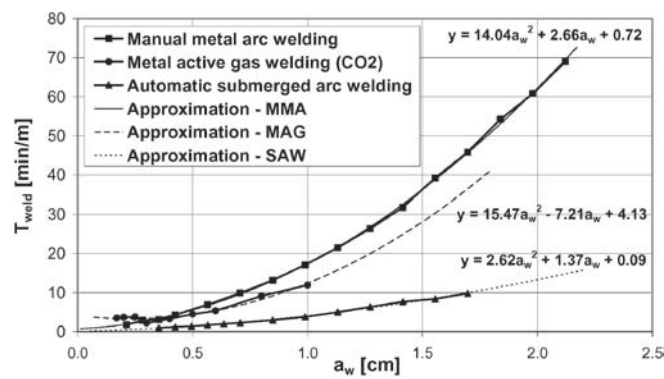
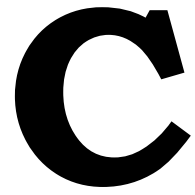


Figure B.2: Welding arc times of different welding technologies for down-hand welding of fillet welds with quadratic function approximations [46, p.288]





## Appendix: Results price comparison Dutch steel traders

## C.1. Material prices

### Long steel

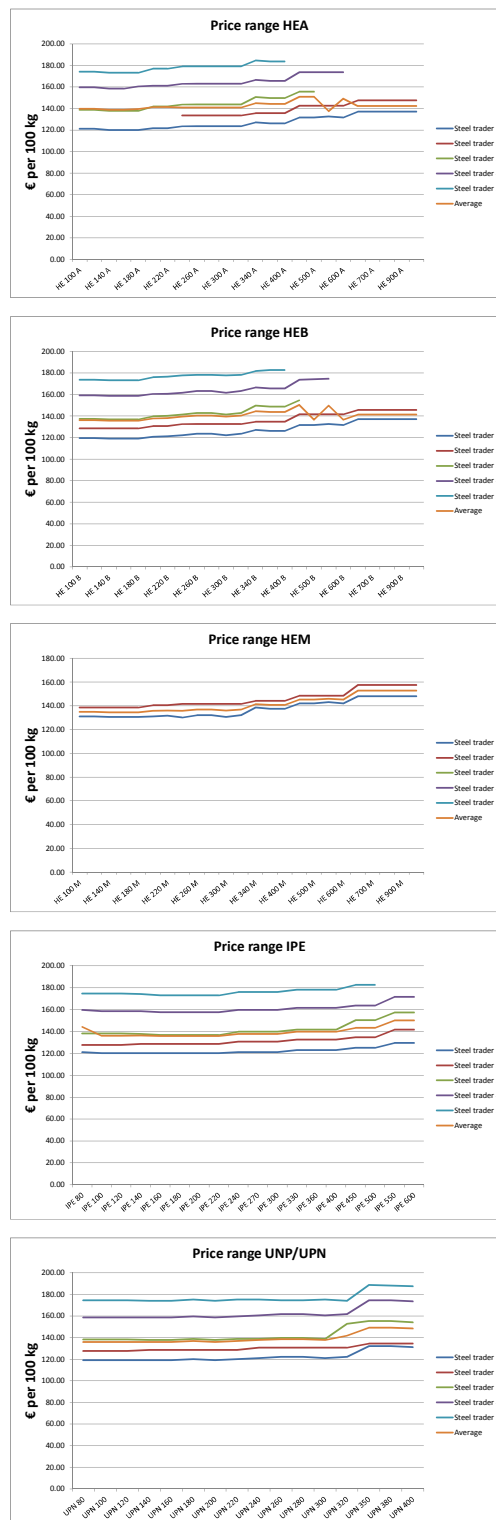


Figure C.1: Price range of Long steel<sup>[38][39][40][41][42]</sup>

## Cold formed Hollow Sections

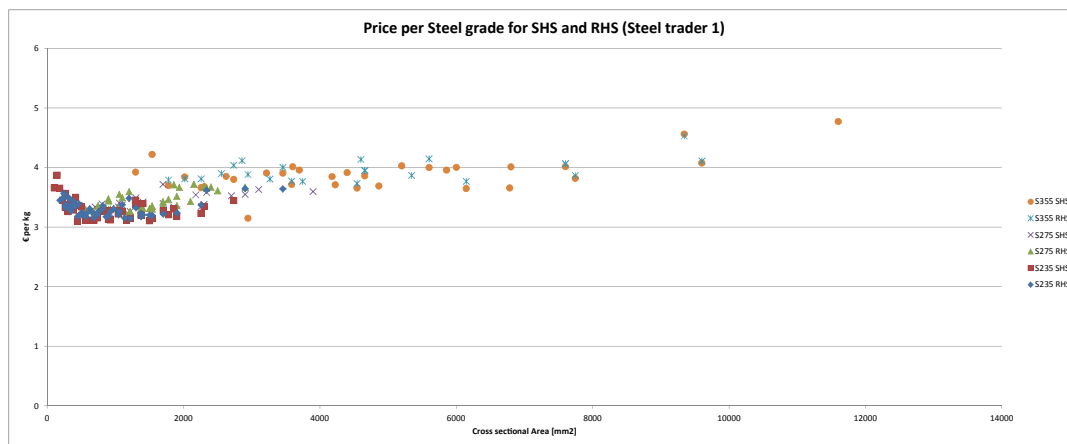


Figure C.2: Price range SHS and RHS, Steel trader 1 [38]



Figure C.3: Price range SHS and RHS, Steel trader 3 [40]

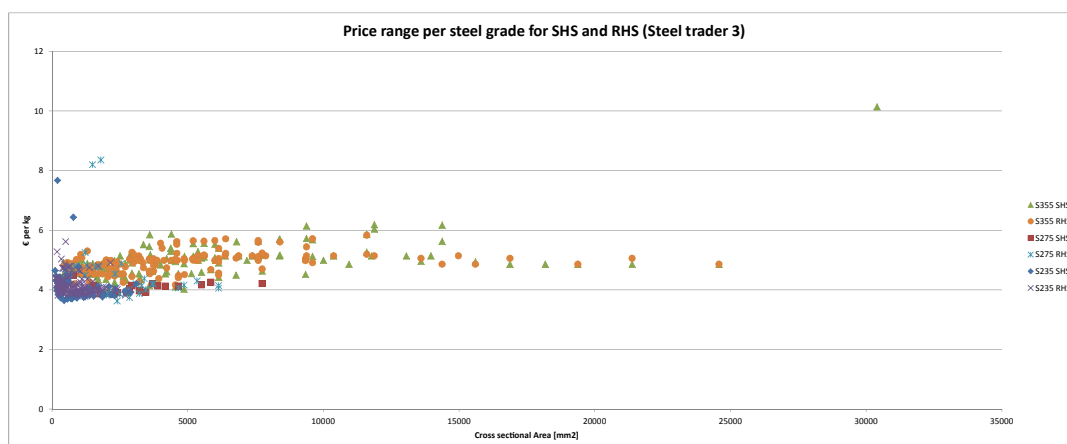


Figure C.4: Price range SHS and RHS, Steel trader 4 [41]

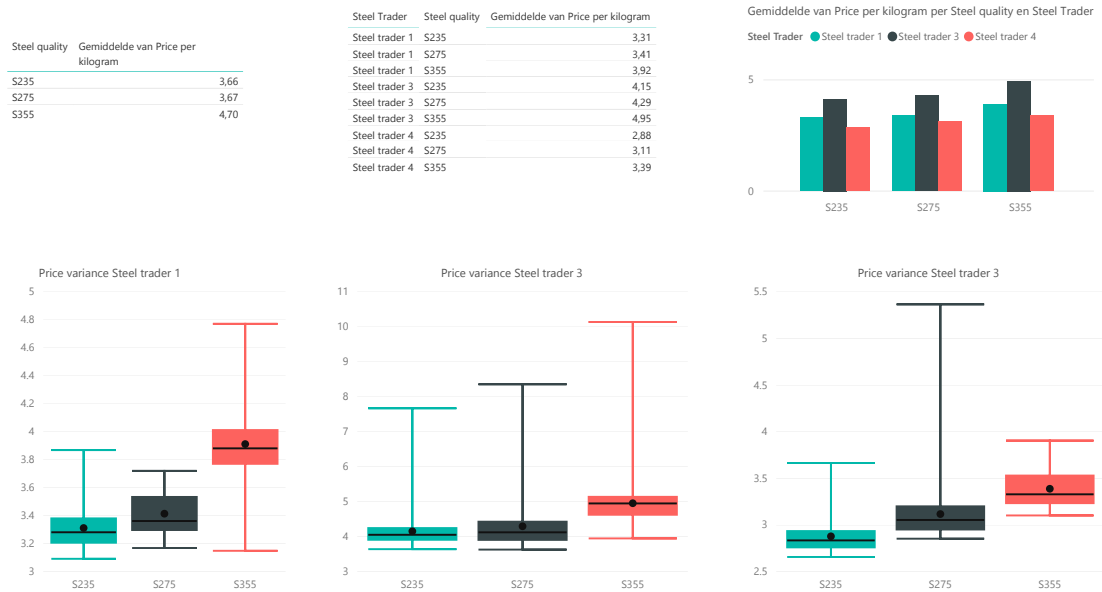


Figure C.5: Box plots SHS and RHS prices of Steel trader 1, 3 and 4 [38] [40][41]

## Plate-steel

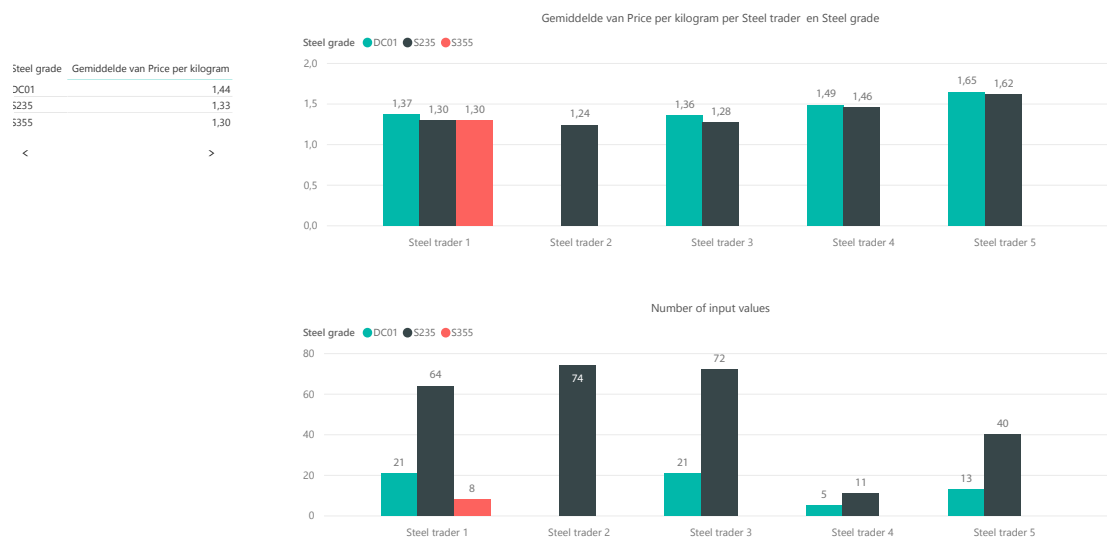


Figure C.6: Average prices of plate steel per steel trader

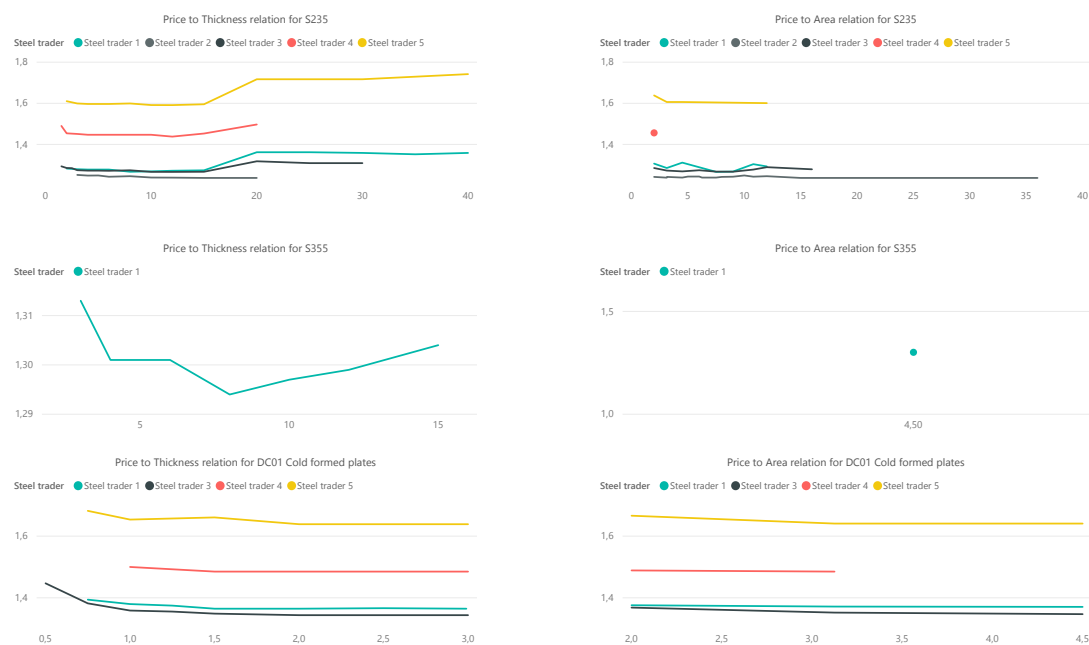


Figure C.7: Price to thickness and price to area relations per steel grade



## C.2. Sawing prices

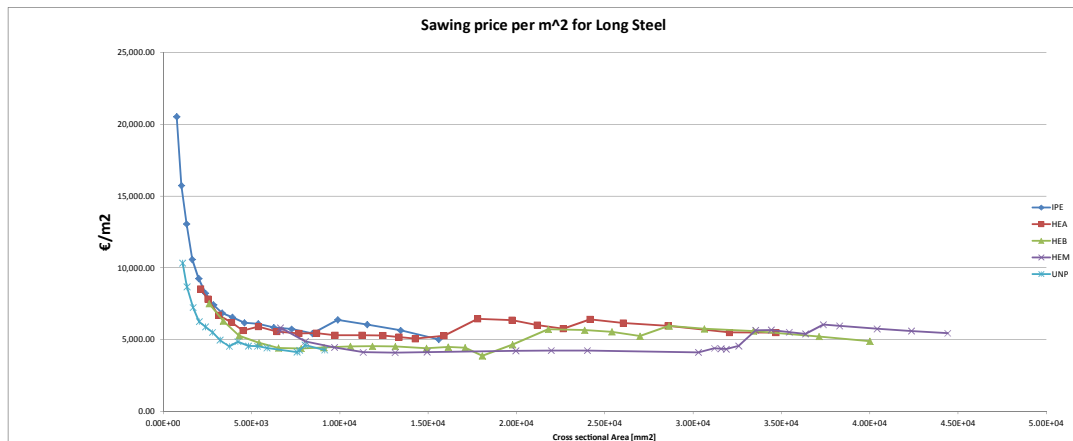


Figure C.8: Average sawing costs for Long steel[38][39][40][41][42]



Figure C.9: Sawing cost of SHS and RHS sections, Steel trader 1 [38]

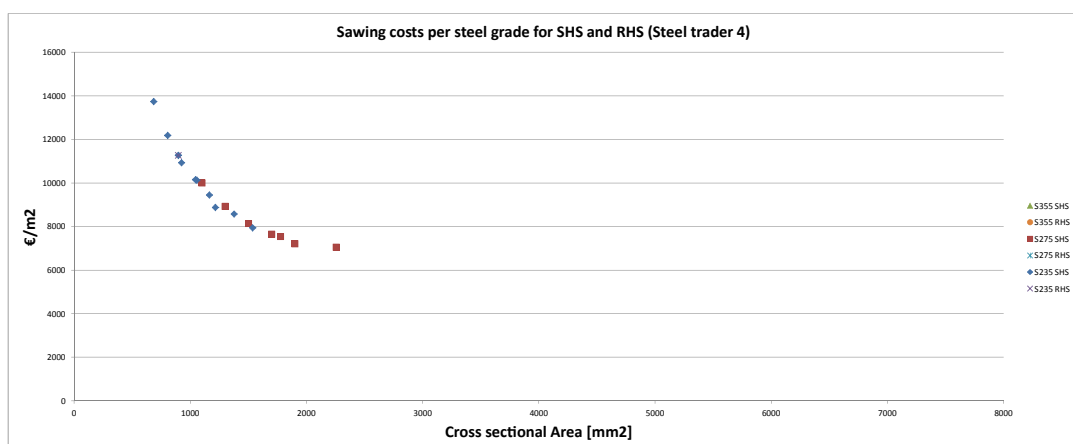


Figure C.10: Sawing cost of SHS and RHS sections, Steel trader 4 [41]

### C.3. Shot-blasting and Priming

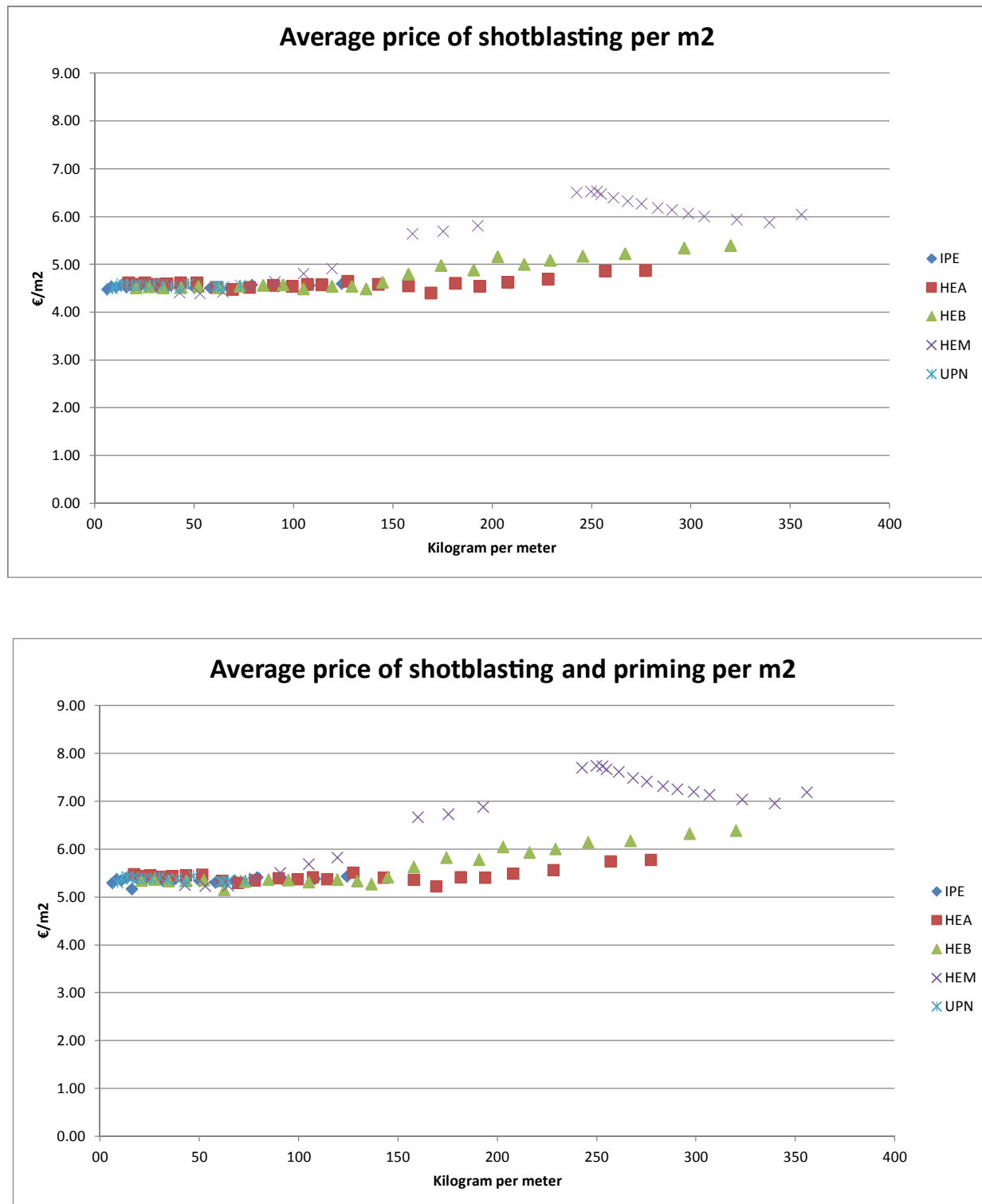


Figure C.11: Average prices for shot-blasting and priming of long steel



# D

## Appendix: Test-case cost-model "Simply supported beam"

In order to verify the cost-model a simple structural model is set up. The model used to test the cost-model is a simple supported beam with two rotational springs. In excel a parametric model is build to create a data set. In table D.1 assumptions can be found that are used to produce the data set.

Table D.1: Assumptions for simply supported beam model

|   |
|---|
| Only Symmetric I-beams are considered (IPE, HEA, HEB & HEM)                         |
| Four connection typologies are considered (Figure D.2)                              |
| Only steel-strength S235 is considered  |
| All welds are fillet welds  |
| Throat thickness fillet welds based on full strength criteria ( $a > 0.46t$ ) 6.3.1 |
| M. Steenhuis method used to determine rotational stiffness. [3, p.262]              |
| Geometric assumptions   |
| Radius bolt is 1.5 times thickness plate  |
| Thickness end-plate is the same thickness as column flange                          |
| <i>Extended end-plate</i>   |
| 6 Bolts   |
| extension plate = 50 mm (not ratio dependent)                                       |
| $z = h_{beam}$  |
| <i>Haunch</i>   |
| 8 Bolts   |
| height haunch = 200 mm (not ratio dependent)  |
| $z = h_{beam} + h_{haunch}$   |
| <i>diagonallength/height ratio = 2/1 (angle of 30 degrees)</i>                      |
| $t_{flange,haunch} = t_{flange,beam}$   |
| $t_{web,haunch} = t_{web,beam}$   |

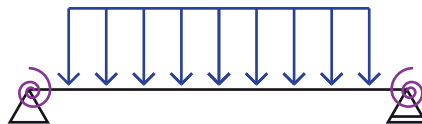


Figure D.1: Simply supported beam with rotation stiffness  $k$

The simply supported beam is analyzed with the Euler-Bernoulli beam theory. With appropriate boundary conditions which describe the rotational stiffness of the nodes with the factor  $k$ , a formula to determine the sag at mid span is formulated.

$$EIw'''' = q \quad (D.1)$$

$$w = -\frac{dw}{dx} = -\phi \quad \kappa = \frac{d\phi}{dx} \quad M = EI\kappa \quad V = \frac{dM}{dx} \quad (D.2)$$

$$\begin{aligned} w(0) &= 0 & w(L) &= 0 \\ M(0) &= k * \phi(0) & M(L) &= -k * \phi(L) \end{aligned} \quad (D.3)$$

$$w_{(x=L/2)} = -\frac{ql^4}{384EI} + \frac{L^5 k q}{96EI(2EI+Lk)} + \frac{L^4 q}{24(EI+Lk)} \quad (D.4)$$

#### Joint verification: Simplified Component method

To verify the joints a simplified component method is used developed by M. Steenhuis [3, p.262]. In this method a simplified formula is set for frequently used I-beam connections. The formula gives a value for the rotational stiffness  $S_{j,ini,ben}$ . From this stiffness the classification of Eurocode whether the connection can be classified as hinged, rigid or semi-rigid can be determined [5, part 1, p.6]. When the connections is classified as rigid or semi-rigid, the rotational stiffness can be taken into account for the structural analysis.

With equation D.7 the rotational stiffness parameter for equation D.4 is determined. The sag at mid-span can be calculated and this value can be compared with a beam without rotational stiffness in the joints. This will show the profit of taking into account rotational stiffness's for a simply supported beam.

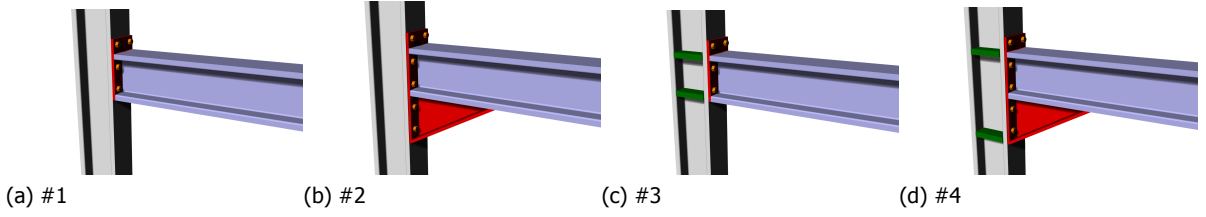


Figure D.2: Connection-typologies of frame structure

$$S_{j,ini,ben} = \frac{Ez^2 t_{fc}}{k_f} \quad (D.5)$$

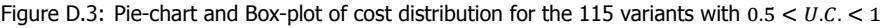
$$\begin{aligned} &\text{Hinged if:} && \text{Moment resisting if:} \\ &S_{j,ini,ben} \leq \frac{0.5EI_b}{L_b} && S_{j,ini,ben} \geq \frac{k_b EI_b}{L_b} \end{aligned} \quad (D.6)$$

$k_b = 25(\text{unbraced system})$   
 $k_b = 8(\text{braced system})$

$$k = \frac{S_{j,ini}L}{EI_b} \quad (D.7)$$

#### Analysis

Excel is used to perform the calculations. Here a model is set up that performs all the required calculations, the main interface of the Excel is displayed in figure D.4 With the input defined in table D.2 data is generated. The input consist out of 74 unique section types and produces 888 different combinations. With this data conclusion can be drawn what the biggest cost influencers are in the used cost-model.



| Parameter      | Input   |
|----------------|---|
| Beams          | IPE100 up till IPE600<br>HEA100 up till HEA1000<br>HEB100 up till HEB1000<br>HEM180 up till HEM1000 |
| Lengths        | 6, 8, 10 meter  |
| qload          | 25 kN/m   |
| Joint-typology | #1,#2,#3,#4   |

After running the analysis of the 888 variants with the Excel spreadsheet, solutions with a unity check for deflection at mid-span between 0.5 and 1 are filtered out. This leaves a list of 115 variants. On these variants cost behaviour is analyzed. Excluding the other variants with unsatisfactory unity checks will produce more thrust-worthy conclusions for cost-effective decision making of steel structures.

The rotational stiffness of the different joints have been taken into account. This can positively influence the amount of sag at mid-span compared to beam that has hinged connections. As seen in equation D.7 the rotational stiffness is dependent on the ratio between the beam stiffness and the beams length. When the beam is long and slender, this will increase the stiffness of the the connection. However a slender beam will have a lot of deflection. This can also be seen in the results of the analysis. Variants where there is a stiff connection are often coupled with slender beams. These

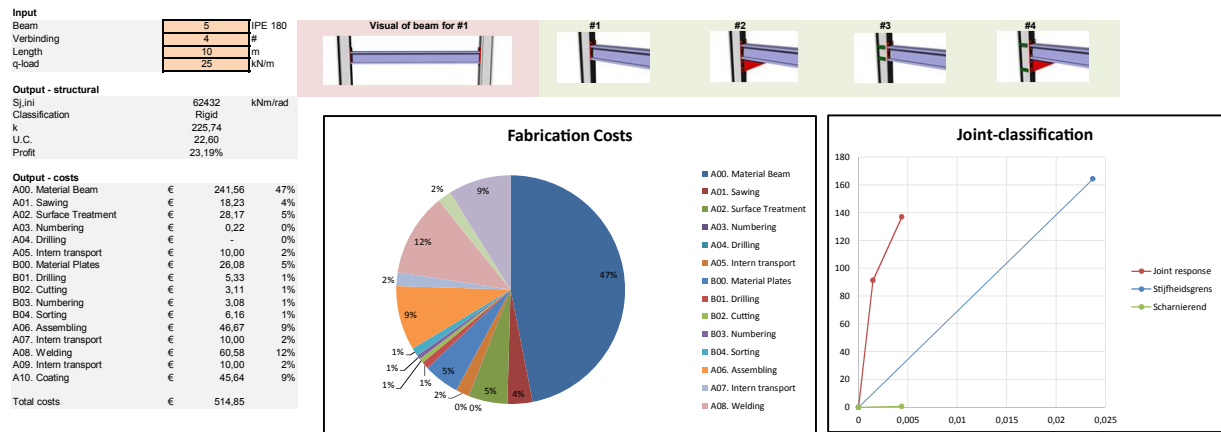


Figure D.4: Input and output sheet of cost-model

slender beams show high deflections in mid-span despite the stiffer connections. This makes these variants unattractive since the maximum deflection requirement is not met.

In figures D.5, D.6 and D.7 the average costs per joint typology for IPE cross-sections are displayed. The average is taken here of the three different lengths. Here the cost behavior per individual cost component can be analyzed. Notable is that the behaviour over increasing beam-height can be either constant, linear or nonlinear, see table D.3.

The only process that is non-linear is the costs for welding. In figure D.6 can be seen how the price increases over increasing beam height. Which does not necessarily seem expected, because a fixed haunch height of 200 mm for joint typology #2 and #4 is assumed in table D.1. However the plate thicknesses of the haunch are equal to the plate thicknesses of the beam. Bigger beams possess bigger thickness and this influences the amount of welding-volume since the full strength method is considered.

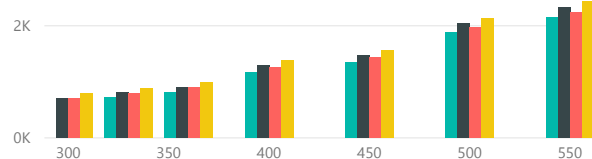
In a case like this all the processes that show a constant relationship do not have influence on the cost optimisation process. Contradictory when the cost-model is used for a steel structure with multiple beam elements, the processes with a constant relation will have an influence on the optimisation towards minimum costs.

Table D.3: Summary of cost component relation for simply supported beam

| Code | Name process      | Relation    |
|------|-------------------|-------------|
| A00  | Material Beam     | Linear      |
| A01  | Sawing            | Linear      |
| A02  | Surface Treatment | Linear      |
| A03  | Numbering         | Constant    |
| A04  | Drilling          | Not Applied |
| A05  | Intern transport  | constant    |
| B00  | Material Plate    | Non-linear  |
| B01  | Drilling          | Constant    |
| B02  | Cutting           | Linear      |
| B03  | Numbering         | Constant    |
| B04  | Sorting           | Constant    |
| A06  | Assembling        | Constant    |
| A07  | Intern transport  | Constant    |
| A08  | Welding           | Non-linear  |
| A09  | Intern transport  | Constant    |
| A10  | Coating           | Linear      |

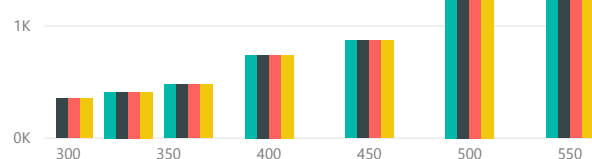
Average of 0totalcosts by BeamHeight and Joint-typologie

Joint-typologie 1 2 3 4



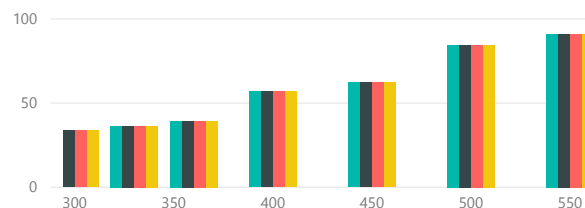
Average of A00\_Material\_Beam by BeamHeight and Joint-typologie

Joint-typologie 1 2 3 4



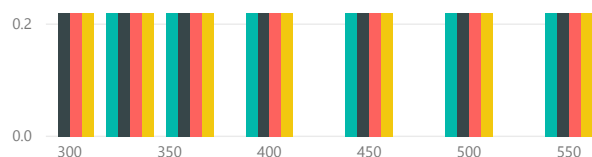
Average of A02\_Surface\_Treatment by BeamHeight and Joint-typologie

Joint-typologie 1 2 3 4



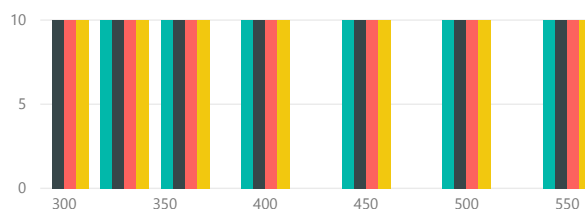
Average of A03\_Numbering by BeamHeight and Joint-typologie

Joint-typologie 1 2 3 4

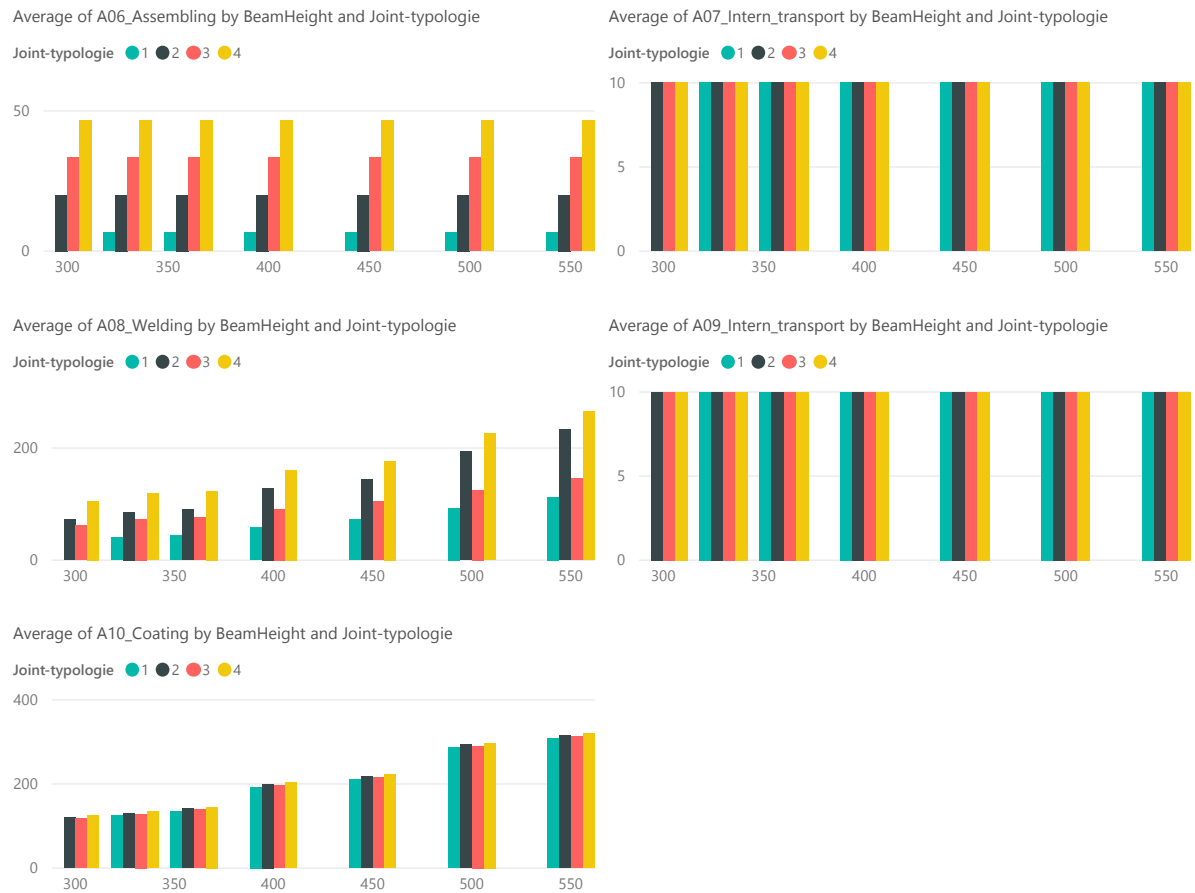


Average of A05\_Intern\_transport by BeamHeight and Joint-typologie

Joint-typologie 1 2 3 4

Figure D.5: Average Costs of A00 up till A05 per Joint typology for IPE cross-sections with  $0.5 < U.C. < 1$



Figure D.6: Average Costs of A06 up till A10 per Joint typology for IPE cross-sections with  $0.5 < U.C. < 1$

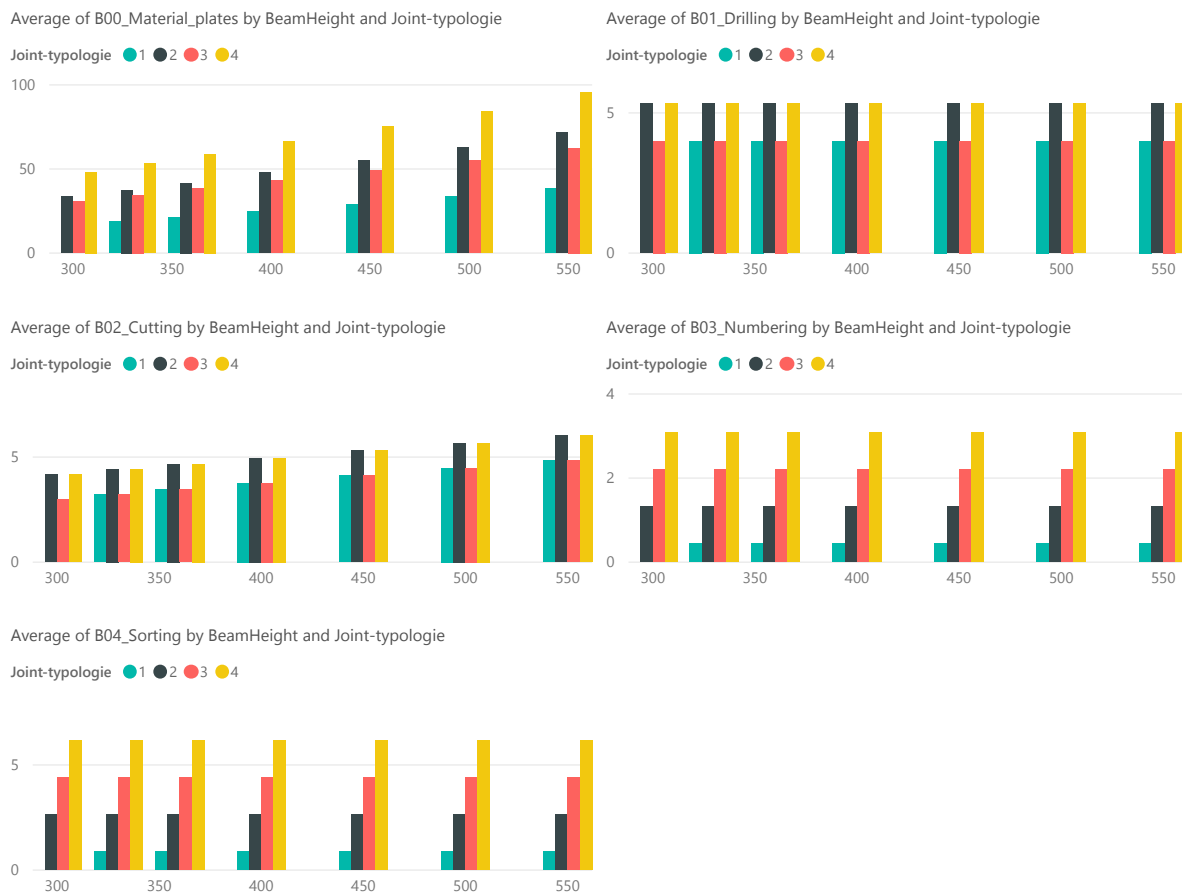
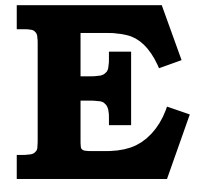


Figure D.7: Average Costs of B00 up till B04 per Joint typology for IPE cross-sections with  $0.5 < U.C. < 1$





## Appendix: Surface area study on welds

## E.1. skewed fillet weld



Figure E.1: Welding surface of Fillet welds per angle

## E.2. skewed but welds

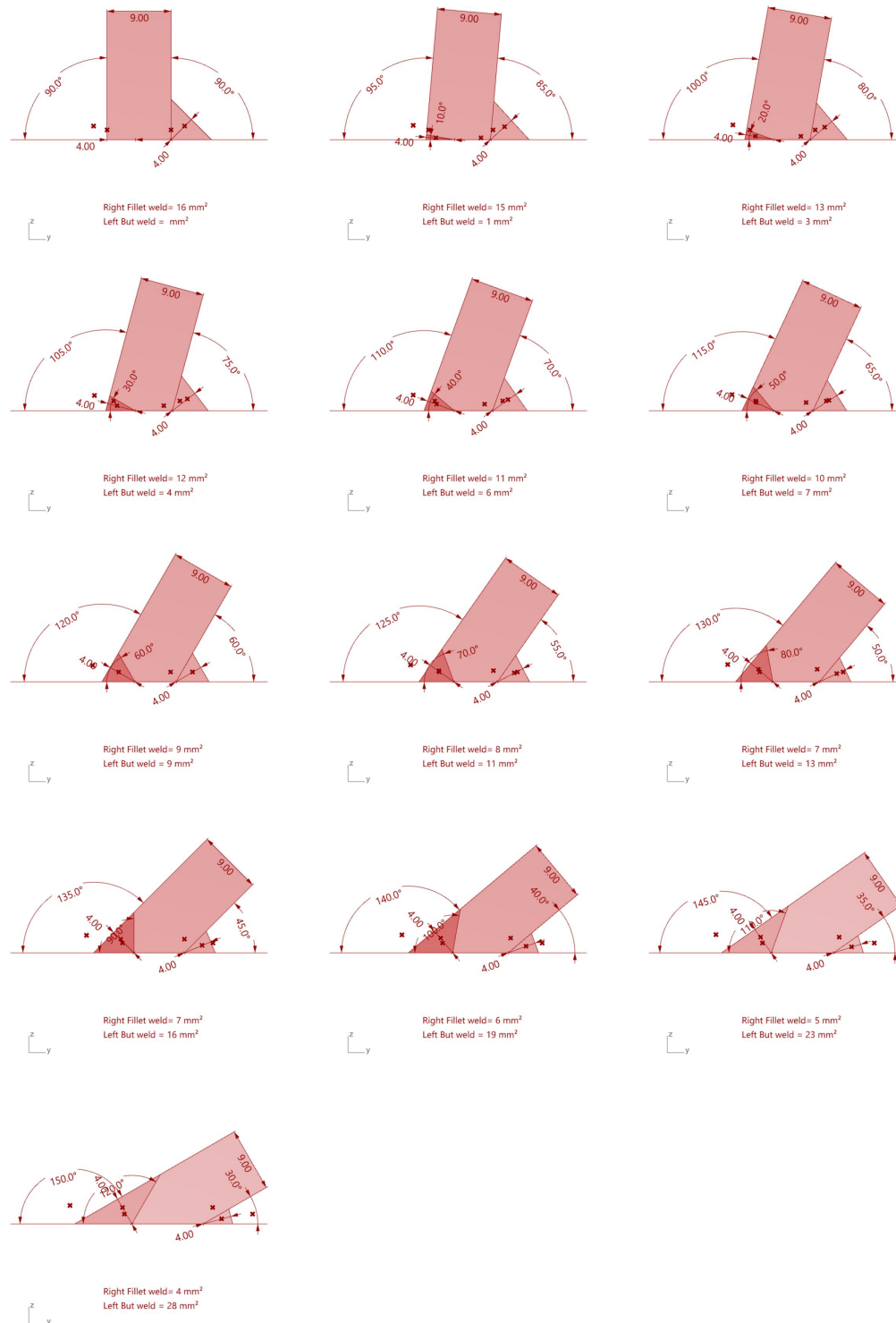


Figure E.2: Welding surface of Butt welds per angle

### E.3. triangle welds



Figure E.3: Welding surface of Triangular welds per angle

## E.4. Directional method for skew fillet welds

### Skew fillet weld of flange plate and web plate

|            |      |
|------------|------|
| Steelgrade | S235 |
| gammaM2    | 1.25 |
| fu         | 360  |
| BetaW      | 0.8  |

|   | fu   | BetaW |
|---|------|-------|
| 1 | S235 | 0.8   |
| 2 | S275 | 0.85  |
| 3 | S355 | 0.8   |

| x        | y     | y2    |
|----------|-------|-------|
| 0        | 360   | 259.2 |
| 144.2398 | 259.2 | 259.2 |
| 180      | 180   |       |
| 207.8461 | 0     |       |

|       |           |
|-------|-----------|
| N     | 400 kN    |
| a     | 6.5 mm    |
| angle | 50 graden |
| L     | 100 mm    |

Check  
max 90

Assumption: N distributed equally over both welds, both welds have the same a

| In case of flange plate |                |            |                |
|-------------------------|----------------|------------|----------------|
| alpha_left              | 65 graden      | alpha      | 25 graden      |
| Left weld               |                | Right weld |                |
| sigma_perp              | 278.8639 N/mm2 | sigma_per  | 130.0364 N/mm2 |
| tau_perp                | 130.0364 N/mm2 | tau_perp   | 278.8639 N/mm2 |
| tau_par                 | 0 N/mm2        | tau_par    | 0 N/mm2        |
| von_mises               | 260.0728 N/mm2 | von_mises  | 500.2047 N/mm2 |
| a_suggested             | 6.47 mm        | a          | 9.03 mm        |
| von_mises               | Voldoet        | von_mises  | Error          |
| Sigma                   | Error          | Sigma      | Voldoet        |

| In case of web plate |                |            |                |
|----------------------|----------------|------------|----------------|
| Left weld            |                | Right weld |                |
| sigma_perp           | 166.6693 N/mm2 | sigma_per  | 166.6693 N/mm2 |
| tau_perp             | 166.6693 N/mm2 | tau_perp   | 166.6693 N/mm2 |
| tau_par              | 197.7808 N/mm2 | tau_par    | 197.7808 N/mm2 |
| von_mises            | 466.4731 N/mm2 | von_mises  | 466.4731 N/mm2 |
| a                    | 8.63 mm        | a          | 8.63 mm        |
| von_mises            | Error          | von_mises  | Error          |
| Sigma                | Voldoet        | Sigma      | Voldoet        |

$$q := \sqrt{\frac{\beta^2 \gamma M^2 N^2 (2 \cos(\alpha)^2 + 1)}{L^2 f_u^2}}$$

$$a := \sqrt{\frac{\beta^2 \gamma M^2 N^2 (\cos(\alpha)^2 + 2)}{L^2 f_u^2}}$$

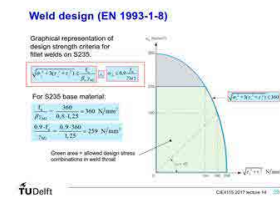
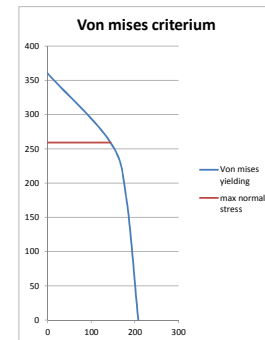


Figure E.4: Interface Weld Calculator made in Excel





# Bibliography

- [1] F. Maatje, *Ronde Tafel Bijeenkomst VO-UO problematiek*, (2018).
- [2] Voortman, *Make it Makeable, Robotics*, Smart Steel, connecting design, data and material , 51 (2017).
- [3] K. Weynand and J.-P. Jaspart, *Design of Structural Steel Joints* (ECCS - European Convention for Constructional Steelwork, 2016) p. 385.
- [4] R. Van Mellaert, *Optimal design of steel structures according to the Eurocodes using mixed-integer linear programming methods*, *Ph.D. thesis*, KU Leuven (2017).
- [5] J. Stark and J. Wardenier, *Knopen* (Bouwen met Staal, Zoetermeer, 2014).
- [6] SteelConstruction.info, *Cost planning through design stages*, (2012).
- [7] K. Mela, *Mixed Variable Formulations for Truss Topology Optimization* (2013) p. 132.
- [8] M. Helminen, *Mika helminen optimization of a trussed steel portal frame*, (2017).
- [9] J. Jalkanen, *Tubular Truss Optimization Using Heuristic Algorithms* (2007).
- [10] K. Mela, T. Tiainen, and M. Heinisuo, *Economical design of high strength steel trusses using multi-criteria optimization*, *Eurosteel 2017* **1**, 9 (2017).
- [11] R. Jankowski, *MODELLING OF TRUSS WITH COLD-FORMED SECTIONS AND POSITIVE ECCENTRICITY IN THE NODES*, **0**.
- [12] G. de Vree, *Company visit ASK Romein, 21-02-2018, Roosendaal*, (2018).
- [13] A. van Dijk, *Company visit Voortman staal bv, 04-06-2018, Rijssen*, (2018).
- [14] F. Reijrink, *Company visit Reijrink staalconstructies, 11-06-2018, Esbeek*, (2018).
- [15] Zeman, *Zeman SBA Costumers information*, (2018).
- [16] J. Paul, *Casting, Forming & Welding*, (2014).
- [17] J. Ifanullah, *Direct Costs and Indirect Costs*, (2013).
- [18] J. Stark, *Verbinden* (Bouwen met Staal, Zoetermeer, 2012).
- [19] K. Watson, S. Dallas, N. van der Kreek, and T. Main, *Costing of Steelwork from Feasibility through to completion*, *AISC* (1996).
- [20] P. Kraljic, *Purchasing must become supply management*, *Harvard Business Review* **61**, 109 (1983).
- [21] S. C. Gottlieb and K. Haugbølle, *Building*, Tech. Rep. (Aalborg Universitet, 2010).
- [22] A. van Douwen, *Connection design and Economy (in Dutch)*, *Bouwen met Staal* **47** (1979).
- [23] W. Foundation, *WageIndicator2018 - Loonwijzer.be*, (2018).
- [24] Statista, *Projected hrc steel prices worldwide from 2017 to 2020, by major market (in U.S. dollars per metric ton)*, (2018).
- [25] F. Hart, H. Henn, and H. Sontag, *Multi-storey Buildings in Steel*, Tech. Rep. (University Press, Camebridge, 1985).

- [26] L. Xu and D. E. Grierson, *Computer Automated Design of Semirigid Steel Frameworks*, [Journal of Structural Engineering](#) **119**, 1740 (1993).
- [27] S. O. Degertekin and M. S. Hayalioglu, *Harmony search algorithm for minimum cost design of steel frames with semi-rigid connections and column bases*, [Structural and Multidisciplinary Optimization](#) **42**, 755 (2010).
- [28] M. S. Hayalioglu and S. O. Degertekin, *Minimum cost design of steel frames with semi-rigid connections and column bases via genetic optimization*, [Computers & Structures](#) **83**, 1849 (2005).
- [29] L. M. Simões, *Optimization of frames with semi-rigid connections*, [Computers and Structures](#) **60**, 531 (1996).
- [30] M. Steenhuis, K. Weynand, and A. M. Gresnigt, *Strategies for economic design of unbraced steel frames*, [Journal of Constructional Steel Research](#) **46**, 88 (1998).
- [31] J. Scherrenberg, *'Het iteratieve proces tussen hoofdberekening en detailberekening'*, Tech. Rep. (Bouwen met Staal, 2017).
- [32] Kreo, *Why are construction profit margins so low?* (2018).
- [33] N. Bel Hadj Ali, M. Sellami, A. F. Cutting-Decelle, and J. C. Mangin, *Multi-stage production cost optimization of semi-rigid steel frames using genetic algorithms*, [Engineering Structures](#) **31**, 2766 (2009).
- [34] N. B. H. Ali, J. C. Mangin, and A. F. Cutting-Decelle, *An overall approach to structural design of steelworks using genetic algorithms*, [System-based vision for strategic and creative design—Proceedings of the 2nd international conference on structural and construction engineering, Balkema, Rome](#), 481 (2003).
- [35] Bouwen met Staal, *Kostenmodel staalskeletbouw Handleiding voor het gebruik*, Tech. Rep. november (Bouwen met Staal, Zoetermeer, 2012).
- [36] J. Haapio, *Feature-Based Costing Method for Skeletal Steel Structures based on the Process Approach*, [Ph.D. thesis](#), Tampere University of Technology (2012).
- [37] K. Jármai and J. Farkas, *Cost calculation and optimisation of welded steel structures*, [Journal of Constructional Steel Research](#) **50**, 115 (1999).
- [38] ArcelorMittal, *Prijslijst nr. 87, 15 januari 2018*, (2018).
- [39] Bressers, *Prijslijst alle artikelen, 05-02-2018*, (2018).
- [40] Douma, *Staalprijzen, 29 januari 2018*, (2018).
- [41] Reesink, *Prijslijst, 29-01-2018*, (2018).
- [42] Vlietjonge, *Prijslijst, 29 januari 2018*, (2018).
- [43] K. Oudshoorn, *Company visit Oostingh ASK Romein, 29-10-2018, Katwijk*, (2018).
- [44] F. Maatje, *Interview company director Bouwen met Staal, 04-04-2018, Zoetermeer*, (2018).
- [45] F. Neessen, *Zin én Onzin over laskostenbeheersing*, [Product Informatie Bulletin](#), 1 (2008).
- [46] L. Pavlovčič, A. Krajnc, and D. Beg, *Cost function analysis in the structural optimization of steel frames*, [Structural and Multidisciplinary Optimization](#) **28**, 286 (2004).
- [47] Dlubal, *Snow Load Zones, Wind Zones and Earthquake Zones*, (2018).
- [48] L. Wagemans, *Quick Reference, Academic year 2011, TU Delft* (2011).
- [49] S. Krenk and J. Høgsberg, *Statics and Mechanics of Structures* (2013) pp. 1–506.

- [50] J. Wardenier, J. A. Packer, X.-L. Zhao, and A. van der Vegte, *Comité International pour le Développement et l'Etude de la Construction Tubulaire* (Bouwen met Staal, Zoetermeer, 2010) p. 199.
- [51] C. Preisinger, *Parametric Structural Modelling (Karamba) User Manual for Version 1.2.2*, (2016).
- [52] IDEA Statica, *IDEA Statica - IDEA Open Model - IOM*, .
- [53] IDEA Statica, *IDEA Statica Connection, Theoretical Background*, (2018).
- [54] i. S. RC, *Waarom S235 achterhaald is*, *Bouwen met Staal* **1**, 62 (2013).
- [55] i. J. Roosendaal and Dr.ir.A.F.Hamerlinck, *S235 niet langer evident*, *Bouwen met Staal* **1**, 1 (2017).
- [56] A. bv, *Project folder Nationaal Militair Museum [projectnumber: 11612]*, (2015).
- [57] W. Spangenberg, *Interview Structural Engineer of project Nationaal Militair Museum, Soesterberg*, (2018).
- [58] H.-J. Kuijer, *Interview Structural Engineer of project Nationaal Militair Museum, Soesterberg*, (2018).
- [59] J. Galjaard, *Interview Structural Engineer of project Sportcampus Zuiderpark, Den Haag*, (2018).
- [60] A. bv, *Project folder Sportcampus Zuiderpark [projectnumber: 12029]*, (2017).
- [61] C. Hatzopoulos, *Mailcontact Support Manager IDEA Statica Connections, United Kingdom*, (2018).